AD-756 854

AERODYNAMIC STABILITY AND CONTROL, DATA, MODEL 844-2035

Boeing Company
Seattle, Washington

14 February 1972

DISTRIBUTED BY:

NTIS
National Technical Information Service
U. S. DEPARTMENT OF COMMERCE
5285 Port Royal Road, Springfield Va. 22151

[redacted]

BOEING AIRPLANE COMPANY

SEATTLE 24, WASHINGTON

AD 256854

FC
TI
AH
AF

Details of illustrations in this document may be better studied on microfiche.

DOCUMENT NO. D2-8174

UNCLASSIFIED TITLE Aerodynamic Stability and Control Data, Model 844-2035

MODEL NO ________ CONTRACT NO. AF 33(600)-41517

ISSUE NO. 17 ISSUED TO ________

CLASSIFIED TITLE ________
(STATE CLASSIFICATION)

PRELIMINARY INFORMATION

WORK ORDER NO UNIT NO. ITEM NO.

SPECIAL ... ON ASTIA DISTRIBUTION

... checked only because of ...

Classification Cancelled
~~(or changed to ______)~~
Auth. AFSDCS ltr, 5 May 70
By AFFDL/CD
Date 14 Feb 72

"Approved for public release; distribution unlimited"

PREPARED BY Flight Controls Group

SUPERVISED BY ________ 2-27-61
A. H. Lee

APPROVED BY ________ 2-28-61
L. G. Mason

CLASS. & DISTR. APPROVED BY ________ ________
J. S. Lesko (DATE)

NO. OF PAGES 164 (EXCLUDING TITLE AND REVISION AND ADDITION PAGES.)

DISTRIBUTION STATEMENT A
Approved for public release;
Distribution Unlimited

[redacted]

DOCUMENT TITLE PAGE

[redacted]

TABLE OF CONTENTS

TABLE OF CONTENTS - Cont'd

FIGURE INDEX

FIGURE INDEX

6.1 LATERAL - DIRECTIONAL STABILITY [illegible]

6.2 AILERON CHARACTERISTICS AND EFFECTIVENESS

6.3 RUDDER CHARACTERISTICS AND EFFECTIVENESS

6.4 ROLL AND YAW ROTARY DERIVATIVES

FIGURE INDEX

FORWARD

The glider configuration represented by the stability and control characteristics presented in this document is not current. Information derived from analysis and wind-tunnel tests as the document was being completed indicated the need for some configuration changes. However, the document is released for distribution to update the information being used by various agencies for stability and control analysis.

The most significant change to the configuration in a stability and control sense is a change in the incidence angle of the folding wing tip extensions. The tip extensions in the document are set at an incidence of −15° degrees relative to a water line. Currently, the tip extensions are considered at an incidence of zero degrees. This change principally affects the zero lift pitching moment with relatively little affect on longitudinal stability. However, it does affect the directional stability at transonic speeds favorably. With this change in tip incidence, the speed for tip extension must also be altered. Currently, tip extensions are considered retracted at speeds higher than Mach 1.[illegible].

Other changes are being considered to correct some stability and control deficiencies evident in the document. The effects of these changes will be distributed in a revision of this document when they are available.

ACKNOWLEDGEMENT

The following people contributed to the preparation of this document:

R. J. Montgomery
G. K. Dragseth
D. C. Leisy
M. A. Carter
J. L. Francis
P. M. Jacobsen
E. J. Hamilton
P. M. McGinnese
R. W. Meinke
D. E. Phillips
W. S. Cox
B. F. Ray
P. T. Victor
J. W. Ball
W. J. Moore
K. A. Noess
R. T. Barth
G. O. Mount
E. A. Piper
D. J. Rossini
L. A. Bodin
N. T. Underwood
R. K. Rice

1.0 INTRODUCTION

The aerodynamic stability and control characteristics of the 844-2035 Dyna Soar glider are presented in the following sections of this document. Data are presented for the glider and for the glider plus third stage.

These data are based on wind tunnel tests, where data are available. Where not available, theoretical estimates have been made for the vehicle characteristics.

This is the interim glider configuration. Some vehicle characteristics peculiar to this configuration are not satisfactory and will be modified for the final configuration. The wing tip extension configuration is subject to change. A good speed brake location is still to be defined. The vertical tail and rudder size may increase. The elevon configuration may change. The possibility of asymmetric deflection of the elevon for roll control to reduce couplings is being considered.

The data presented will be revised as additional wind tunnel data are received and better estimates of the vehicle characteristics are made.

Information presented in the document is estimated for an obsolete configuration, Model 844-2035. The document is being released to up-date data now in the possession of the customer and associates.

2.0 REFERENCES

Reference a — BAC D2-6909-1 "Interim System Description of the Dyna Soar Step I", R. L. Campbell, November 29, 1960.

Reference b — C119-ER-10440 "Dyna Soar I Configuration Evaluation Wind Tunnel Test Report Series II", Bell Aircraft Corporation, May 1959.

Reference c — NACA TN 2409 "Summary of Methods for Calculating Dynamic Lateral Stability and Response and for Estimating Lateral Stability Derivatives", Campbell and Mc Kinney, July 1951.

Reference d — NASA TM X - 287 "Theoretical Stability Derivatives for the X-15 Research Airplane at Supersonic and Hypersonic Speeds Including a Comparison with Wind Tunnel Results, Walker and Wolowicz, August 1960.

3.0 CONFIGURATION

3.1 The general arrangement of the 844-2035 configuration is shown on Figure 3.1.1. The configuration is shown in the manufactured shape (referred to as the "cold" shape).

A heat shield is shown covering the pilots wind shield. This is separated from the glider at supersonic speeds. The drag brake, shown on top the body, is actuated at subsonic and low supersonic speeds, only. The wing tip extensions, located on the vertical tails, are extended at supersonic speeds. The rudders are deflected outboard only.

The elevons are split in two panels. This was done to reduce the sensitivity of the elevons for roll control at transonic and supersonic speeds and at high dynamic pressures when the elevons have high effectiveness. In these flight conditions, roll commands are transmitted to the inboard panels only. If a continuous signal is required by the adaptive feature of the flight control system, it will be transmitted to the inboard panel only to conserve A.P.U. fuel.

The inboard elevon panel is shown to have a wedged section to eliminate possible "dead" zones in elevon effectiveness at small deflections at hypersonic speeds. This wedging is probably unnecessary. The elevon section of the inboard panel has been considered modified to the same as that outboard panel for the data in this document.

Elevon actuator housings, not shown on the drawing, are located on the upper wing surface. These are positioned at approximately midspan of the two elevon panels and extend forward of the elevon hinge line. Actuators for the rudders are located in the bottom section of the vertical tail.

A more complete configuration is presented in Reference 2.

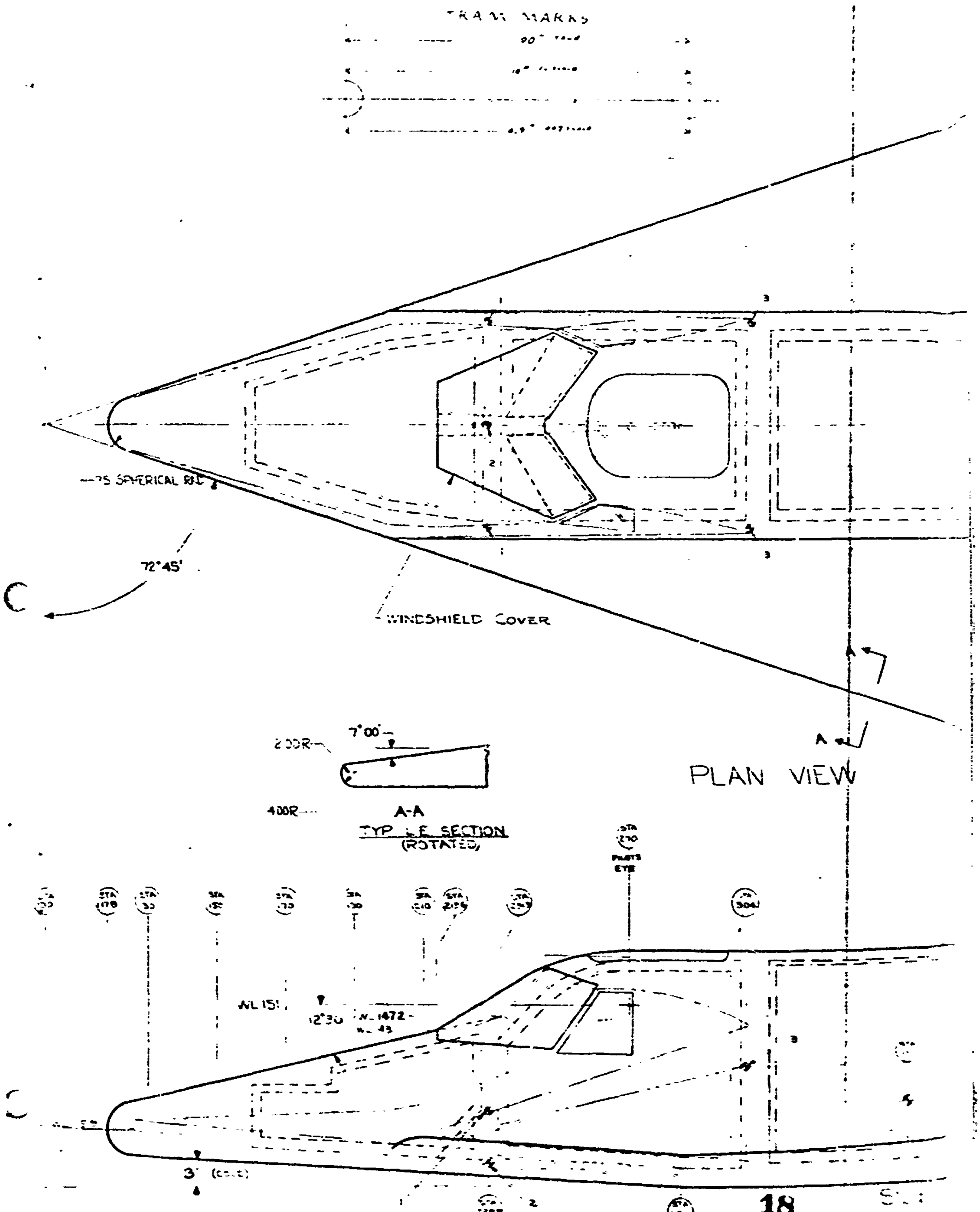

TRAM MARKS
75 SPHERICAL RAD
72°45'
WINDSHIELD COVER
7°00'
200R
400R
A-A
TYP L.E. SECTION
(ROTATED)
PLAN VIEW
A
STA 270
PILOTS EYE
WL 151
12°30'
WL 147.2
3" (CONST)

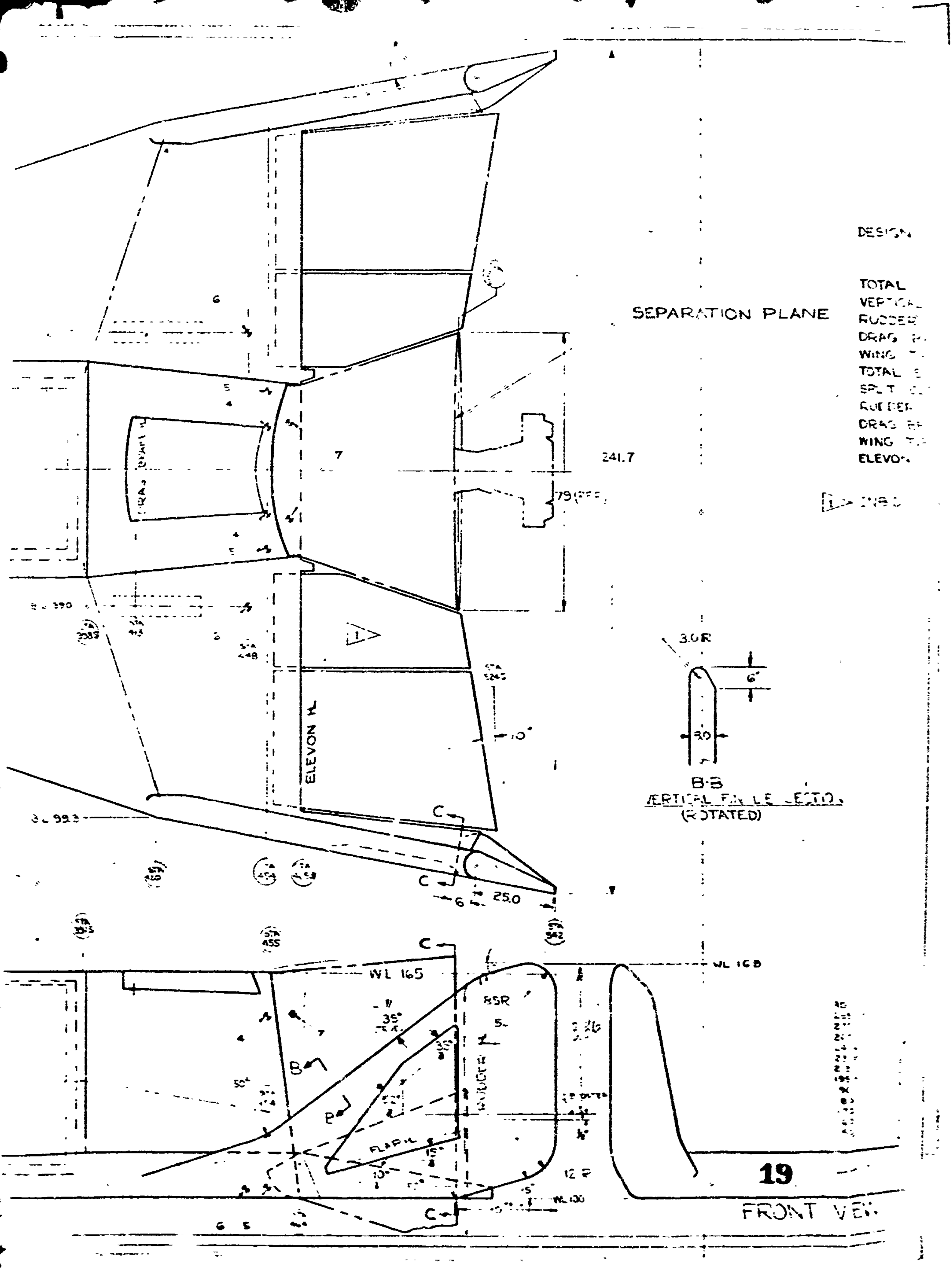
SEPARATION PLANE
DESIGN
TOTAL
241.7
79 (REF)
ELEVON
DRAG
3.0 R
6"
3.0
B-B
VERTICAL FIN LE SECTION
(ROTATED)
25.0
WL 165
WL 168
35°
15°
10°
RUDDER
FLAP
85R
12 R
FRONT VIEW

DESIGN LAUNCH GROSS WEIGHT — — — — — — 9600 LBS.

TOTAL LIFTING SURFACE AREA — — — — — — 343 SQ FT
VERTICAL FIN SURFACE AREA — — — — — — 3.0 SQ FT
RUDDER SURFACE AREA — — — — — — 10.6 SQ FT
DRAG BRAKE AREA — — — — — — [illegible] SQ FT
WING TIP EXTENSION AREA (TOTAL) — — — — — 11 SQ FT
TOTAL ELEVON SURFACE AREA — — — — — 48.0 SQ FT
SPLIT ELEVON SURFACE AREA (TOTAL) — — — — 16.0 SQ FT
RUDDER ANGULAR MOVEMENT — — — — — — 25 OUTBD
DRAG BRAKE ANGULAR MOVEMENT — — — — — 60°
WING TIP EXTENSION ANGULAR MOVEMENT — — — 90°
ELEVON ANGULAR MOVEMENT — — — — — 55° UP
22° DOWN

INBD SECTION OF ELEVON FIXED SPLIT ANGLE 20°

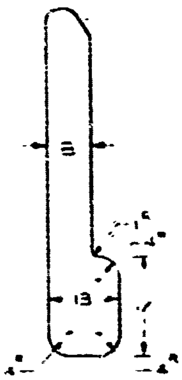

C-C

HOIST AND HANDLING POINTS

CONDITION	ATTACHMENT POINTS
AIR TRANSPORT	2 AND 4
AIR LAUNCH	[illegible] AND [illegible], 3 AND 4
SLING	[illegible] 4, AND 5 [illegible] AND [illegible]
DOLLY	2 AND 4
TRAILER	2 AND 5
[illegible] ATTACH	4 AND 5
[illegible]	2 AND 3

[illegible] ADAPTER LIFTING PYLON

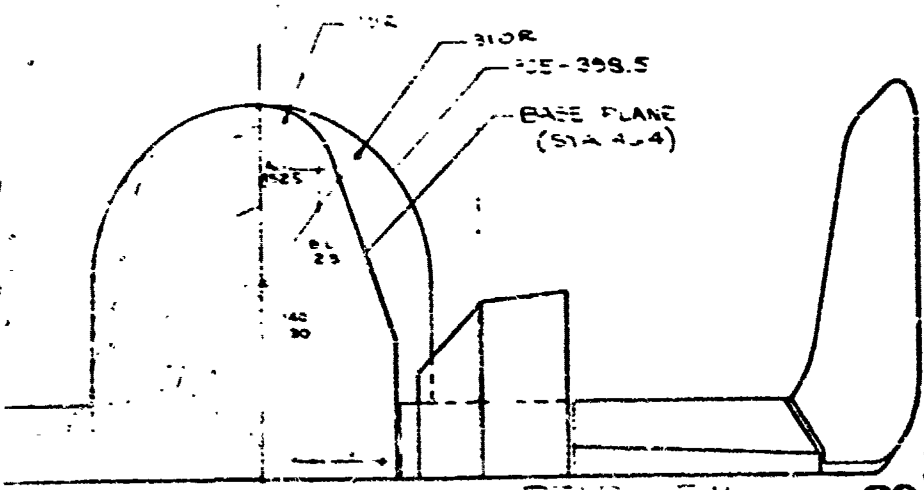

REAR VIEW

FIG 3.1.1

[illegible] GENERAL ARRANGEMENT
DYNA SOAR
MODEL 844-2035

D2-8174

3.2 WEIGHTS AND MOMENTS OF INERTIA

The design weights and moments of inertia for the glider vehicle are presented below.

For the glider alone (transition section off):

Weight = 9600 lbs.

Principal Moments of Inertia about C.G.:

$I_y = 18,600$ slugs - ft^2 (pitch)

$I_x = 4,000$ slugs - ft^2 (roll)

$I_z = 21,000$ slugs - ft^2 (yaw)

The x principal axis is assumed parallel to glider water lines.

For the 9600 lb. glider plus the third stage, Figure 3.2.1 gives the moments of inertia during third stage burning, and the weights and the center of gravity locations at beginning and end of third stage burning.

The center of gravity location for the glider alone is shown on Figure 3.3.3 .

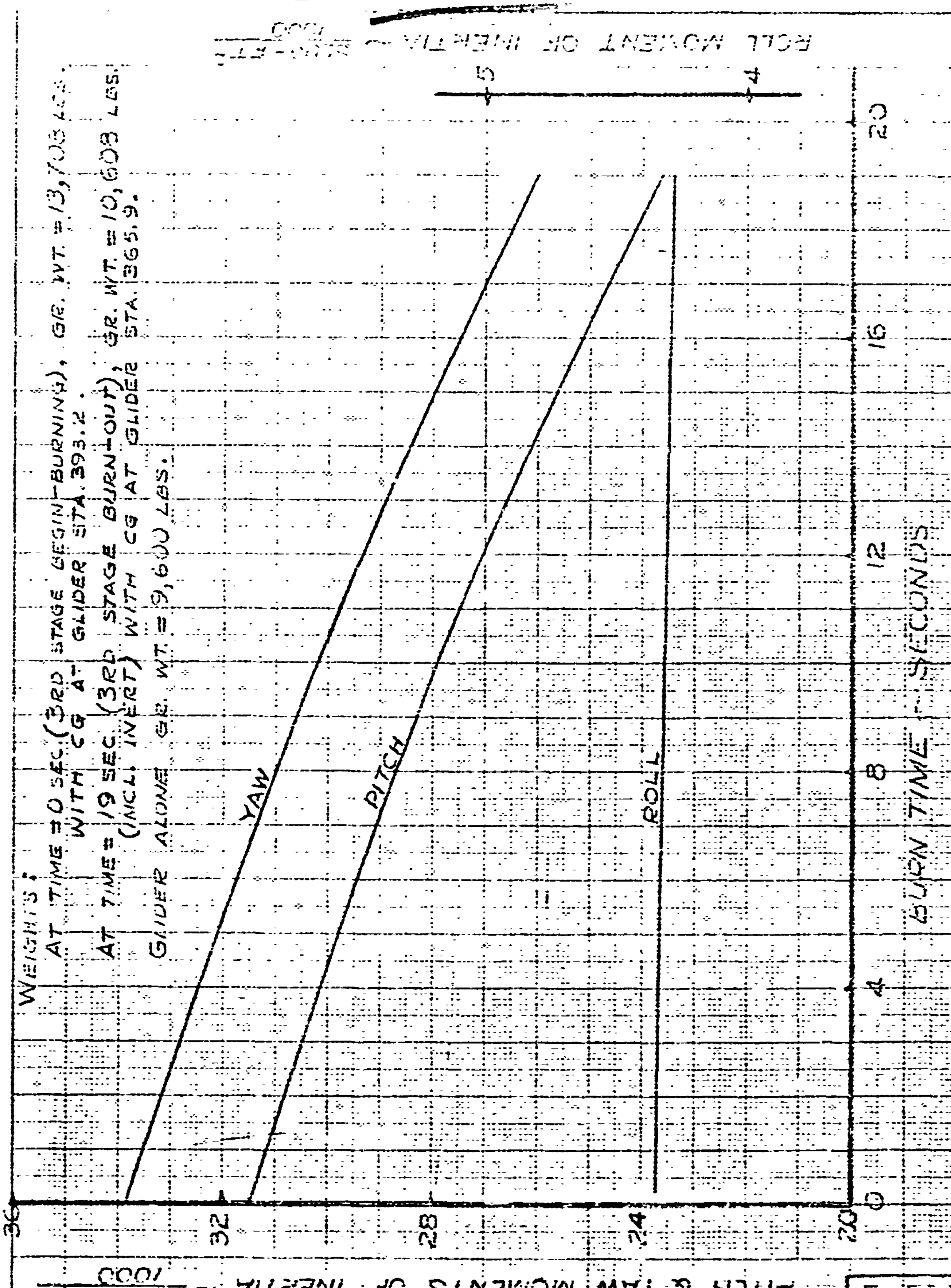

Fig 3.4

C. W. CANNON 12-21

✓ 12-25

REDMANN M.A.C. 12-23

MASS DATA FOR 9600 LB GLIDER AND THIRD STAGE

844-2035

D2-3174

BOEING AIRPLANE COMPANY

PAGE 3.4

3.3 AERODYNAMIC DATA AND REFERENCE CONSTANTS

Aerodynamic data in the document are presented on a fixed body axis system. The axis system is shown on Figure 3.3.1 . Definition of angle of attack and sideslip and the sign convention for the force and moment coefficients are also shown. The sign conventions for control deflections are shown on Figure 3.3.2 .

Reference constants and glider alone center of gravity location are shown on Figure 3.3.3 . Some significant aerodynamic configuration constants are also presented.

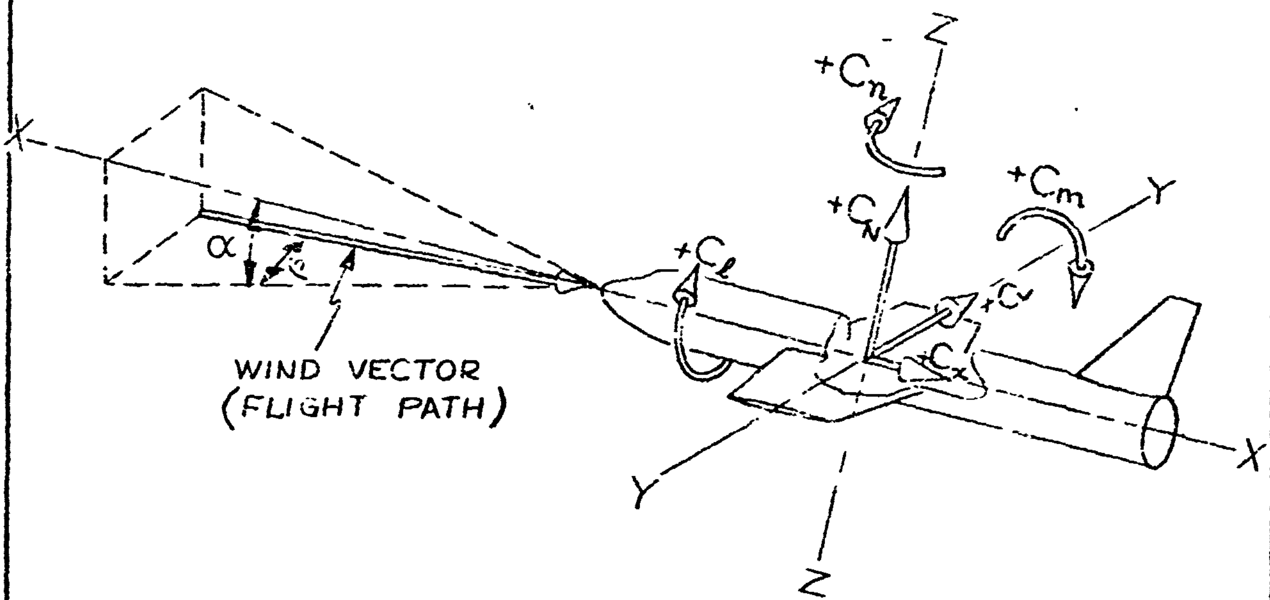

NOTES:

1.) THE MUTUALLY PERPENDICULAR X, Y, AND Z AXES ARE FIXED ON THE AIRPLANE, REGARDLESS OF FLIGHT ATTITUDE.

2.) ANGLE OF ATTACK IS MEASURED IN THE AIRPLANE PLANE OF SYMMETRY (X-Z PLANE), BETWEEN THE AIRPLANE X-AXIS AND THE PROJECTION OF THE WIND VECTOR INTO THE X-Z PLANE.

3.) ANGLE OF SIDESLIP IS MEASURED IN OR PARALLEL TO THE PLANE DEFINED BY THE AIRPLANE Y-AXIS AND THE WIND VECTOR, BETWEEN THE WIND VECTOR AND THE PROJECTION OF THE AIRPLANE X-AXIS INTO THE ABOVE-DEFINED PLANE.

4.) FOR THE DYNA SOAR 844-2035 CONFIGURATION, THE X-Y PLANE IS PARALLEL TO THE FLAT, AFT PART OF THE WING UNDERSURFACE.

FIG. 3.3.1

CALC		REVISED	DATE	BODY AXIS SYSTEM NOMENCLATURE ~ COMBINED ANGLE OF ATTACK & SIDESLIP	844-2035
CHECK					D2-8174
APR				BOEING AIRPLANE COMPANY	PAGE 3.6
APR					
DWN M. CARTER 12-23-0					

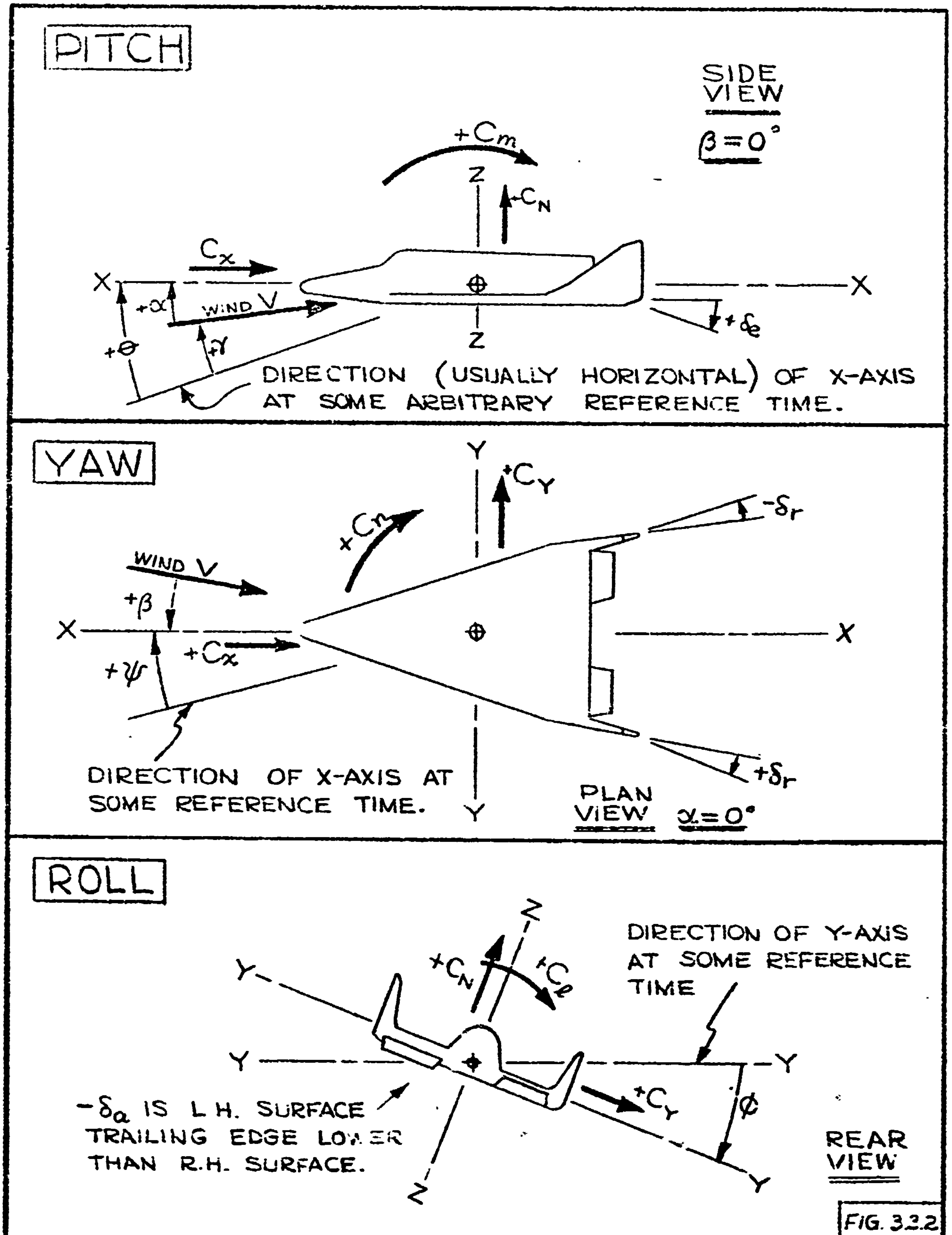

FIG. 3.2.2

		REVISED	DATE	
CALC				BODY AXIS SYSTEM ~ NOMENCLATURE
CHECK				844-2035
APR				D2-8174
APR				BOEING AIRPLANE COMPANY
DWN M. CARTER 12-27-60.				PAGE 3.7

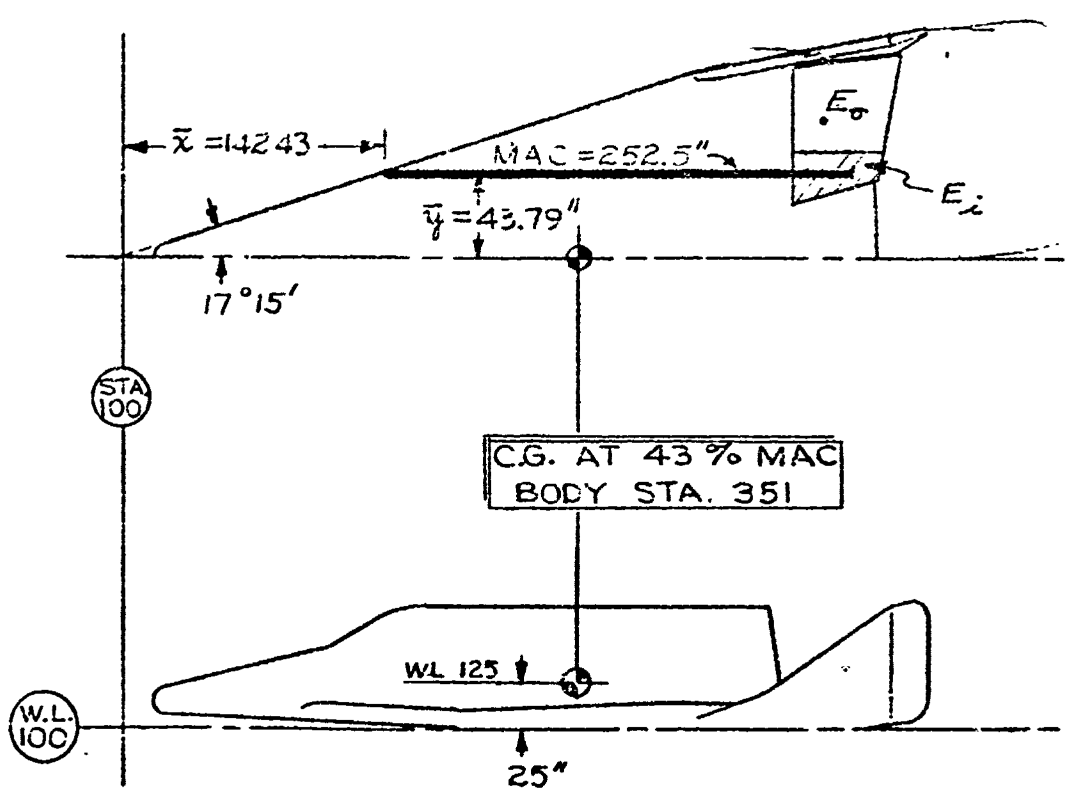

AERODYNAMIC REFERENCE CONSTANTS:

WING AREA, $S_W = 343.24\ FT^2$
EFFECTIVE SPAN, $b = 236.7$ IN.
ASPECT RATIO, $AR = 1.13$
ROOT CHORD, $C_R = 406.1$ IN.
TIP CHORD, $C_T = 107.8$ IN.
$\lambda = C_T / C_R = .265$

ELEVONS:

FULL ELEVON AREA, $S_E = .14\ S_W$
INBOARD PORTION AREA, $E_i = .047\ S_W$
OUTBOARD PORTION AREA, $E_o = .093\ S_W$

FIG. 3.3.3

	REVISED	DATE	AERODYNAMIC REFERENCE CONSTANTS & PERTINENT DIMENSIONS	844-2035
CHECK				D2-8174
APR				
APR			BOEING AIRPLANE COMPANY	PAGE 3.8
DWN M. CARTER				

4.0 DEFINITION OF SYMBOLS

Symbol	Definition
a.c.	aerodynamic center
AR	aspect ratio
b	wing span
B.S.	body station
$\bar{c}$, m.a.c. or M.A.C.	mean aerodynamic chord
c_e	elevon chord
c.g. or C.G.	center of gravity
c_r	wing root chord
c_t	wing tip chord
HM	hinge moment
i_t	incidence angle of wing tip extensions
I_x	moment of inertia in roll
I_y	moment of inertia in pitch
I_z	moment of inertia in yaw
ℓ	rolling moment
L	lift force
m	pitching moment
M	Mach number or pitching moment
n	yawing moment
N	normal force
p	roll rate
q	pitch rate or dynamic pressure in PSF
r	yaw rate

S_e or S_E	elevon area
S_r or S_R	rudder area
S_t	wing tip extension area
S_w	wing area
V	velocity
X	force along X (roll) axis
Y	force along Y (pitch) axis
α	angle of attack
α_{0L}	angle of attack at zero lift
β	angle of sideslip
δ_a	aileron deflection angle
δ_{e_L}	left elevon deflection angle
δ_{e_R}	right elevon deflection angle
δ_e or δ_E	elevon deflection angle, elevons deflecting together
δ_R	rudder deflection angle
θ	pitch angle
ϕ	roll angle
ψ	yaw angle
λ	wing taper ratio $\frac{c_t}{c_r}$
C_l	rolling moment coefficient, $\frac{L}{q S_w b}$
C_{l_p}	$= \partial C_l / \partial (pb/2V)$
C_{l_r}	$= \partial C_l / \partial (rb/2V)$
C_{l_β}	$= \partial C_l / \partial \beta$
$C_{l_{\dot\beta}}$	$= \partial C_l / \partial (\dot\beta b/2V)$
$C_{l_{\delta_a}}$	$= \partial C_l / \partial \delta_a$
$C_{l_{\delta_R}}$	$= \partial C_l / \partial \delta_a$

C_L	lift coefficient, $\frac{L}{q S_w}$
C_m	pitching moment coefficient, $\frac{M}{q S_w \bar{c}}$
C_{m_o}	pitching moment coefficient at zero lift
C_{m_q}	$= \partial C_m / \partial (q\bar{c}/2V)$
C_{m_α}	$= \partial C_m / \partial \alpha$
$C_{m_{\dot{\alpha}}}$	$= \partial C_m / \partial (\dot{\alpha}\bar{c}/2V)$
$C_{m_{\delta a}}$	$= \partial C_m / \partial \delta a$
$C_{m_{\delta e}}$	$= \partial C_m / \partial \delta e$
C_n	yawing moment coefficient, $\frac{N}{q S_w b}$
C_{n_p}	$= \partial C_n / \partial (pb/2V)$
C_{n_r}	$= \partial C_n / \partial (rb/2V)$
$C_{n_{\delta a}}$	$= \partial C_n / \partial \delta a$
$C_{n_{\delta R}}$	$= \partial C_n / \partial \delta R$
C_{n_β}	$= \partial C_n / \partial \beta$
$C_{n_{\dot{\beta}}}$	$= \partial C_n / \partial (\dot{\beta} b/2V)$
C_N	normal force coefficient, $\frac{N}{q S_w}$
C_{N_α}	$= \partial C_N / \partial \alpha$
$C_{N_{\dot{\alpha}}}$	$= \partial C_N / \partial (\dot{\alpha}\bar{c}/2V)$
$C_{N_{\delta a}}$	$= \partial C_N / \partial \delta a$
$C_{N_{\delta e}}$	$= \partial C_N / \partial \delta e$
C_{N_q}	$= \partial C_N / \partial (q\bar{c}/2V)$
C_x	axial force coefficient, $\frac{X}{q S_w}$
C_y	side force coefficient, $Y/q S_w$
C_{y_β}	$= \partial C_Y / \partial \beta$
$C_{y_{\dot{\beta}}}$	$\partial C_Y / \partial (\dot{\beta} b/2V)$

$C_{y_{\delta a}}$	=	$\partial C_Y / \partial \delta_a$
$C_{y_{\delta r}}$	=	$\partial C_Y / \partial \delta_R$
C_{y_p}	=	$\partial C_Y / \partial (pb/2V)$
C_{y_r}	=	$\partial C_Y / \partial (rb/2V)$
C_h		hinge moment coefficient, $\frac{HM}{q S_e C_e}$
C_{h_α}	=	$\partial C_h / \partial \alpha$
$C_{h_{\delta e}}$	=	$\partial C_h / \partial \delta_e$

5.0 LONGITUDINAL STABILITY AND CONTROL (GLIDER)

5.1 SUMMARY

Longitudinal stability and control data are presented in the following sections for the 844-2035 glider configuration. Data are presented through the speed range of the glider. The elevon configuration of the glider has been modified from the 844-2035 such that the inboard panel has no wedging (same section as the outboard panel) for the data to be presented.

The glider aerodynamic configuration varies as a function of speed. At subsonic and supersonic speeds, wing tip extensions, located on the outboard surface of the vertical tails, are extended for increased stability. At hypersonic speeds, the glider is subjected to high temperatures resulting in structural deformation. Data are presented for these changes of configuration.

Normal force, axial force and pitching moment coefficients comprise the data presented in the following sections. The data are presented at the nominal center of gravity position of 43% of the M.A.C. and a vertical c.g. location at water line 125.

Summary curves of these coefficient data are presented on Figures 5.1.1 through 5.1.7. Trimmed aerodynamic center as a function of Mach number and trimmed lift coefficient is presented on Figures 5.1.1 and 5.1.2. Normal force curve slope, at trimmed elevon deflection for a given C_L, is presented on Figures 5.1.6 and 5.1.7. A minor amount of fairing was required to produce these curves from the basic data to be presented, except at $M = 0.7$. The data at $M = 0.7$ produce appreciable discontinuities in the curves and have been faired out of the summary data.

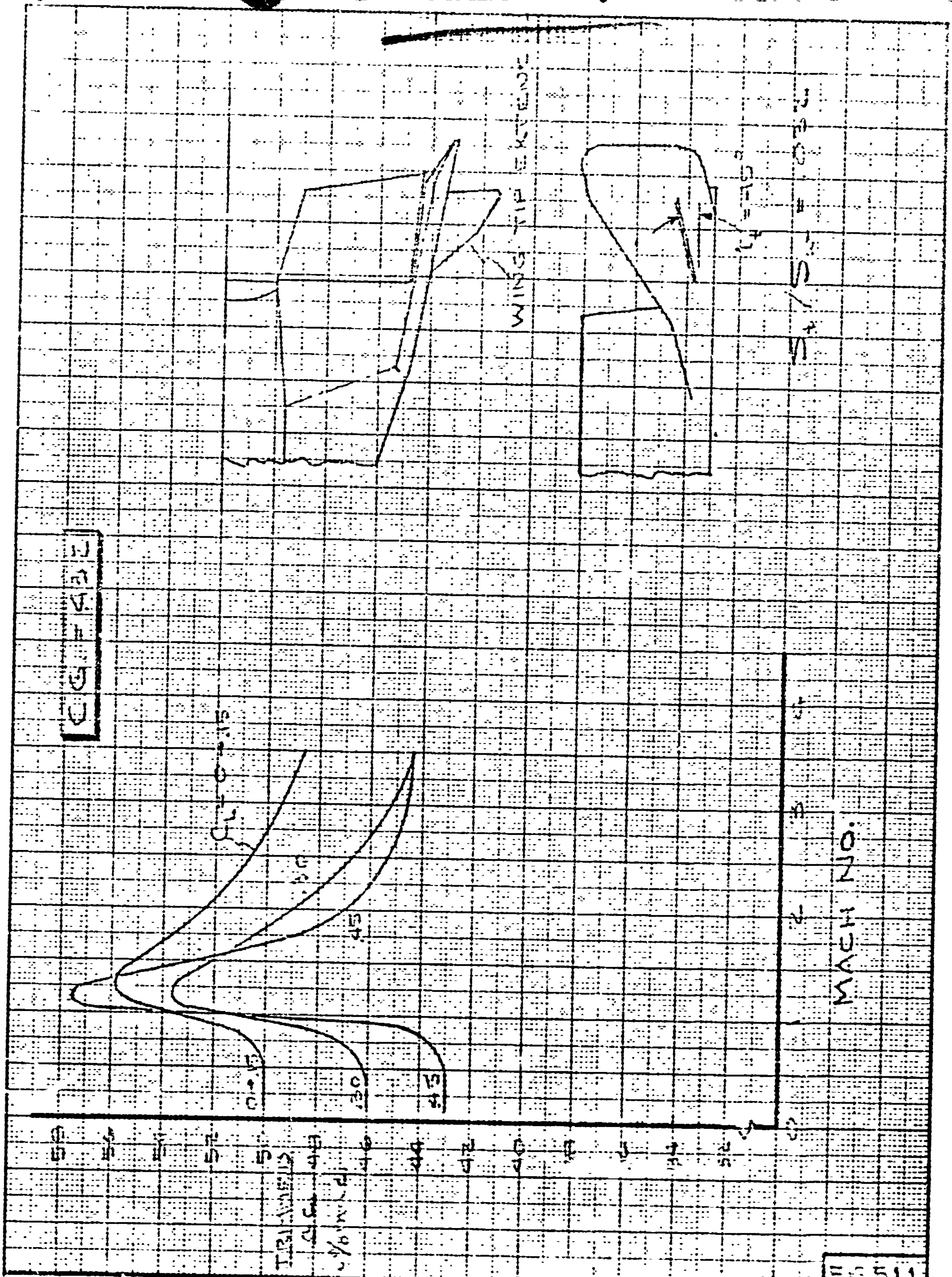

CALC	D C L	12/5/51	REVISED / DATE
CHECK			
APR			
APR			

FIG. 5.11

AERODYNAMIC CENTER
WING TIPS EXTENDED

844-2035

D2-8174

BOEING AIRPLANE COMPANY

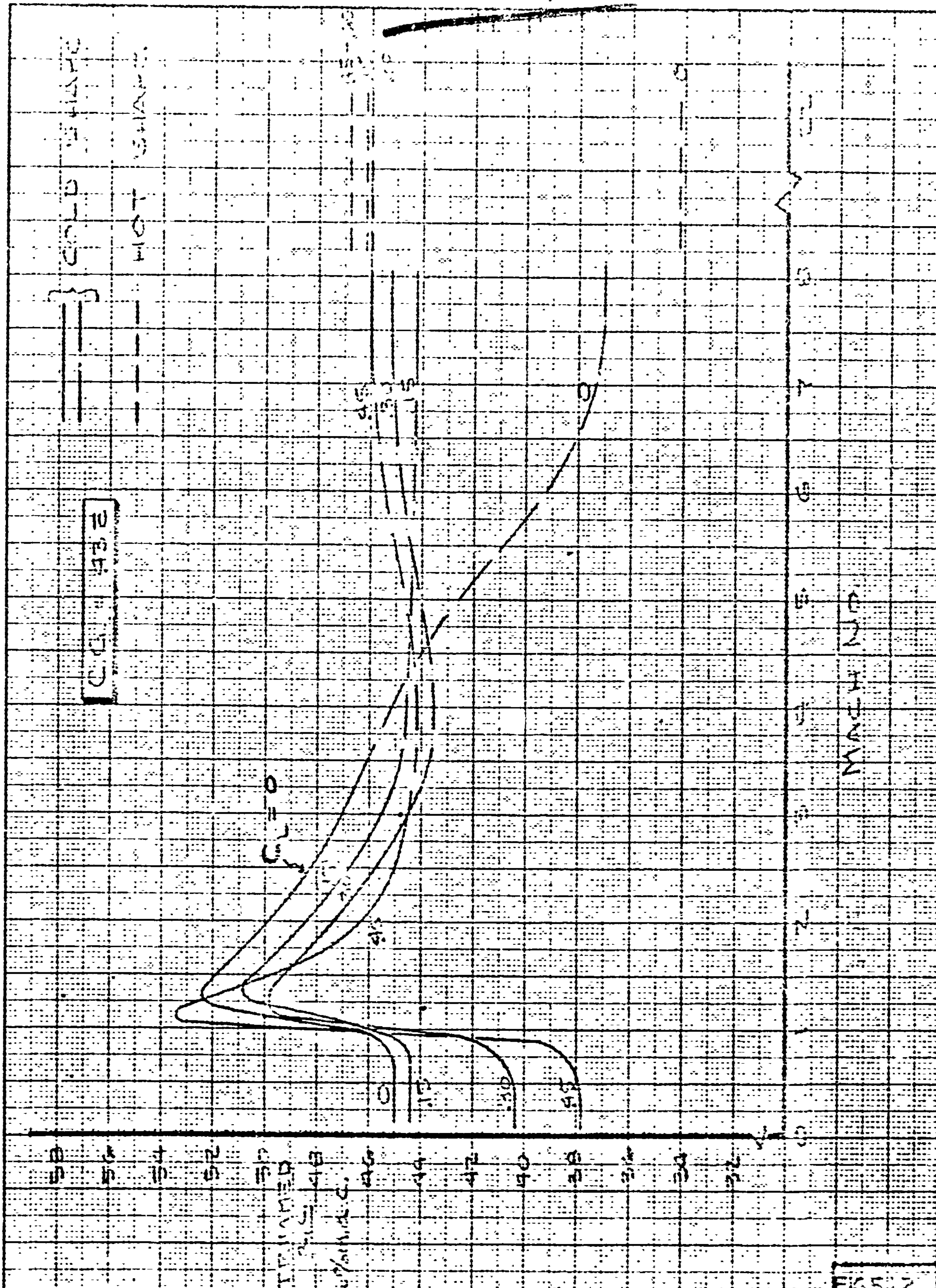

FIG 5.1.2

CALC	D.C.L.	12/15/50	REVISED	DATE
CHECK				
APR				
APR				

AERODYNAMIC CENTER
WING TIPS RETRACTED

844-2035

D2-8174

BOEING AIRPLANE COMPANY 33

PAGE 5.3

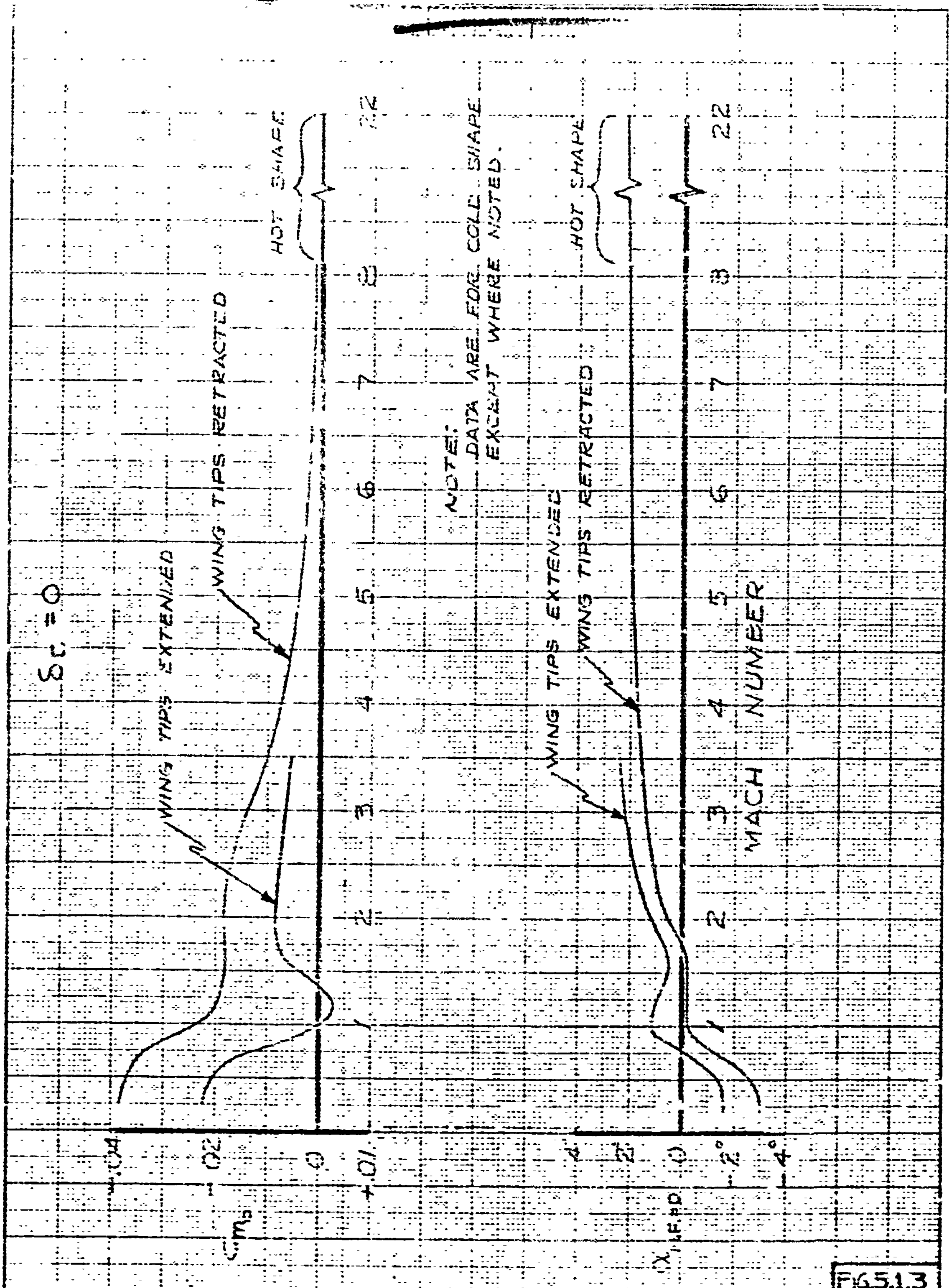

FIG. 5.1.3

M. CARTER 12-16-60

ANGLE OF ATTACK AND PITCHING MOMENT AT ZERO NORMAL FORCE

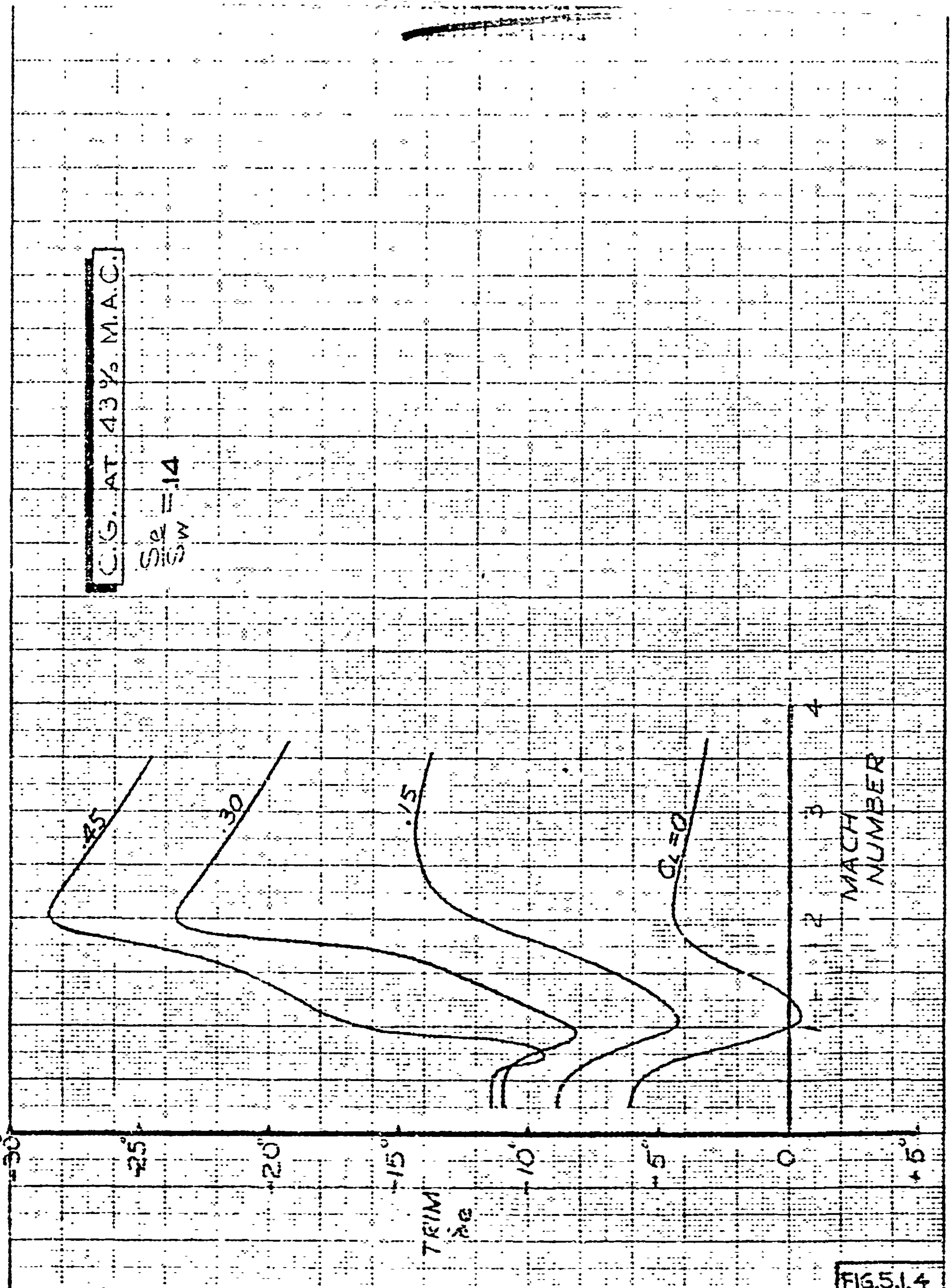

FIG.5.1.4

M. CARTER 12-16-60

ELEVATOR REQUIRED TO TRIM — WING TIPS EXTENDED

844-2035

D2-8174

BOEING AIRPLANE COMPANY 35

PAGE 55

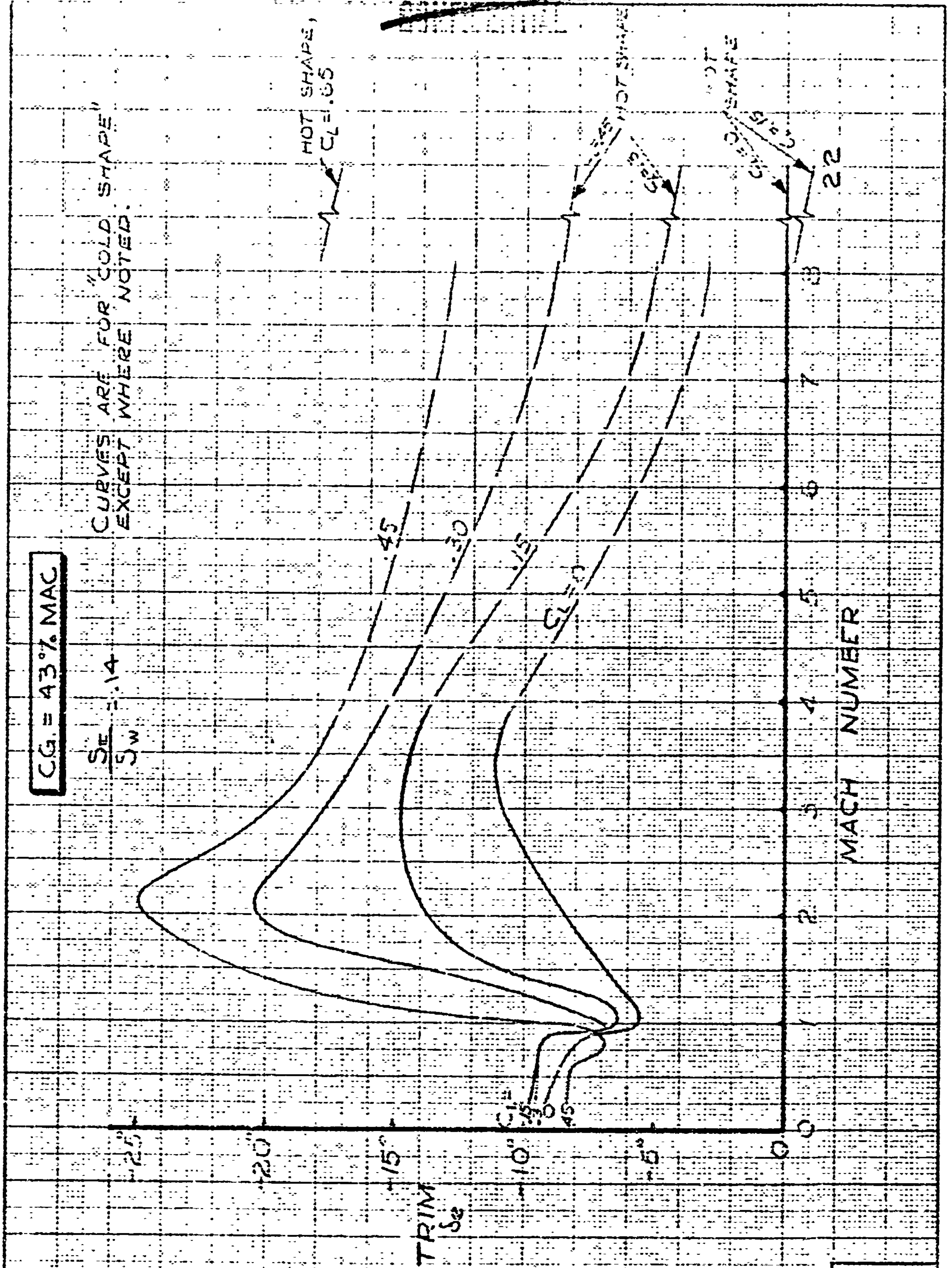

M. CARTER 12-16-60

FIG. 5.1.5

844-2035

ELEVATOR REQUIRED TO TRIM — WING TIP EXTENSIONS RETRACTED

D2-8174

BOEING AIRPLANE COMPANY **36**

PAGE 5.6

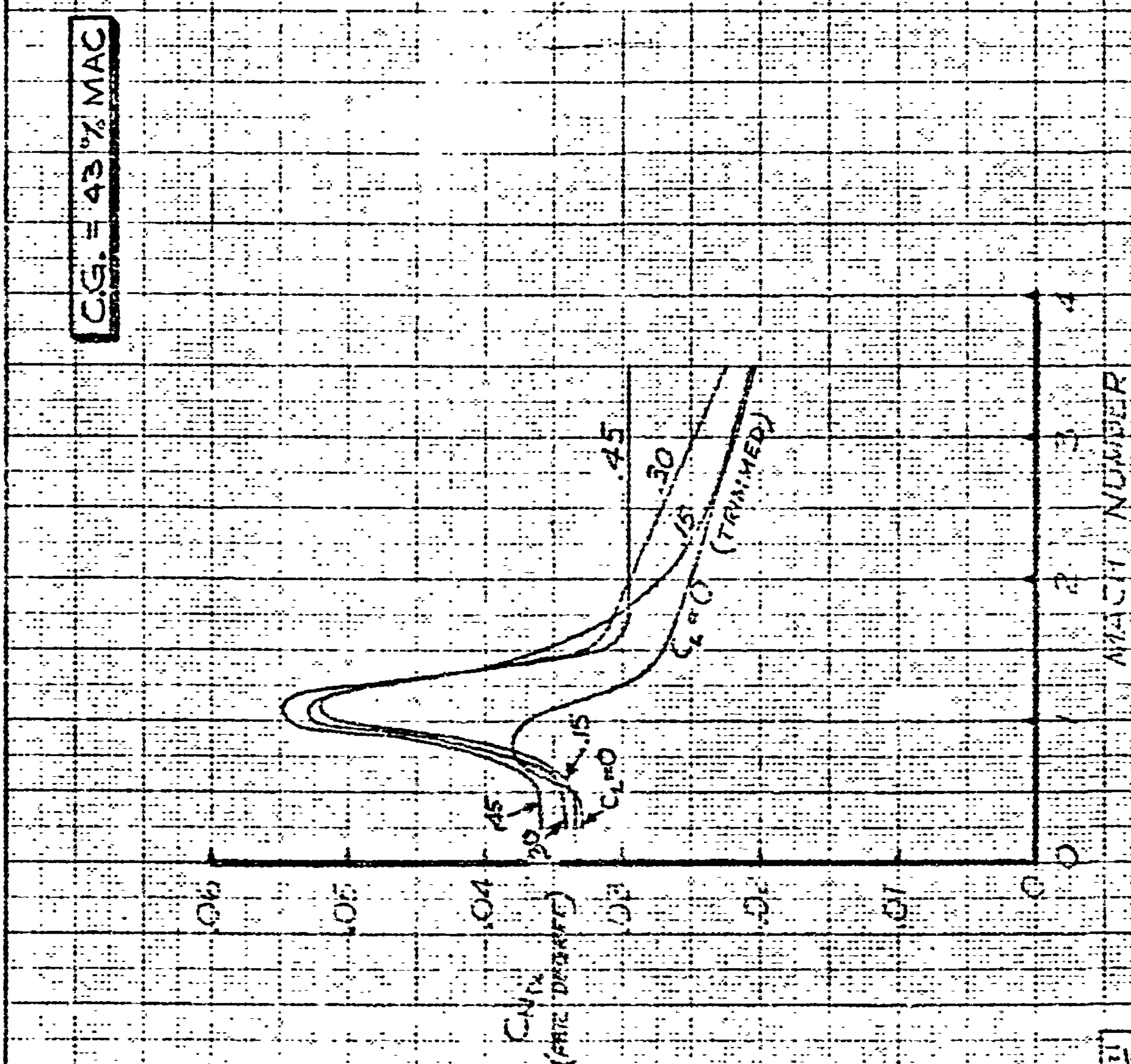

FIG 5.16

M. CARTER 12-21-0	NORMAL FORCE CURVE SLOPE WING TIPS EXTENDED		844-2035
			D2-8174
	BOEING AIRPLANE COMPANY	37	PAGE 5.7

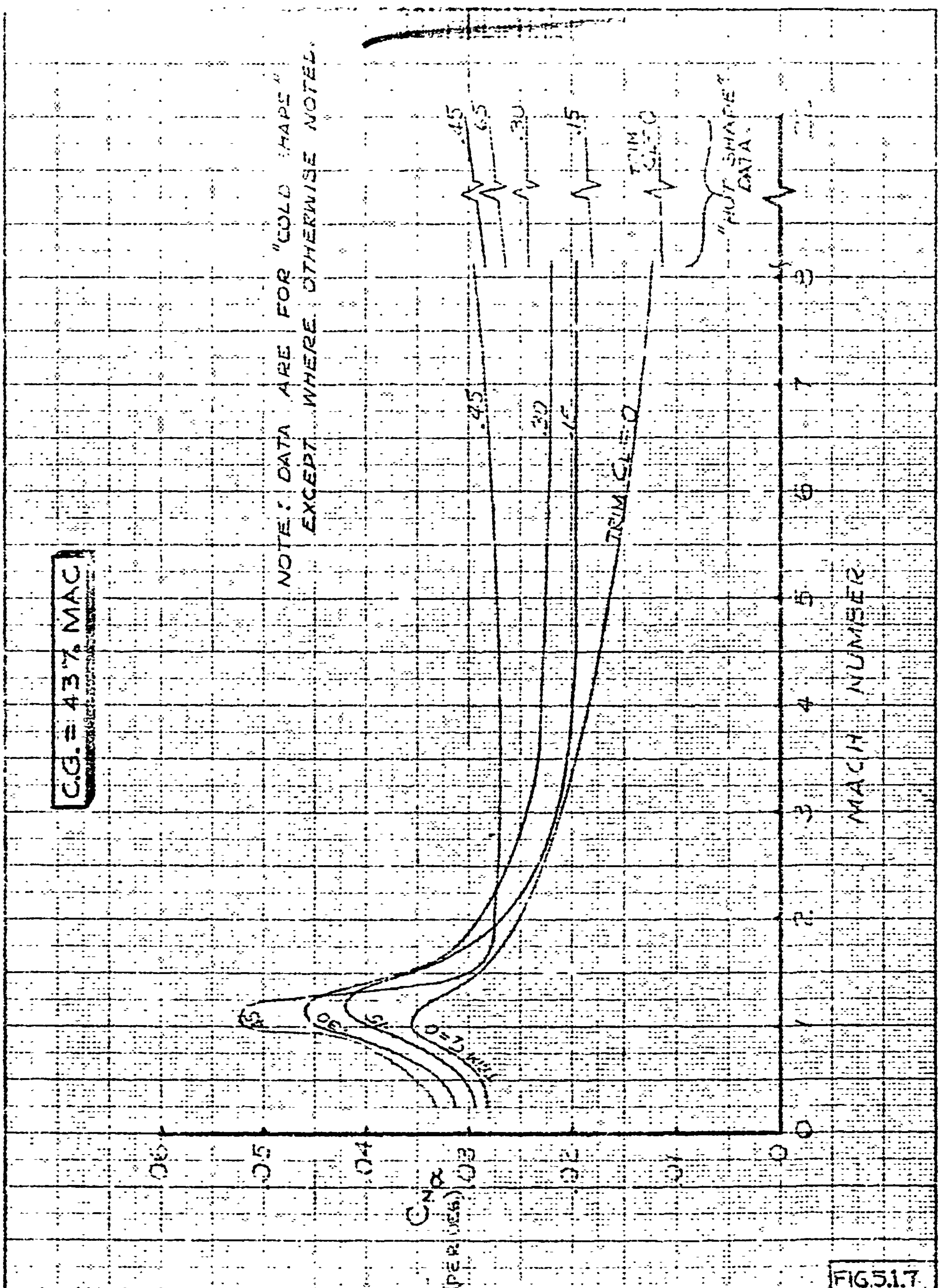

FIG.5.1.7

M. CARTER 12-20-0

NORMAL FORCE CURVE SLOPE
WING TIPS RETRACTED

844-2035

D2-8174

BOEING AIRPLANE COMPANY

5.2 LANDING SPEED

Basic stability and elevon effectiveness plots are presented on Figures 5.2.1 and 5.2.2 for the glider at a Mach number typical of landing speed. These data were determined from wind tunnel tests performed in the A.R.C. 12-Foot Pressure Wind Tunnel and the Boeing Transonic Wind Tunnel on a .15 scale model of the 844-2 05 configuration. These data have been modified to the 844-2035 configuration as required.

The change in stability and control effectiveness with landing gear extended and in close proximity to the ground is shown on Figure 5.2.3. These data were determined from wind tunnel tests in the Boeing Transonic Wind Tunnel on a similar configuration and modified for the present configuration. The incremental effect of extending the landing gear is shown on Figure 5.2.4. It was assumed that proximity to the ground would have little effect on these increments.

Axial force coefficients as a function of angle of attack are shown on Figures 5.3.11 and 5.3.12 at $M = .26$ which is typical of landing. The axial force increment due to landing gear extension is shown on Figure 5.2.5. Axial force is assumed to be unaffected by the presence of the ground.

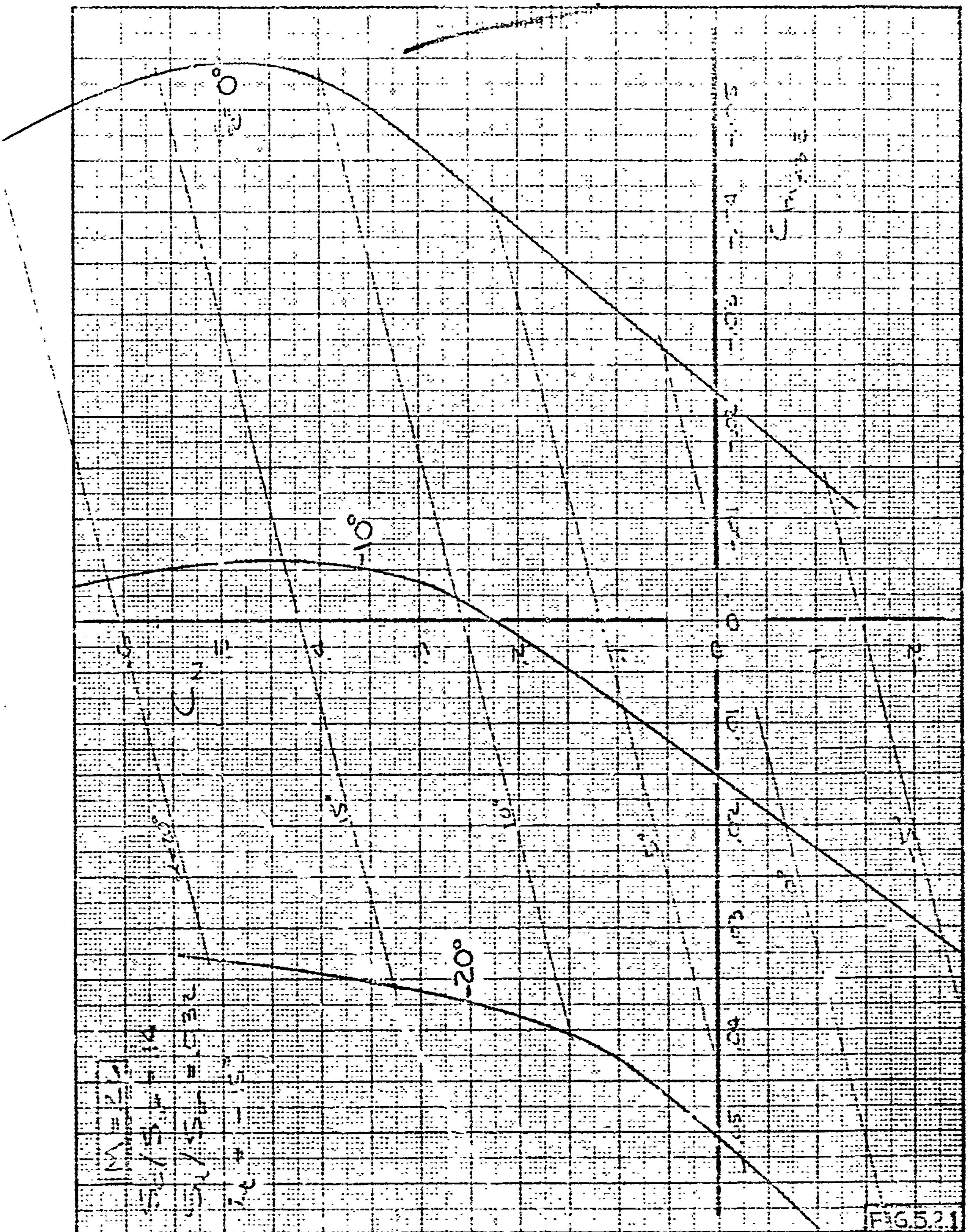

FIG 5.21

CALC			REVISED	DATE	LONGITUDINAL STABILITY WING TIPS EXTENDED M = 2.6	844-2035
CHECK						D2-8174
APR						
APR					BOEING AIRPLANE COMPANY 40	PAGE 5.10

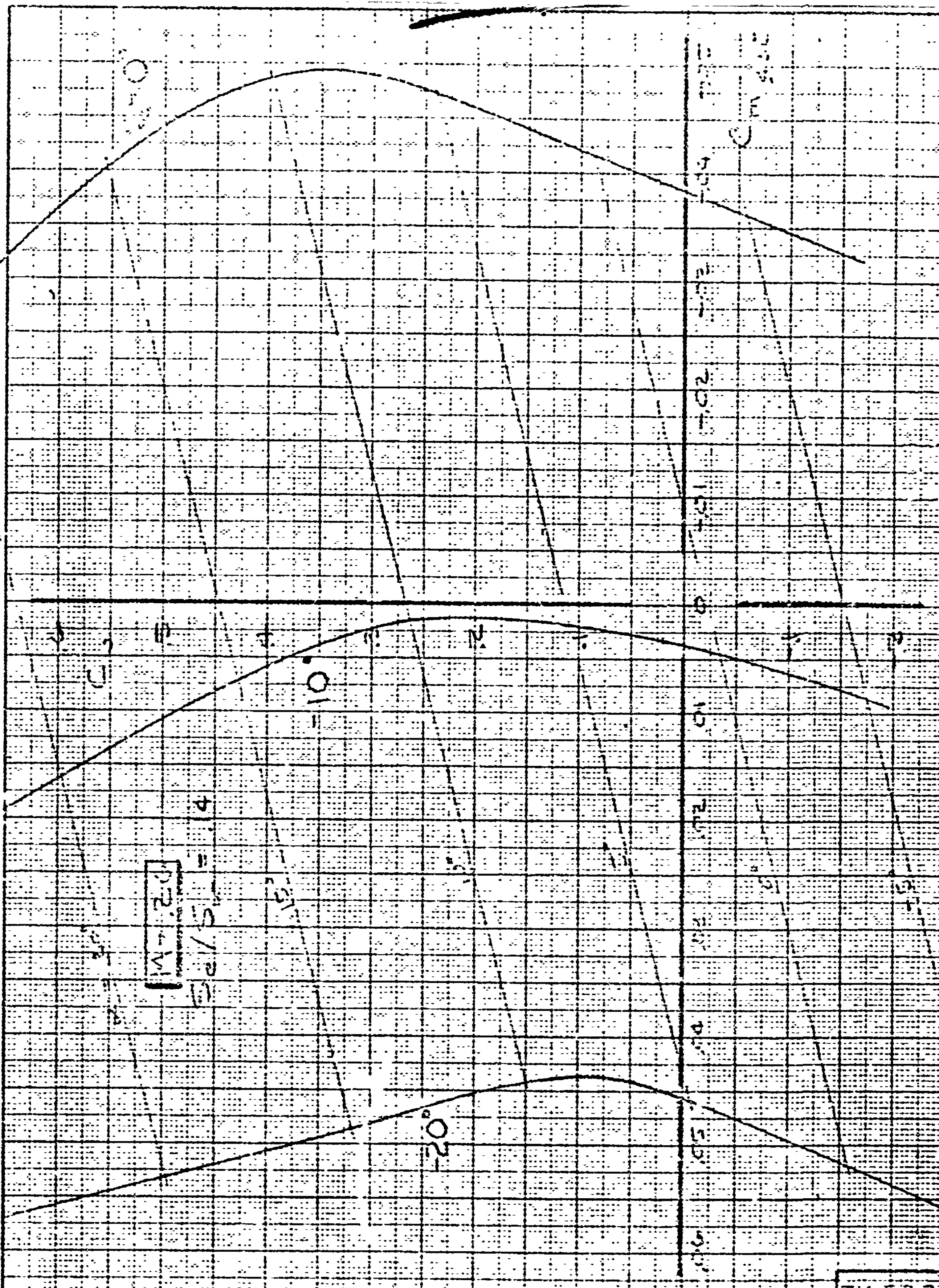

FIG 5.2.2

CALC	LCL	2-11-??	REVISED	DATE	LONGITUDINAL STABILITY WING TIPS RETRACTED M = .26	644-2035
CHECK						D2-8174
APR						
APR					BOEING AIRPLANE COMPANY **41**	PAGE 5.11

K-E

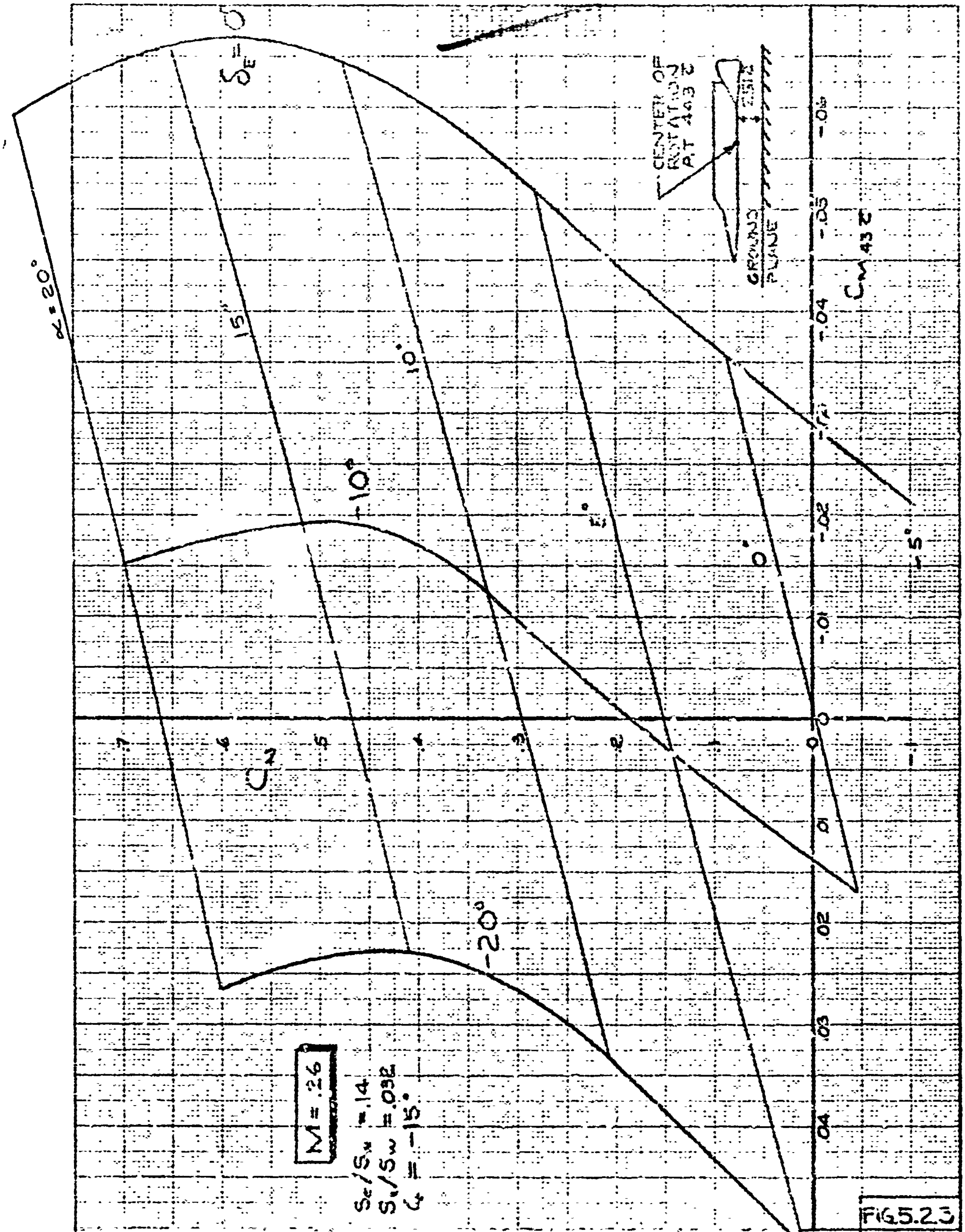

J.L. Francis 12/14/66

LONGITUDINAL STABILITY, WING TIPS & LANDING GEAR DOWN. IN PRESENCE OF GROUND PLANE

FIG 5.2.3
644-2035
D2-8174

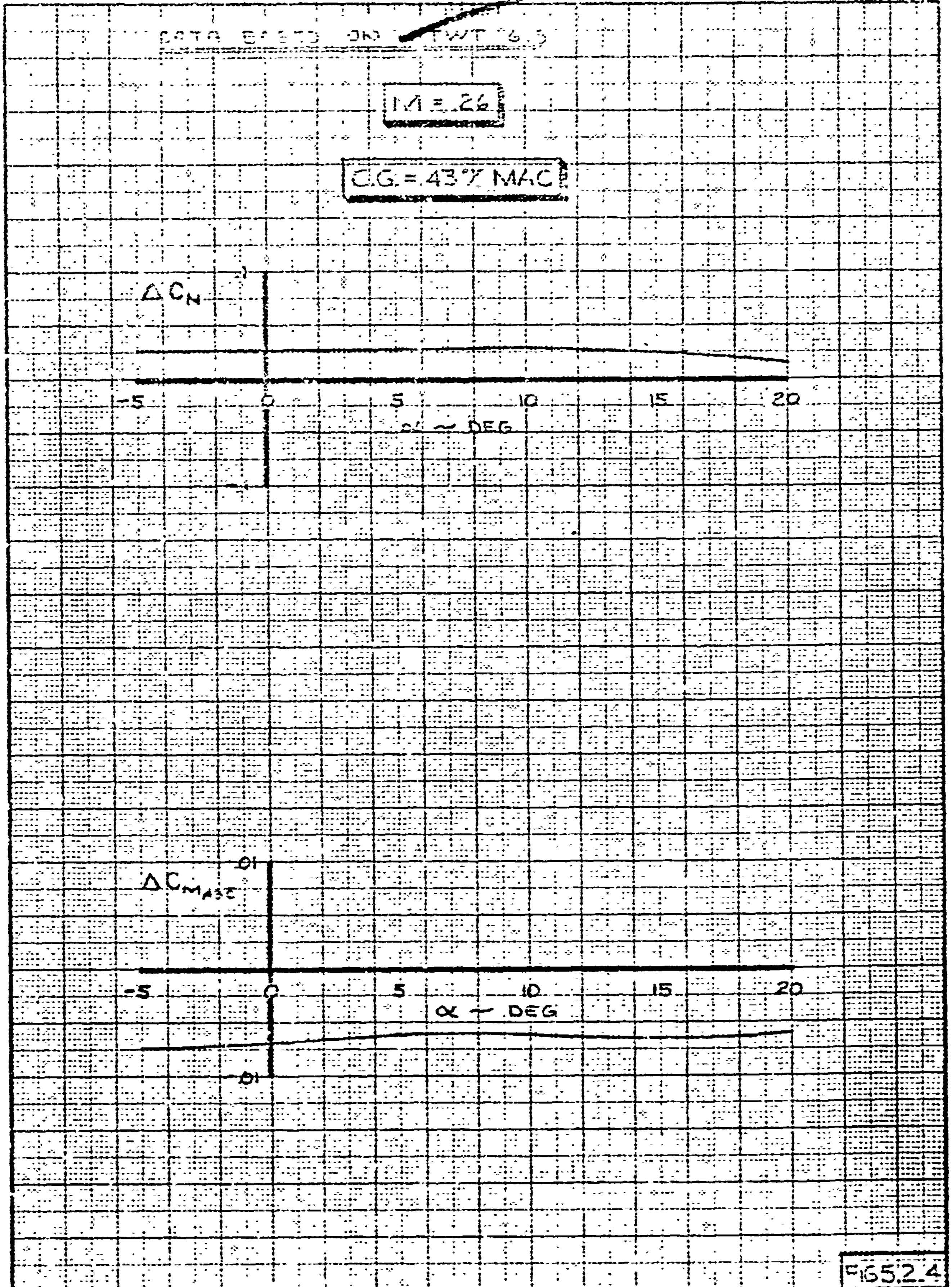

FIG 5.2.4

CALC	J.L. FRANCIS	12/19/60	REVISED	DATE	EFFECT OF LANDING GEAR
CHECK					
APR					
APR					BOEING AIRPLANE COMPANY

844-2035

D2-8174

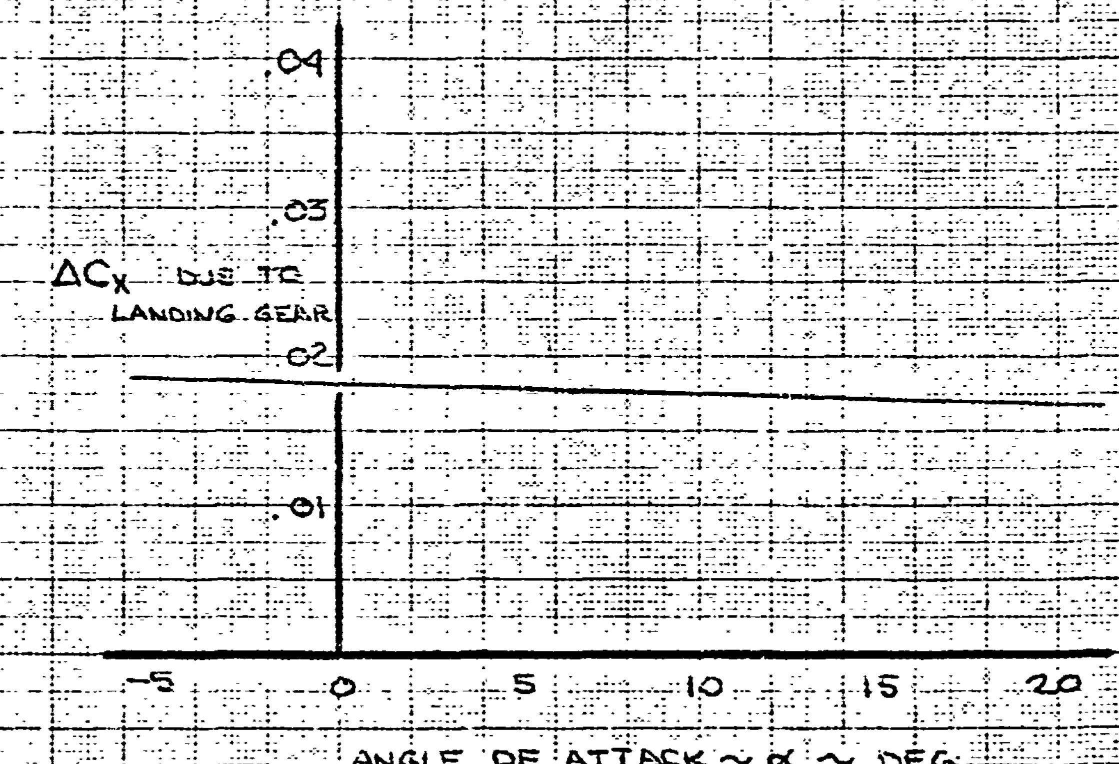

FIG. 5.2.5

EFFECT OF LANDING GEAR ON CHORD FORCE

M = .26

WEJ 12-27-6

844-2035

D2-8174

5.3 SUBSONIC - TRANSONIC SPEEDS

Basic stability and control effectiveness data are presented on Figures 5.3.1 through 5.3.10. Data are shown at Mach numbers of 0.5, 0.7, 0.9, 0.95, and 1.05 for both the wing tip extensions retracted and extended. The data are presented in this fashion and for the various Mach numbers due to the appreciable non-linearities of the aerodynamics. The data are based on results of wind tunnel tests in the Boeing Transonic Wind Tunnel and preliminary results of tests in the L.R.C. 16-Foot Transonic Wind Tunnel. Due to the preliminary nature of some of these data, some modification to the characteristics shown can be anticipated. The tunnel data were modified to the current configuration by empirical and theoretical analysis.

Data shown at M=0.7 show discontinuity with the other data as a function of Mach number as discussed in the summary. These trends of the M=0.7 data were corroborated to some degree by the two tunnel tests mentioned. Further testing will be done to define these data better.

Axial force data as function of angle of attack are shown on Figure 5.3.11 for the glider with wing tips extended and on Figure 5.3.12 for wing tips retracted. These data are for the glider in trimmed flight.

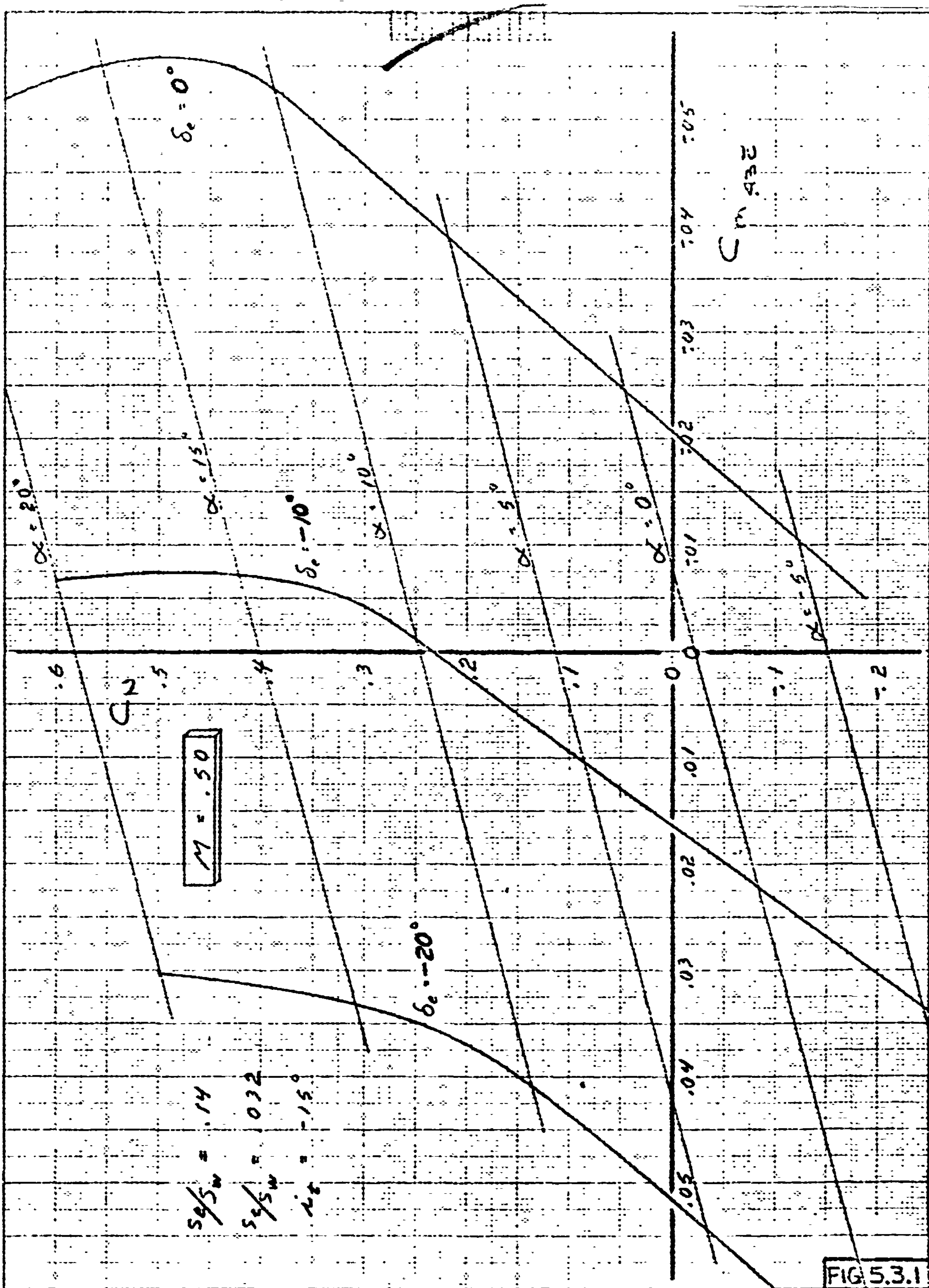

FIG 5.3.1

DCL. 12-9-60	LONGITUDINAL STABILITY WING TIPS EXTENDED M = .50	844-2035
CHECK		D2-8174
DWN. PW	BOEING AIRPLANE COMPANY	5.6

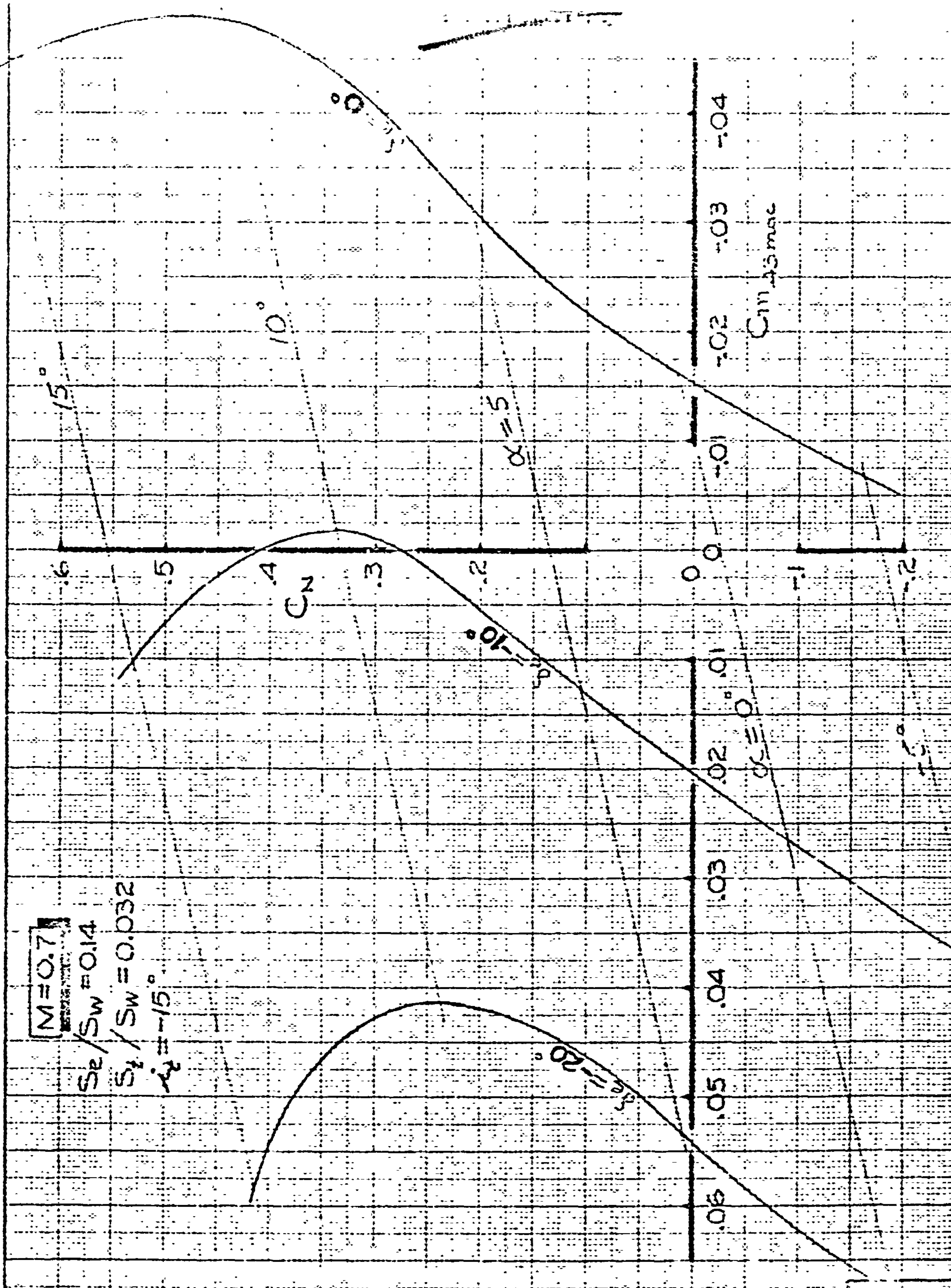

FIG 5.32

M. CARTER 12-12-60	LONGITUDINAL STABILITY WING TIPS EXTENDED M = 0.7		844-2035 D2-8174
	BOEING AIRPLANE COMPANY	47	PAGE 5.17

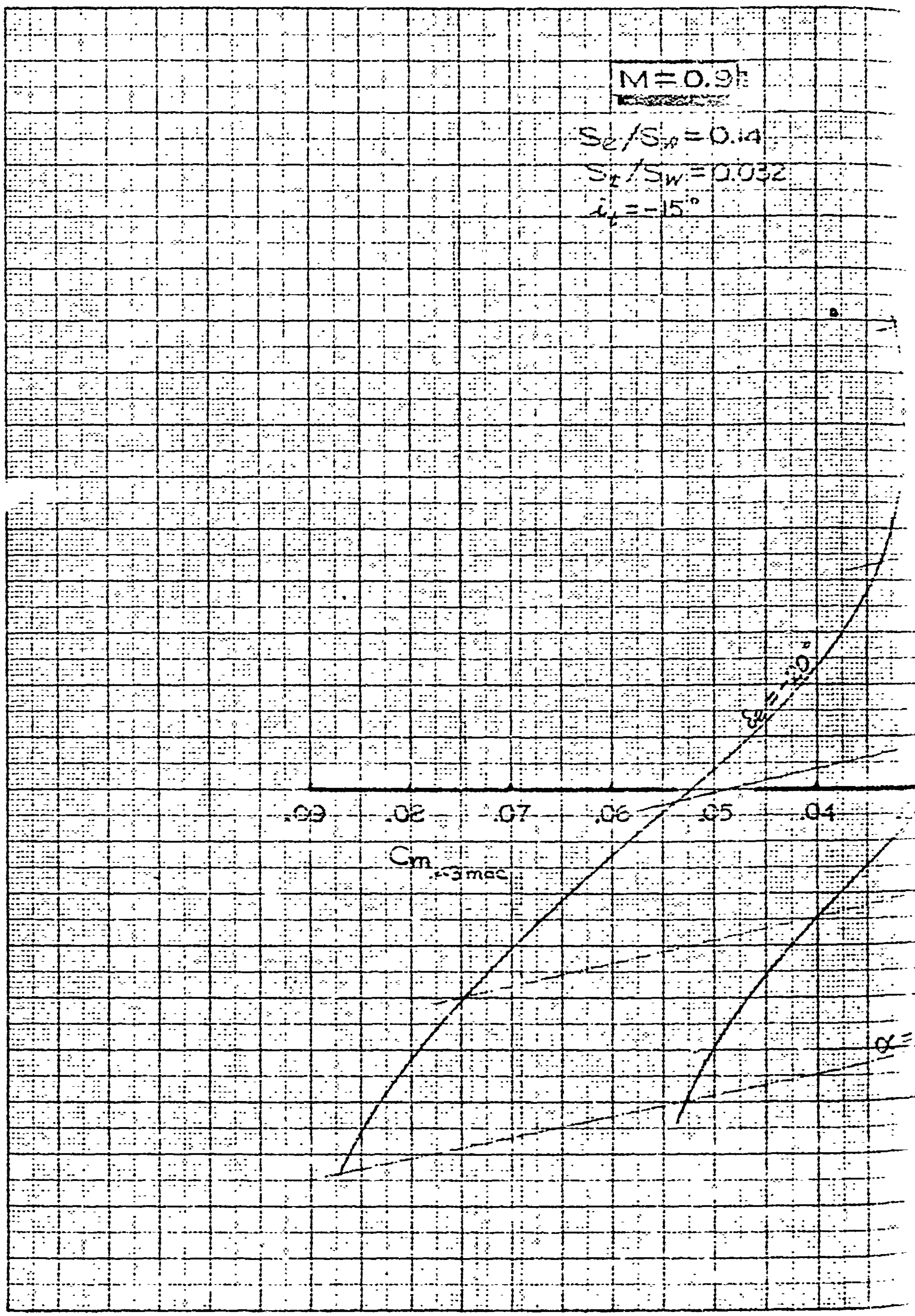
M = 0.9
Se/Sw = 0.14
St/Sw = 0.032
it = -15°
.09
.08
.07
.06
.05
.04
Cm

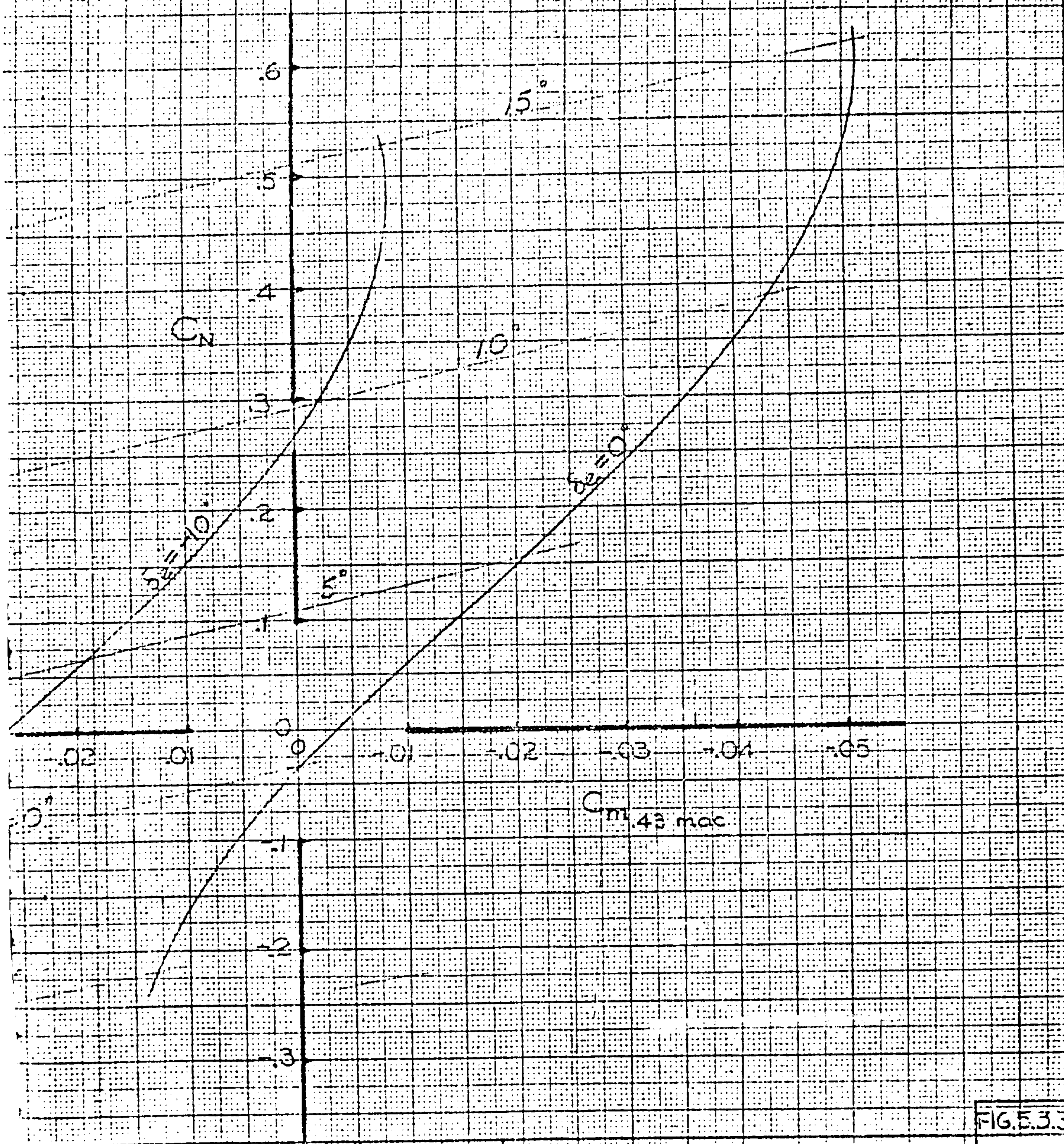

CALC	M. CARTER 12-12-60	REVISED	DATE	LONGITUDINAL STABILITY WING TIPS EXTENDED M=0.9	FIG. 5.3.3
CHECK					844-2035
APPD					D2-8174
APPD					PAGE 5.18

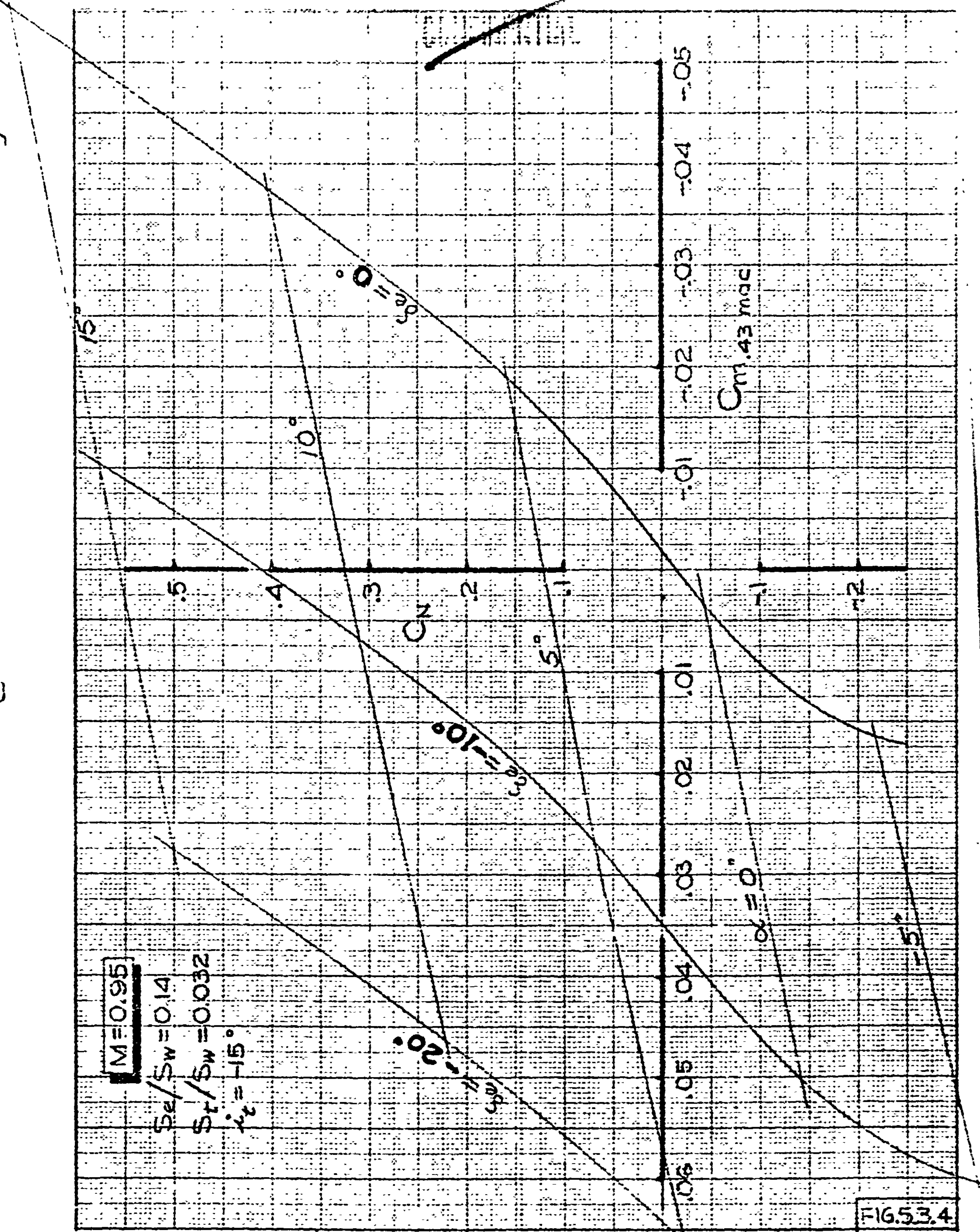

FIG 5.3.4

CALC M. CARTER 12-12-60	REVISED	DATE	LONGITUDINAL STABILITY WING TIPS EXTENDED M = .95
CHECK			
APR			
APR			BOEING AIRPLANE COMPANY 50

844-2035

D2-8174

PAGE 5.19

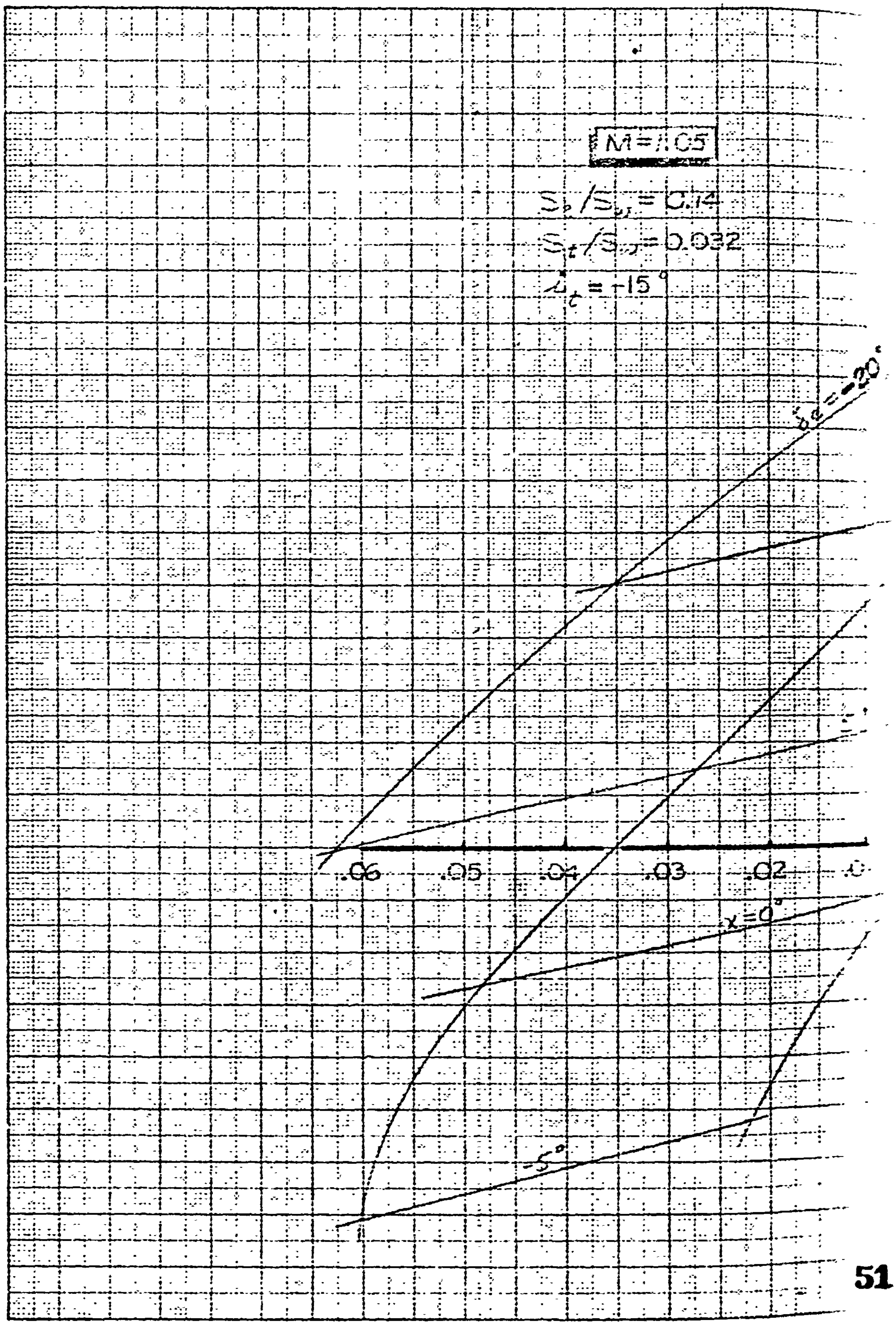

M = 1.05
S_b/S_w = 0.14
S_t/S_w = 0.032
i_t = -15°
δ_e = -20°
.06
.05
.04
.03
.02
x = 0°
-5°

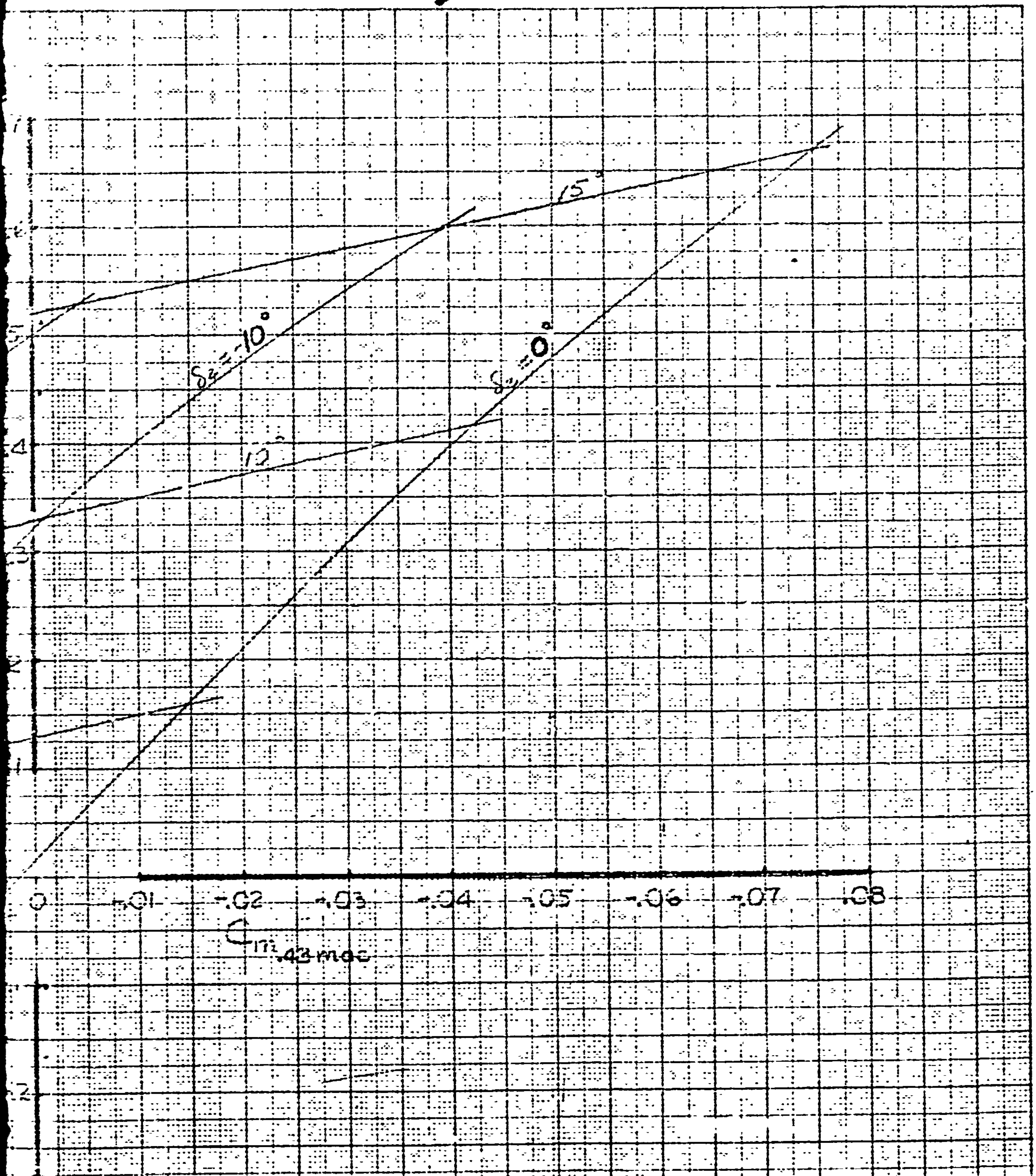

CALC	M. Cox	12-9-60	REVISED	DATE
CHECK				
APPD				
APPD				

LONGITUDINAL STABILITY
WING TIPS EXTENDED
M=1.05

FIG 535
844-2035
D2-8174
PAGE 52

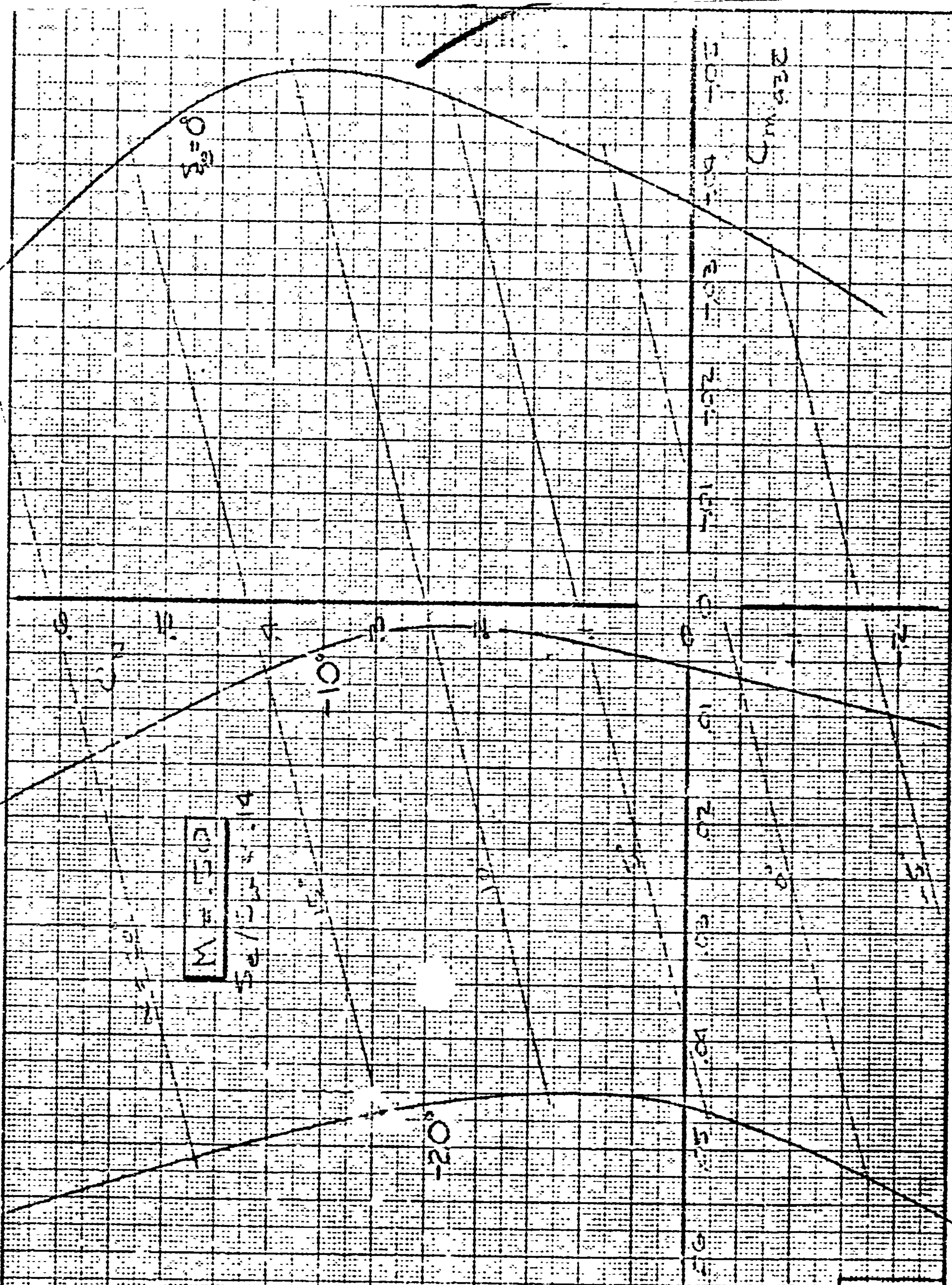

FIG. 53.6

CALC	DCL	12/9/0	REVISED	DATE
CHECK				
APR				
APR				

LONGITUDINAL STABILITY
WING TIPS RETRACTED
M = .5

BOEING AIRPLANE COMPANY

844-2035

D2-8174

53

PAGE 521

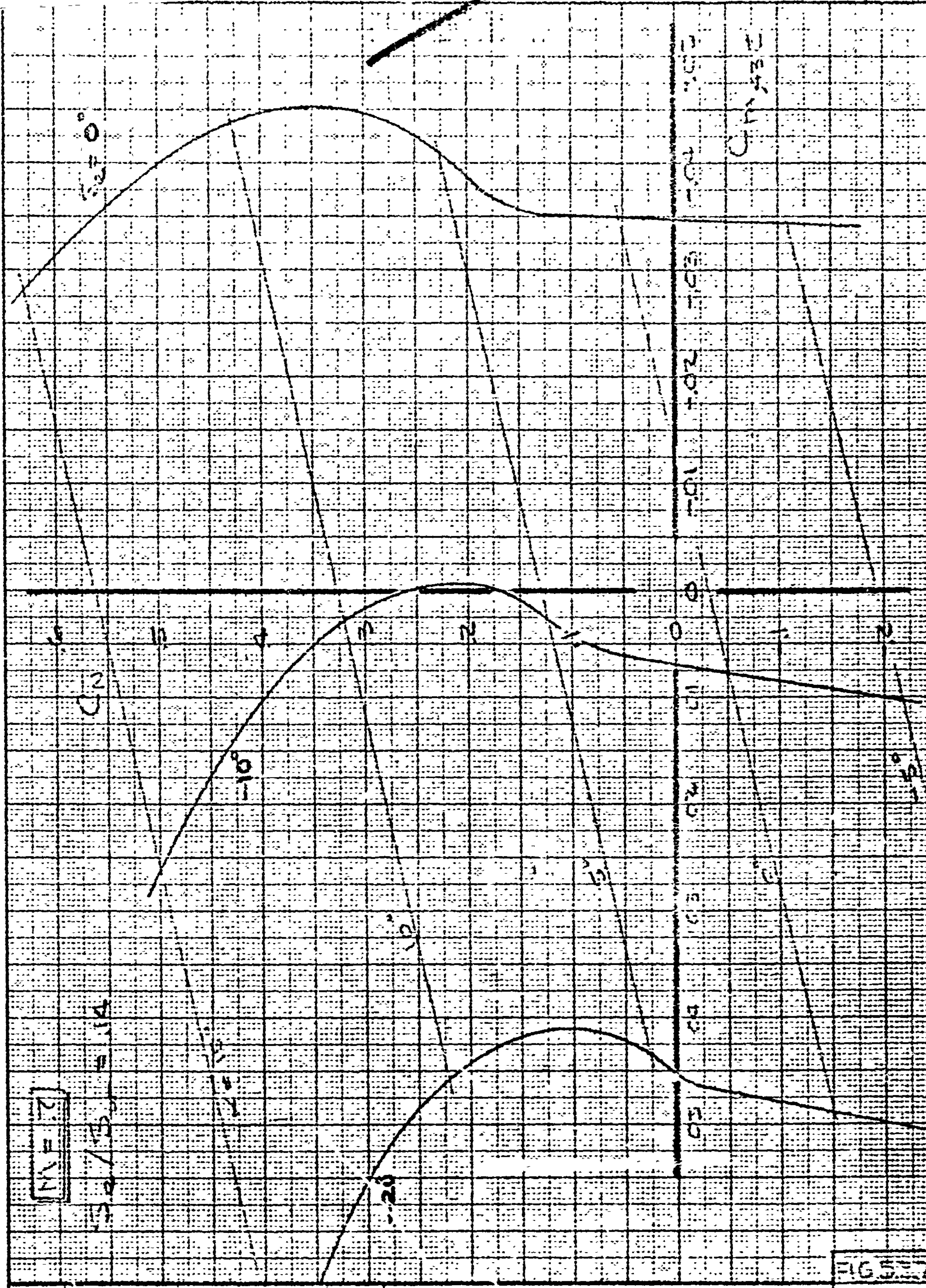

FIG 5.27

CALC	DCL	12/12/5?	REVISED	DATE
CHECK				
APR				
APR				

LONGITUDINAL STABILITY
WING TIPS RETRACTED
M = .7

BOEING AIRPLANE COMPANY

844-2035

D2-8174

PAGE 5.22

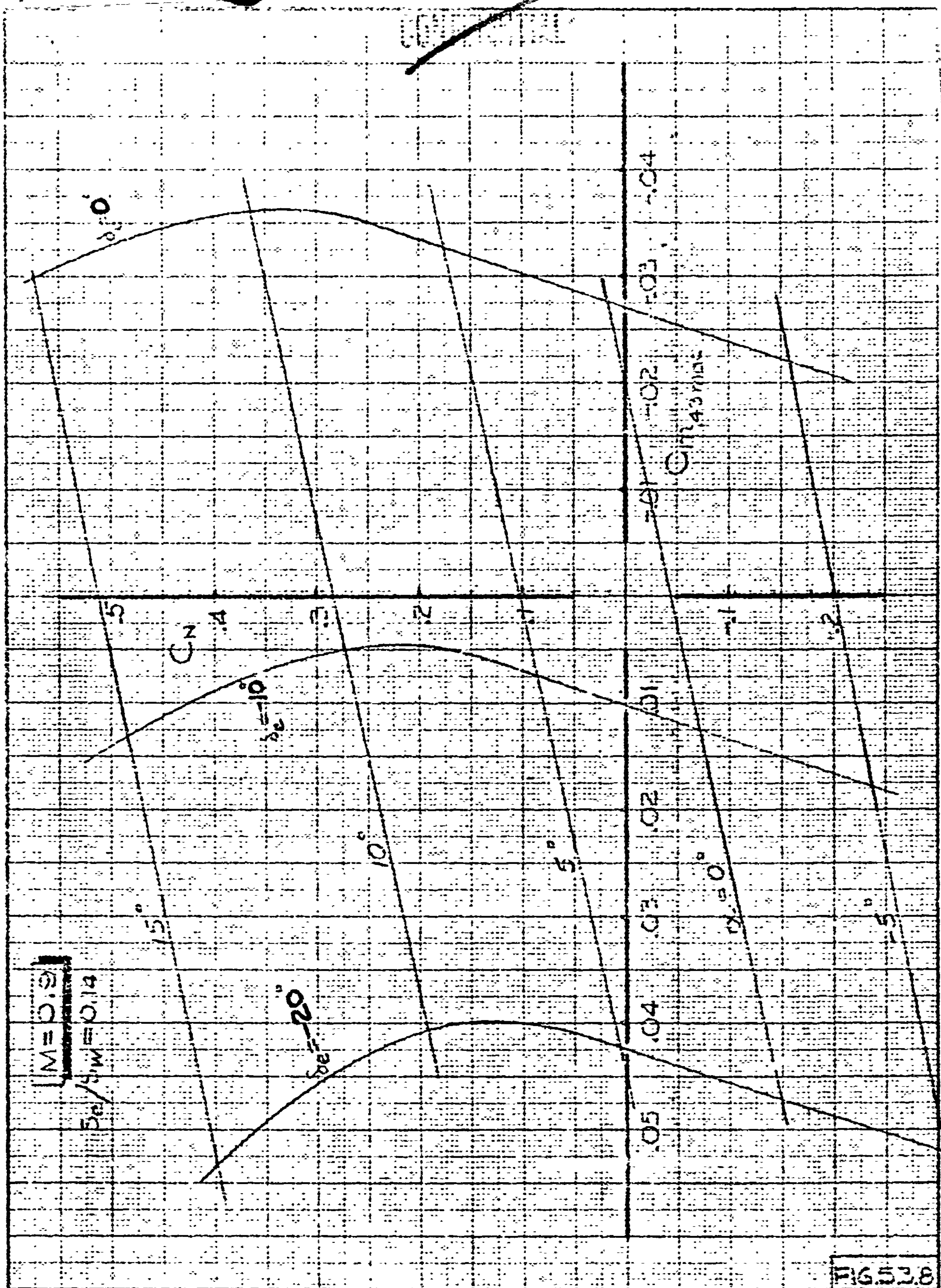

CA M. CARTER 12-7-60	LONGITUDINAL STABILITY WING TIPS RETRACTED, M=.9	844-2035 D2-8174
CHECK	BOEING AIRPLANE COMPANY	
APR	55	PAGE 5.23

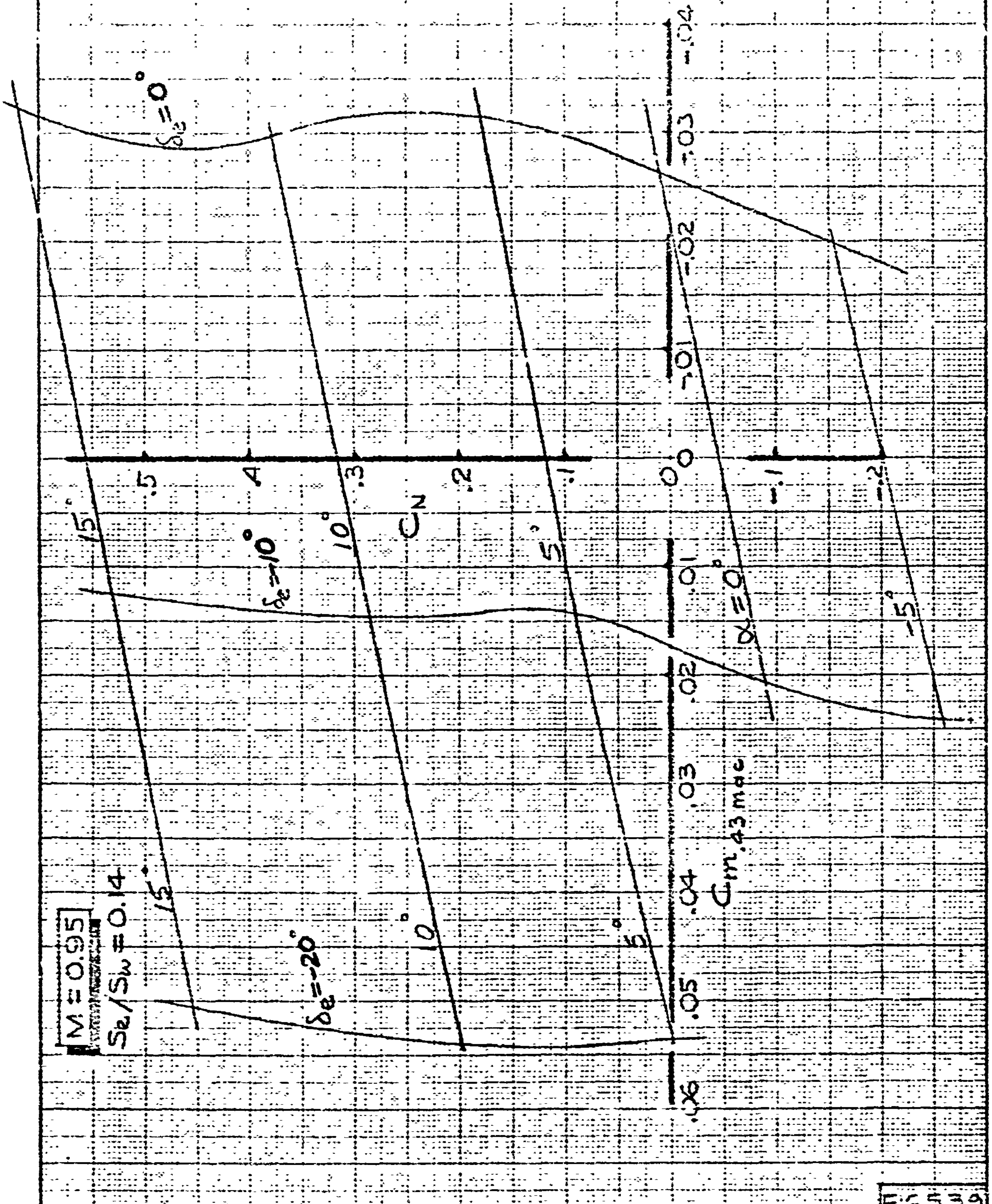

FIG 5.39

M. CARTER 12-9-60	LONGITUDINAL STABILITY		644-2035
	WING TIPS RETRACTED, M=.95		D2-6174
	BOEING AIRPLANE COMPANY	56	PAGE 5.24

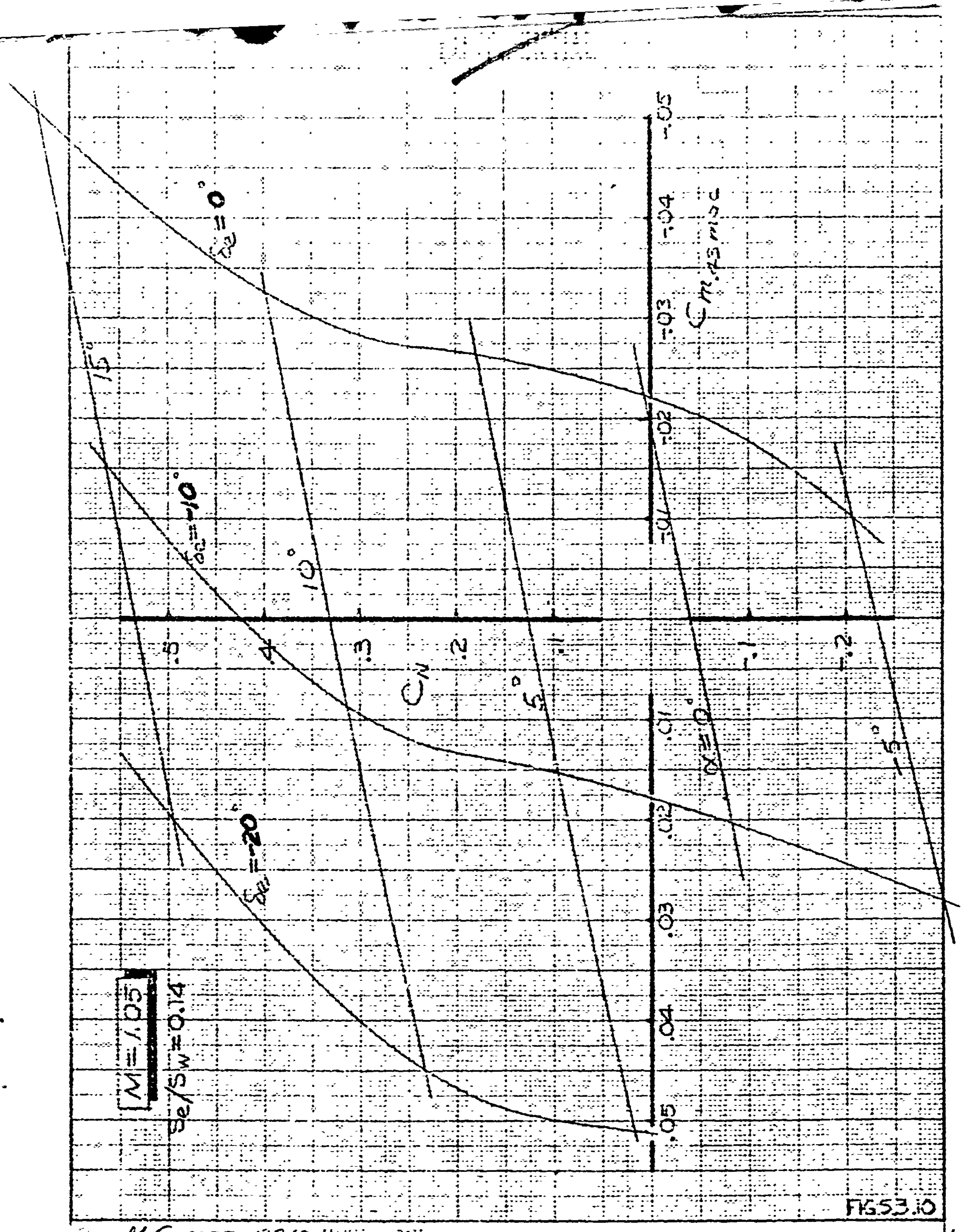

FIG 5.3.10

CALC M. CARTER 12-9-60	LONGITUDINAL STABILITY WING TIPS RETRACTED, M=1.05	844-2035
CHECK		D2-8174
APP	BOEING AIRPLANE COMPANY	PAGE 5.25

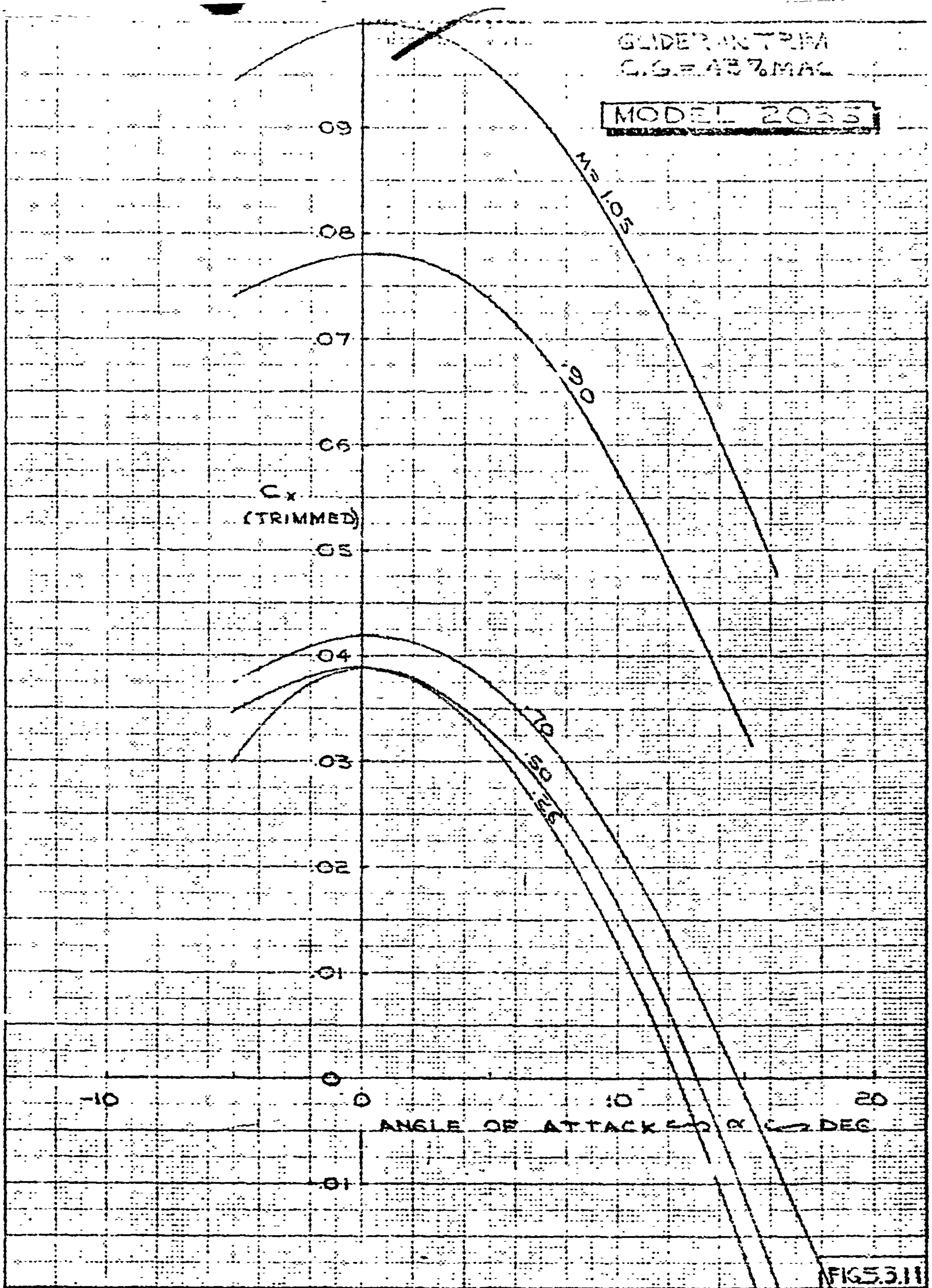

FIG.5.3.11

DEZ 12/22/60

CHORD FORCE COEFFICIENT
WING TIPS EXTENDED

844-2035

D2-8174

BOEING AIRPLANE COMPANY

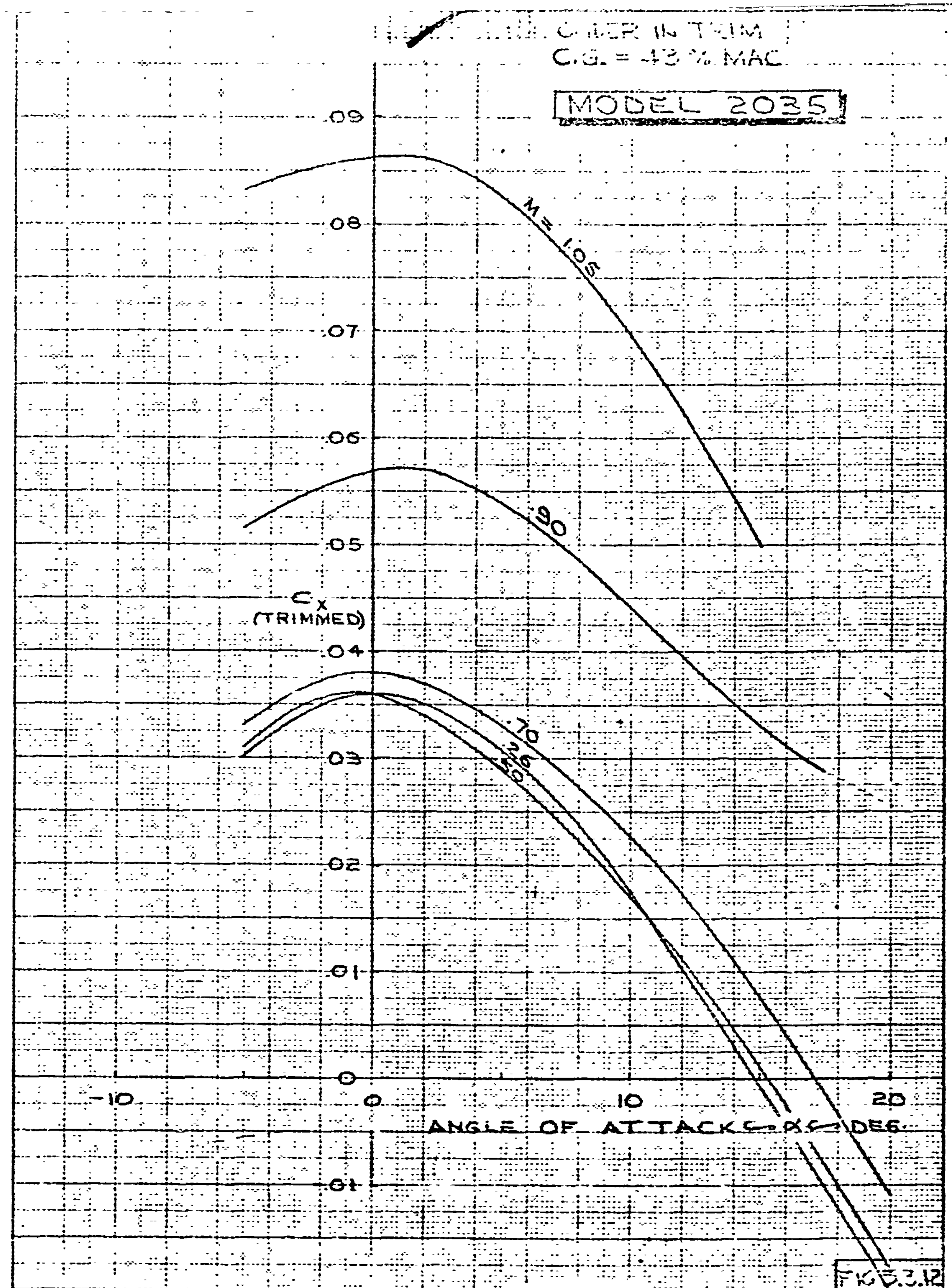

FIG 5.3.12

DEZ 12/22/60

CHORD FORCE COEFFICIENT
WING TIPS RETRACTED

644-2035
D2-8174

BOEING AIRPLANE COMPANY

5.4 SUPERSONIC

Longitudinal stability and control characteristics at supersonic speeds for Mach numbers of 1.6, 2.0 and 3.5 are shown for wing tip extensions retracted, Figures 5.4.4 through 5.4.6 and for wing tip extensions extended, Figures 5.4.1 through 5.4.3. These curves were derived from wind tunnel tests performed in the Boeing Supersonic Wind Tunnel. The 814-1058 glider configuration was tested with variations in model components to give parametric data. The parametric data were corrected by theoretical methods to obtain predictions of pitch characteristics on the 844-2035 configuration.

Chord force coefficient data for the glider in trim and with wing tips extended are shown on Figure 5.4.7. Data with the tip extensions retracted are shown on Figure 5.4.8.

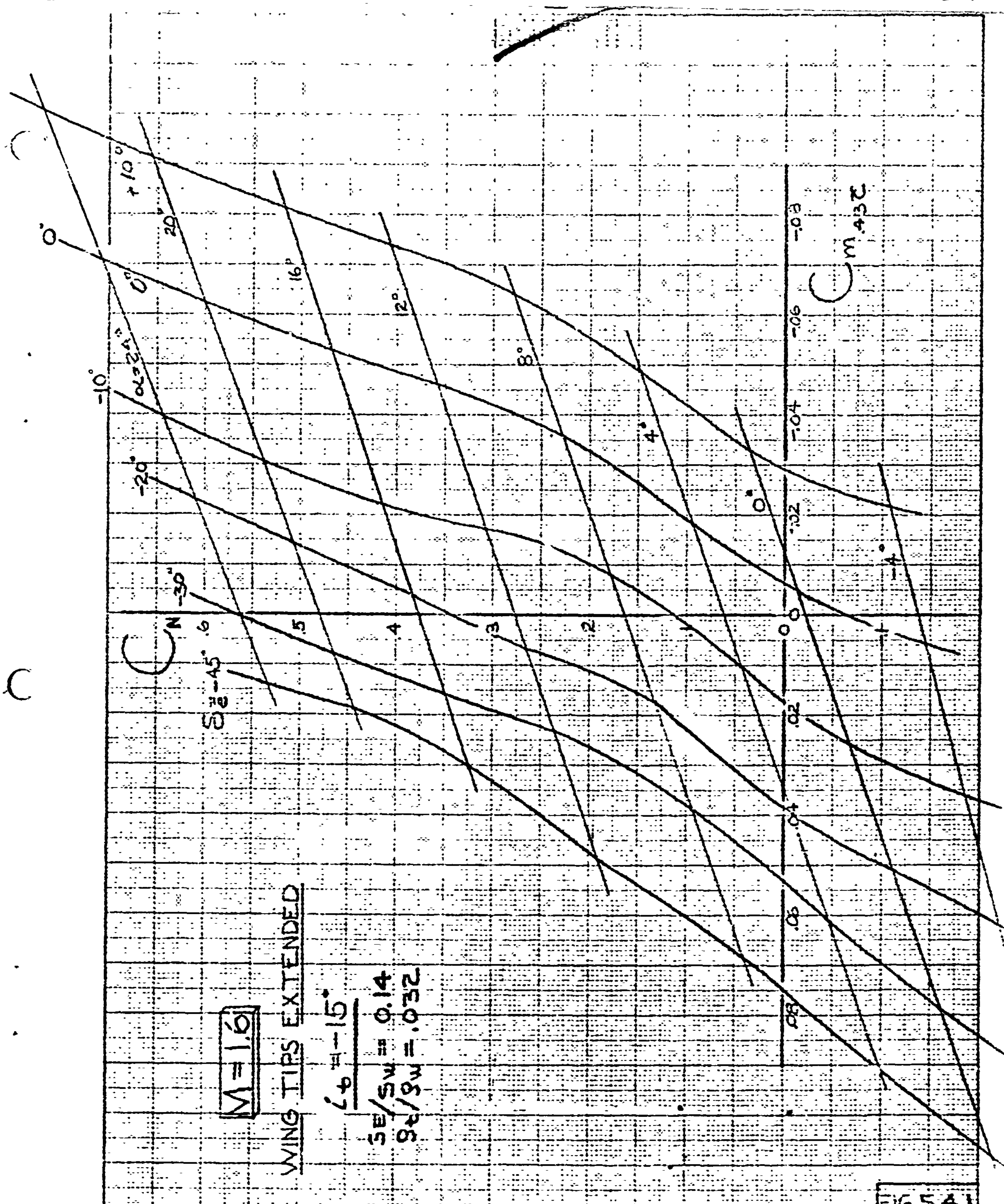

FIG. 5.4.1

DJR 12-8-61

LONGITUDINAL STABILITY
WING TIPS EXTENDED M=1.6

844-2035

D2-8174

BOEING AIRPLANE COMPANY

61

PAGE 5.29

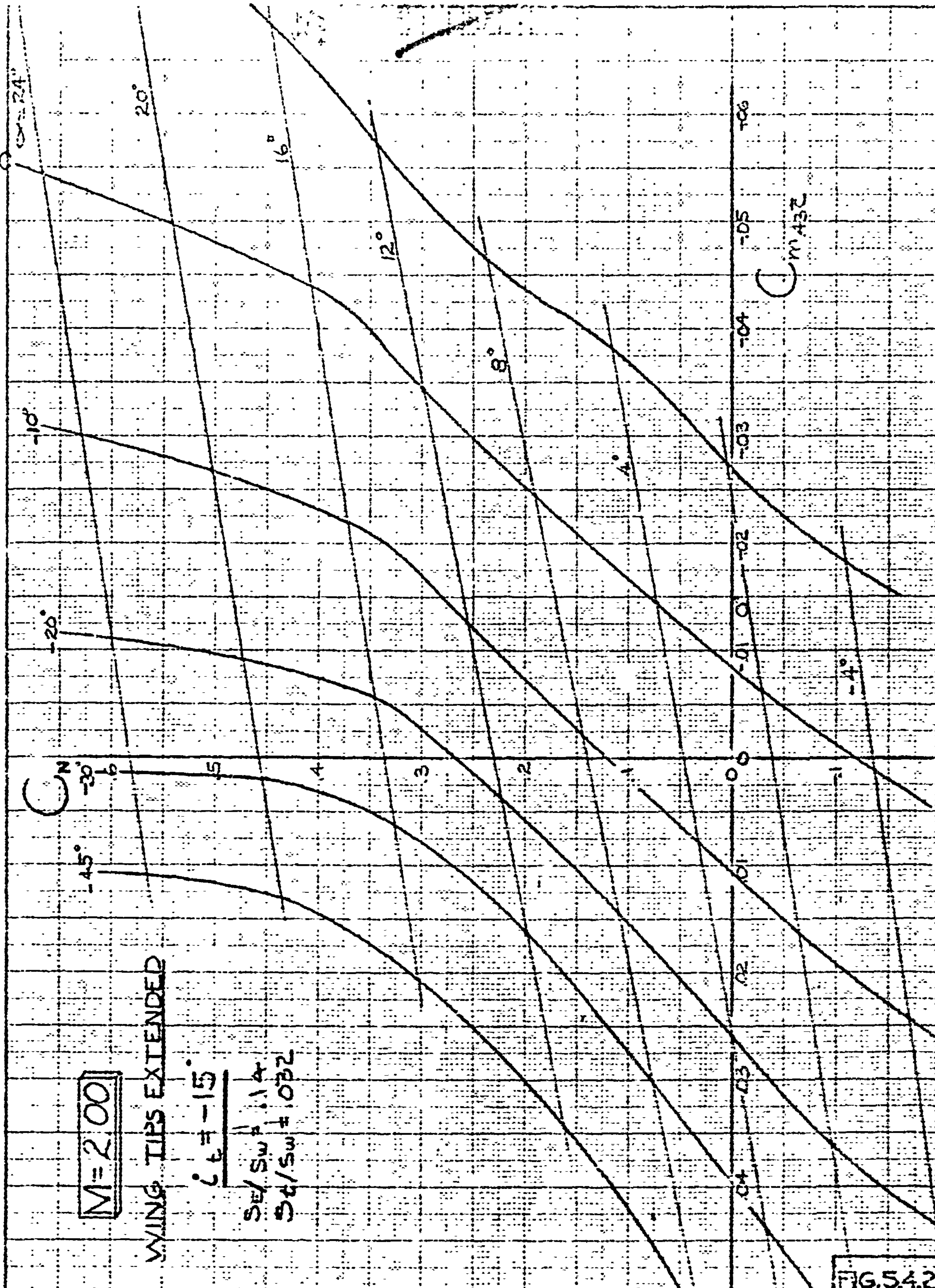

FIG. 5.4.2

DJR	12-7-0	LONGITUDINAL STABILITY WING TIPS EXTENDED M=2.0	844-2035
CHECK			D2-8174
APR		BOEING AIRPLANE COMPANY	62 PAGE 5.30
APR			

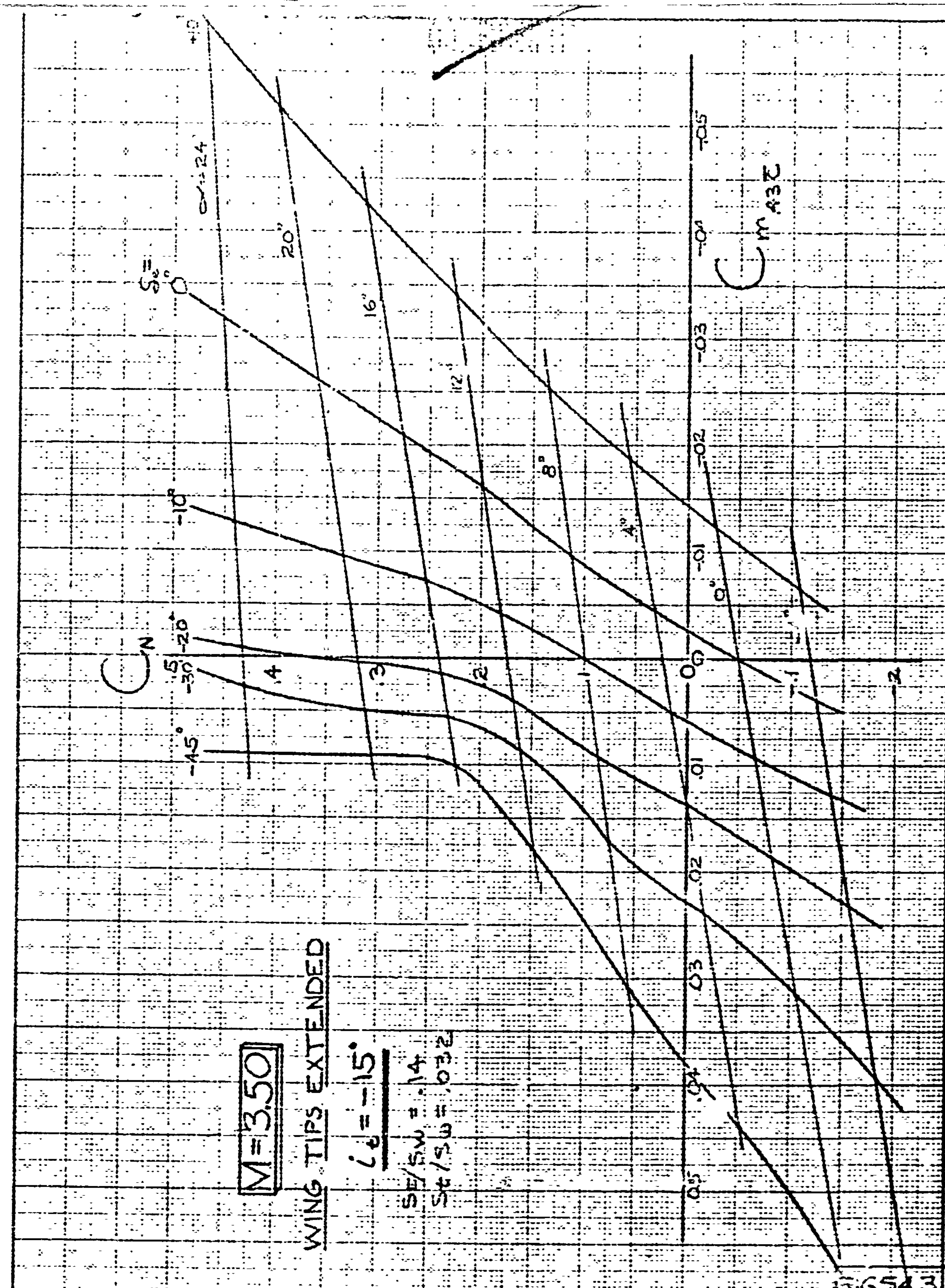

FIG 5.4.3

DJR	R-7-0	REVISED	DATE	LONGITUDINAL STABILITY WING TIPS EXTENDED M=3.5	844-2035
CHECK					D2-8114
APP				BOEING AIRPLANE COMPANY 63	PAGE 5.31
APR					

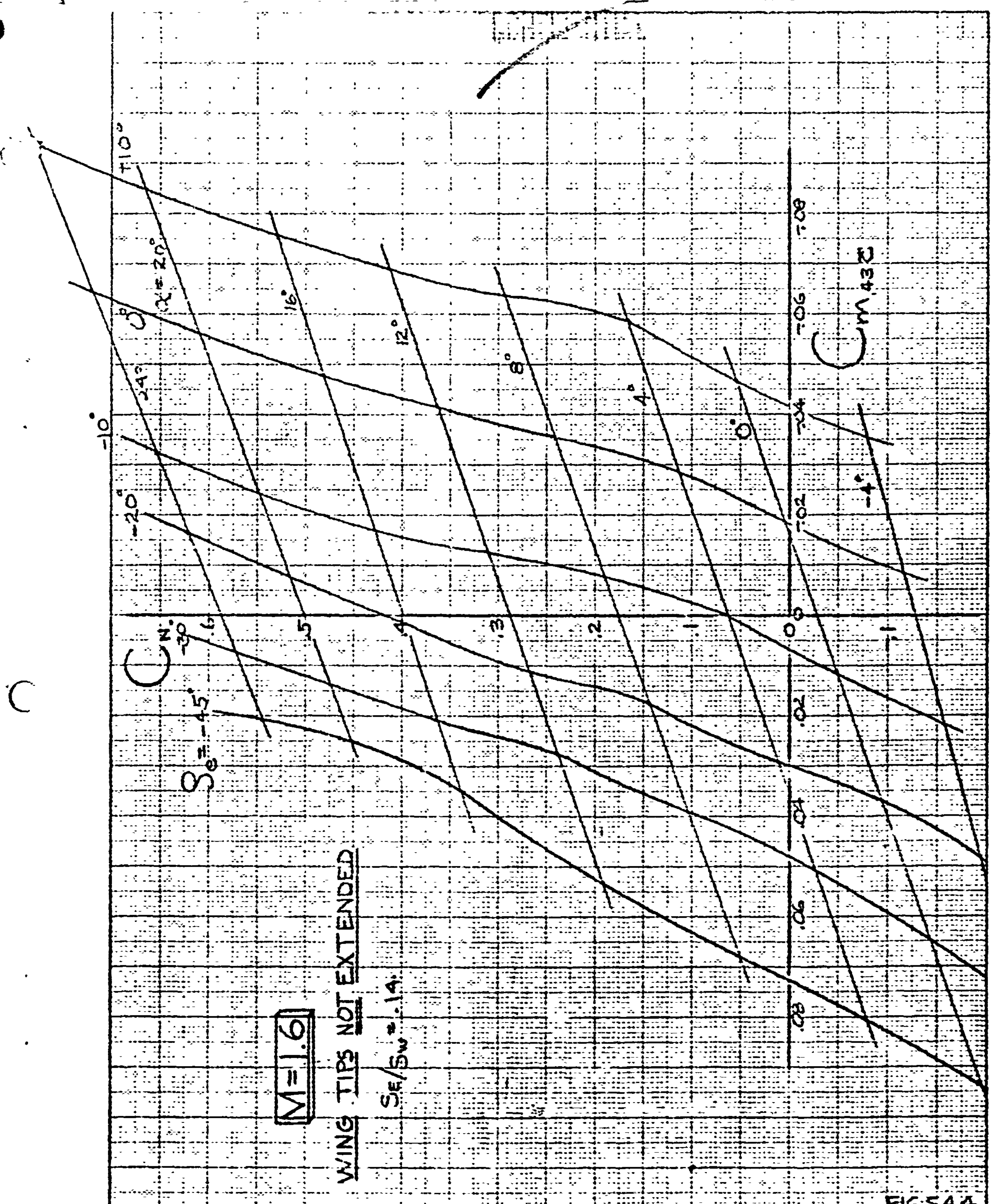

FIG. 5.4.4

DJR	12-2-01	REVISED	DATE	
CHECK				LONGITUDINAL STABILITY WING TIPS RETRACTED M=1.6
APR				844-2035
APR				D2-8174

BOEING AIRPLANE COMPANY 64 PAGE 5.32

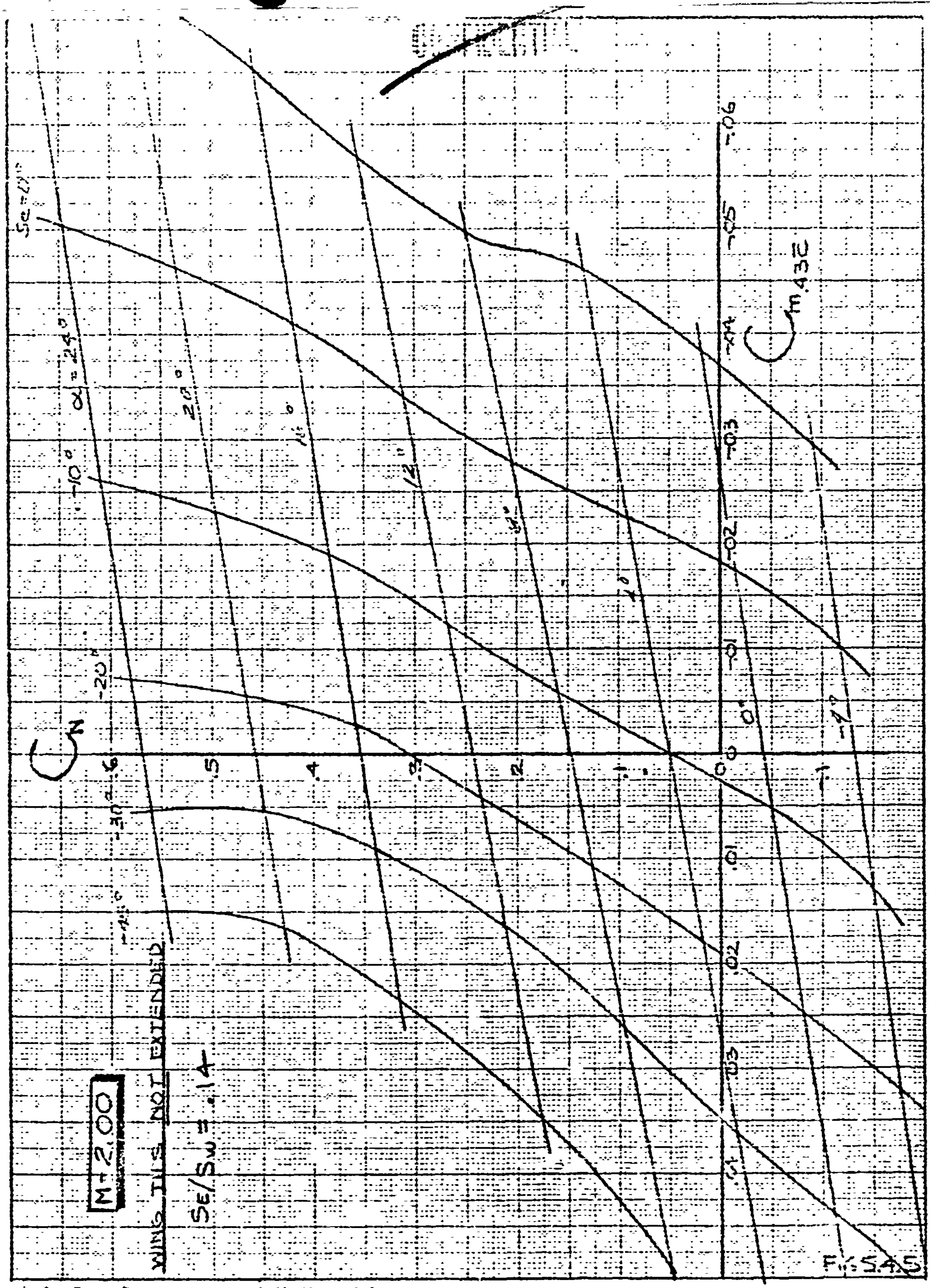

CALC R.K.R. 12-2-60	REVISED	DATE	844-2035
CHECK			LONGITUDINAL STABILITY WING TIPS RETRACTED M=2.0
APR			D2-8174
APR			BOEING AIRPLANE COMPANY 65 PAGE 5.33

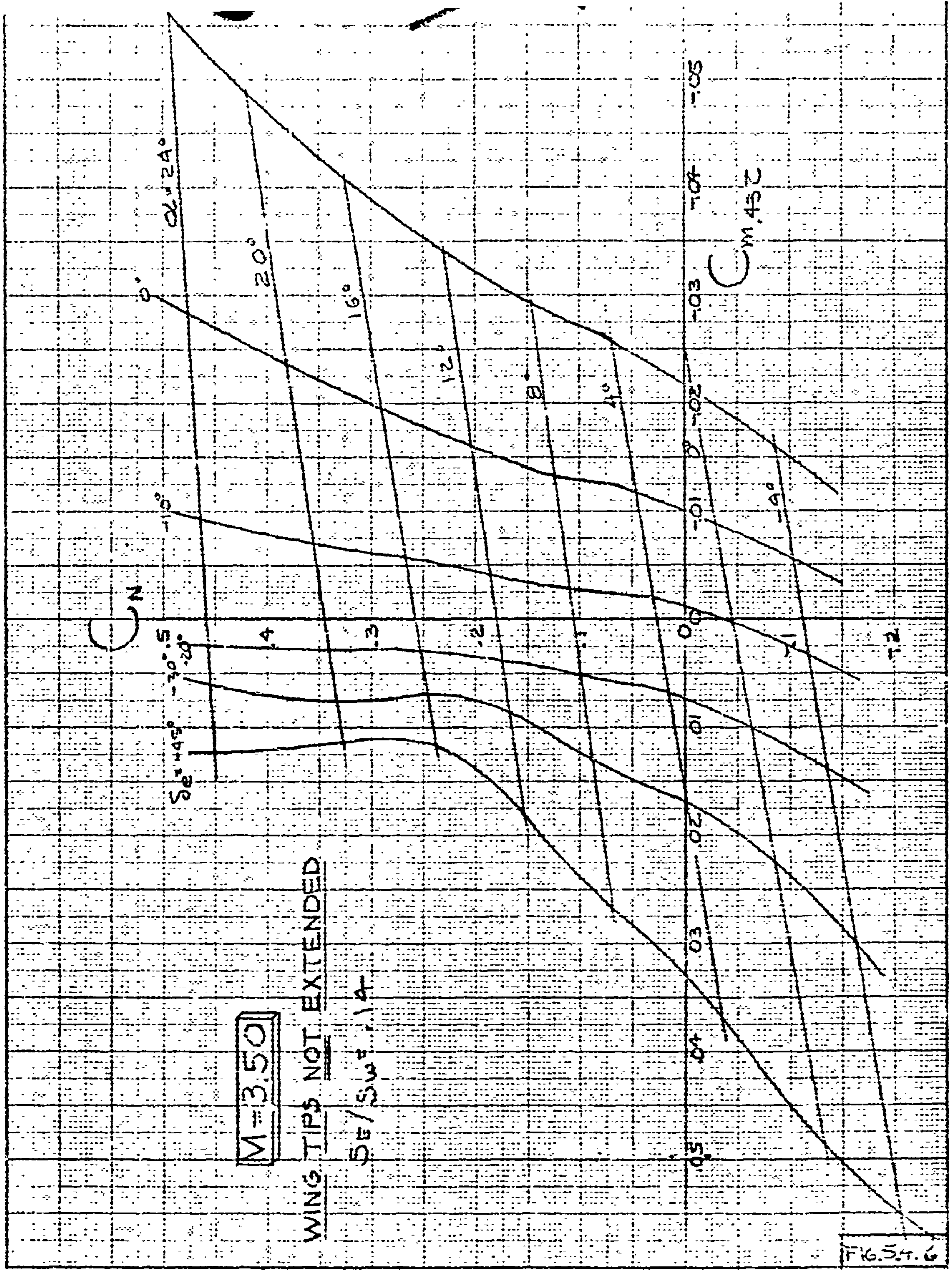

DJR 12-2-0 | REVISED | DATE

CHECK

APP

APP

LONGITUDINAL STABILITY

WING TIPS RETRACTED M=3.5

844-2035

D2-8174

BOEING AIRPLANE COMPANY **66**

PAGE 5.34

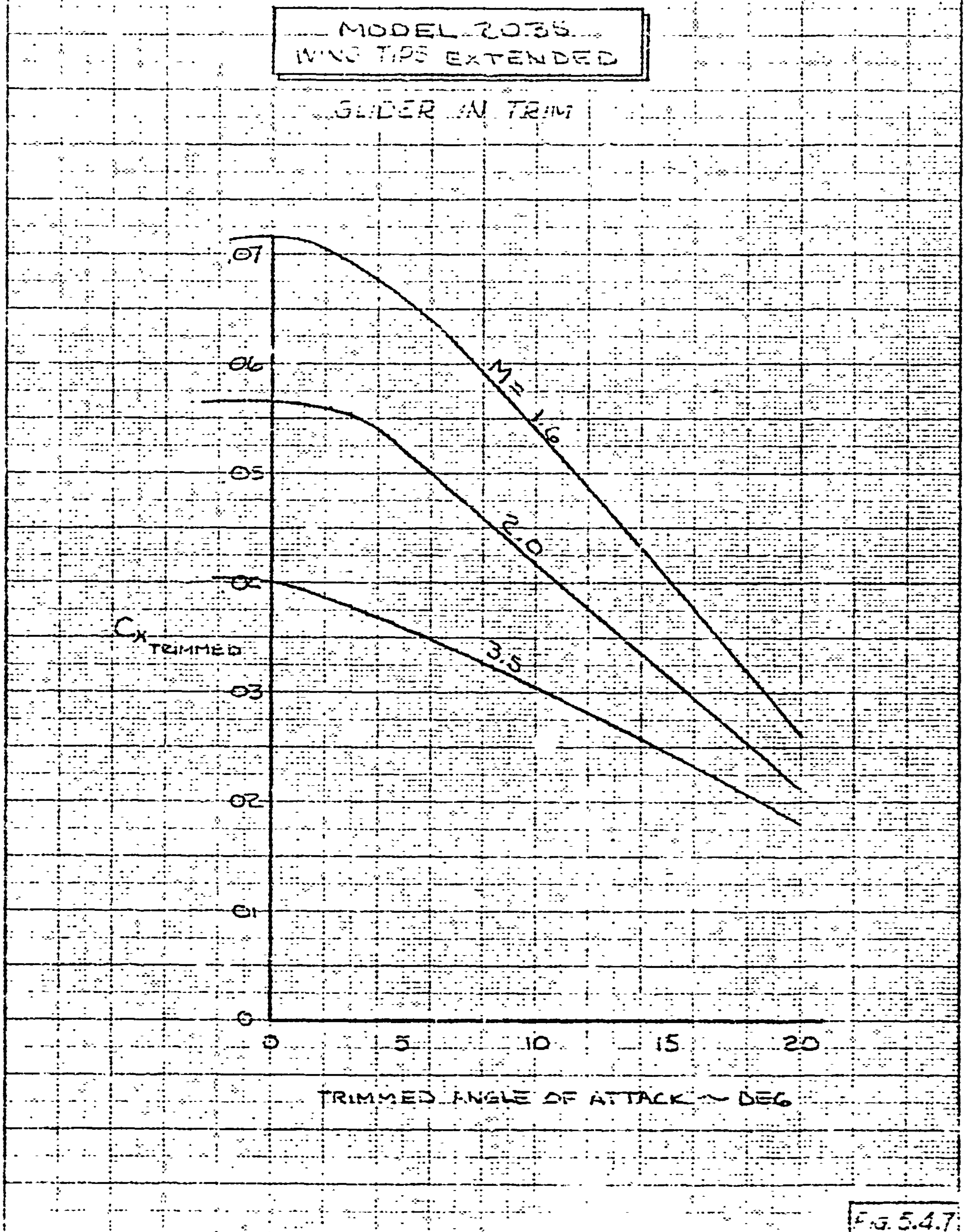

Fig. 5.4.7

WEJ 12/22/60

SUPERSONIC CHORD FORCE COEFFICIENT
WING TIPS EXTENDED

D2-6174

BOEING AIRPLANE COMPANY

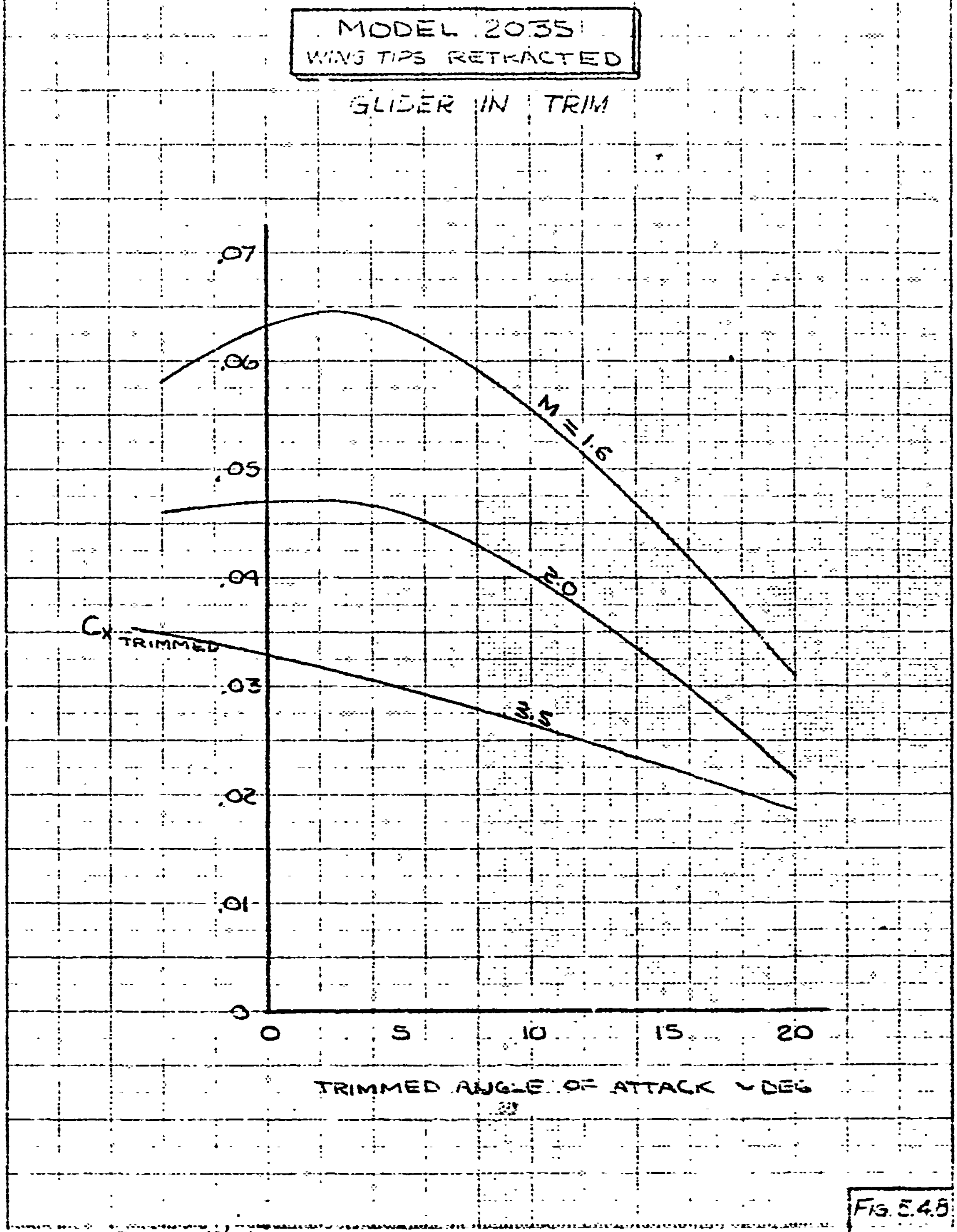

FIG. 5.4.8

WEJ 12/22/60

SUPERSONIC CHORD FORCE COEFFICIENT
WING TIPS RETRACTED

644-2035

D2-8174

5.5 HYPERSONIC SPEEDS

Longitudinal stability and control characteristics for the 744-2035 glider configuration are shown on Figures 5.5.1 through 5.5.3. Data are shown on Figure 5.5.1 for a Mach number of 8 and the cold shape glider. This assumes the glider to have the manufactured, or jig shape, configuration. Data are shown on Figures 5.5.2 and 5.5.3 at a Mach number of 8.0 and 22.0 for the "hot shape" glider. This assumes that the glider has assumed its maximum structural deformation due to thermal effects.

The data presented are based on wind tunnel tests in the following facilities:

1) A.E.D.C. Tunnel B, M=8.08

2) J.P.L. 21-Inch Hypersonic Tunnel, M=9.5

3) L.R.C. 11-Inch Hypersonic Tunnel, M=9.6

4) Boeing 44-Inch Hotshot Tunnel, M=16 and 22

These data were corrected to the present configuration by theoretical methods (Modified Newtonian Flow Theory and Shock Expansion Theory, particularly for elevon effectiveness). The incremental effect of the "hot shape" glider was determined by Modified Newtonian Flow Theory.

The effect of altitude or Reynolds number change at a constant Mach number is not included. Work is currently in progress in this area. Some variation of characteristics between M=8 and 22 can also be anticipated. Wind tunnel tests are currently in progress to define this variation.

Chord force data as a function of angle of attack for Mach numbers of 8 and 22 are presented on Figure 5.5.4. These data are for the glider trimmed at the various angles of attack.

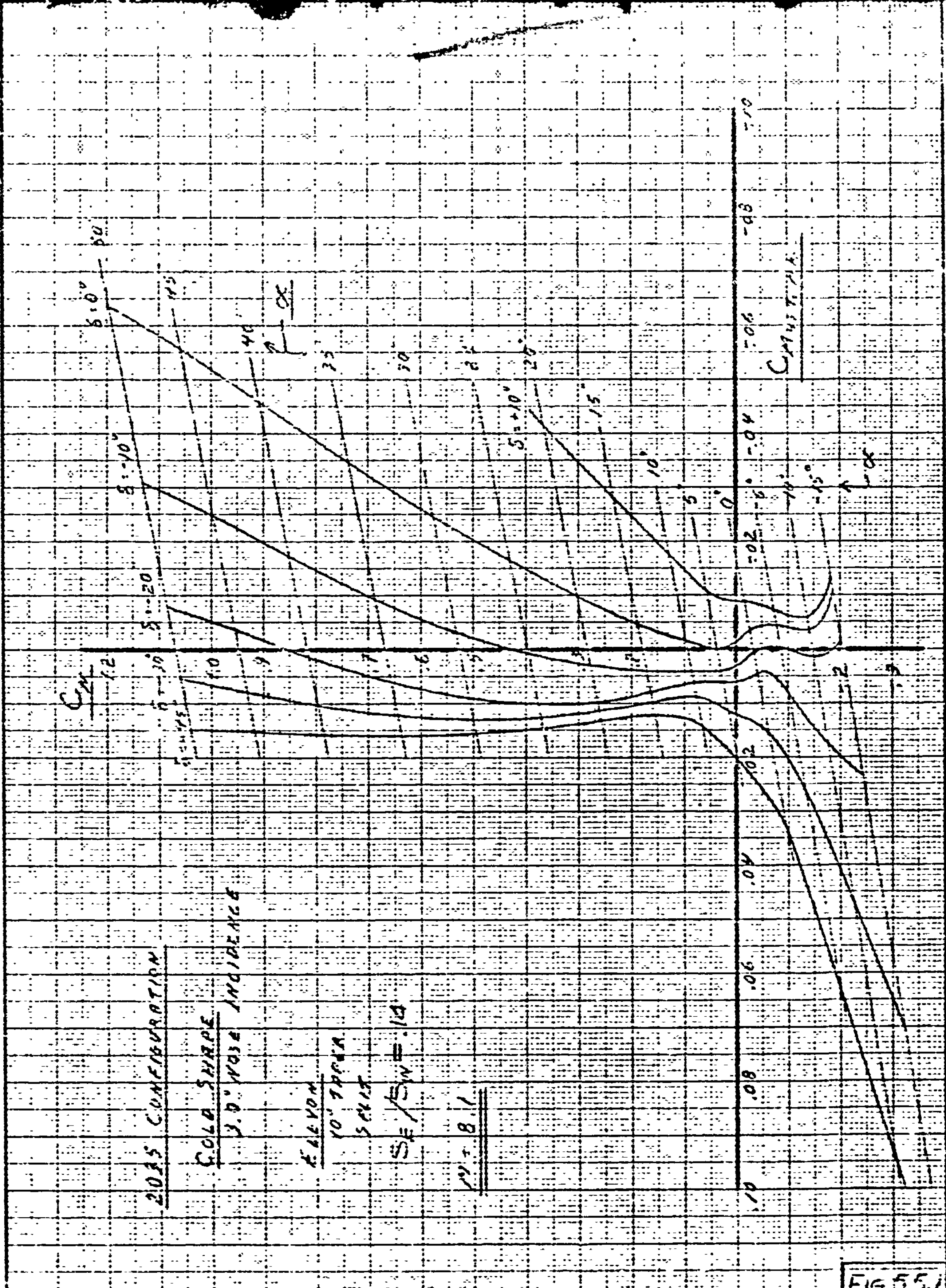

FIG. 5.5.1

CALC	PW	12-2-60	REVISED	DATE	LONGITUDINAL STABILITY COLD SHAPE M = 8.1
CHECK					
APR					
APR					

70

BOEING AIRPLANE COMPANY
SEATTLE 24, WASHINGTON

844-2035

D2-8174

SAC 461 C-R4

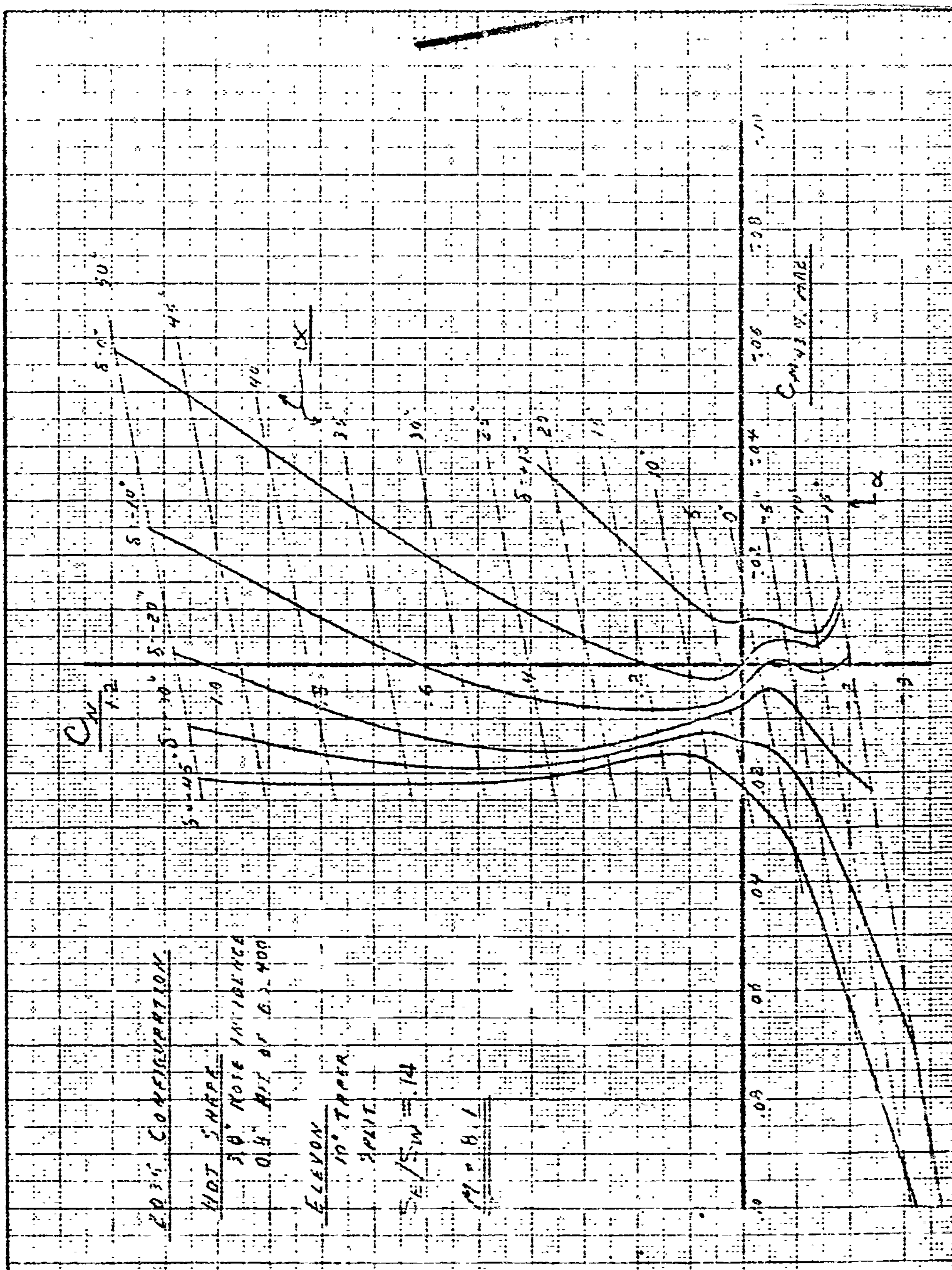

Fig 5.5.2

CALC	PW	12-?-60	REVISED	DATE	LONGITUDINAL STABILITY HOT SHAPE M = 8.1
CHECK					
APR					
APR					BOEING AIRPLANE COMPANY SEATTLE 24, WASHINGTON

71

844-2035

D2-8174

PAGE 5.39

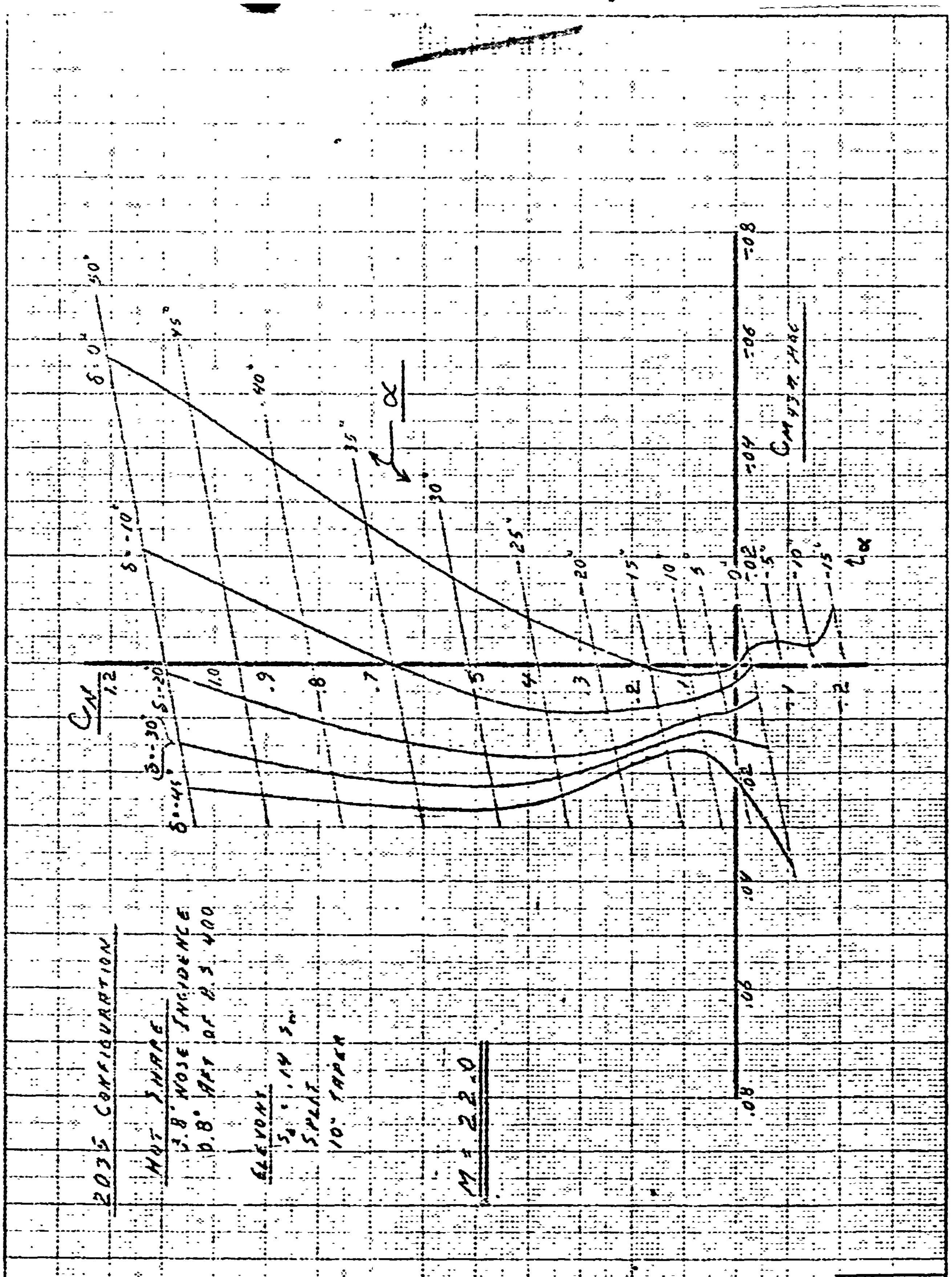

Fig. 5.5.3

AW 12-5-60

LONGITUDINAL STABILITY
HOT SHAPE
M = 22.0

72

844-2035

D2-8174

BOEING AIRPLANE COMPANY

PAGE 540

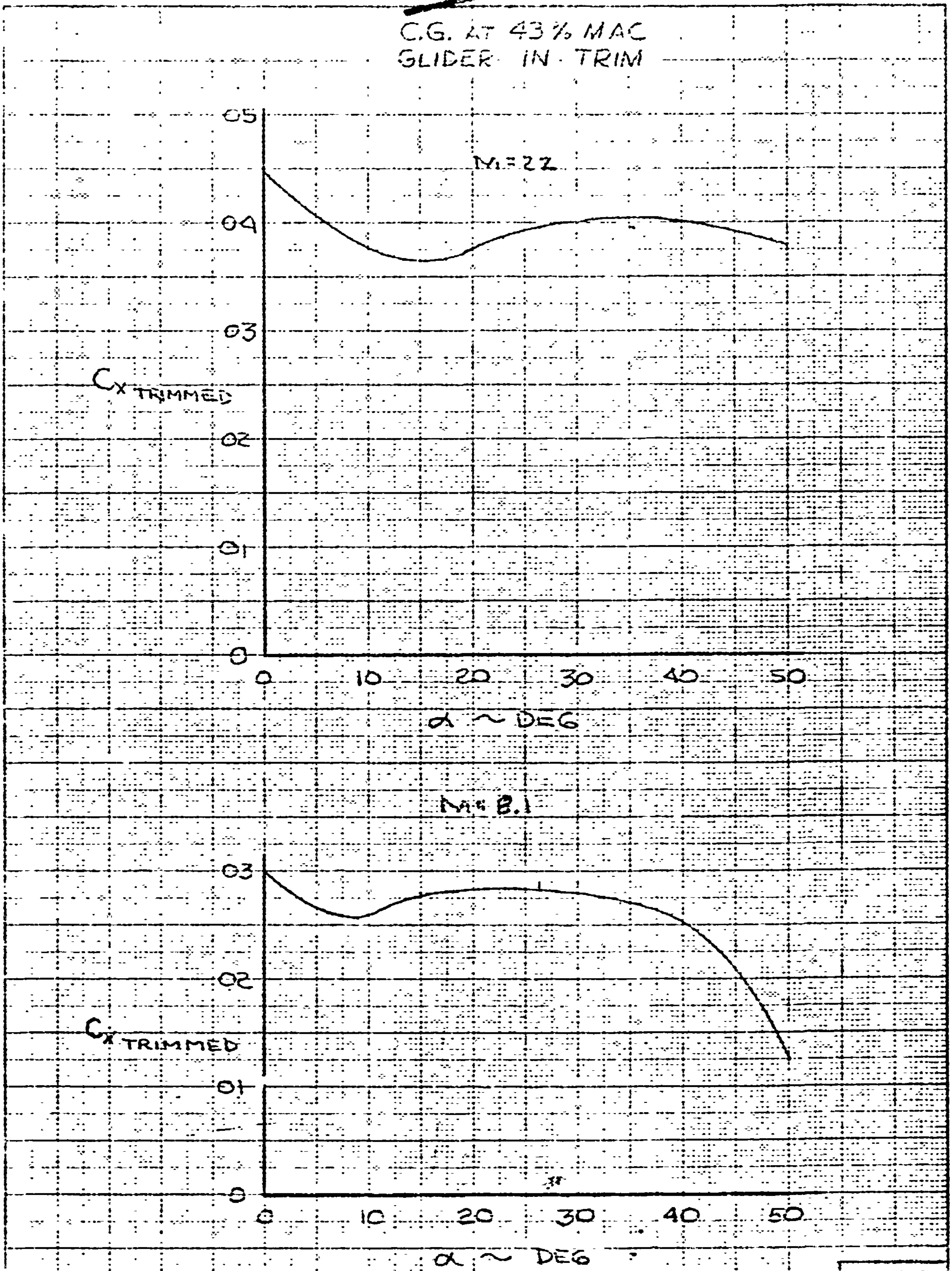

FIG. 5.54

W.E.J. 12-12-0

HYPERSONIC CHORD FORCE COEFFICIENT

844-2035

D2-8174

5.6 SPEED BRAKES (DRAG BRAKE)

The incremental effect of extending the speed brakes on longitudinal stability is shown on Figure 5.6.1. Data are shown at the three Mach numbers where test data have been obtained. The test data were obtained in the Boeing Transonic and Supersonic Wind Tunnels and have been modified to the present configuration. Further study of speed brake location, to minimize trim and stability changes, is being conducted.

The incremental effect of the speed brakes on axial force is shown on Figure 5.6.2 at supersonic and low speed.

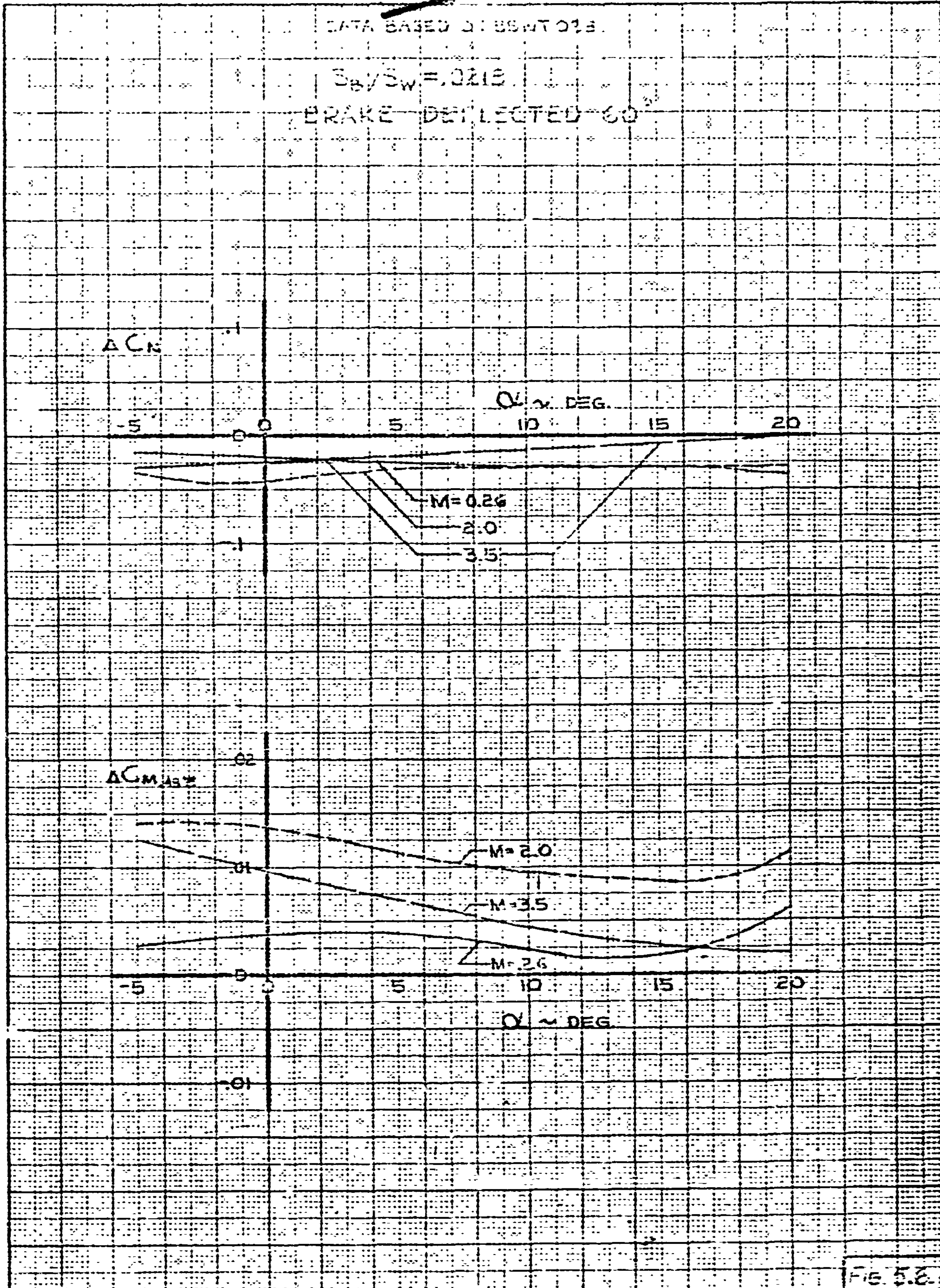

Fig. 5.8.7

CALC	J. FRANCIS	12-9-60	REVISED	DATE
CHECK				
APR				
APR				
TRAC	N.U	12-9-60		

EFFECT OF DRAG BRAKE ON LONGITUDINAL STABILITY

75

844-2035

D2-8174

BOEING AIRPLANE COMPANY

PAGE 5.43

MODEL 2035

$S_E / S_W = .0218$

BRAKE DEFLECTED 60°

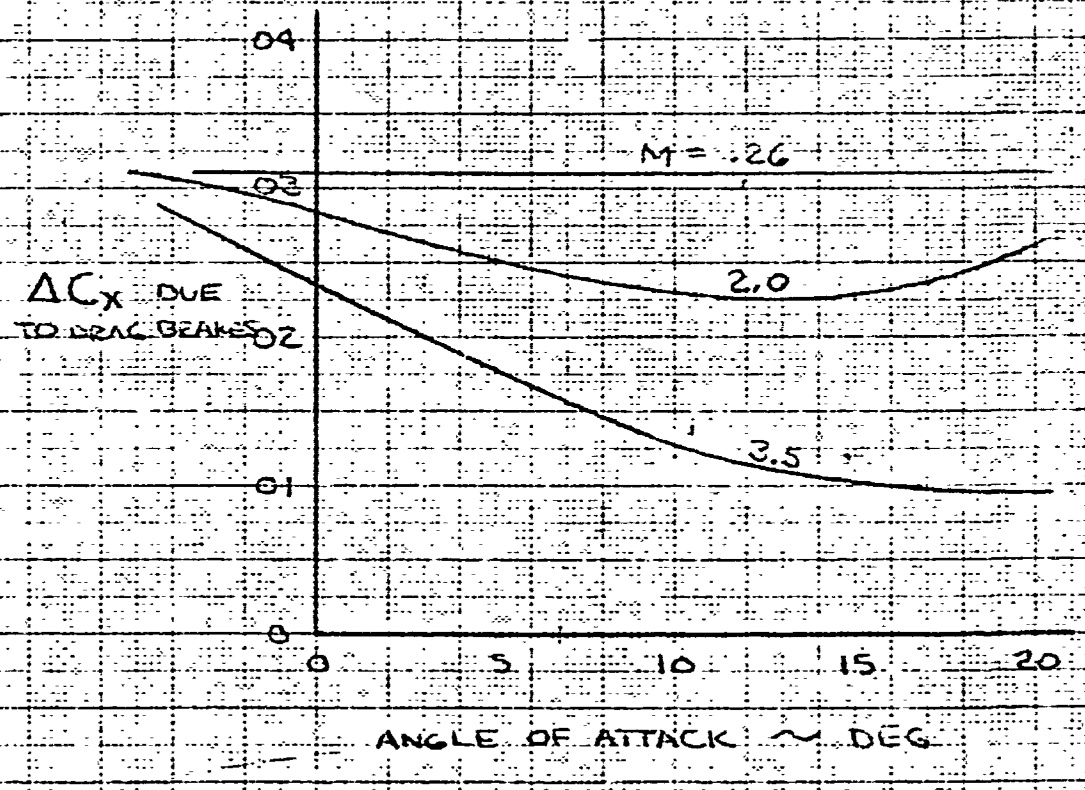

FIG 5.2.2

W.E.J. 12-22

EFFECT OF DRAG BRAKE ON CHORD FORCE COEFFICIENT

76

D2-3174

BOEING AIRPLANE COMPANY

5.7 ELEVON AS AILERON PITCH COUPLING

The effects of symmetrical elevon deflection for roll control on pitch stability and trim at subsonic through supersonic speeds are shown on Figures 5.7.1 and 5.7.2. The data were estimated from limited wind tunnel data and can be subject to major revision.

At hypersonic speeds, the changes in pitching moment and normal force are presented as functions of elevon deflection and angle of attack for one elevon deflected. Test data have shown that the deflection of one elevon has a negligible effect upon the flow about the other elevon at hypersonic speeds. Therefore, the effect of aileron deflection can be obtained by adding the individual effects of the two elevons. The increments in normal force and pitching moment due to deflection of one elevon are shown on Figures 5.7.3 through 5.7.8 for M=8 and 22. Elevon pitch trim requirements for various roll control deflection are shown on Figure 5.7.3 for M=8 and Figure 5.7.6 for M=22.

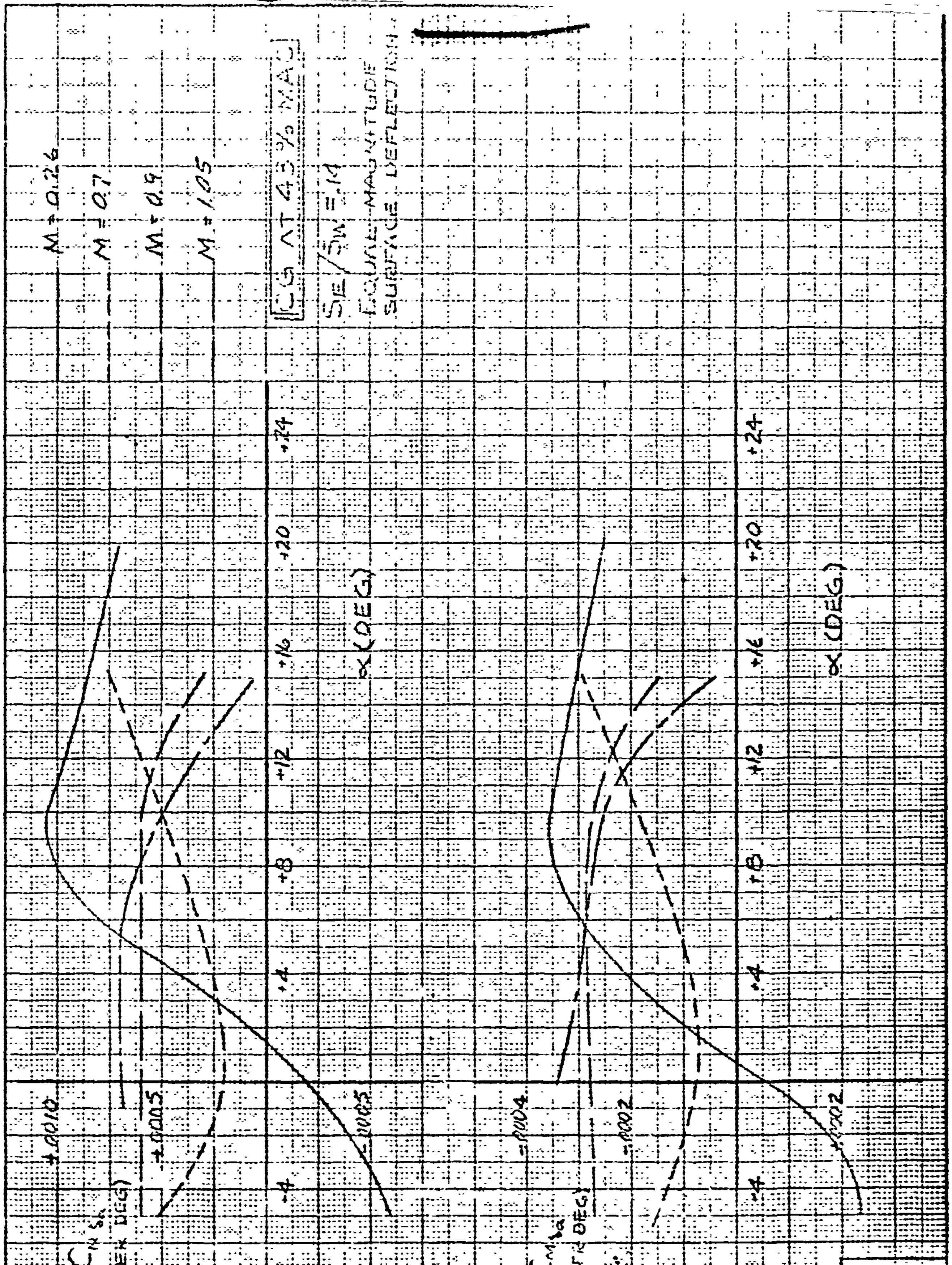

FIG. 5.7.8

CALC	G O M	12-13-61	REVISED	DATE	PITCH EFFECTS DUE TO AILERON DEFLECTION	844-2035
CHECK						
APR					SUBSONIC - TRANSONIC SPEED	D2-8174
APR					BOEING AIRPLANE COMPANY	PAGE 5.46

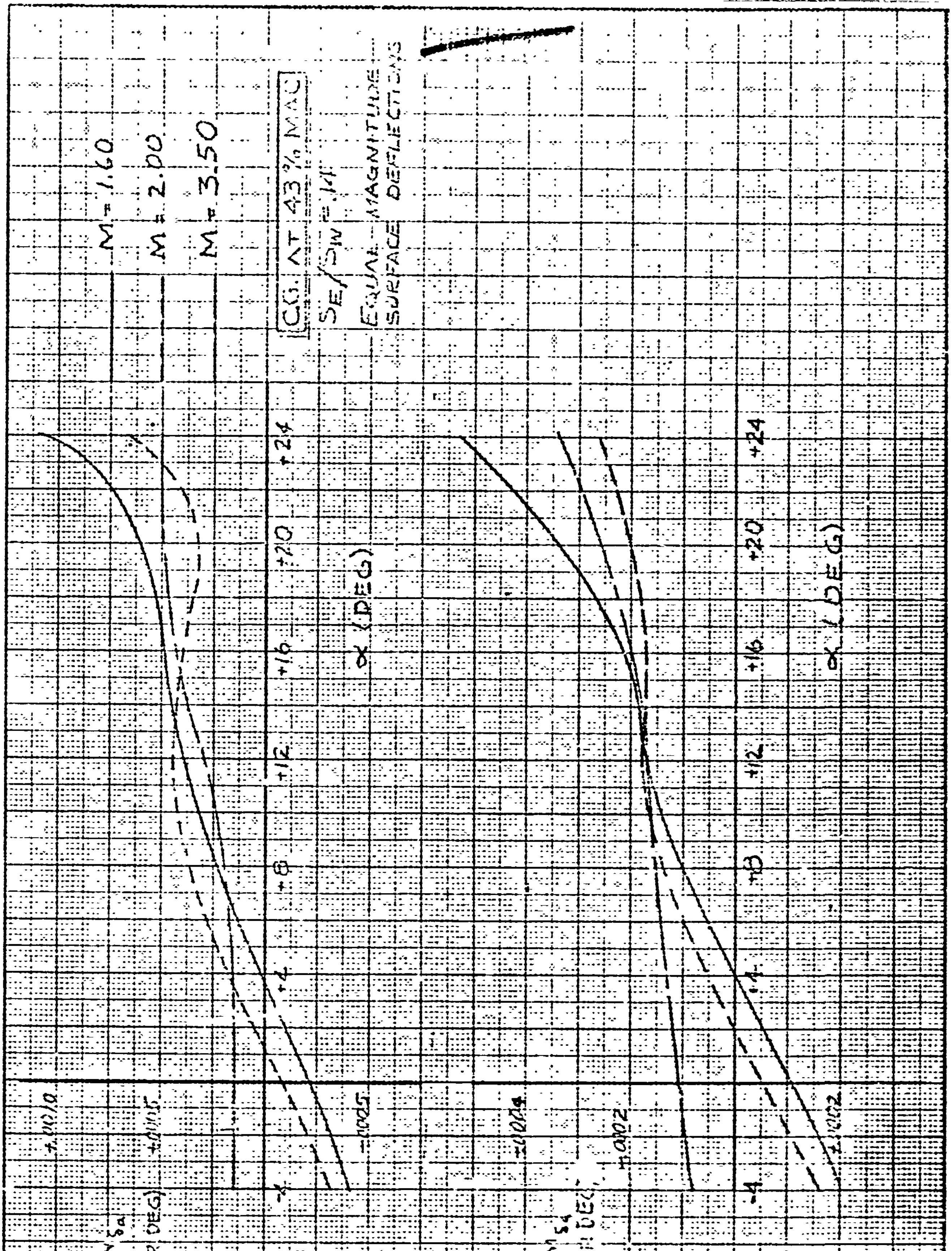

Fig 5.7.2

CALC	GOM	12/13/60	REVISED	DATE
CHECK				
APR				
APR				

PITCH EFFECTS DUE TO AILERON DEFLECTION

SUPERSONIC SPEED

BOEING AIRPLANE COMPANY

344-2035

D2-8174

PAGE 5.47

79

K-E

2035 CONFIGURATION

M = 8.1

CG AT 43% MAC

HOT SHAPE
3.8° NOSE INCIDENCE
0.8° AFT OF B.S. 400

ELEVON
10° TAPER
SPLIT
$S_E / S_W = .14$

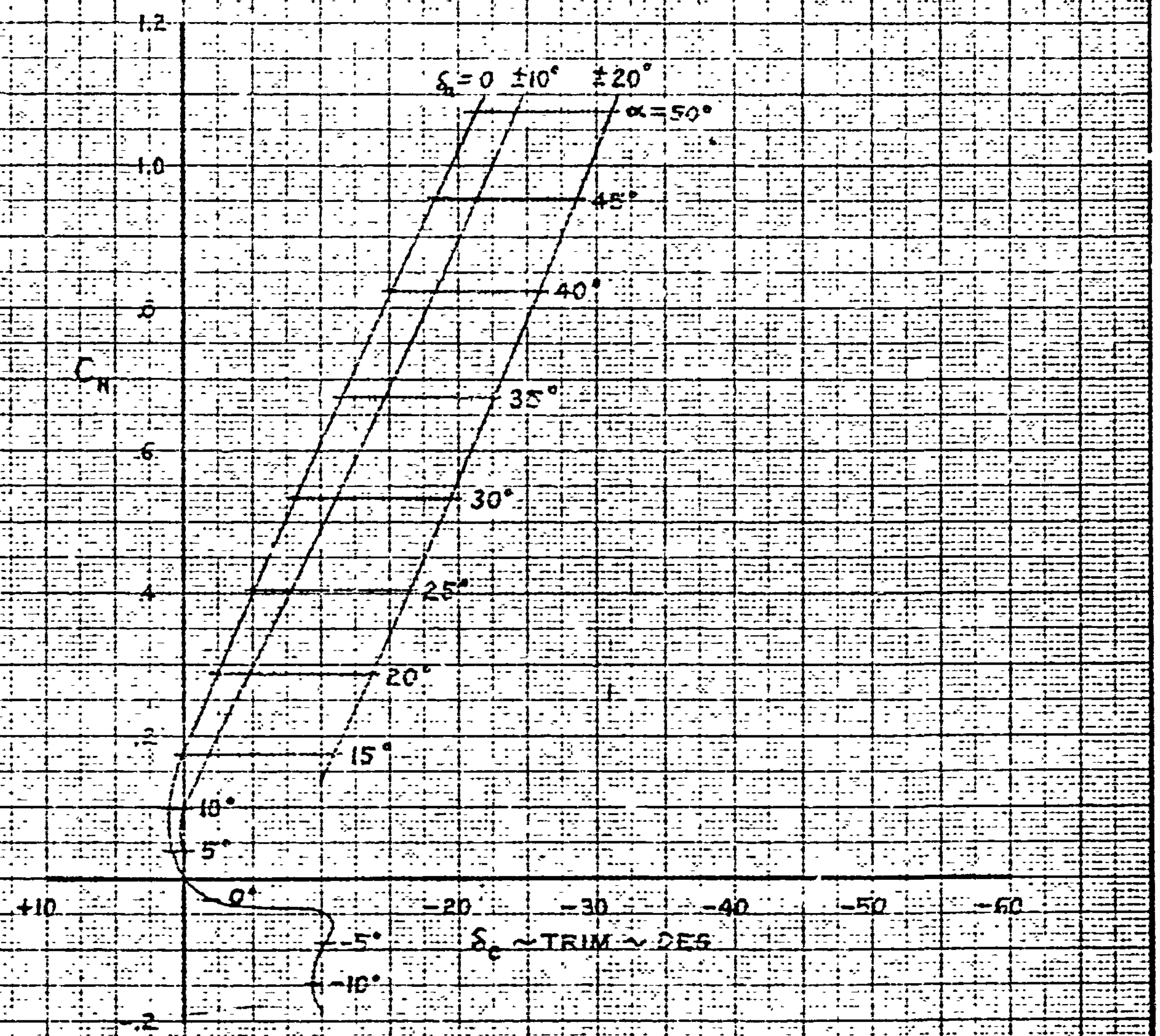

FIG. 5.7.3

CALC	Emp	12/8/58	REVISED	DATE	AILERON PITCH TRIM REQUIREMENTS HOT SHAPE M = 8.1	80	844-2035
CHECK							D2-3174
APR					BOEING AIRPLANE COMPANY SEATTLE 14 WASHINGTON		PAGE 545
APR							

BAC 461 C-R4

BASE CONFIGURATION

M = 3.1

C.G. AT 43 % MAC

HOT SHAPE

3.8° NOSE INCIDENCE

0.8° AFT OF B.S. 400

ELEVON

10° TAPER

SPLIT

$S_E/S_W = .14$

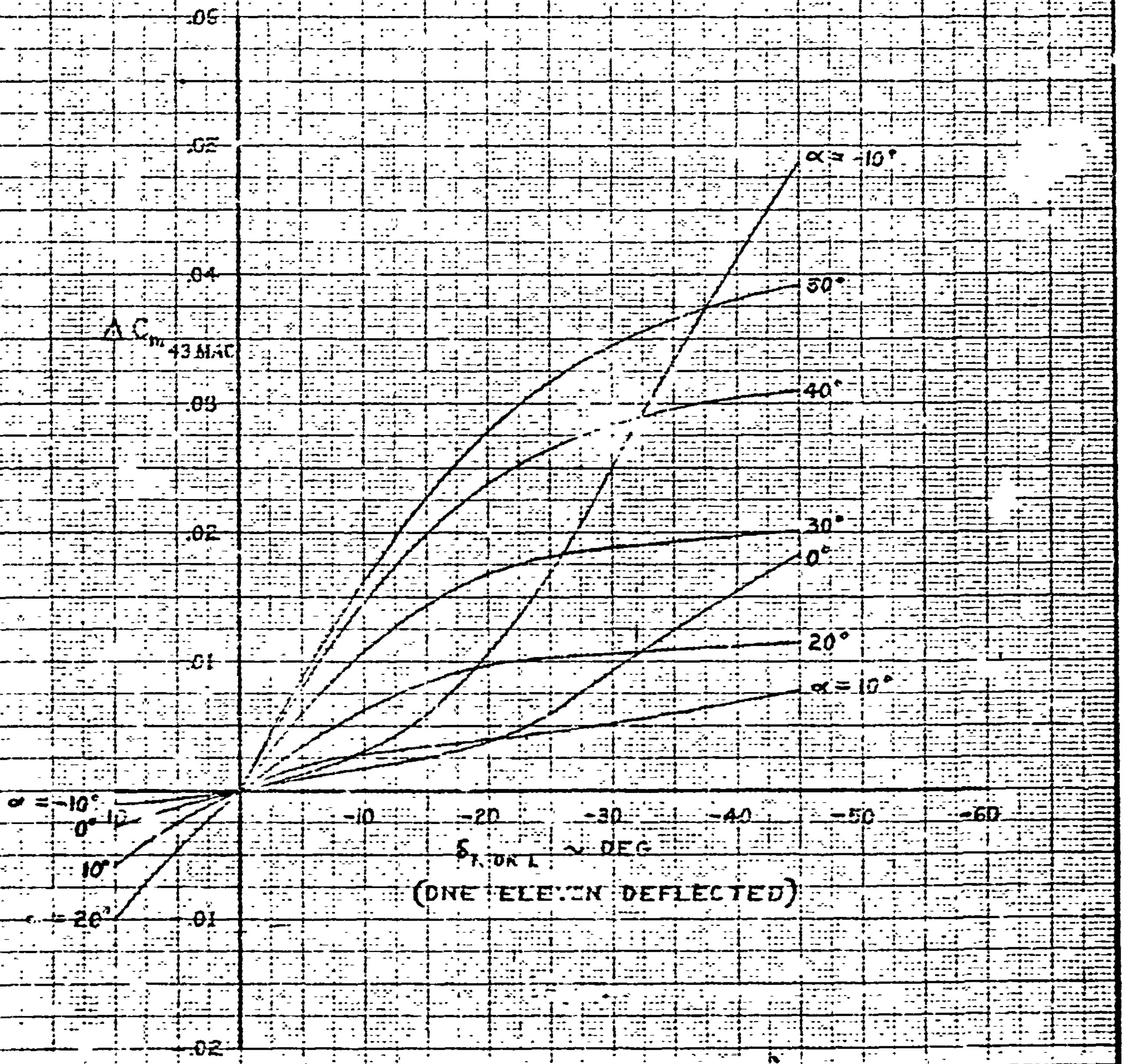

FIG 5.7.4

CAL		12/7/60	REVISED	DATE
CH				
APR				
APR				

EFFECT OF AILERONS ON PITCHING MOMENT

HOT SHAPE M = 3.1

BOEING AIRPLANE COMPANY

SEATTLE 24, WASHINGTON

44-2035

D2-3174

PAGE 5.43

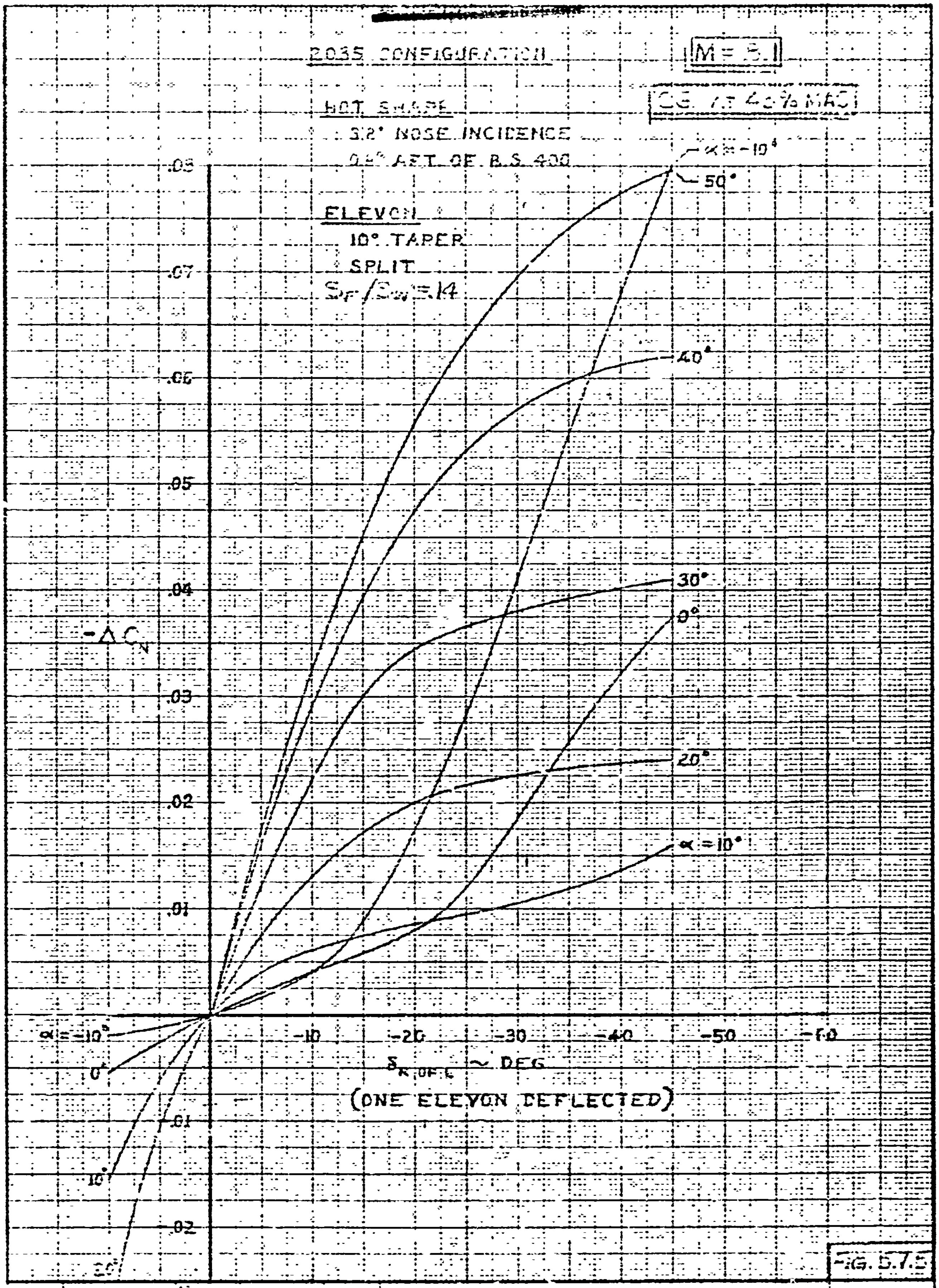

FIG. 5.7.5

CALC	Em+	12/7/60	REVISED	DATE
CHECK				
APR				
APR				

EFFECT OF AILERONS ON NORMAL FORCE

HOT SHAPE M = 5.1

82

844-2035

D2-5174

PAGE 5.59

BOEING AIRPLANE COMPANY
SEATTLE 24 WASHINGTON

BAC 451 C-R4

035 CONFIGURATION

M = 22.0

C.G. = 43% MAC

HOT SHAPE

3.5° NOSE INCIDENCE

2.5° AFT OF B.S. 400

ELEVON

10° TAPER

SPLIT

$S_F/S_W = .14$

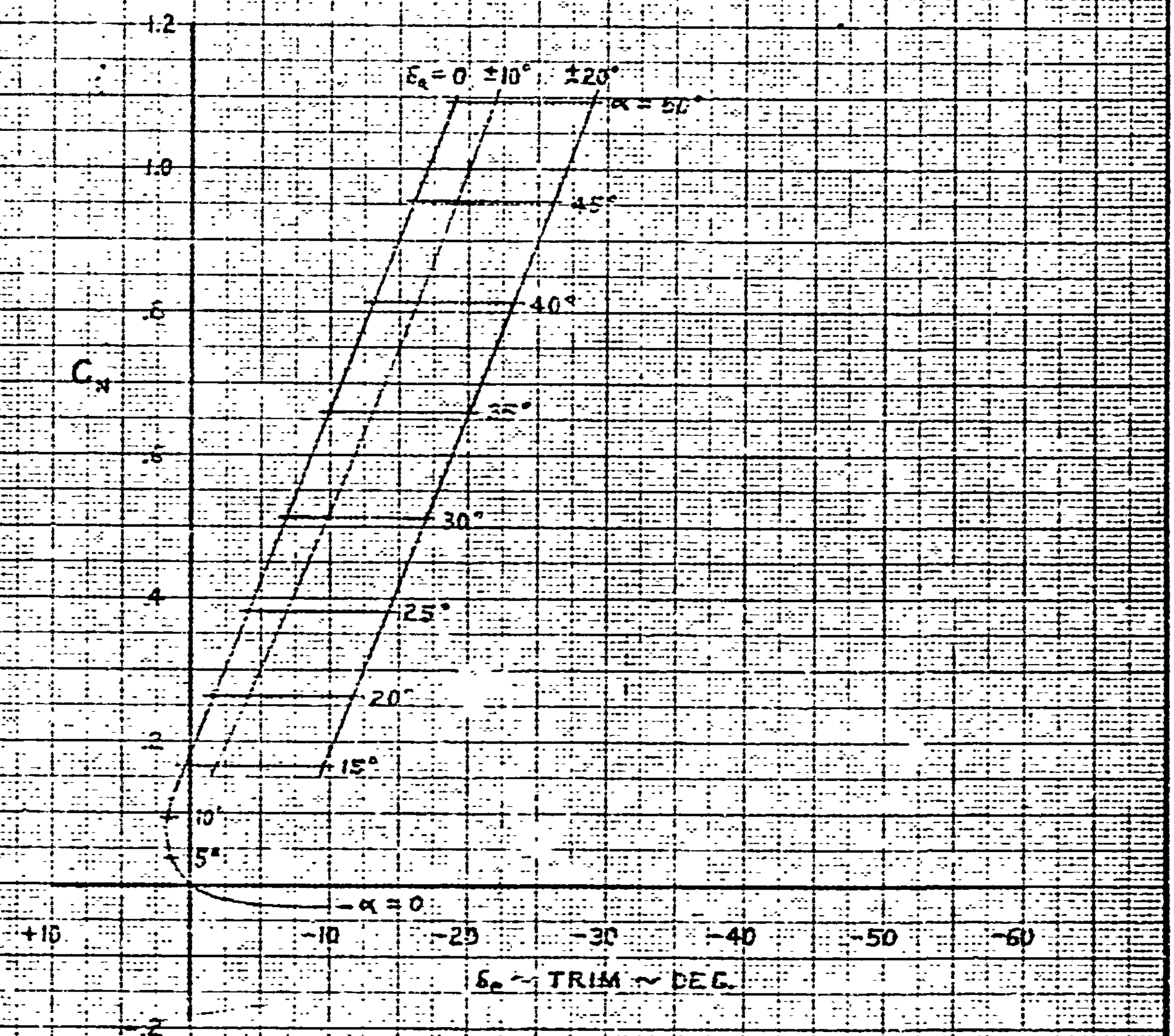

FIG 5.76

CALC	EM	12/9/57	REVISED	DATE
CHECK				
APR				
APR				

AILERON PITCH TRIM REQUIREMENTS 83

HOT SHAPE M = 22.0

E44-2035

D2-8174

BOEING AIRPLANE COMPANY

SEATTLE 24, WASHINGTON

PAGE 5.51

BAC 461 C-R4

60629

2035 CONFIGURATION

M = 22.0

C.G. AT 42% MAC

HOT SHAPE
3.5° NOSE INCIDENCE
0.8° AFT OF B.S. 400

ELEVON
10° TAPER
SPLIT
$S_E/S_W = .14$

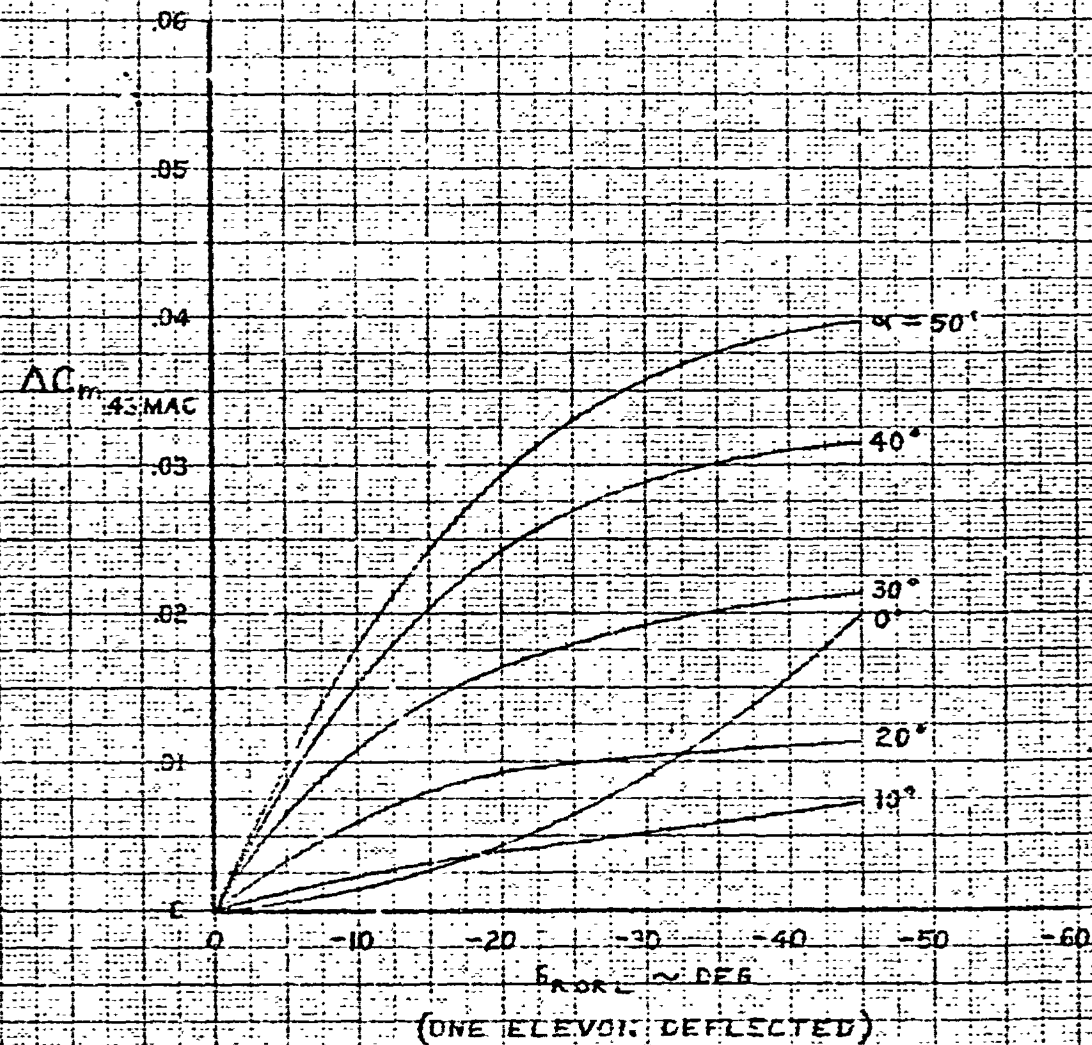

FIG. 5.7.7

CALC	Em.H	12/3/56	REVISED	DATE	EFFECT OF AILERONS ON PITCHING MOMENT HOT SHAPE M = 22.0	844-2035
CHECK						D2-5174
APR					BOEING AIRPLANE COMPANY	
APR					SEATTLE 24 WASHINGTON	PAGE 5.52

84

FAC 461 C-R4

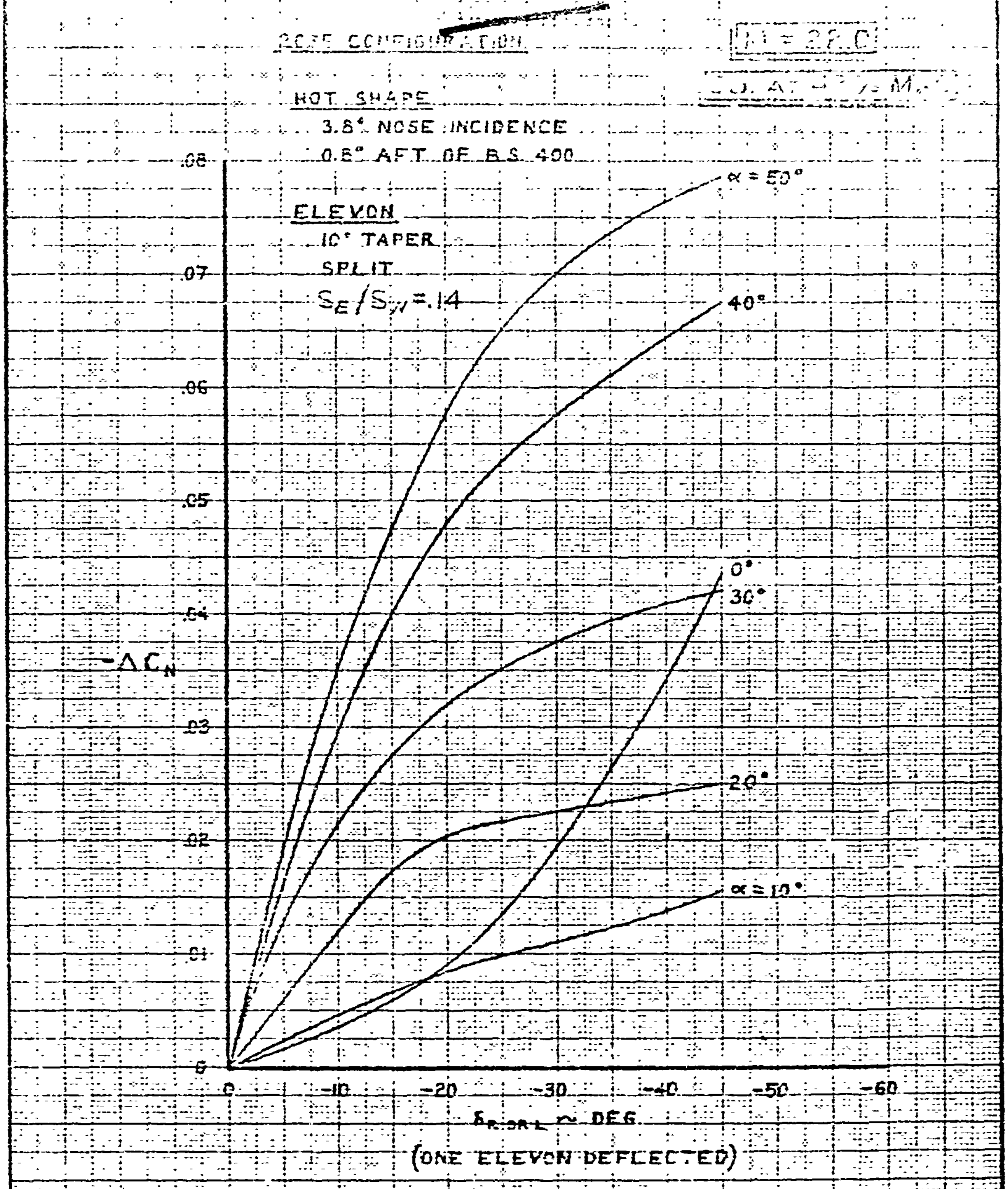

FIG. 5.73

CALC		4/9/60	REVISED	DATE
CHECK				
APR				
APR				

EFFECT OF AILERONS ON NORMAL FORCE

85

344-2035

D2-8174

PAGE 5.53

BOEING AIRPLANE COMPANY
SEATTLE 14 WASHINGTON

BAC 801 C-R4

5.8 ROTARY DERIVATIVES

The pitch damping derivative, C_{m_q} (shown on Figure 5.8.1), was obtained from NASA reports of similar configurations. These data were also compared with linear theory which was found to be in reasonable agreement at supersonic speeds but was nearly double the empirical value at subsonic speeds. Recent wind tunnel data were run showing the effects of angle of attack and oscillation frequency on C_{m_q} and $C_{m_{\dot{\alpha}}}$ at low speed in the L.R.C. Free Flight Wind Tunnel. These data are currently being analyzed. Additional analytical and test work is being done and is planned, to define the necessary rotary derivatives further.

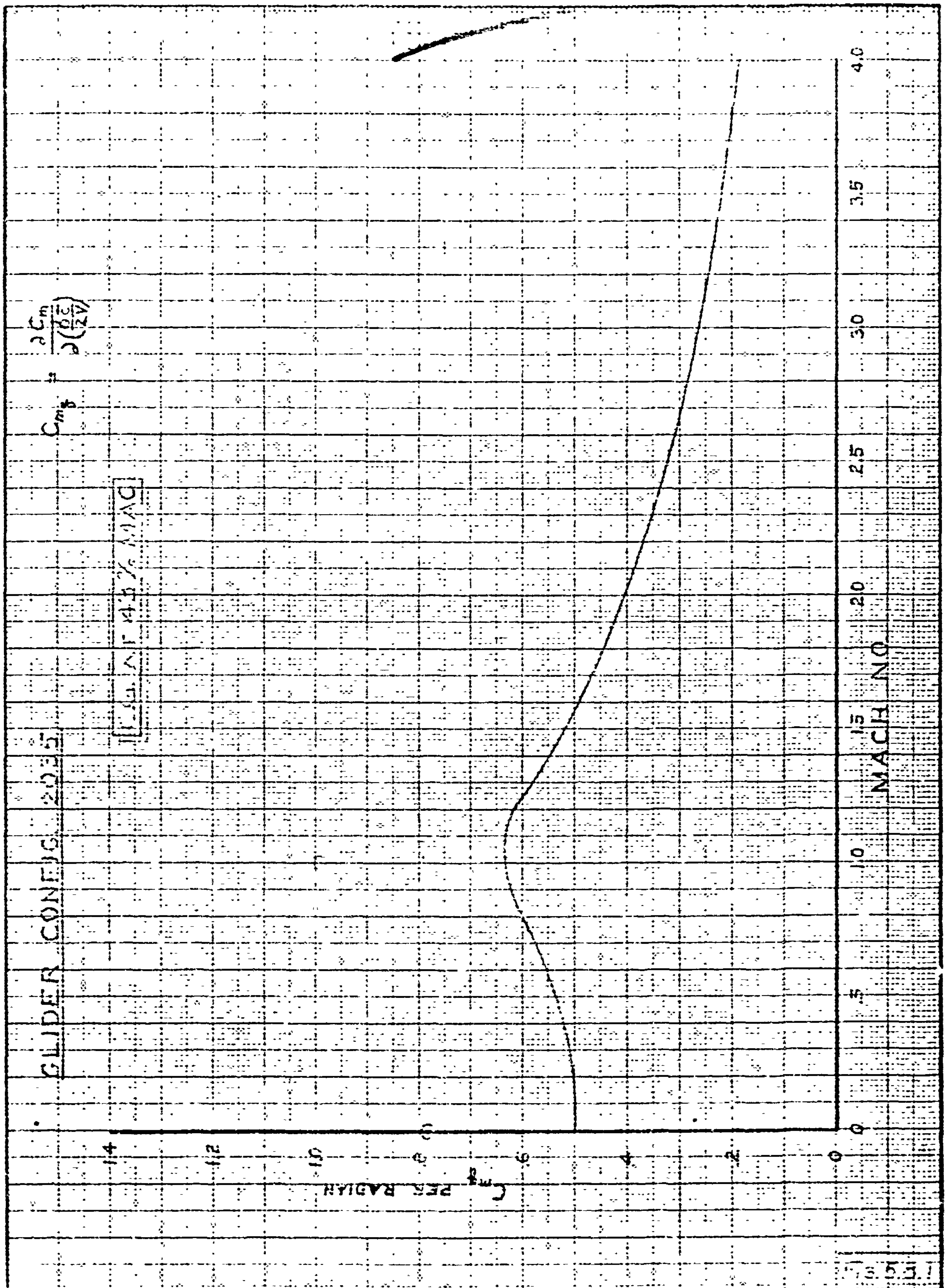

CALC	Cm?	12/5/60	REVISED	DATE
CHECK				
APR				
APR				

PITCHING MOMENT DUE TO PITCHING VELOCITY

844-2035

D2-8174

87

BOEING AIRPLANE COMPANY
SEATTLE 24, WASHINGTON

PAGE 5.55

5.9 ELEVON HINGE MOMENT CHARACTERISTICS

Variation of C_{H_α} and C_{H_δ} with Mach number is shown on Figure 5.9.1. These data were obtained from published N.A.S.A. reports on similar configurations.

Wind tunnel tests in the A.R.C. Unitary Wind Tunnel have been completed recently and further testing is planned to define these characteristics better as a function of Mach number, angle of attack and angle of elevon deflection.

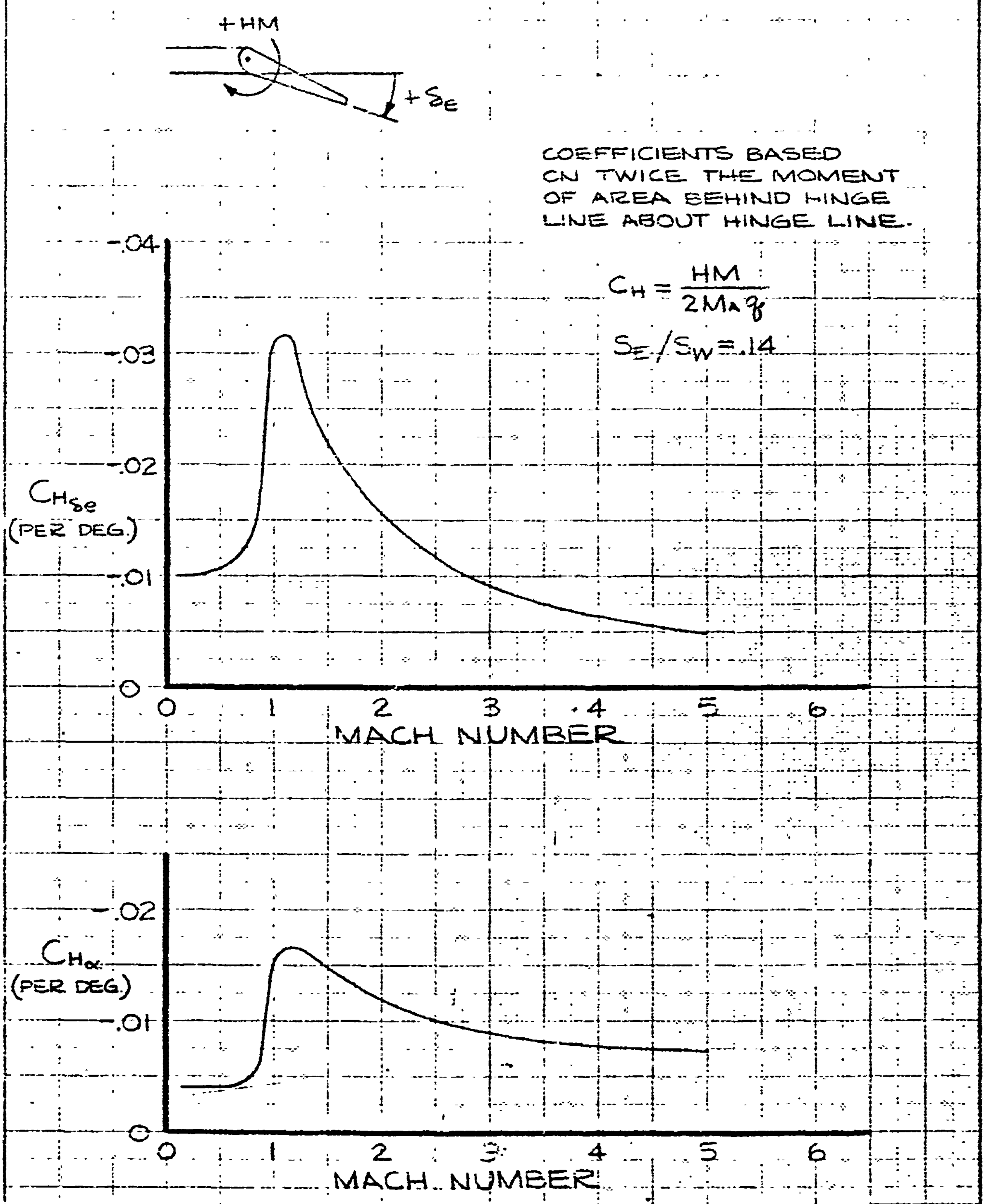

FIG. 5.9.1

PMJ 11/18/60

ELEVON HINGE MOMENT COEFFICIENTS

844-2035

D2-8174

5.10 WING TIP EXTENSIONS

The incremental effect of wing tip extensions, located on the vertical tails, on pitching moment and normal force coefficients is shown on Figures 5.10.1 and 5.10.2. These data are based on tests performed in the A.R.C. 12-Foot Pressure Wind Tunnel and the Boeing Transonic and Supersonic Wind Tunnels. It was assumed that the tip extension would have only secondary effects on elevon effectiveness. The data obtained were not with the precise tip extension configuration for the [illegible]-2035 glider; consequently some variation in the increments shown may be anticipated.

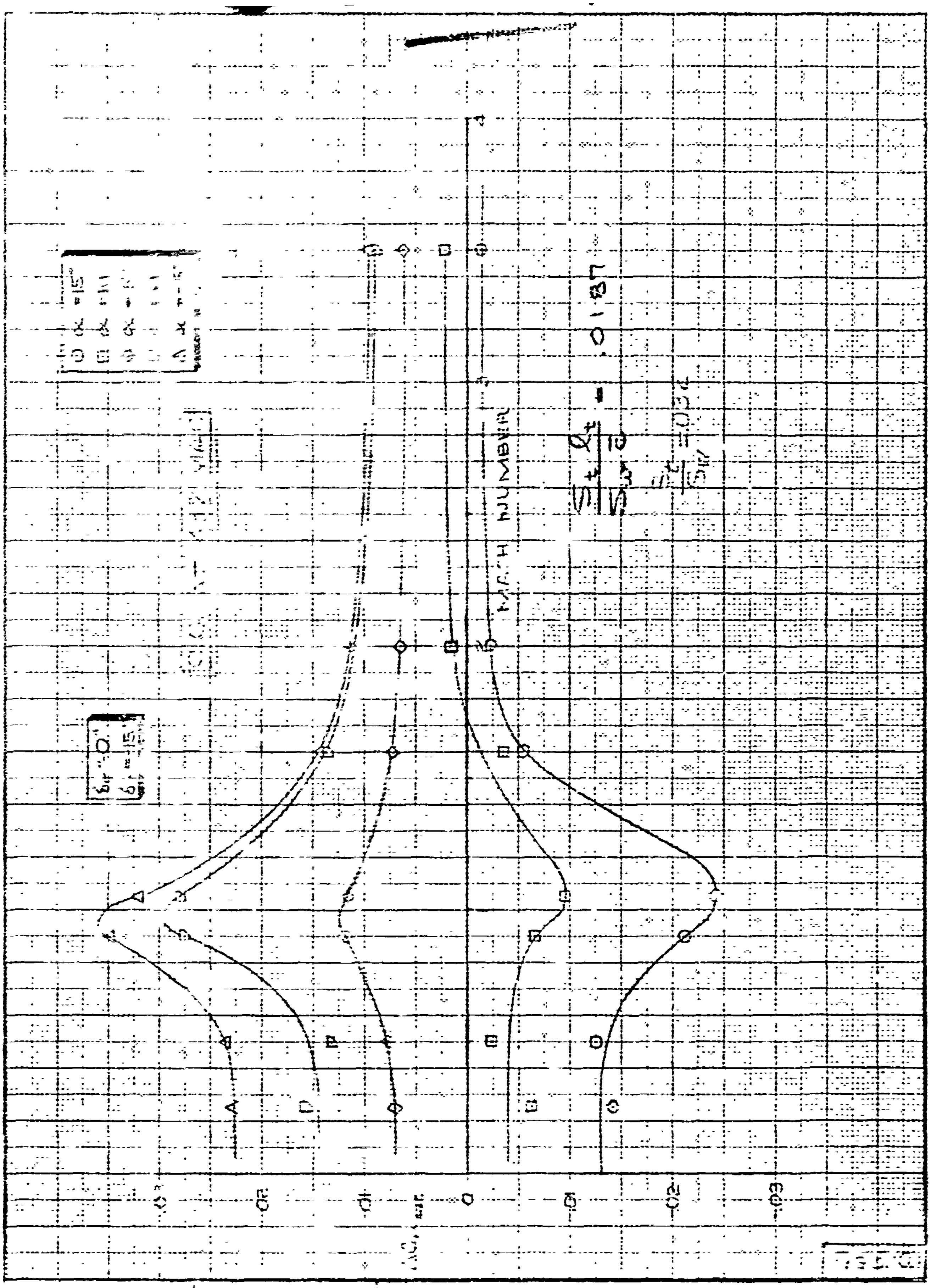

CALC	W.L. Francis	12/6/60	REVISED	DATE
CHECK	EDJR	12-7-60		
APP				
APR				

EFFECT OF WING TIP EXTENSIONS ON PITCHING MOMENT

91

BOEING AIRPLANE COMPANY

PAGE 59

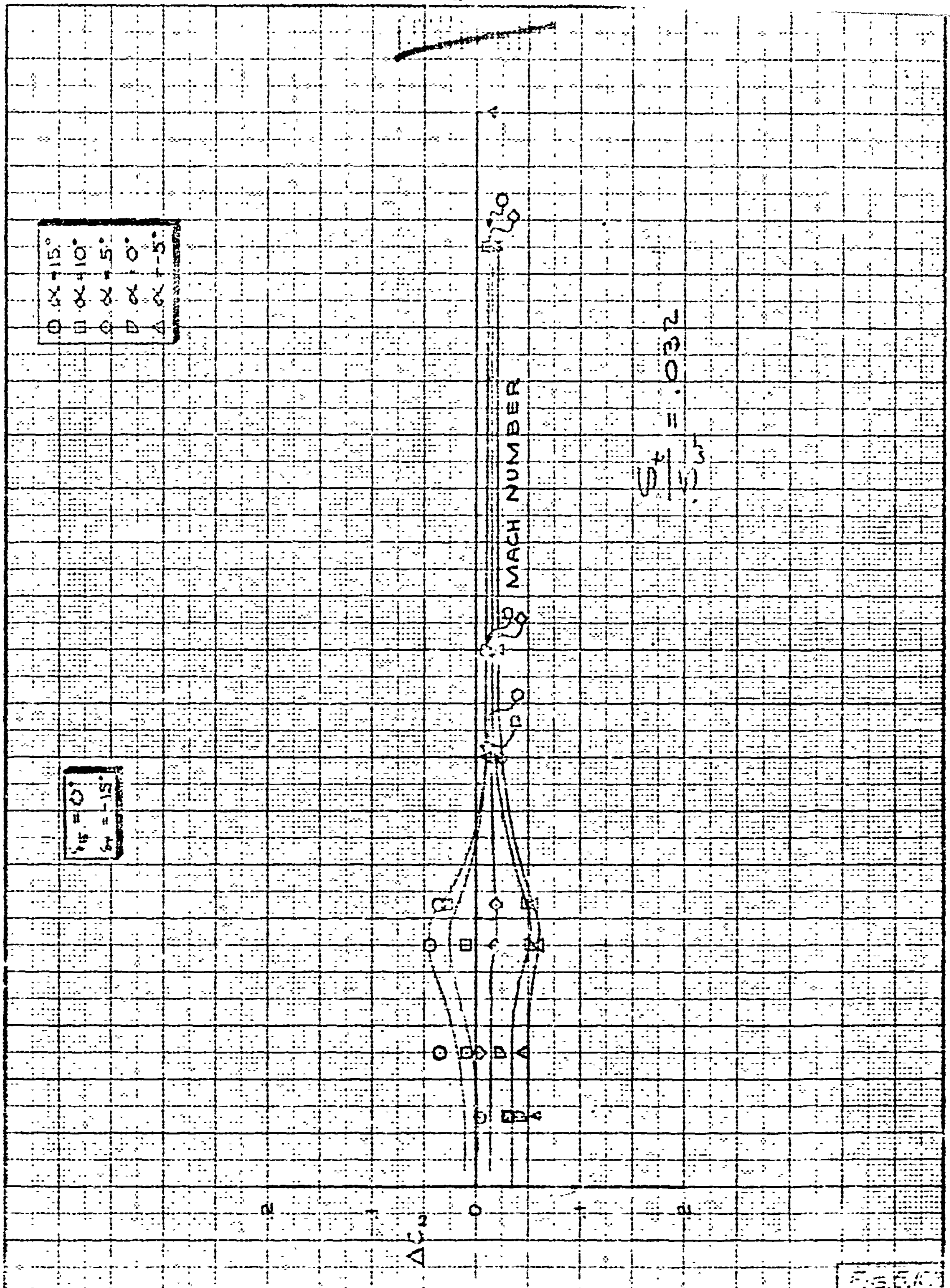

CALC	J L FRANCIS		REVISED	DATE
CHECK	EDJR	12-7-0		
APP				
APP				

FIG.

EFFECT OF WING TIP EXTENSIONS ON NORMAL FORCE

92

844-203

D2-3174

BOEING AIRPLANE COMPANY

PAGE 56

6.0 LATERAL - DIRECTIONAL STABILITY AND CONTROL

The predicted force, moment, and directional control effectiveness characteristics are included in this section. The data are grouped in the following areas. A list of the data in each area is presented at the front of each group.

6.1 Lateral - Directional Stability Characteristics

6.2 Aileron Characteristics and Effectiveness

6.3 Rudder Characteristics and Effectiveness

6.4 Roll and Yaw Rotary Derivatives

The characteristics are presented for the 844-2035 configuration, Figure 3.1.1. The reference dimensions on which the characteristics are based are shown on Figure 3.3.3. All characteristics are presented for conventional body axes fixed in the vehicle.

6.1 LATERAL - DIRECTIONAL STABILITY CHARACTERISTICS

The lateral - directional stability is presented in Figures 6.1 through 6.24 for landing speed to high hypersonic speed. The yawing moment, rolling moment, and side force are presented versus sideslip angle and angle of attack at representative Mach numbers in order to show the non-linearity of the stability characteristics. The stability derivatives C_{n_β}, C_{l_β}, and C_{Y_β} are also presented versus Mach number in order to indicate the interpolation between Mach numbers (Figures 6.1, 6.2, and 6.3). These derivatives are presented only for zero sideslip, and because of the non-linear nature of the stability characteristics, should not be used for large sideslip angles. Stability characteristics are presented for wing-tip extensions both retracted and extended from landing speed to M = 3.5.

The stability characteristics are presented at representative speeds corresponding approximately to wind tunnel test speeds, namely, M = 0.25, .70, .95, 1.65, 2.0, 3.5, 8.0 and 22.0. The landing speed data are based primarily on low speed tests on a similar configuration at the ARC 12-Foot Pressure Tunnel, test 122, and preliminary data from BTWT 619. Effects of Reynolds number (altitude) were shown to be small. The stability at $\alpha = 15°$ and β greater than 12° was extrapolated. The incremental effect of extending the landing gear and extending the speed brakes is shown on Figures 6.7 and 6.8. No data on the influence of the ground is currently available; however, any effect of the ground on yawing moment and side force will probably be negligible, with the major effect a small reduction in aileron effectiveness and roll due to sideslip (dihedral effect).

The transonic characteristics were estimated from preliminary data from BTWT 623 on a similar glider configuration. The data have been extrapolated to the current configuration on the basis of body shape, vertical tail size, location, and planform, and fold-down wing tip size. The static stability is currently minimum in this speed range.

The supersonic stability characteristics were obtained from tests in the Boeing Supersonic Wind Tunnel at Mach numbers 2.0 and 3.5. Since C_n, C_l, and C_Y are quite linear with β in this Mach number region, data are presented for M = 3.5 only (wing tips extended and retracted) on Figures 6.22 and 6.21. These Figures are representative of the variation of these coefficients versus β throughout the supersonic region. Figures 6.15 through 6.20 present C_{n_β}, C_{l_β}, and C_{Y_β} versus α for M = 2.0 and 3.5, and for wing tips extended and retracted.

Lateral - directional stability at low hypersonic speeds were obtained from wind tunnel tests on the model 844-2005, a similar configuration, at Mach numbers of 8.08 (AFDC-B, BAC 13) and 9.6 (LRC 11-Inch, Test 47 in air). The data have been adjusted for vertical tail size, planform and cant angle (Figure 3.1.1). The results are presented in Figure 6.23.

High hypersonic speed data were obtained at Mach 17.8 (LRC 11-Inch, Test 47 in helium) and Mach 16 and 22 (HHST 006). The helium data were obtained on a model identical to the low hypersonic speed model. The hot shot data, however, were on a cone-cylinder body configuration, and additional corrections had to be made for the body shape. This was performed by comparing the cone-cylinder and SW4-2005 body effects at Mach 9.6 and adjust the Mach 22.0 data accordingly. Figure 6.24 shows the lateral - directional stability characteristics at high hypersonic speeds. Characteristics at angles of attack above 20° were extrapolated from lower Mach number data.

No information is currently available on the influence of altitude (i.e., Reynolds number) variation at high hypersonic speeds on the lateral - directional force-moment characteristics. Until data become available, it is assumed that the effect of altitude will be negligible on C_n, C_l and C_Y. The primary effect of altitude will be to increase boundary layer thickness. However, the areas of the glider that are most important in establishing directional stability are the glider fore-body and vertical tail; regions which are not expected to have significant boundary layer growth because of short boundary layer runs.

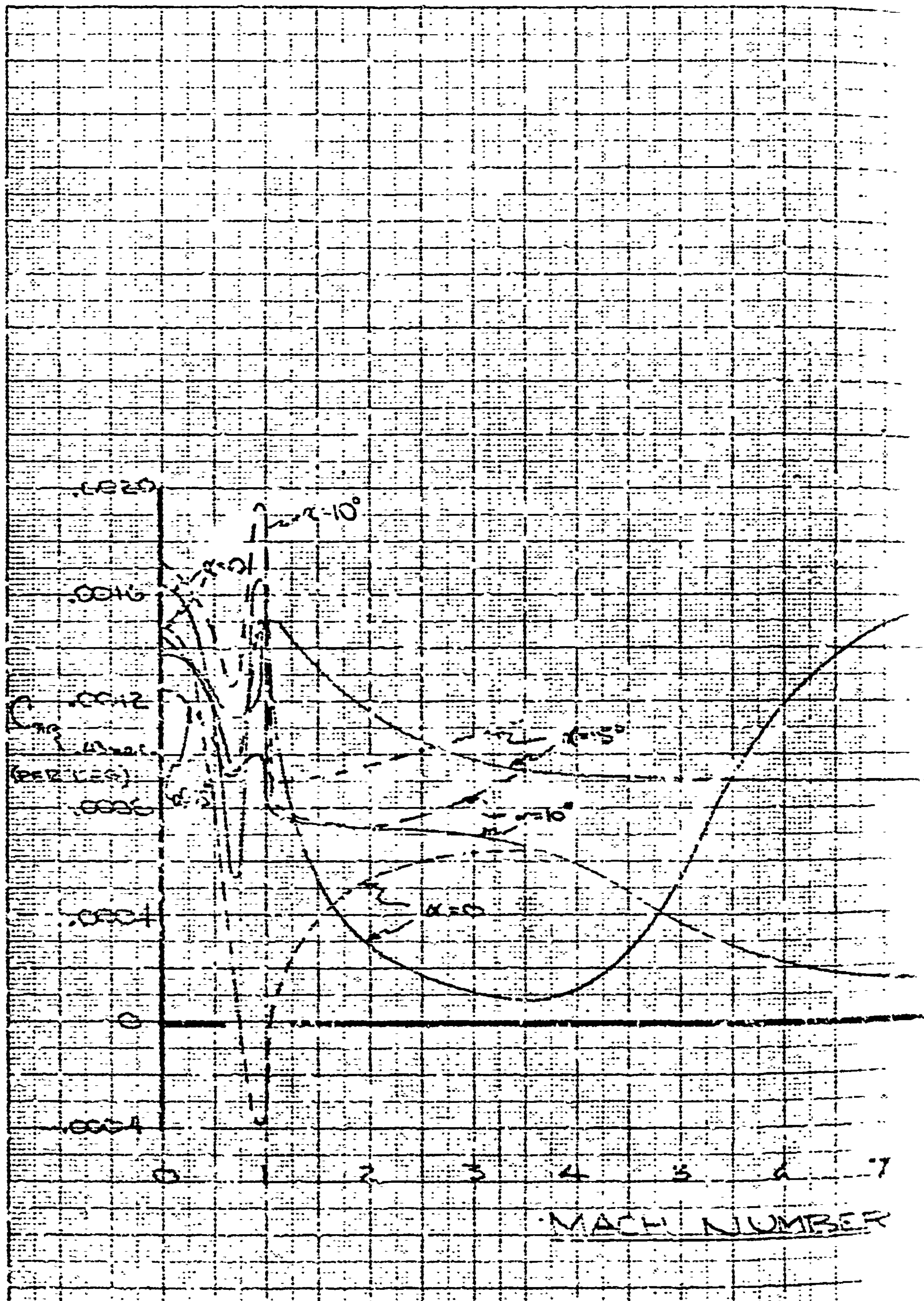
.0020
.0016
.0012
.0008
.0004
0
.0004
0
1
2
3
4
5
6
7
MACH NUMBER
α=0

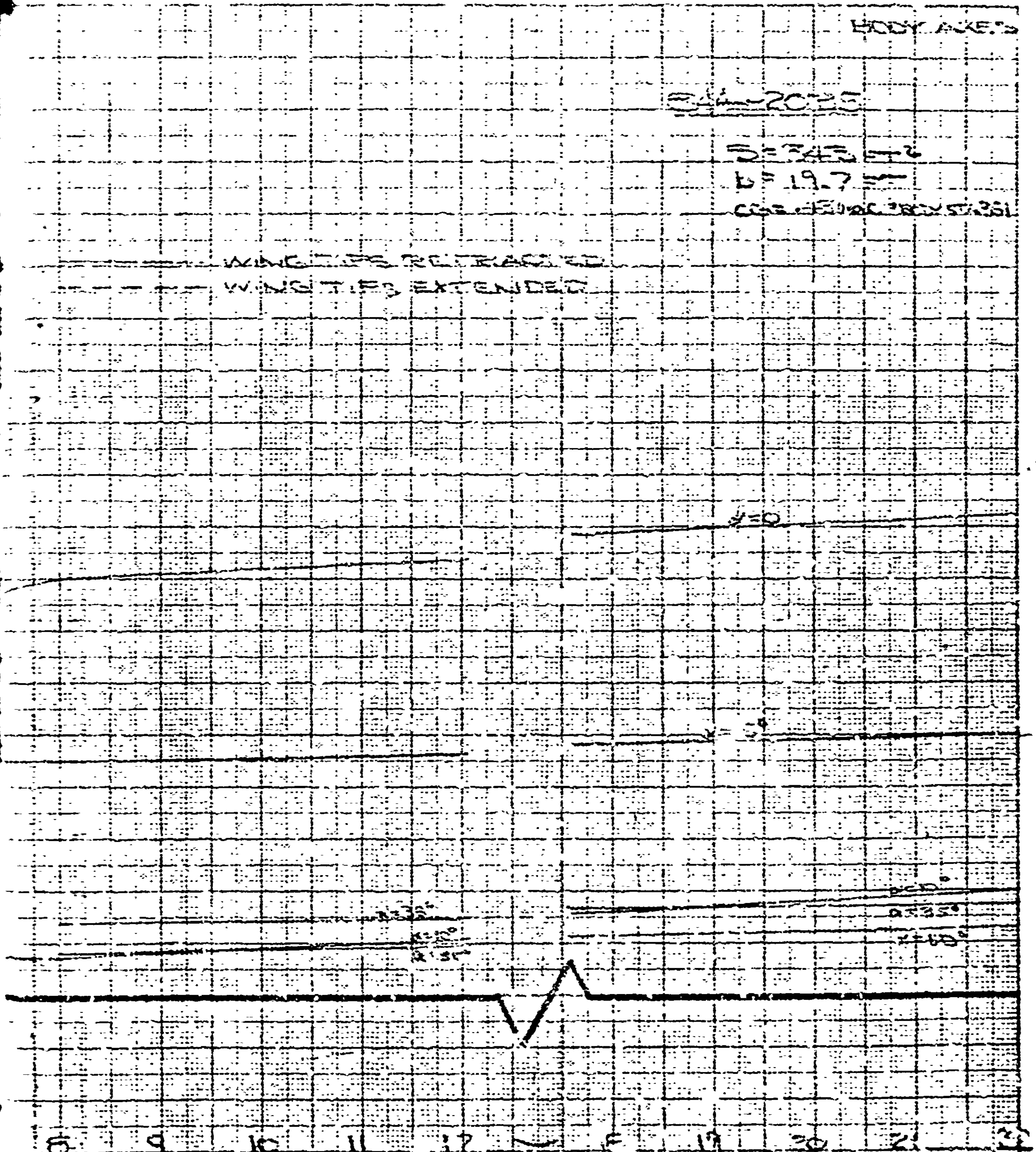

FIG 6.1

DIRECTIONAL STABILITY

D2-8174

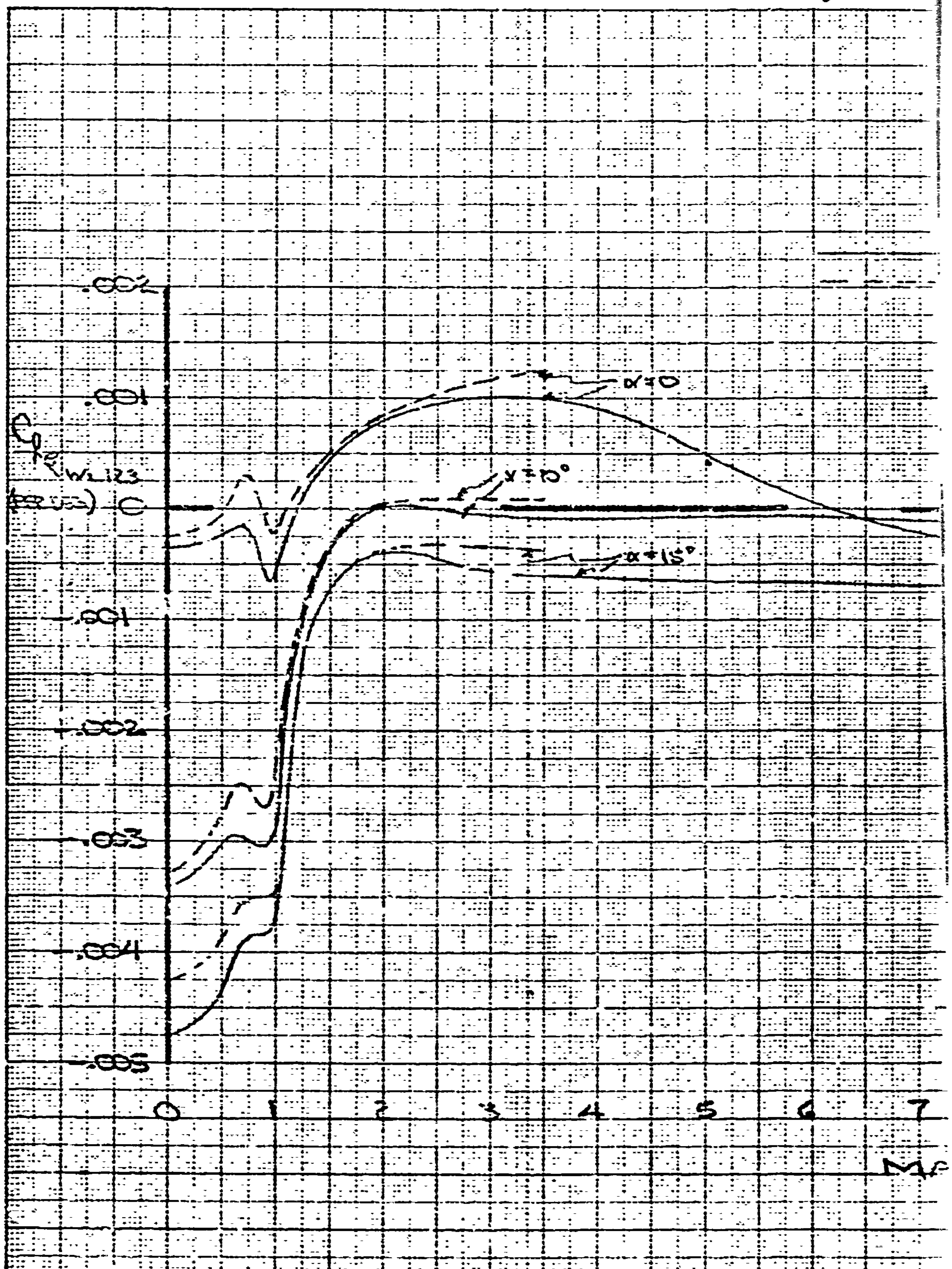

.002
.001
C_{l_β}
WL 123
(PER DEG)
0
-.001
-.002
-.003
-.004
-.005
α = 0
α = 10°
α = 15°
0
1
2
3
4
5
6
7
M

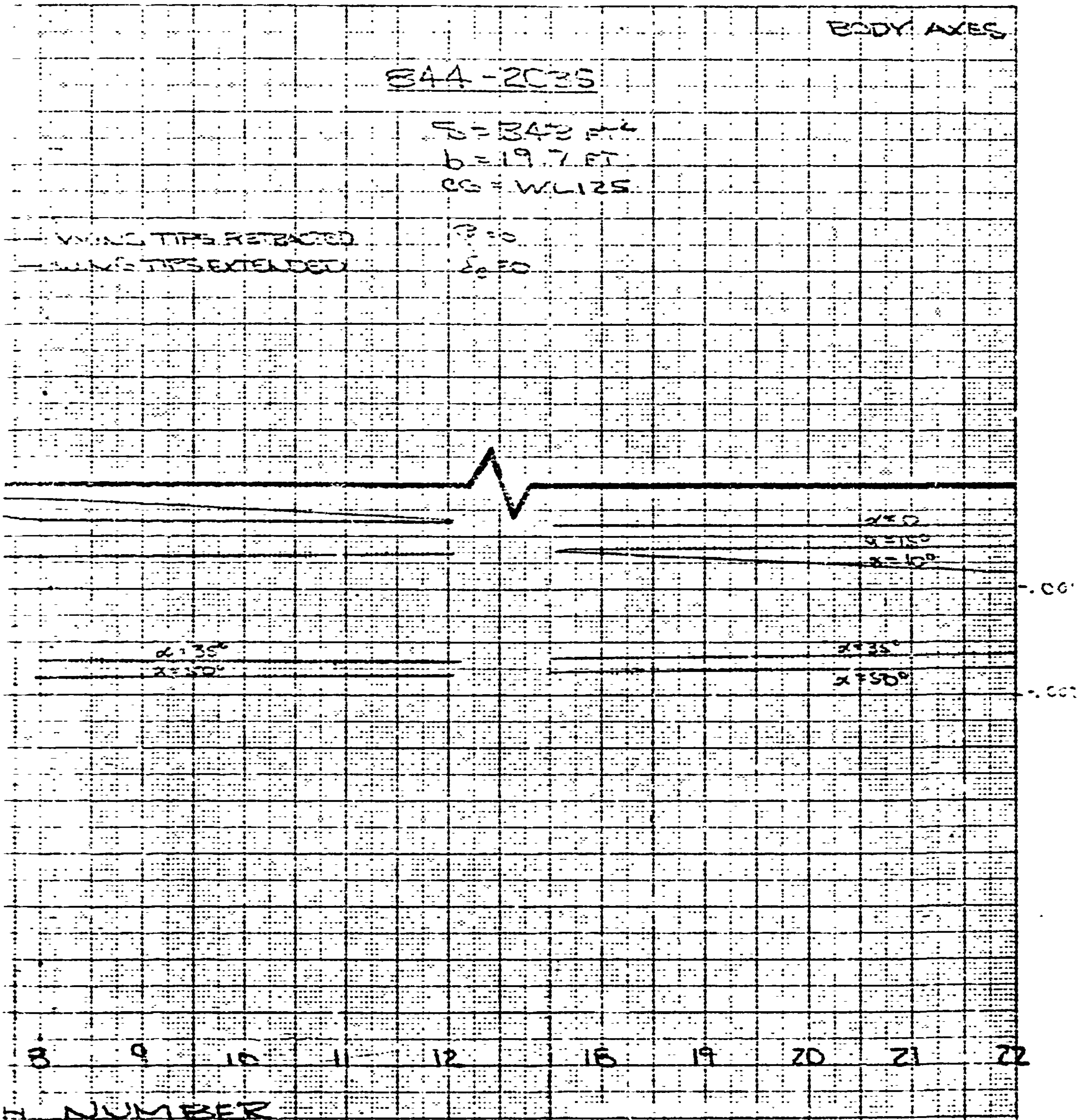

FIG. 6.2
844-2035

LATERAL STABILITY

D2-8174
PAGE 6.5

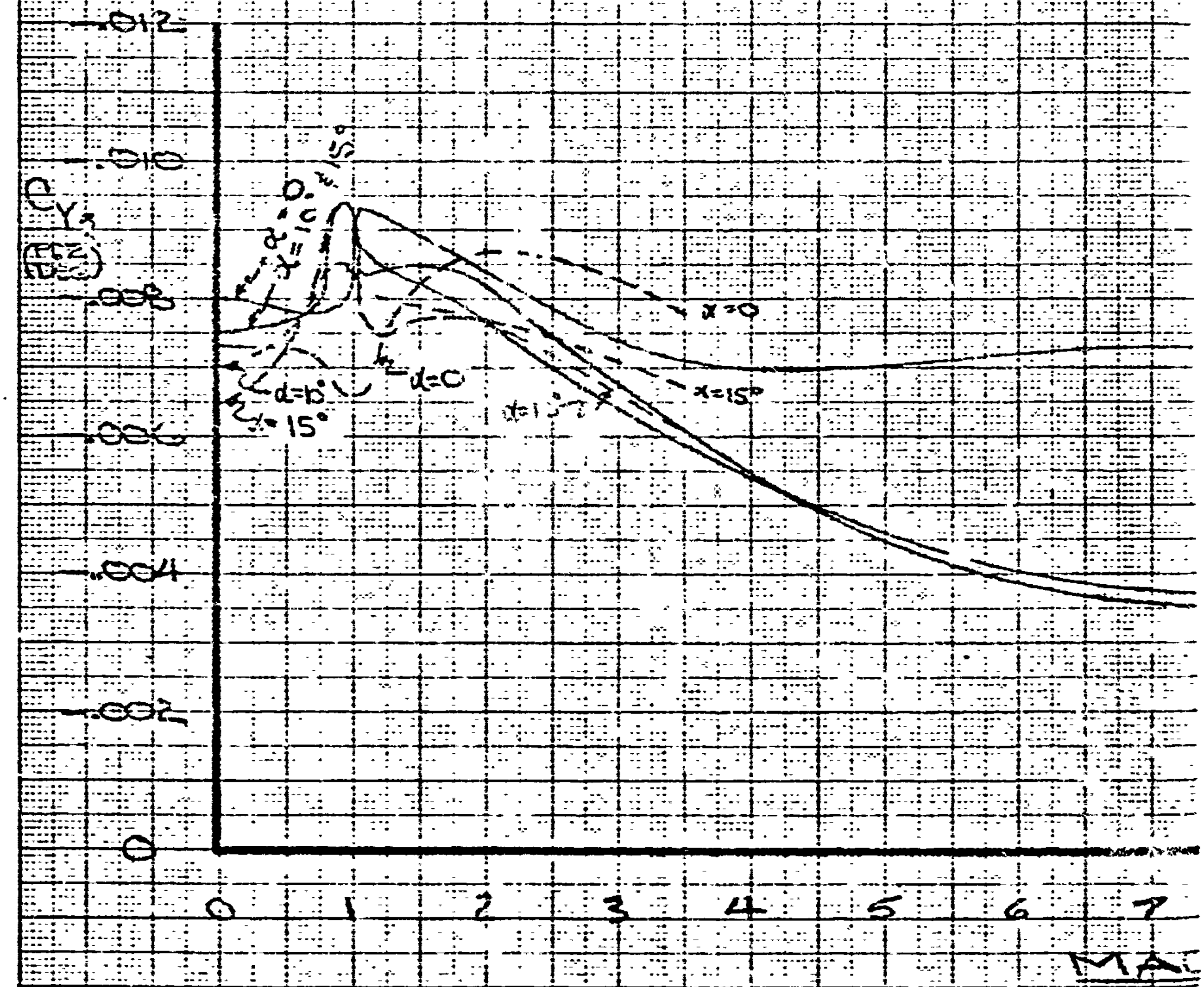
.012
.010
.008
.006
.004
.002
0
0
1
2
3
4
5
6
7
α=0
α=15°
α=0
α=15°

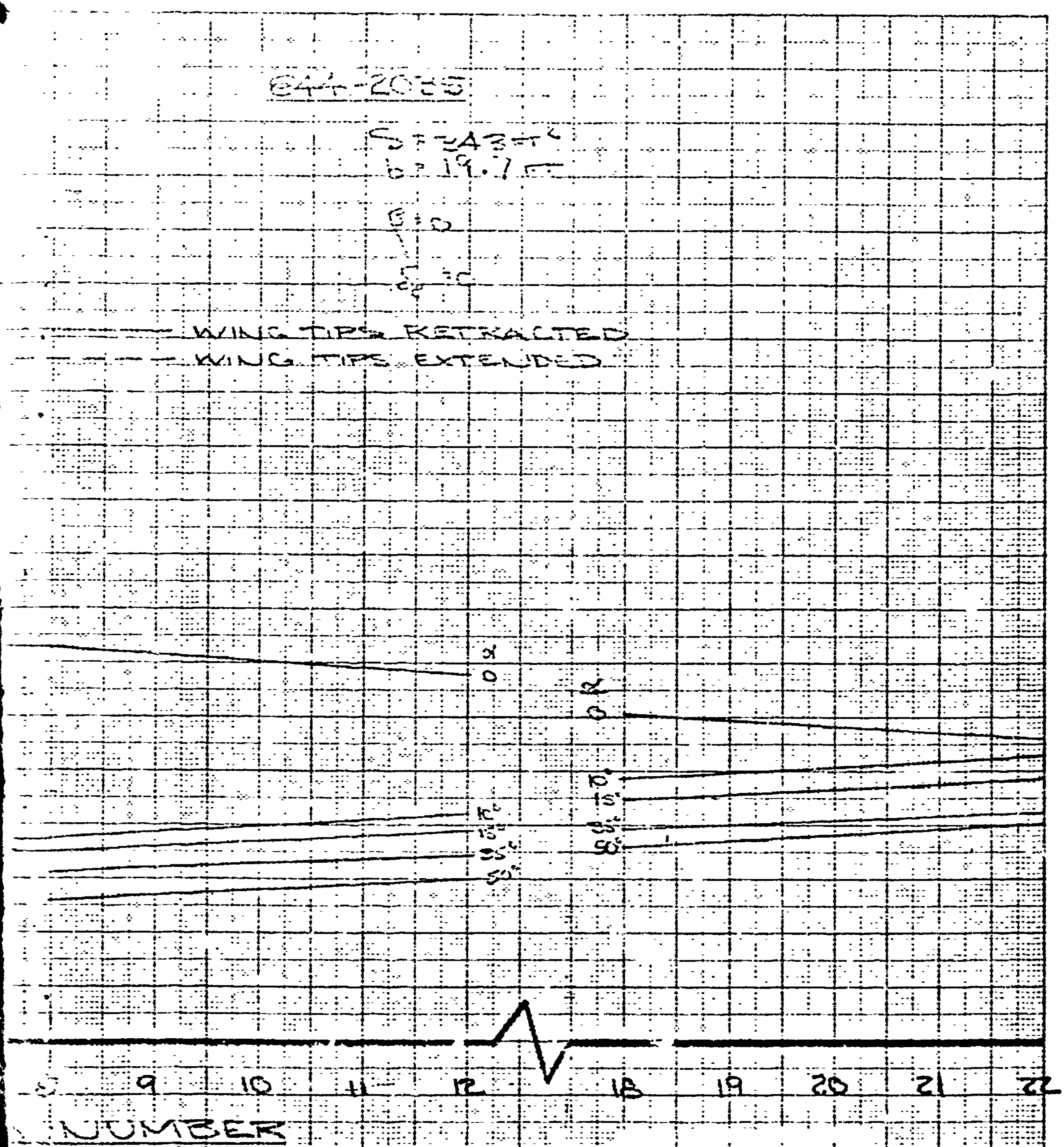

CALC EER	12-22-C	REVISED	DATE	SIDE FORCE
CHECK				
APD				
APD				

FIG 6.9
644-2055
D2-8174
6.6

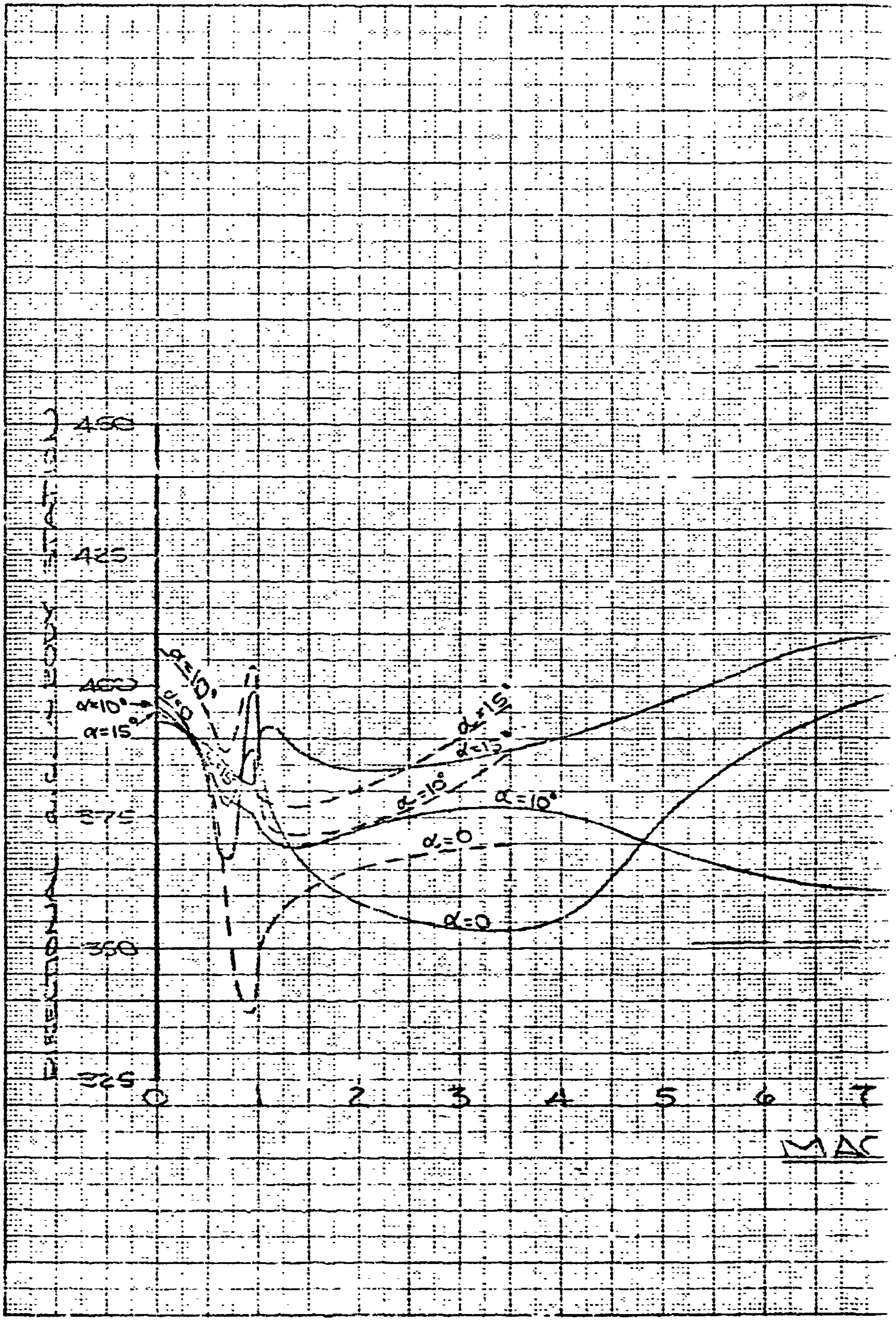
450
425
400
375
350
325
α=10°
α=15°
α=10°
α=0
α=15°
α=15°
α=10°
α=10°
α=0
α=0
0
1
2
3
4
5
6
7
MAC

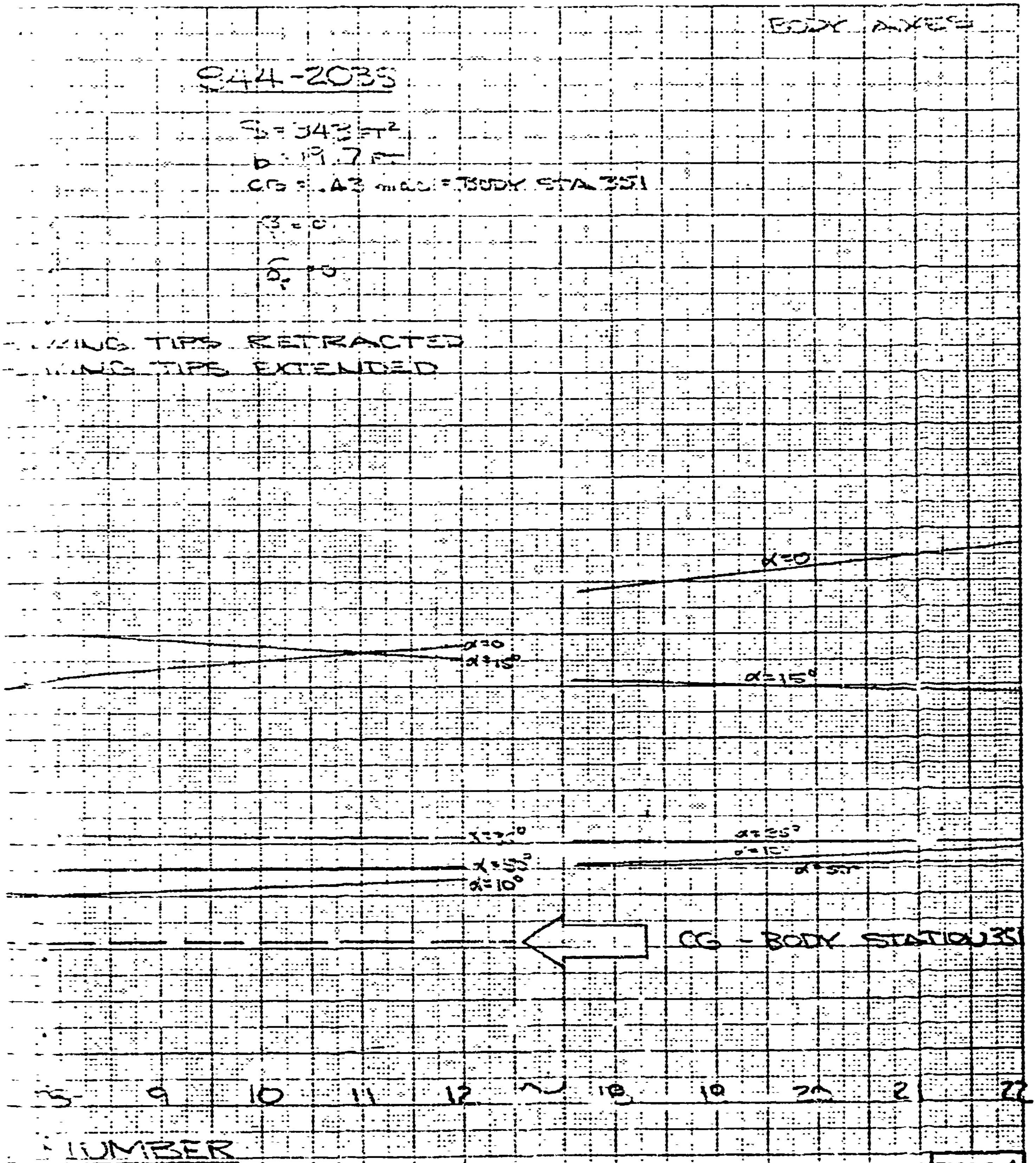

CALC BFR	12-2-0	REVISED	DATE
CHECK			
APPD			
APPD			

DIRECTIONAL a.c.

FIG 6.4
844-2035

D2-8174

PAGE 6.7

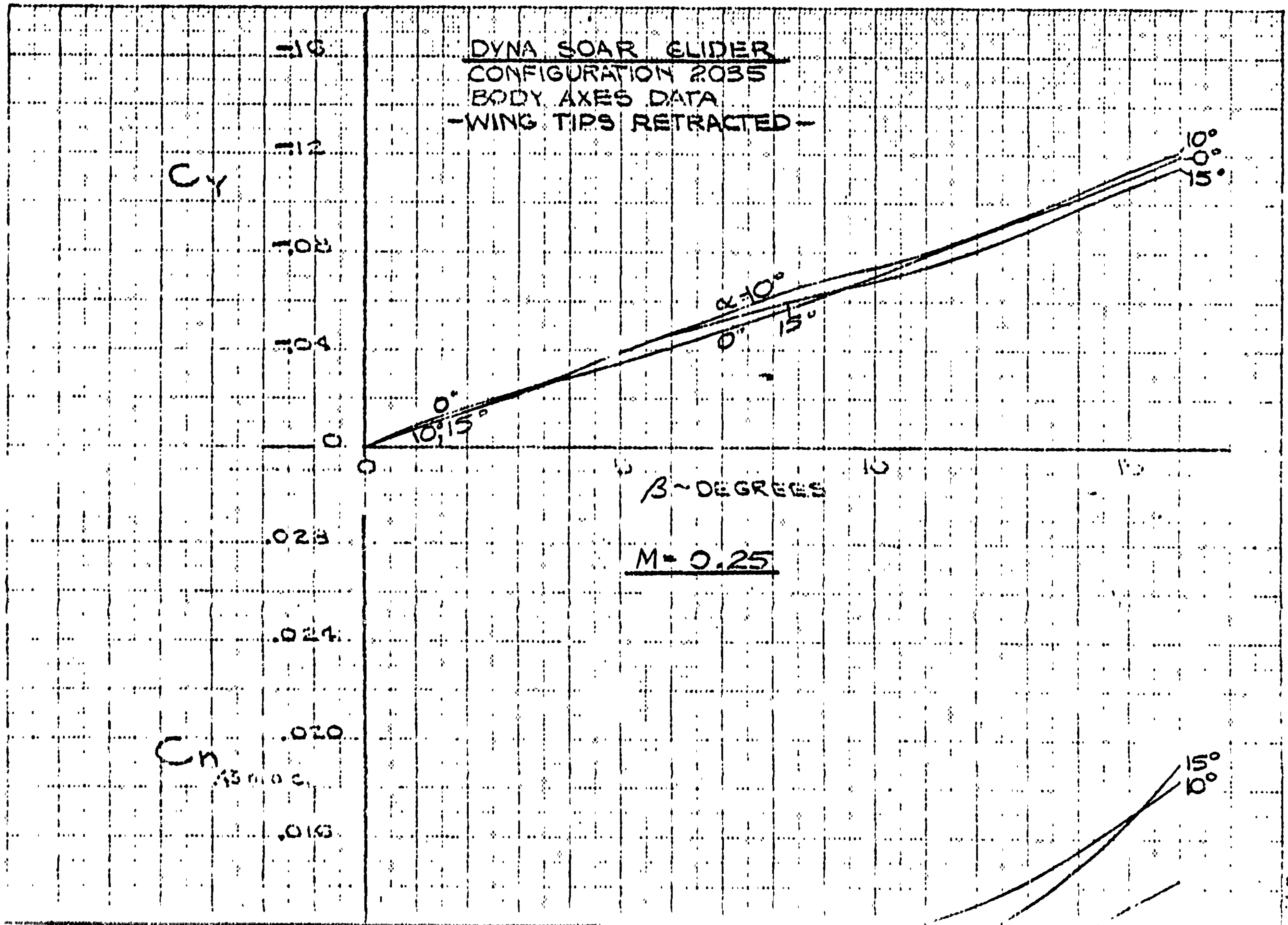

DYNA SOAR GLIDER
CONFIGURATION 2035
BODY AXES DATA
-WING TIPS RETRACTED-
M = 0.25
β ~ DEGREES
C_Y
C_n
-.16
-.12
-.08
-.04
0
.028
.024
.020
.016
0
5
10
15
α=10°
0°
15°
10°
15°

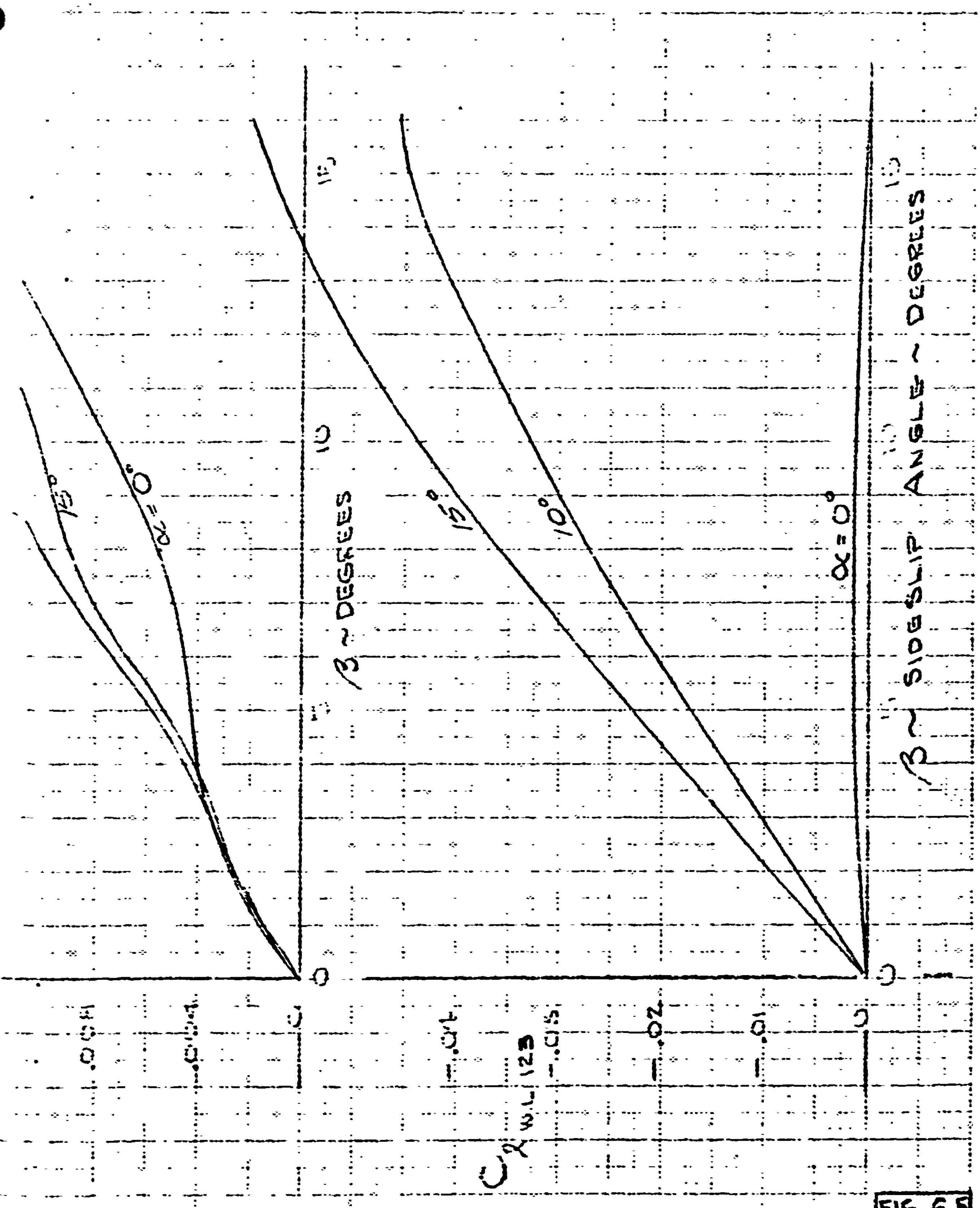

RKR/PTV 12-7	LATERAL - DIRECTIONAL STABILITY CHARACTERISTICS —WING TIPS RETRACTED— —LANDING SPEED—	FIG 6.5 844-2035 D2-8174 6.8

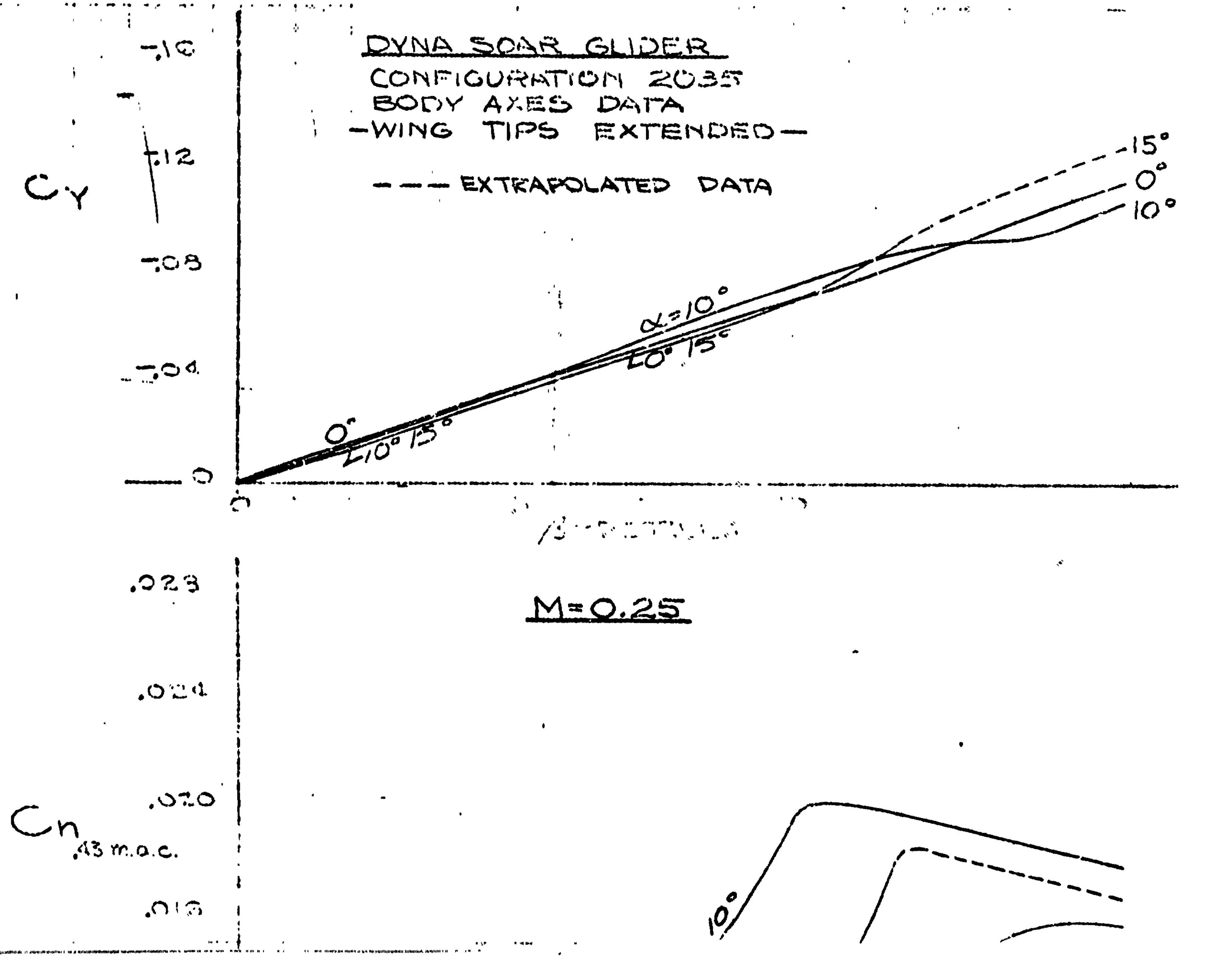
DYNA SOAR GLIDER
CONFIGURATION 2035
BODY AXES DATA
—WING TIPS EXTENDED—
— — — EXTRAPOLATED DATA
-.16
-.12
-.08
-.04
0
C_Y
-15°
0°
10°
α=10°
0° 15°
0°
10° 15°
M=0.25
.028
.024
.020
.016
$C_{n_{.43 m.a.c.}}$
10°

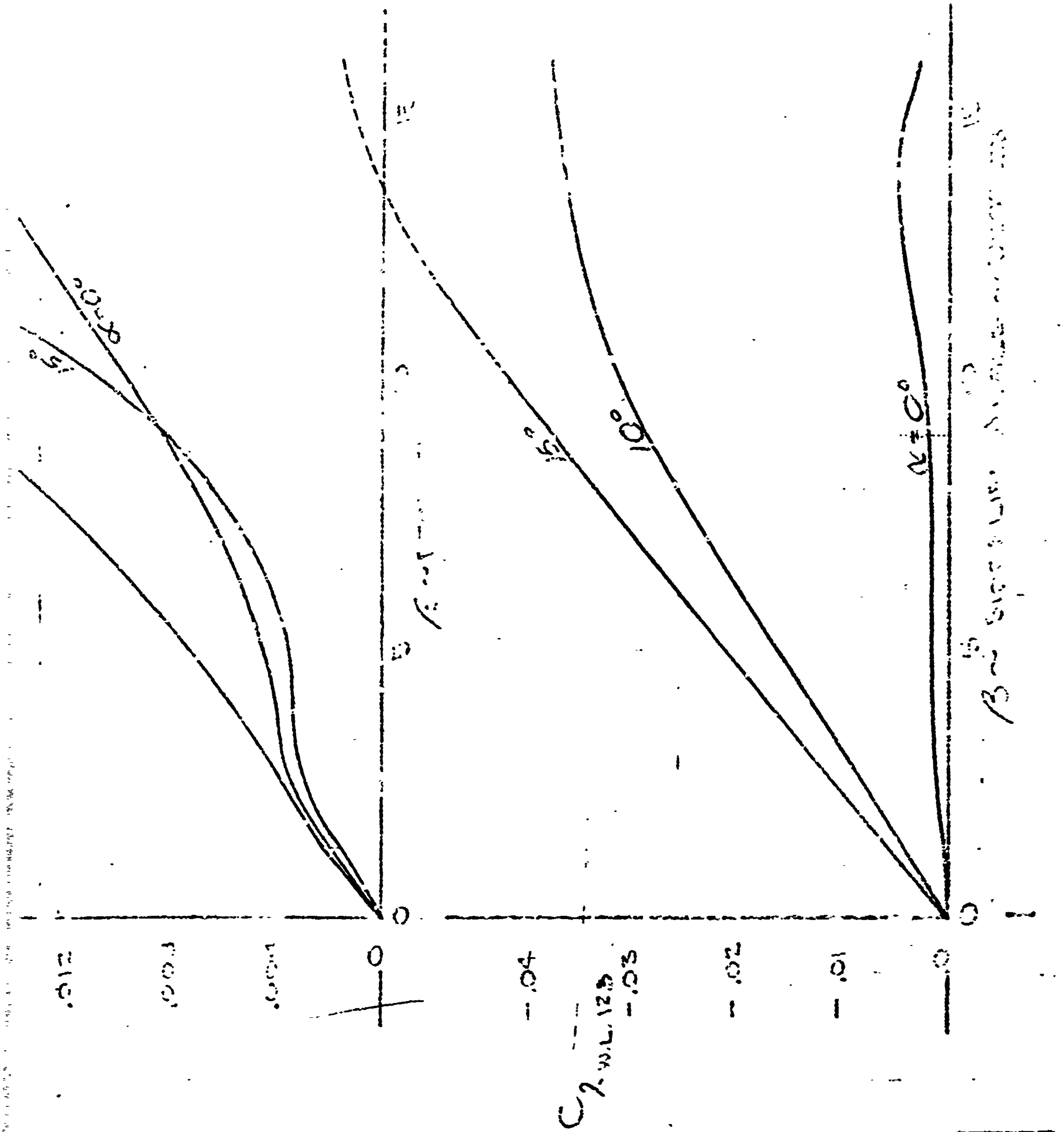

CALC	RWSVITY	12-6	REVISED	DATE	LATERAL - DIRECTIONAL	FIG 6.3
CHECK					STABILITY CHARACTERISTICS	844-2035
APPD					— WING TIPS EXTENDED —	D2-8174
APPD						PAGE
					— LANDING SPEED —	6.9

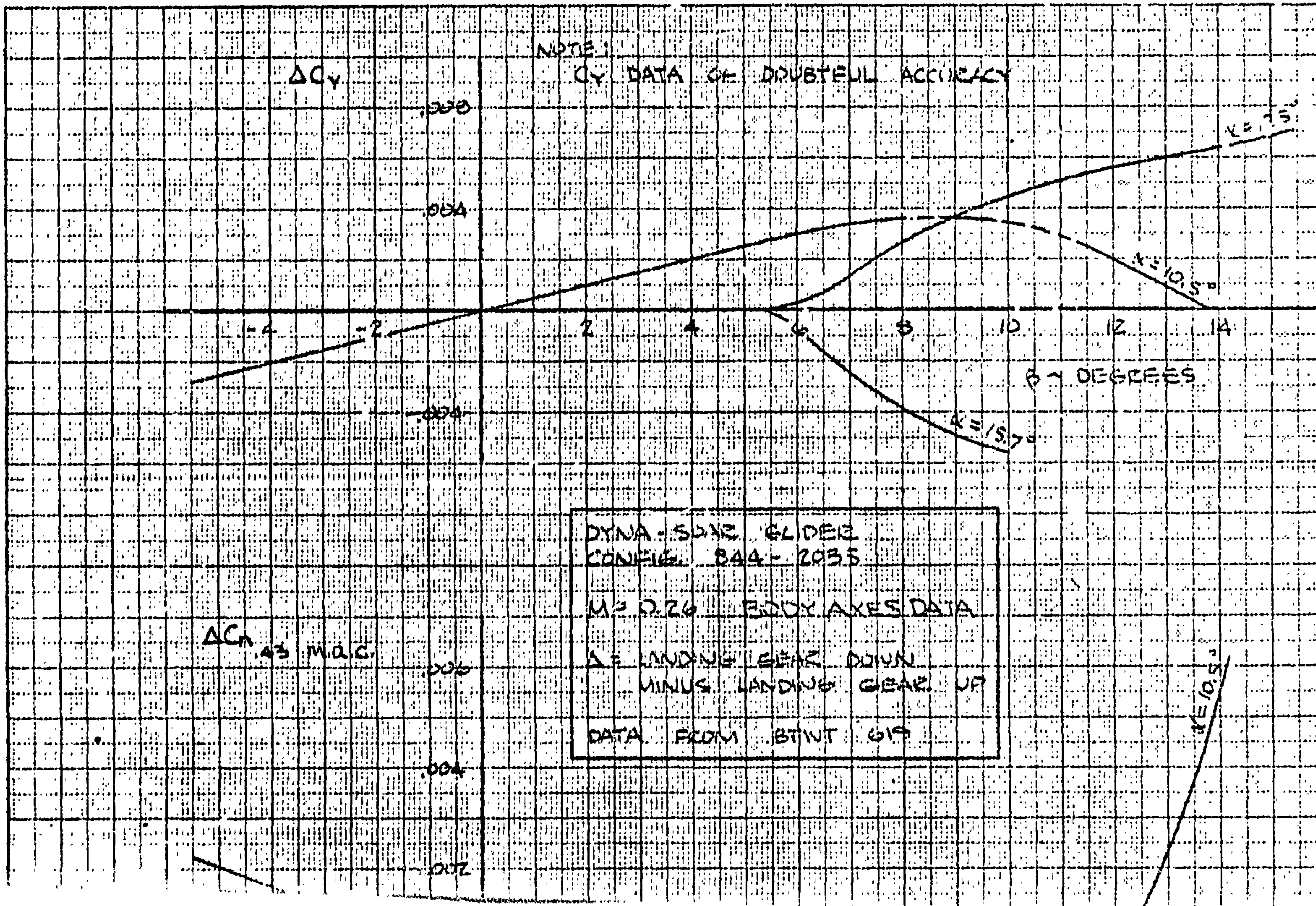

NOTE:
C_Y DATA OF DOUBTFUL ACCURACY
ΔC_Y
.008
.004
-.004
-4
-2
2
4
6
8
10
12
14
β ~ DEGREES
α = 7.5°
α = 10.5°
α = 15.7°
ΔC_{n} .43 M.A.C.
.006
.004
.002
DYNA-SOAR GLIDER
CONFIG. 844-2035
M = 0.26 BODY AXES DATA
Δ = LANDING GEAR DOWN
MINUS LANDING GEAR UP
DATA FROM BTWT 619

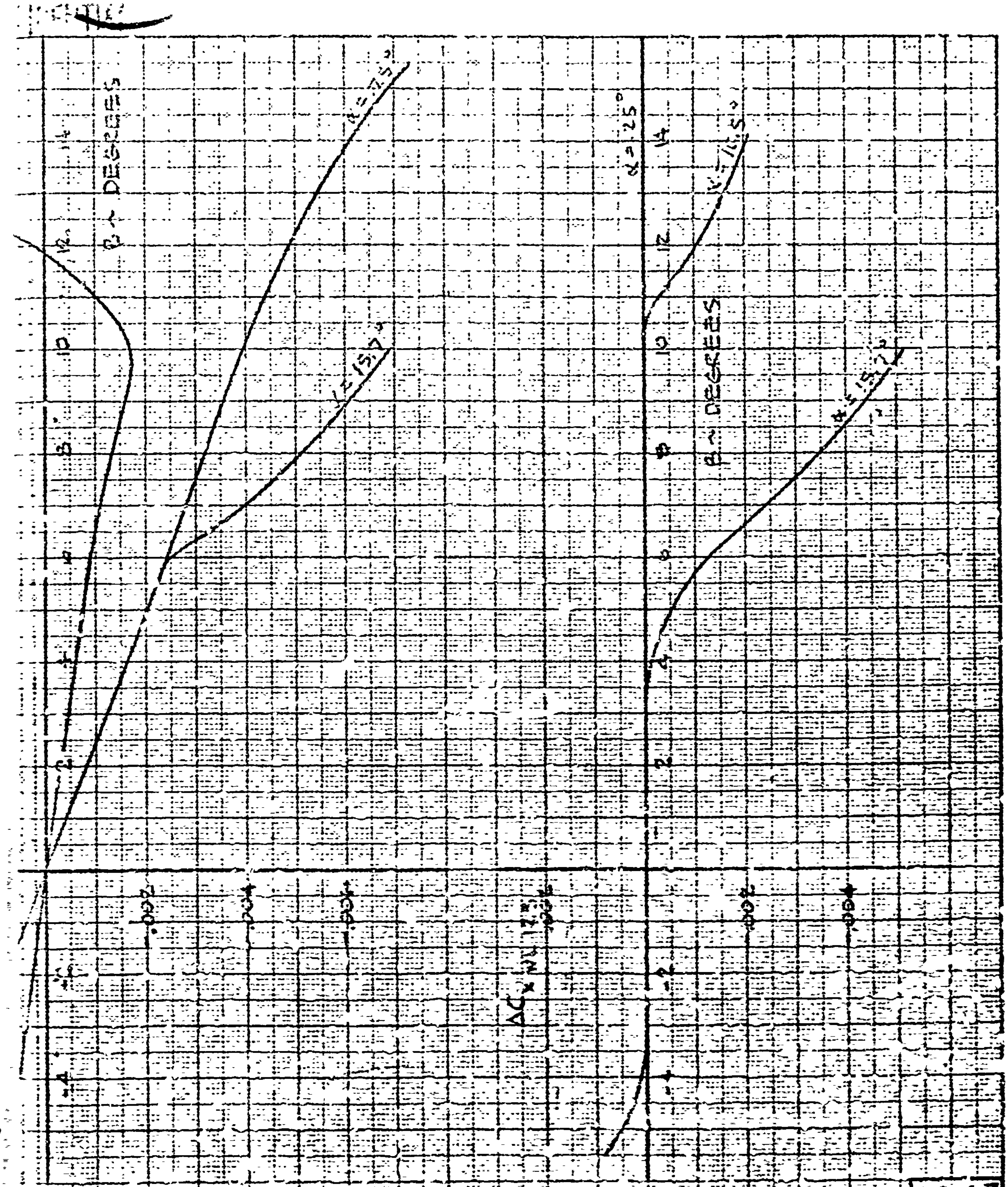

CALC	MOORE	12-9-60	REVISED	DATE	INCREMENTAL EFFECT OF LANDING GEAR
CHECK					
APPD					
APPD					BOEING AIRPLANE COMPANY SEATTLE 14, WASHINGTON

FIG 6.7

844-7035

D2-8174

PAGE 6.10

BAC 1033-R-4

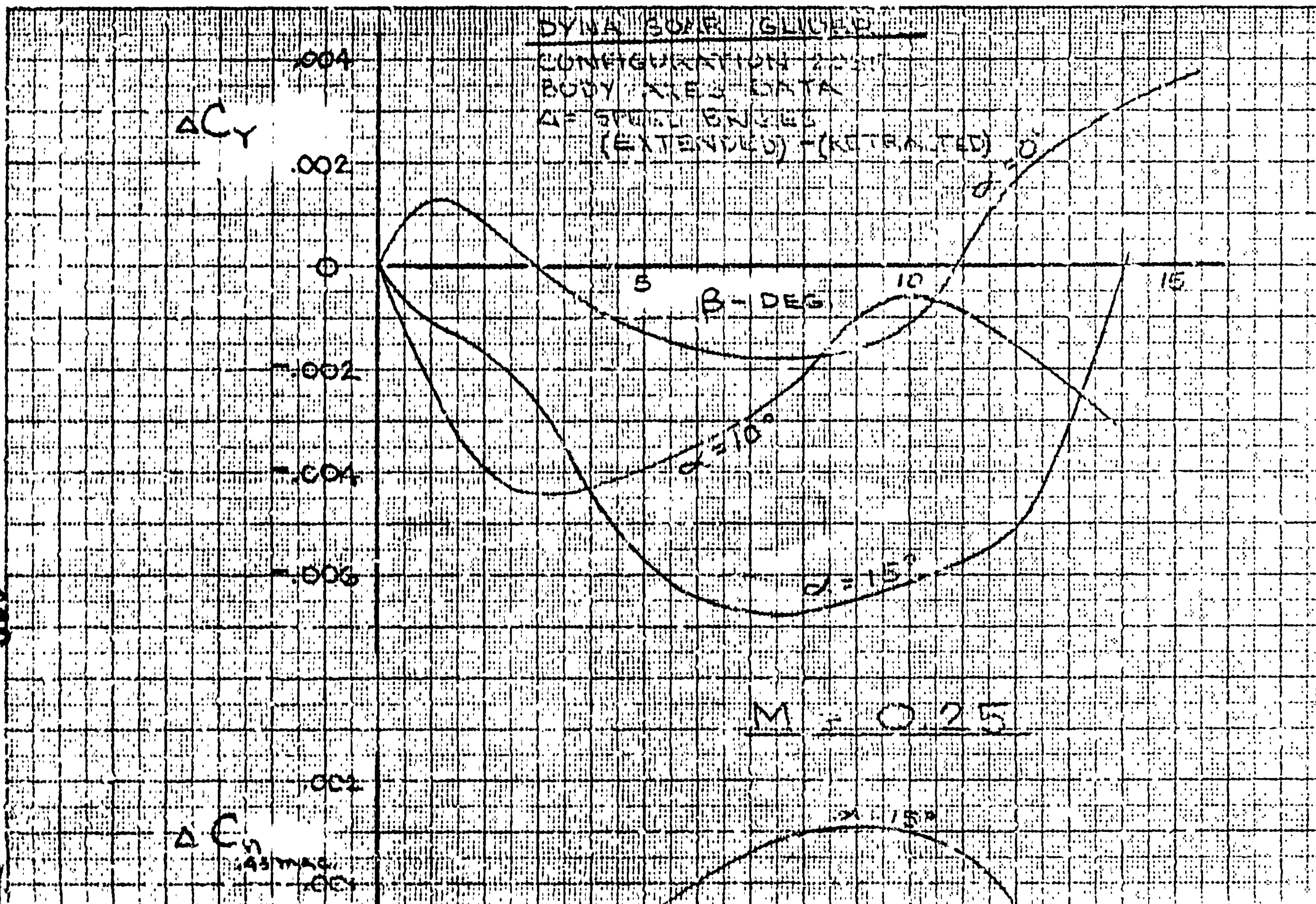
DYNA SOAR GLIDER
CONFIGURATION
BODY AXES DATA
ΔCY
.004
.002
0
-.002
-.004
-.006
5
10
15
β - DEG
α = 0°
α = 10°
α = 15°
M = 0.25
.002
ΔCn
.001
α = 15°

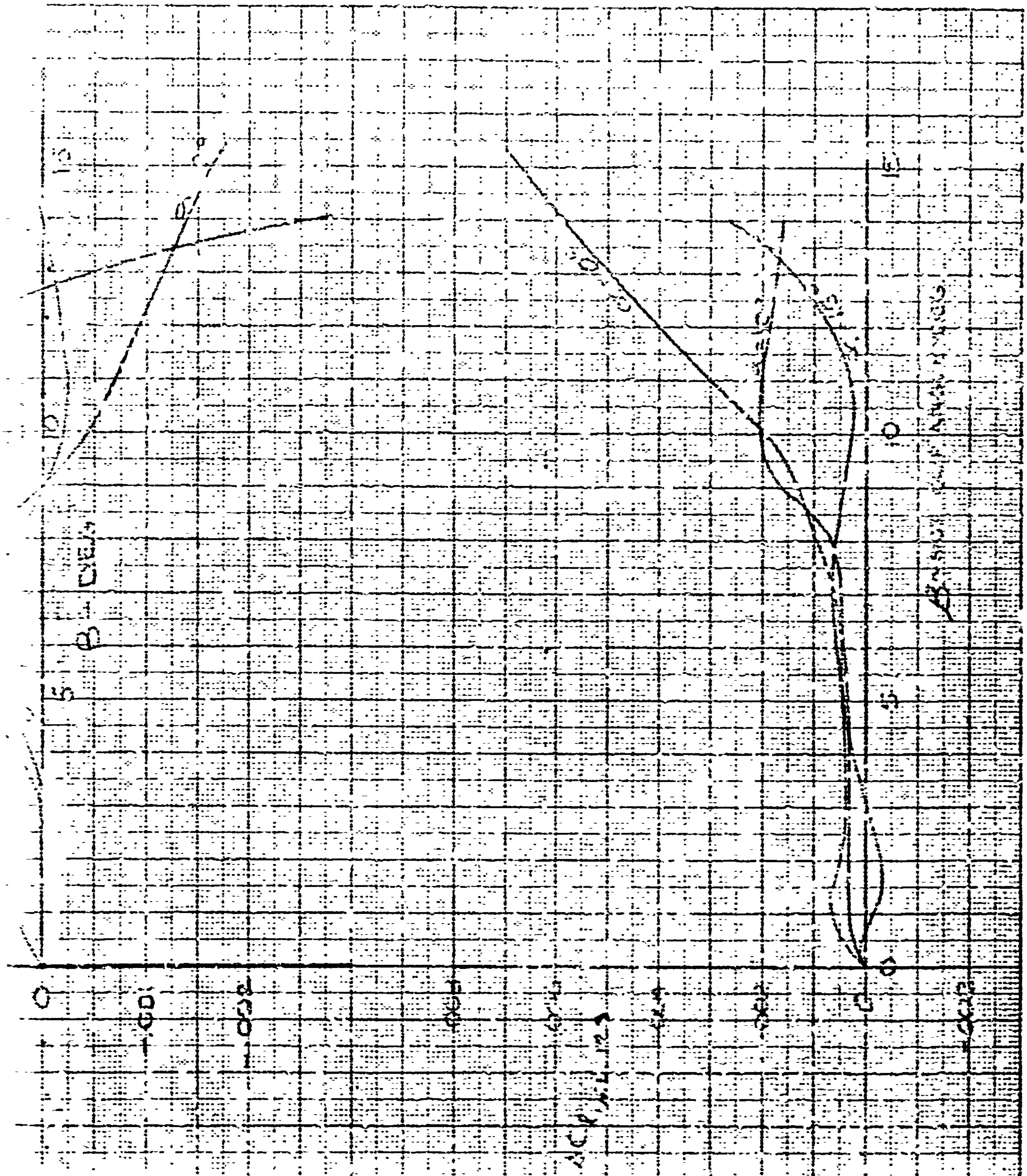

INCREMENTAL EFFECT OF SPEED BRAKES

LANDING SPEED

FTV

FIG 6.B

B44-CC35

D2-6174

PAGE 6.11

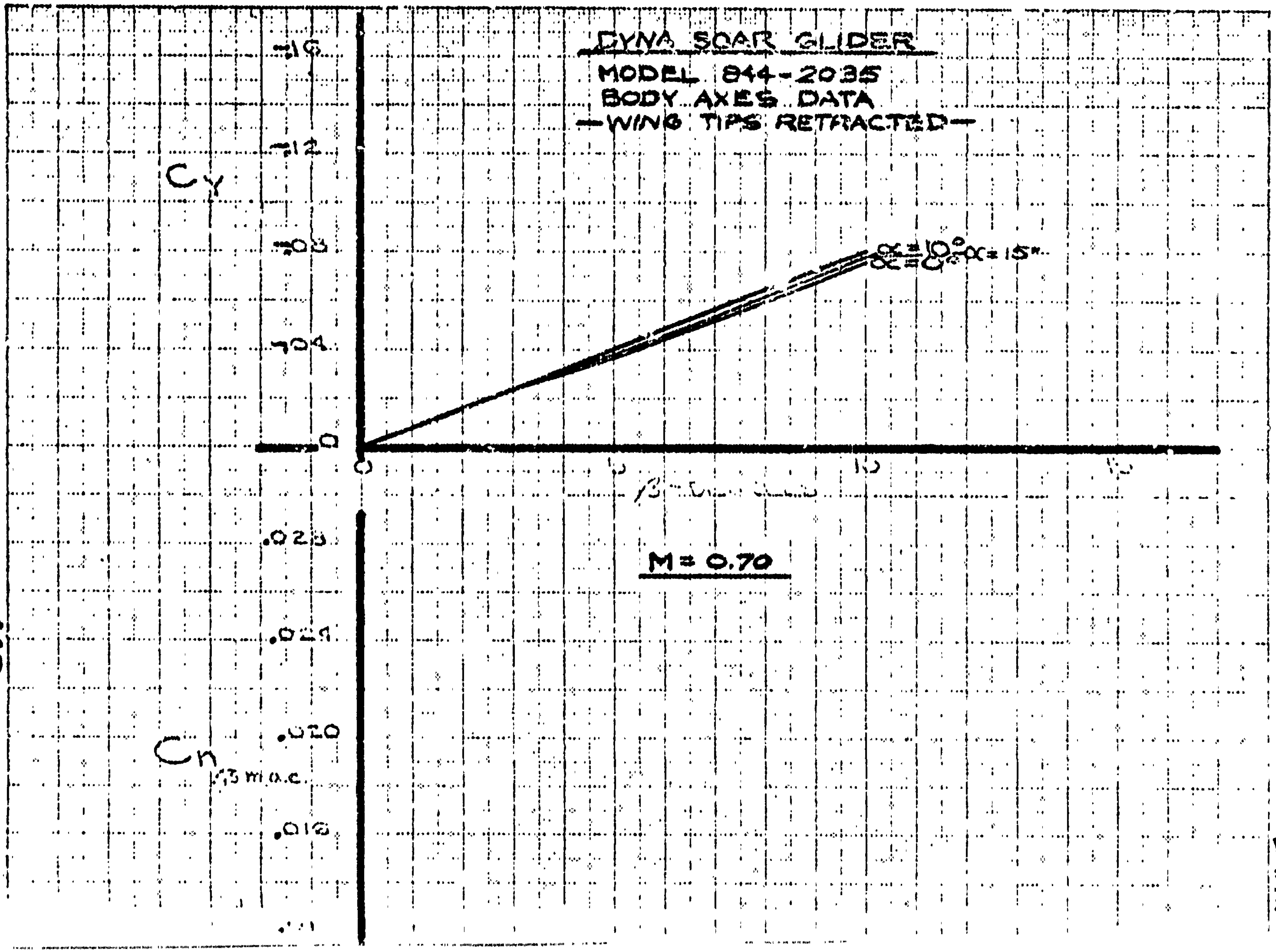
DYNA SOAR GLIDER
MODEL 844-2035
BODY AXES DATA
—WING TIPS RETRACTED—
C_Y
-.16
-.12
-.08
-.04
0
$\alpha = 10°$
$\alpha = 0°$
$\alpha = 15°$
M = 0.70
$C_{n_{.3 m.a.c.}}$
.028
.024
.020
.016

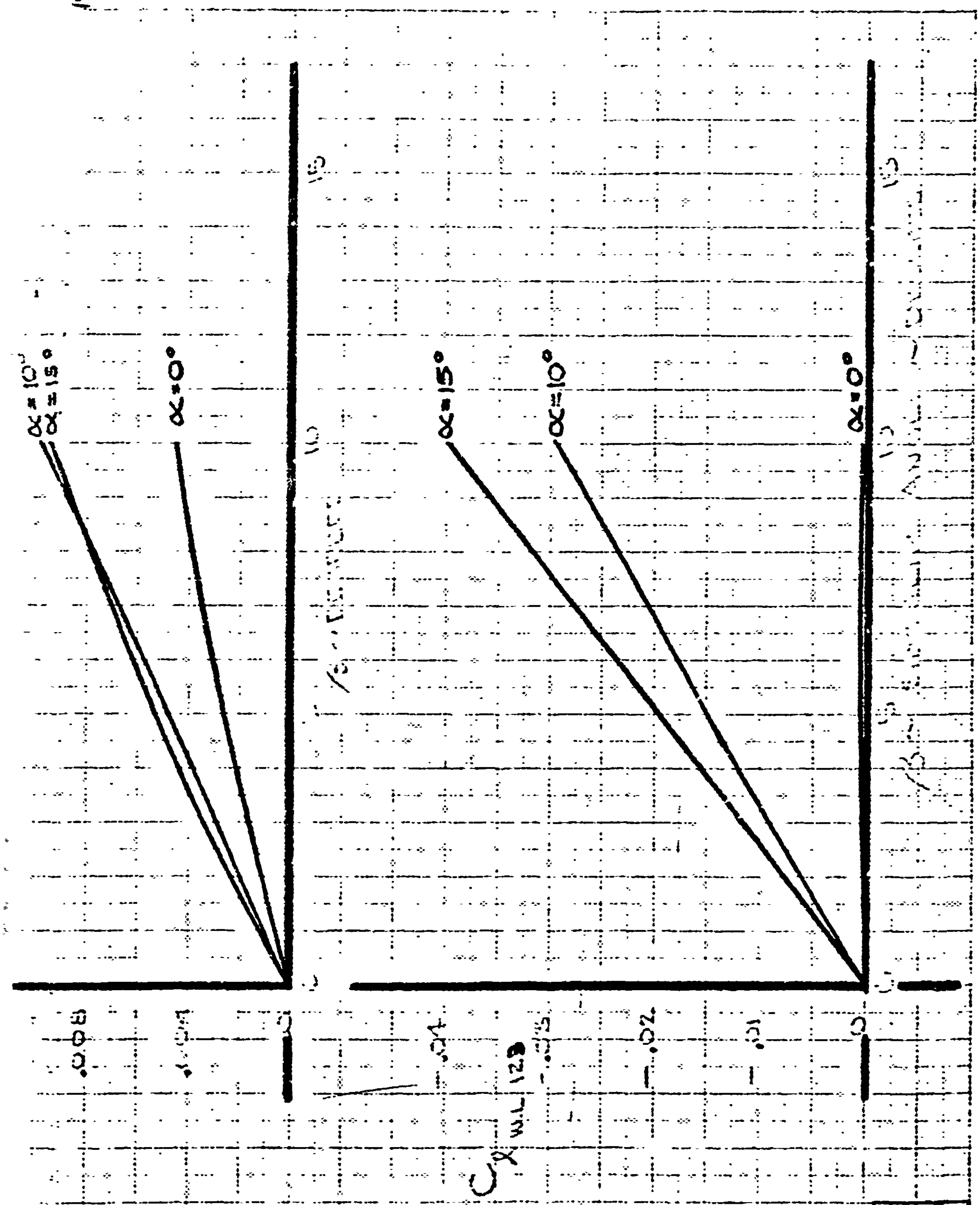

RKR	12-2060	LATERAL-DIRECTIONAL STABILITY CHARACTERISTICS- WING TIPS RETRACTED	FIG 6.9
		M= 0.70	844-2055
			D2-8174
			6.12

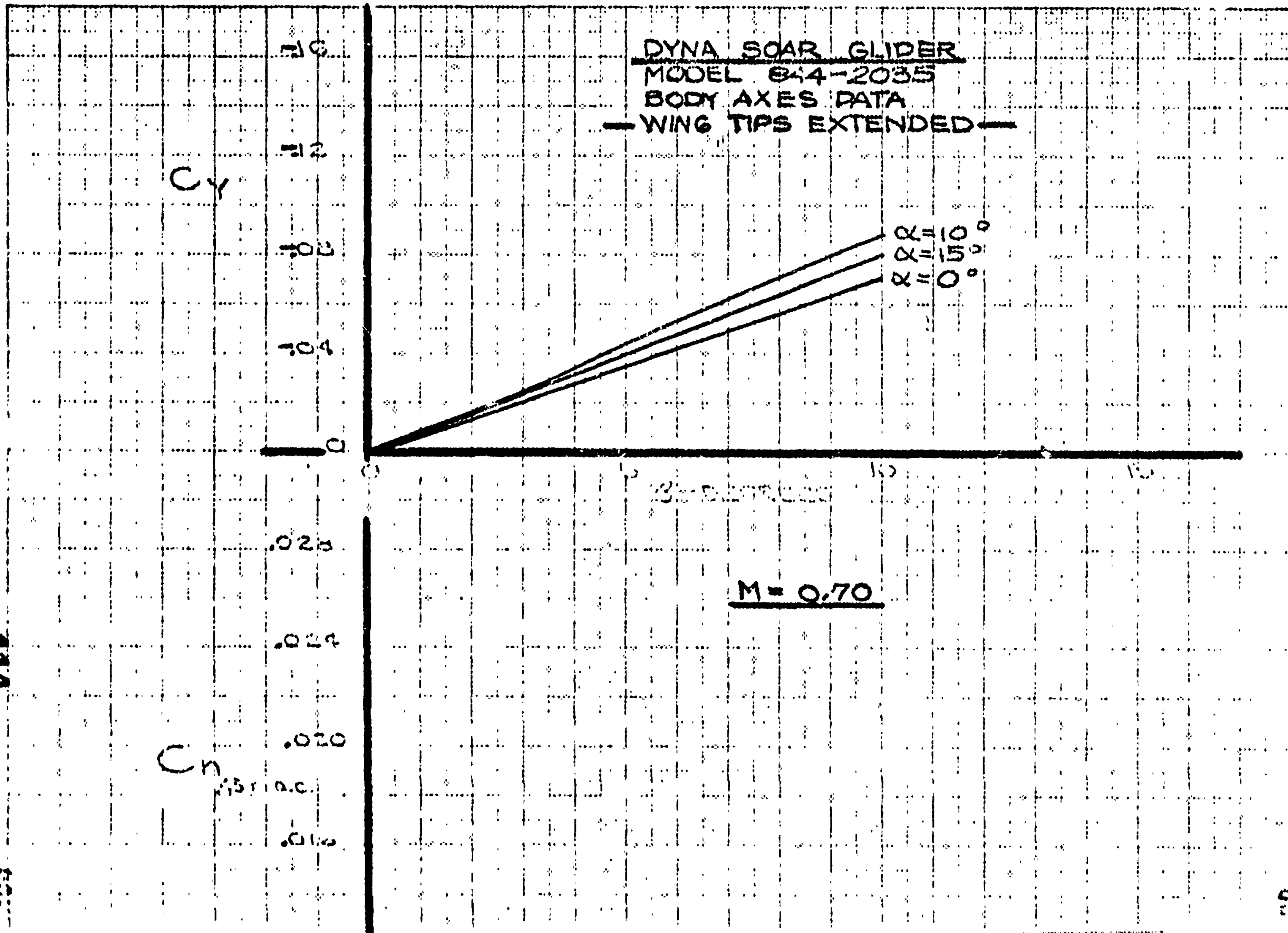
DYNA SOAR GLIDER
MODEL 844-2035
BODY AXES DATA
—WING TIPS EXTENDED—
M = 0.70
α=10°
α=15°
α=0°
Cy
Cn
.028
.024
.020
0

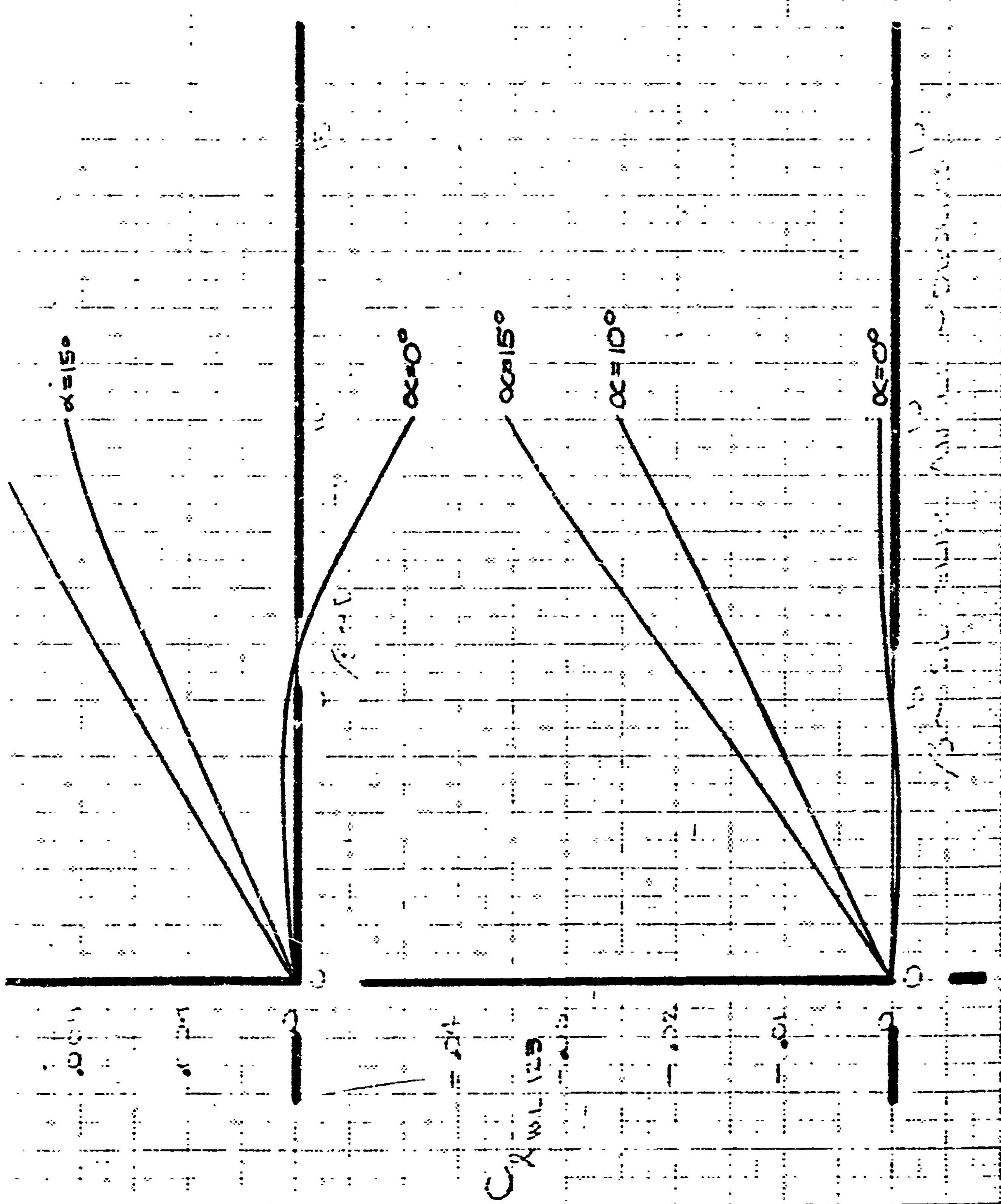

RKR 12-20-61

FIG 6.10

LATERAL - DIRECTIONAL STABILITY CHARACTERISTICS —WING TIPS EXTENDED—

M = 0.70

244-2095

D2-8174

6.13

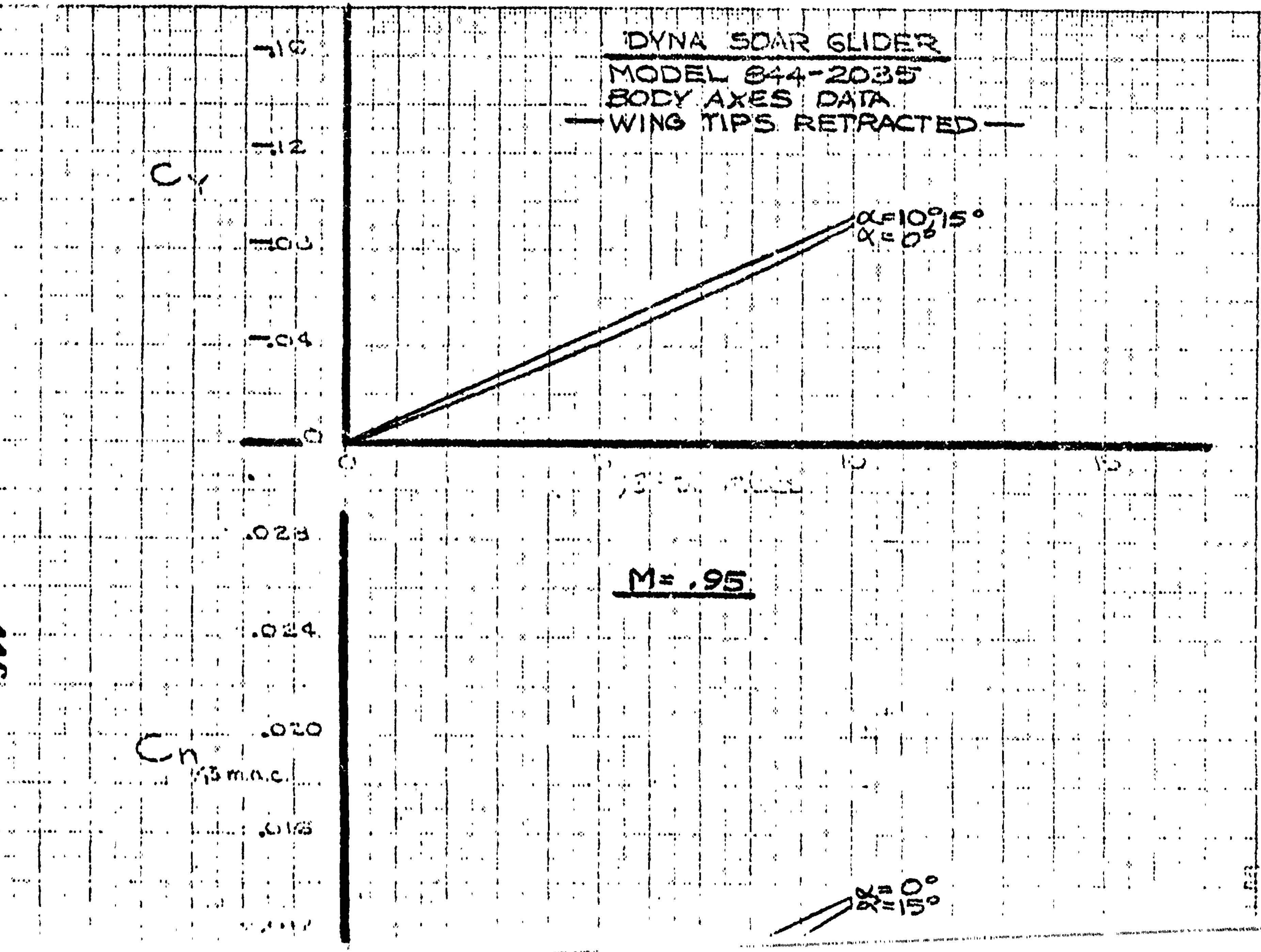
DYNA SOAR GLIDER
MODEL 844-2035
BODY AXES DATA
—WING TIPS RETRACTED—
C_Y
-.16
-.12
-.08
-.04
0
0
5
10
15
α=10°,15°
α=0°
M= .95
.028
.024
.020
.016
$C_{n_{.13\,m.a.c.}}$
α=0°
α=15°

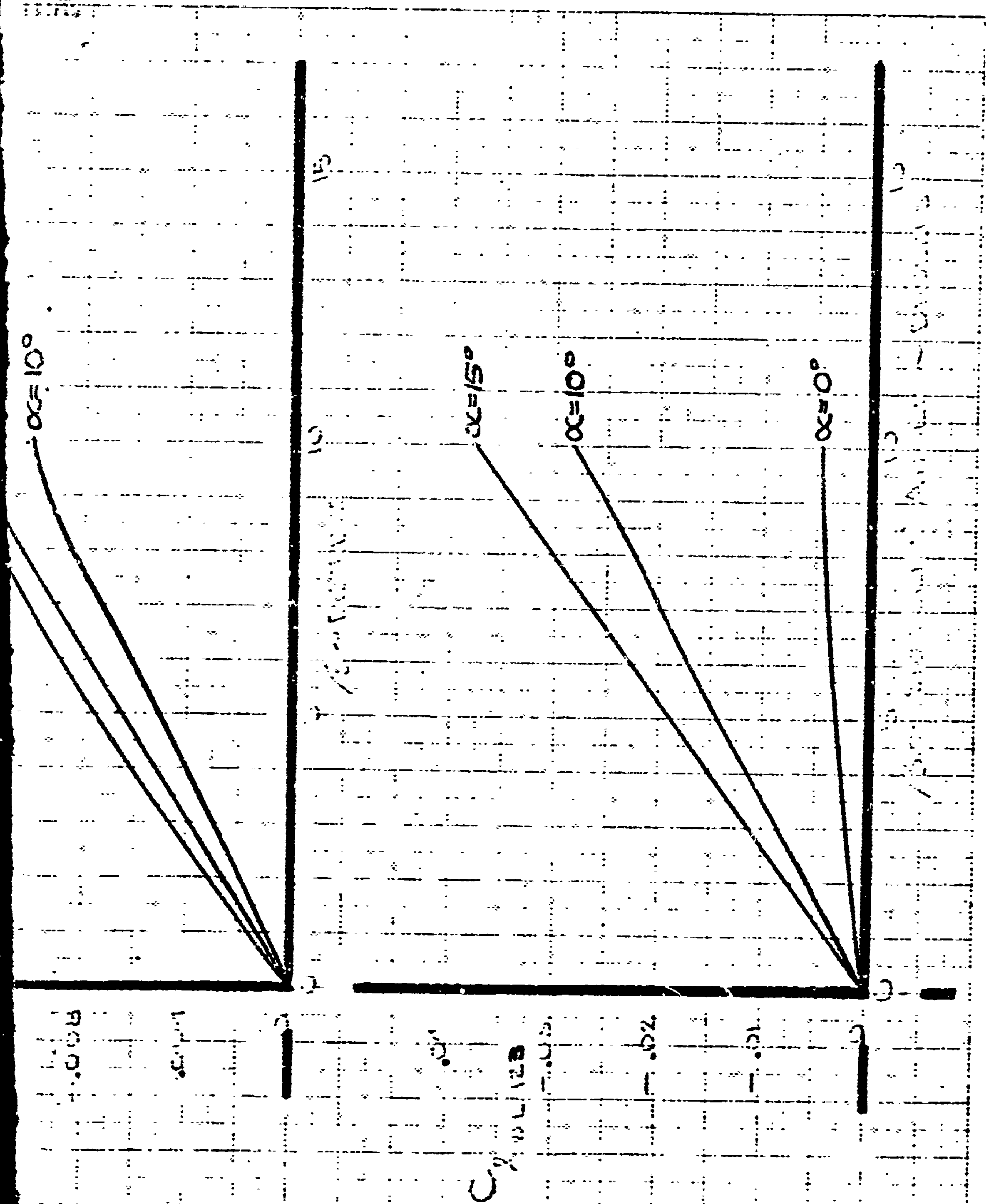

RKR	12-22-60	LATERAL-DIRECTIONAL STABILITY CHARACTERISTICS WING TIPS RETRACTED	FIG 6.11 844-2055 D2-8174
		M=.95 117	6.14

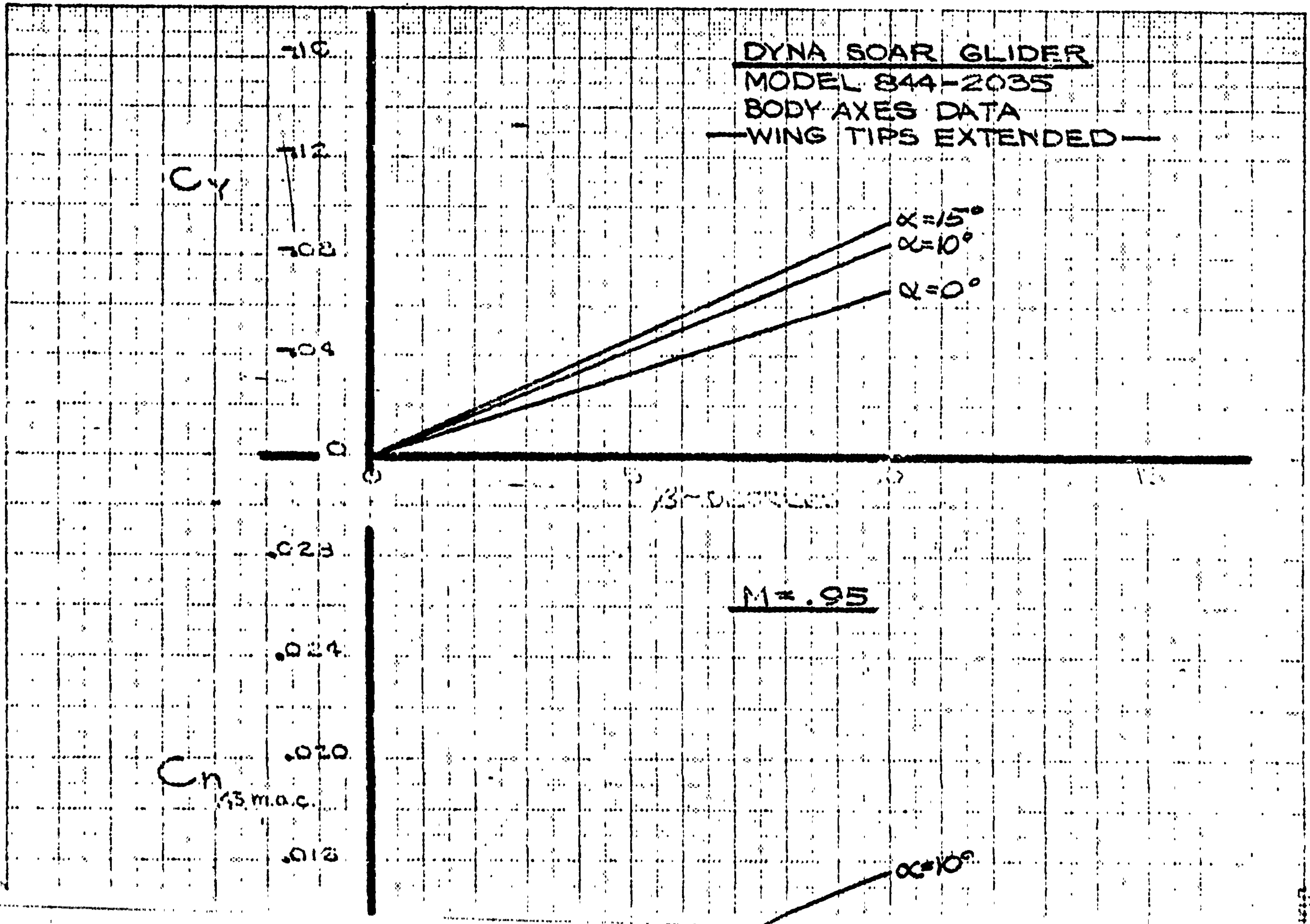

DYNA SOAR GLIDER
MODEL 844-2035
BODY AXES DATA
—WING TIPS EXTENDED—
α=15°
α=10°
α=0°
M=.95
α=10°
C_Y
$C_{n_{.25\,m.a.c.}}$
.16
.12
.08
.04
0
.028
.024
.020
.016

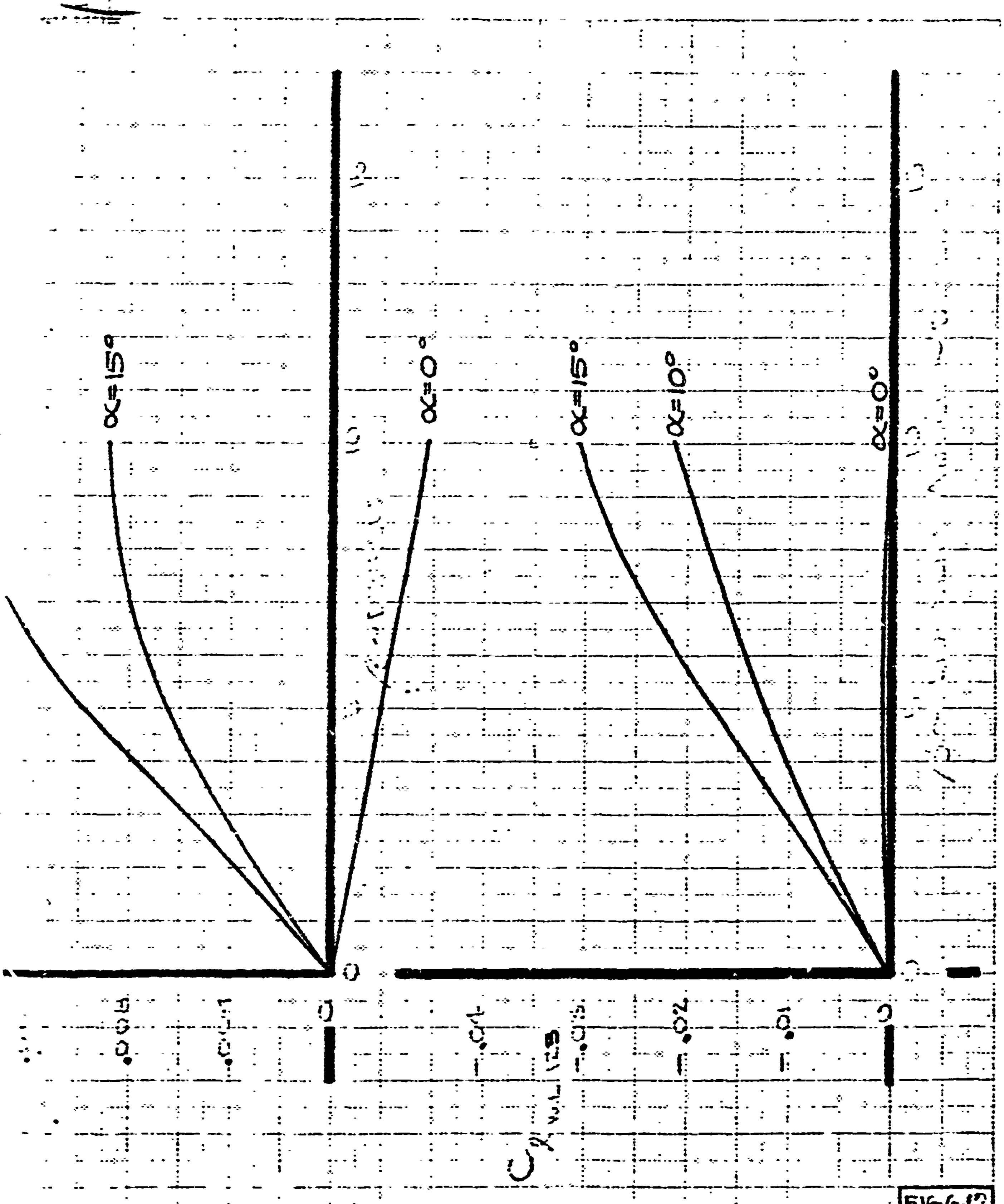

FIG 6.12

RKR/NTU 12-22-0

LATERAL- DIRECTIONAL STABILITY CHARACTERISTICS

— WING TIPS EXTENDED —

M= .95

649-2955

D2-8174

6.15

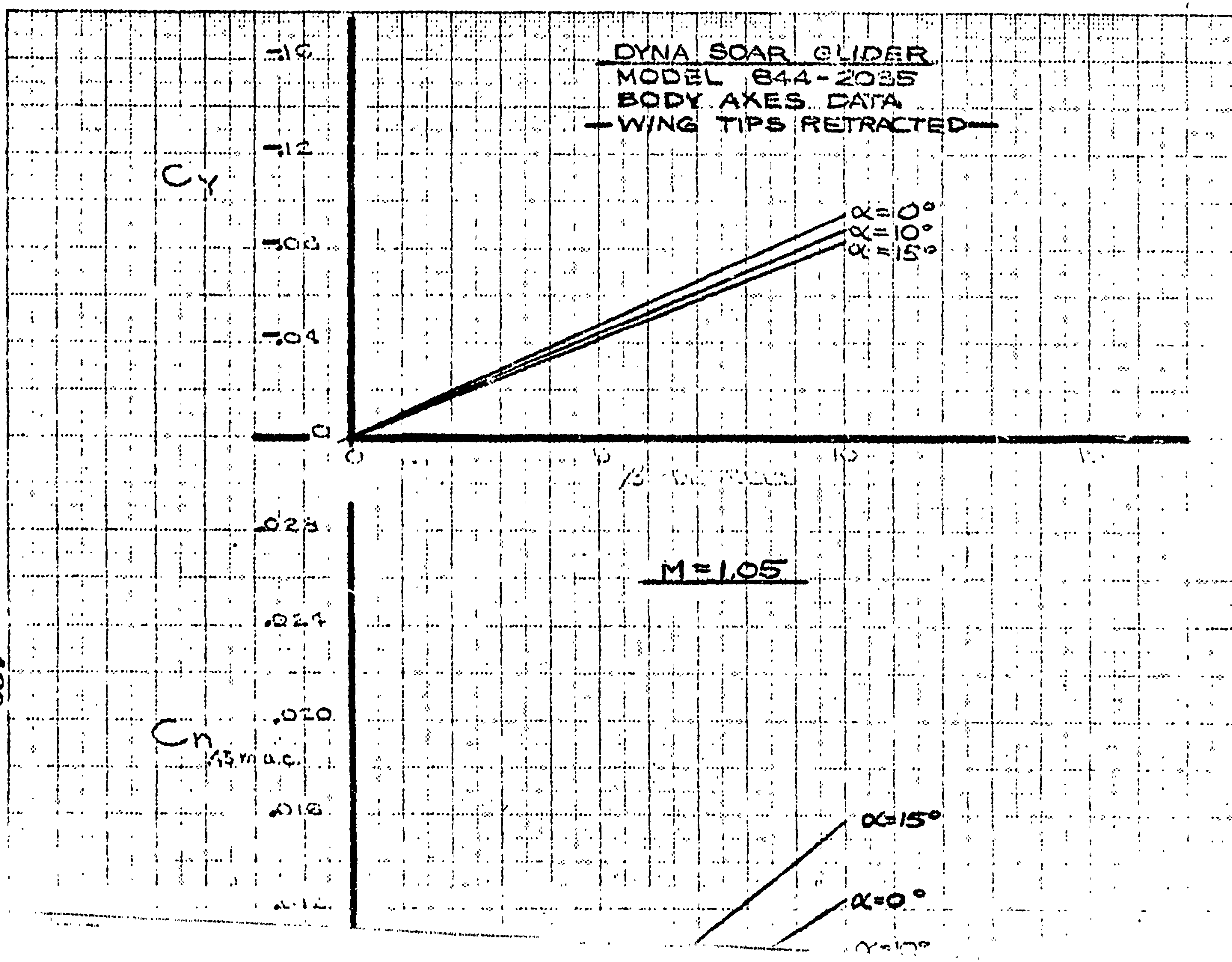
DYNA SOAR GLIDER
MODEL 844-2035
BODY AXES DATA
—WING TIPS RETRACTED—
C_Y
-.16
-.12
-.08
-.04
0
0
5
10
15
α=0°
α=10°
α=15°
M=1.05
$Cn_{.43 m.a.c.}$
.028
.024
.020
.016
.012
α=15°
α=0°

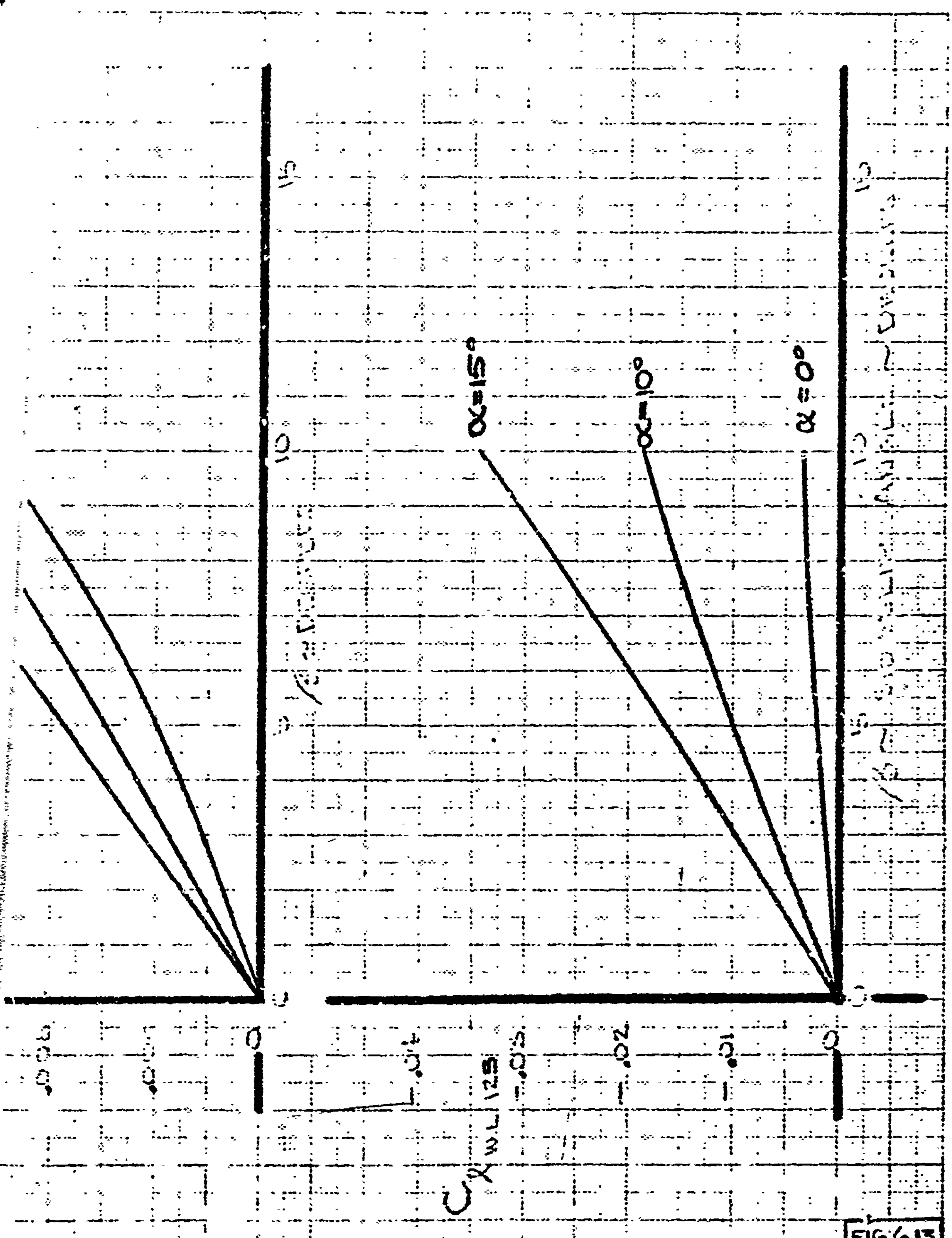

FIG. 6.13

LATERAL - DIRECTIONAL STABILITY CHARACTERISTICS

WING TIPS RETRACTED

M= 1.05

D2-8174

6.16

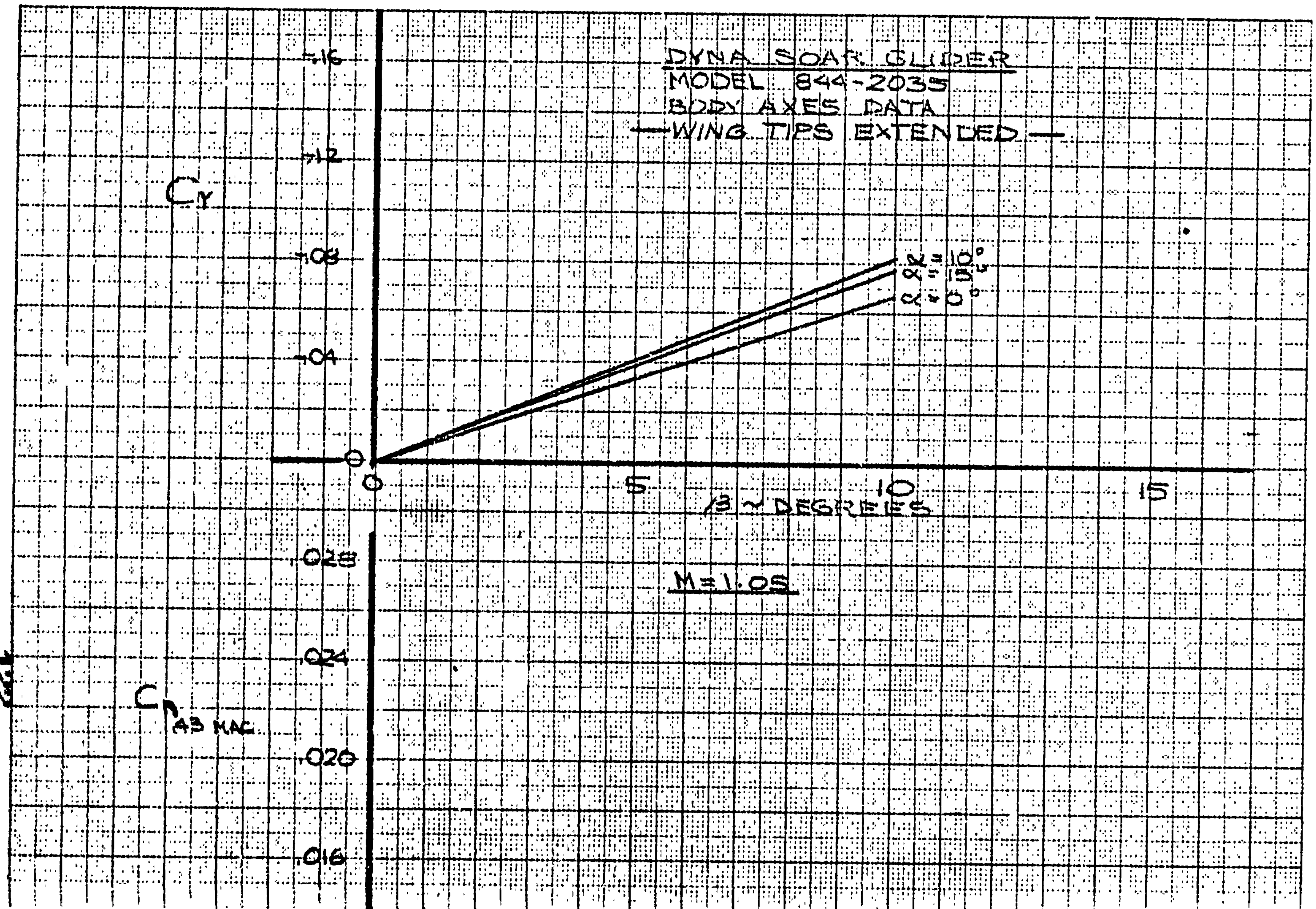

DYNA SOAR GLIDER
MODEL 844-2035
BODY AXES DATA
—WING TIPS EXTENDED—
α = 10°
α = 15°
α = 0°
.16
.12
.08
.04
0
0
5
10
15
β ~ DEGREES
M = 1.05
.028
.024
.020
.016
C_Y
$C_{n_{43\ MAC}}$

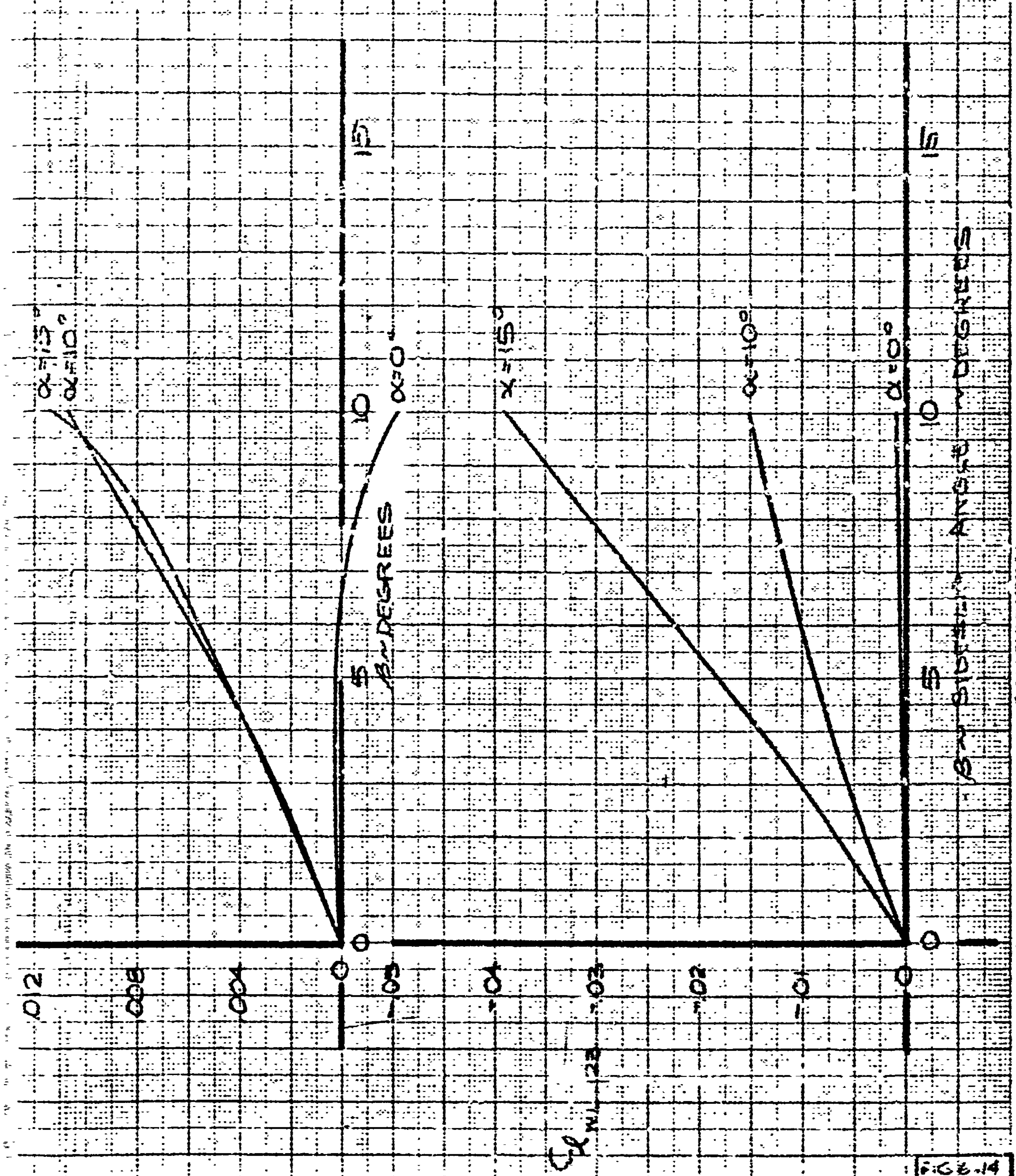

CONFIDENTIAL

CALC	RKR	2/6/??	REVISED	DATE	LATERAL - DIRECTIONAL STABILITY CHARACTERISTICS	FIG. 6.14
CHECK						D2-8174
APPD					WING TIPS EXTENDED — M=1.05	PAGE 6.17
APPD						

84-2035

S = 845 ft²
b = 19.7 ft
[illegible]

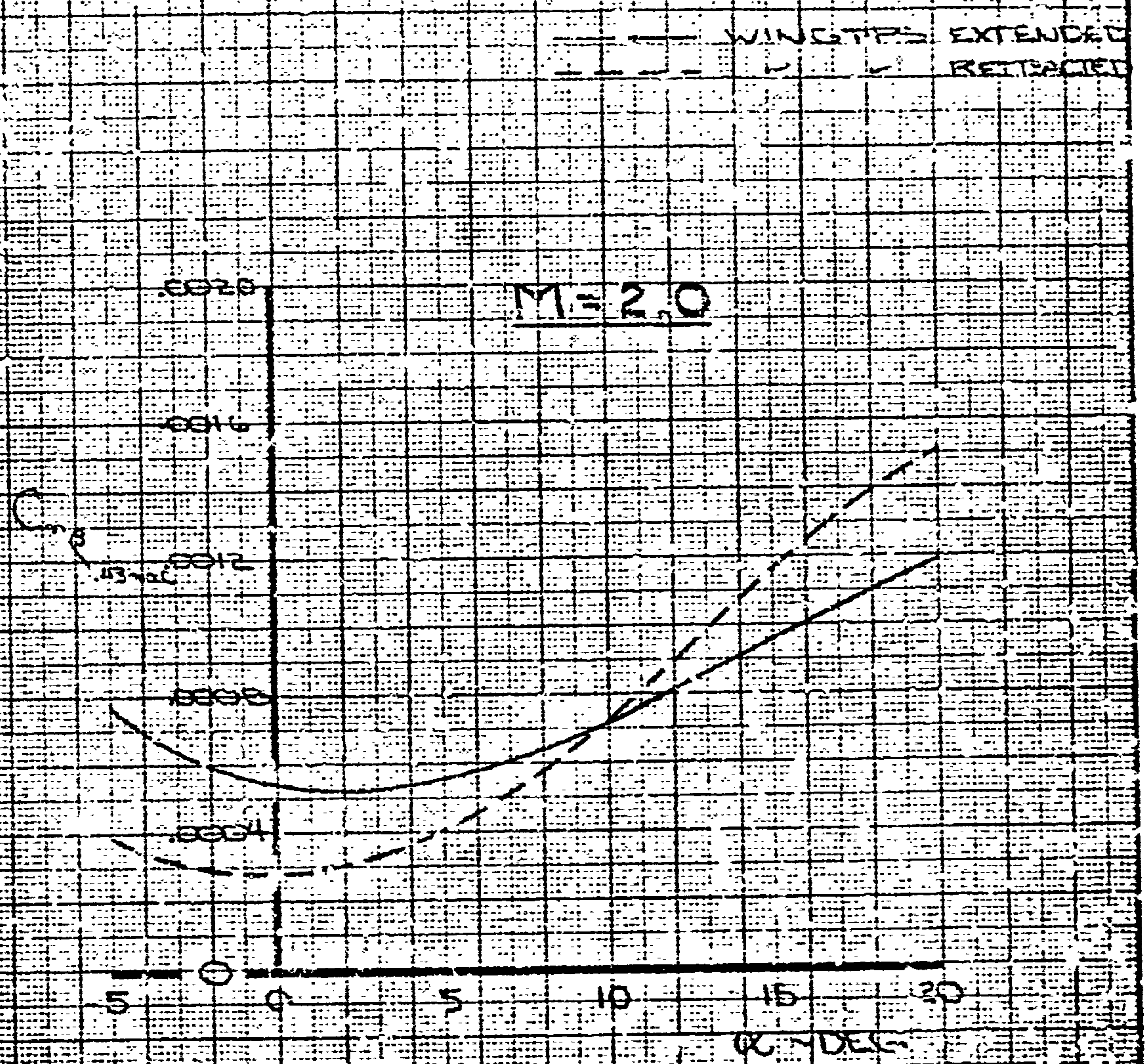

FIG. 6.18

CALC		12-2-60	REVISED	DATE	DIRECTIONAL STABILITY M = 2.0	84-2035
CHECK					124	D2-8174
APR					BOEING AIRPLANE COMPANY	PAGE 6.18
APR						

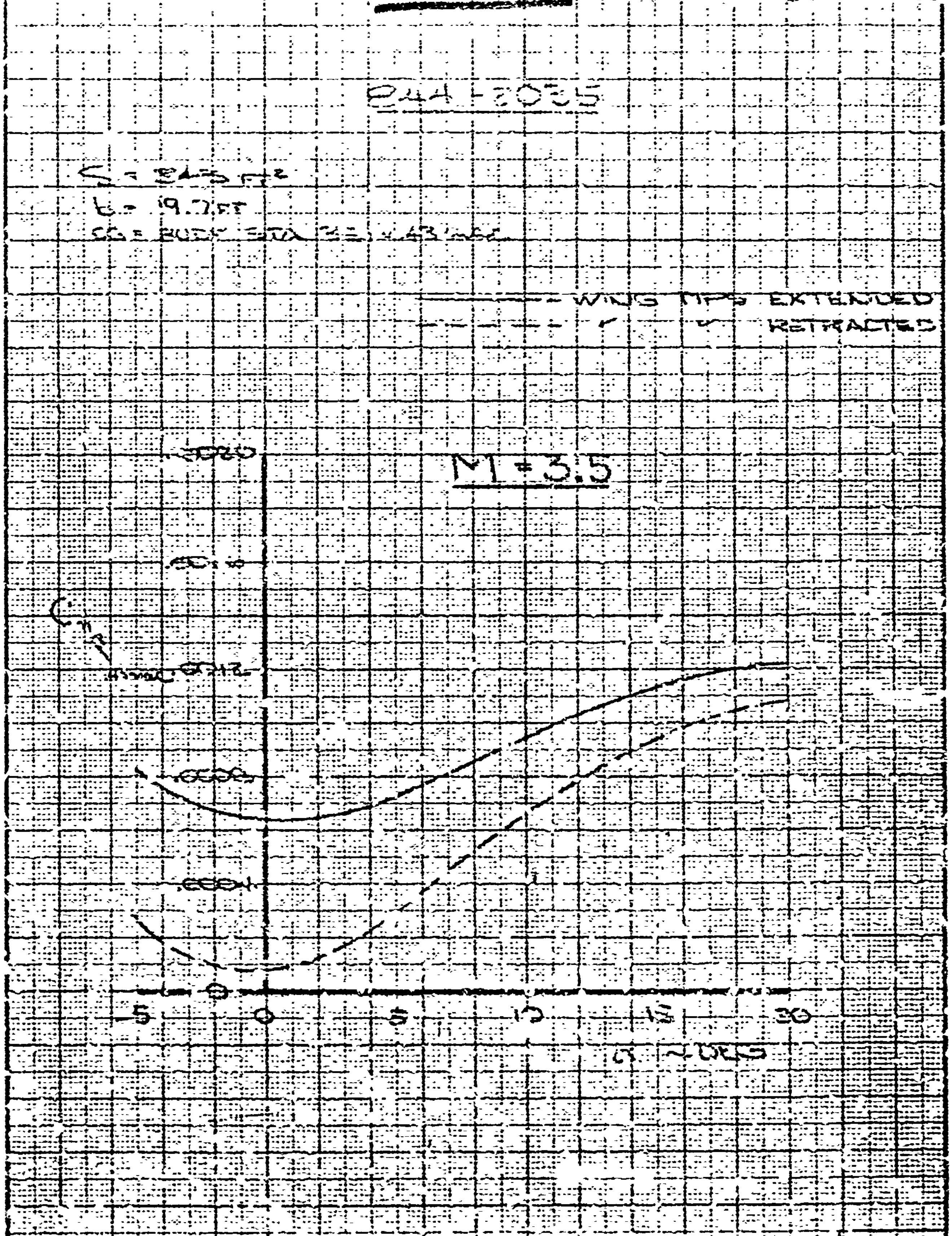

FIG. 6.16

CALC			REVISED	DATE	DIRECTIONAL STABILITY M = 3.5	844-2035
CHECK						D2-6174
APD						
APR					BOEING AIRPLANE COMPANY	PAGE 6.19

BODY AXES

E44-2035

S = 343 FT^2
b = 19.7 FT
CG = W.L.123

——— WING TIPS EXTENDED
- - - - WING TIPS RETRACTED

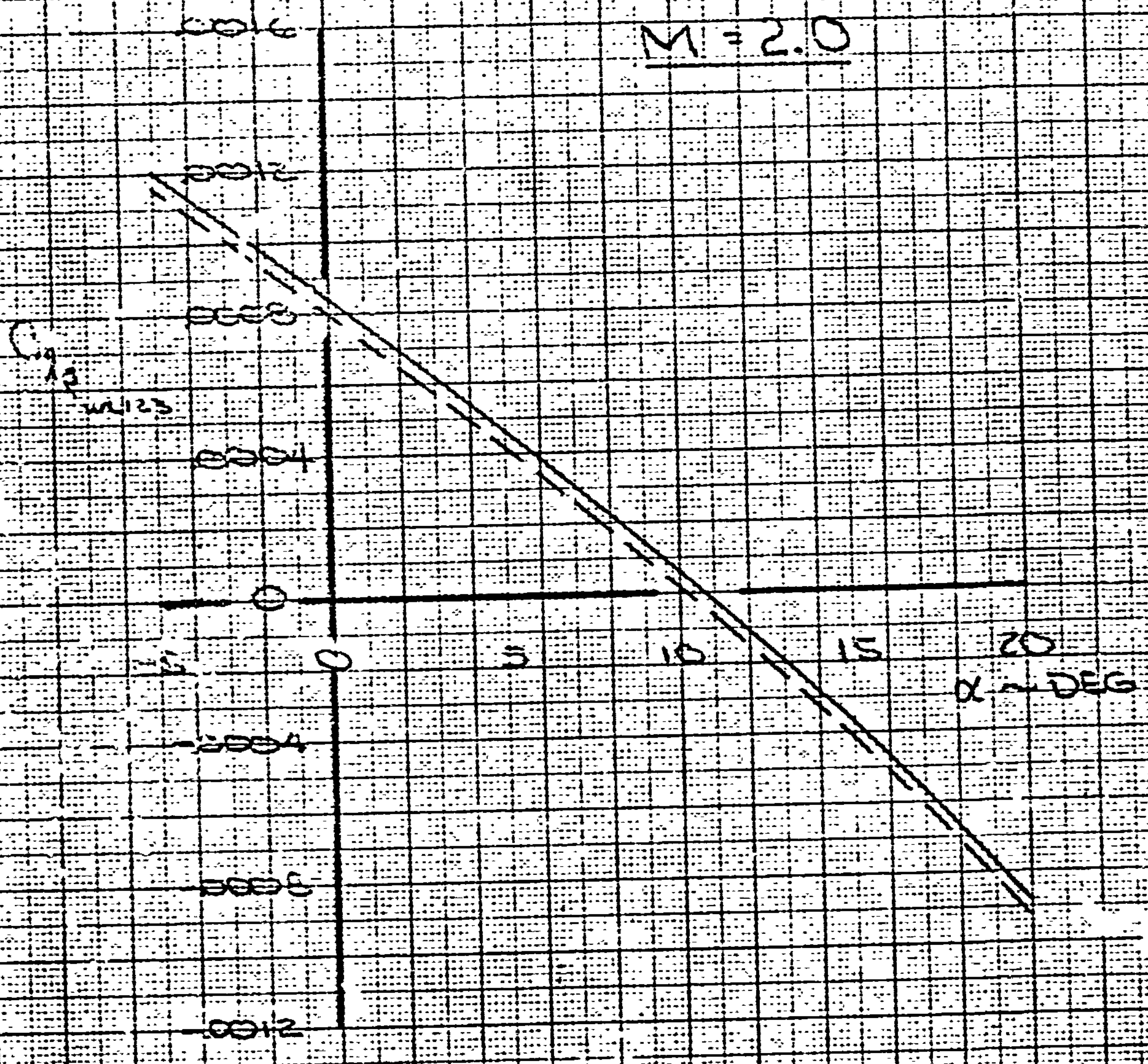

FIG. 6.17

CALC	E.F.K.	12-2-0	REVISED	DATE	LATERAL STABILITY M = 2.0
CHECK					
APR					BOEING AIRPLANE COMPANY
APR					

E44-2035

126

D2-8174

PAGE 6.20

[redacted]

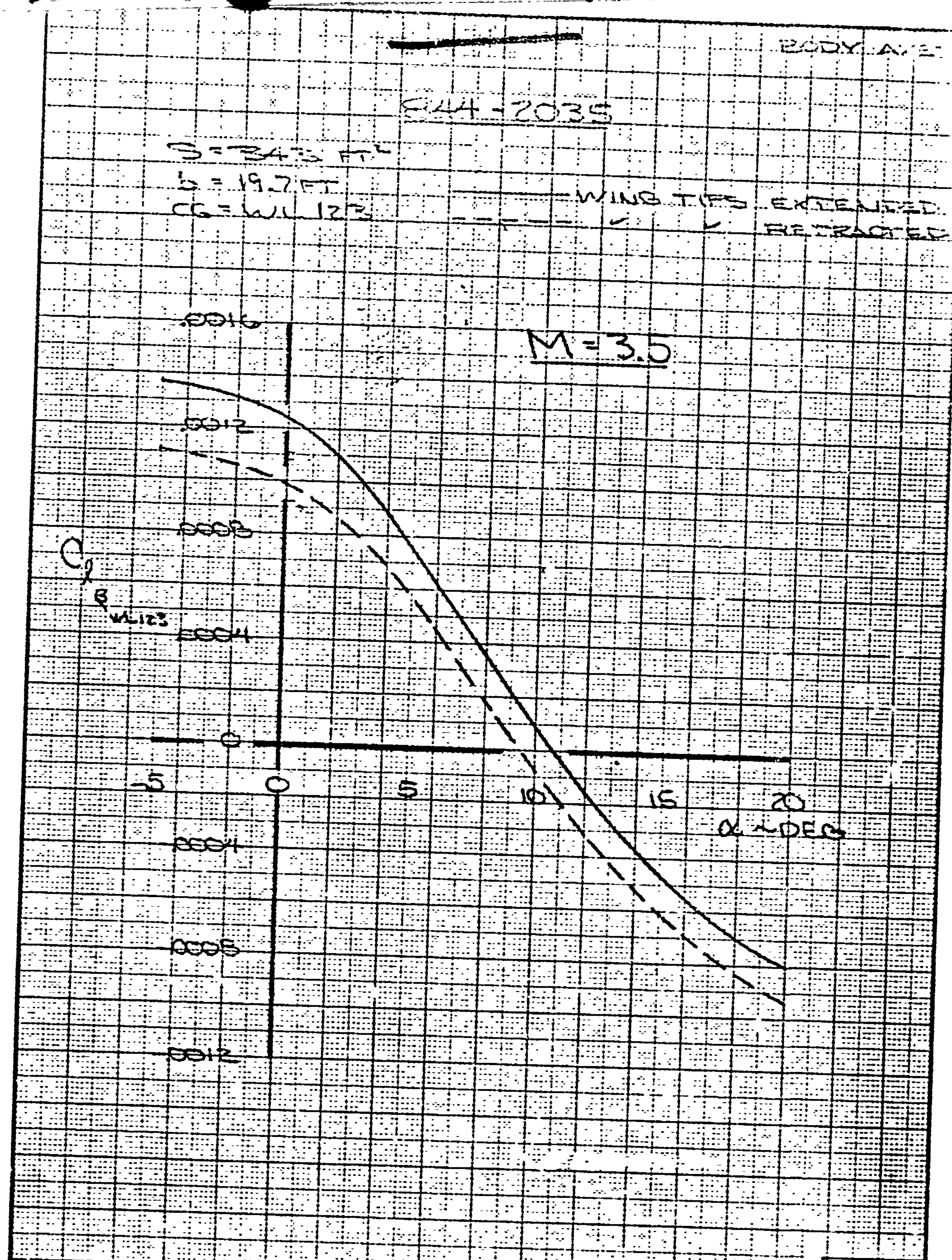

CALC	87R	12-2-0	REVISED	DATE	LATERAL STABILITY M = 3.5 127	FIG. 6.18
CHECK						844-2035
APR						D2-8174
AFR					BOEING AIRPLANE COMPANY	PAGE 6.21

[redacted]

K+E 60029

[redacted]

844-2035

S = 3473 FT²

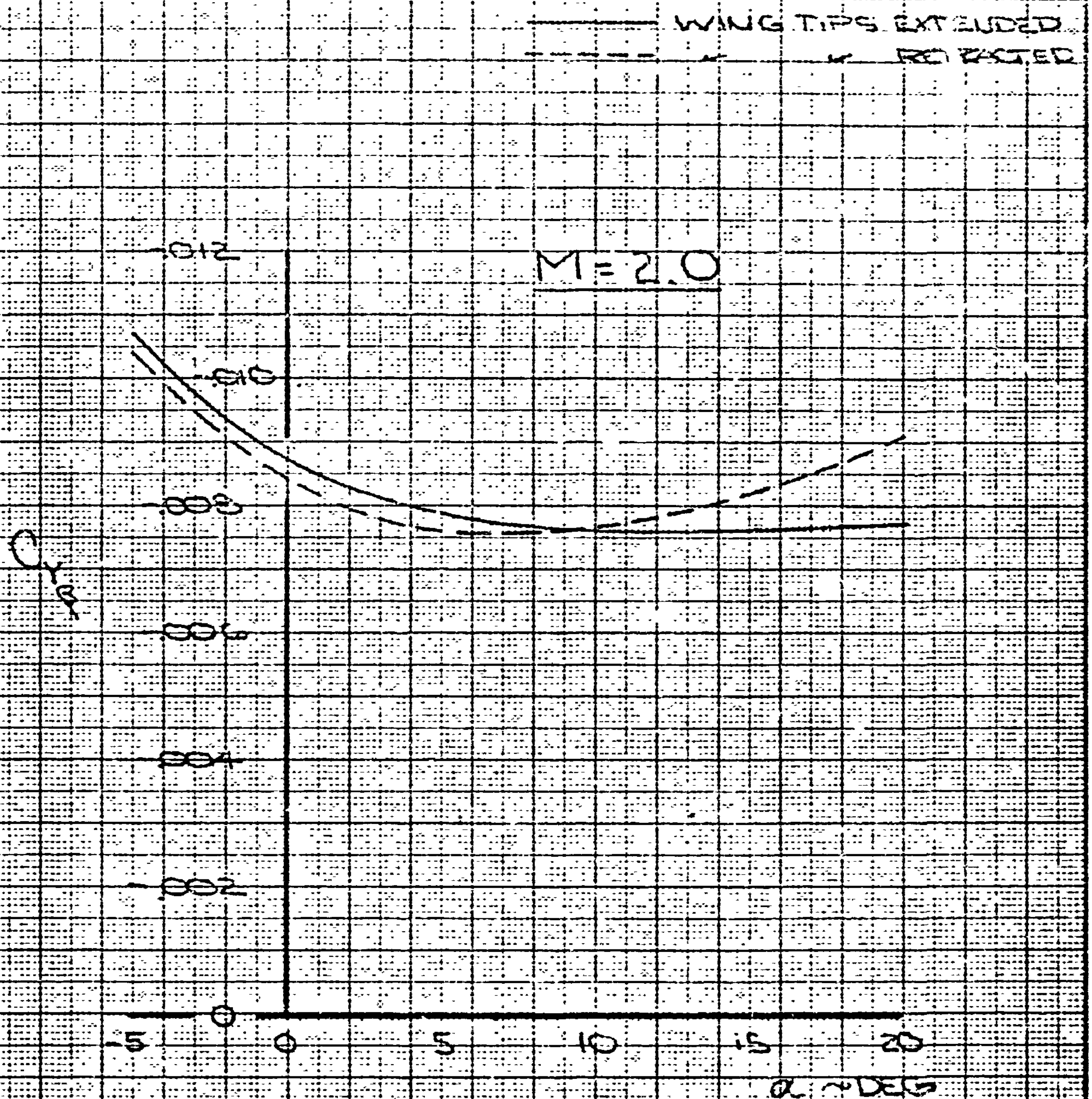

FIG. 6.19

CALC	KFK	12-2-0	REVISED	DATE	SIDE FORCE M = 2.0 **128**	844-2035
CHECK						D2-8174
APR					BOEING AIRPLANE COMPANY	PAGE 6.22
APR						

[redacted]

K·E 60629

844-2035

S = 343 FT²

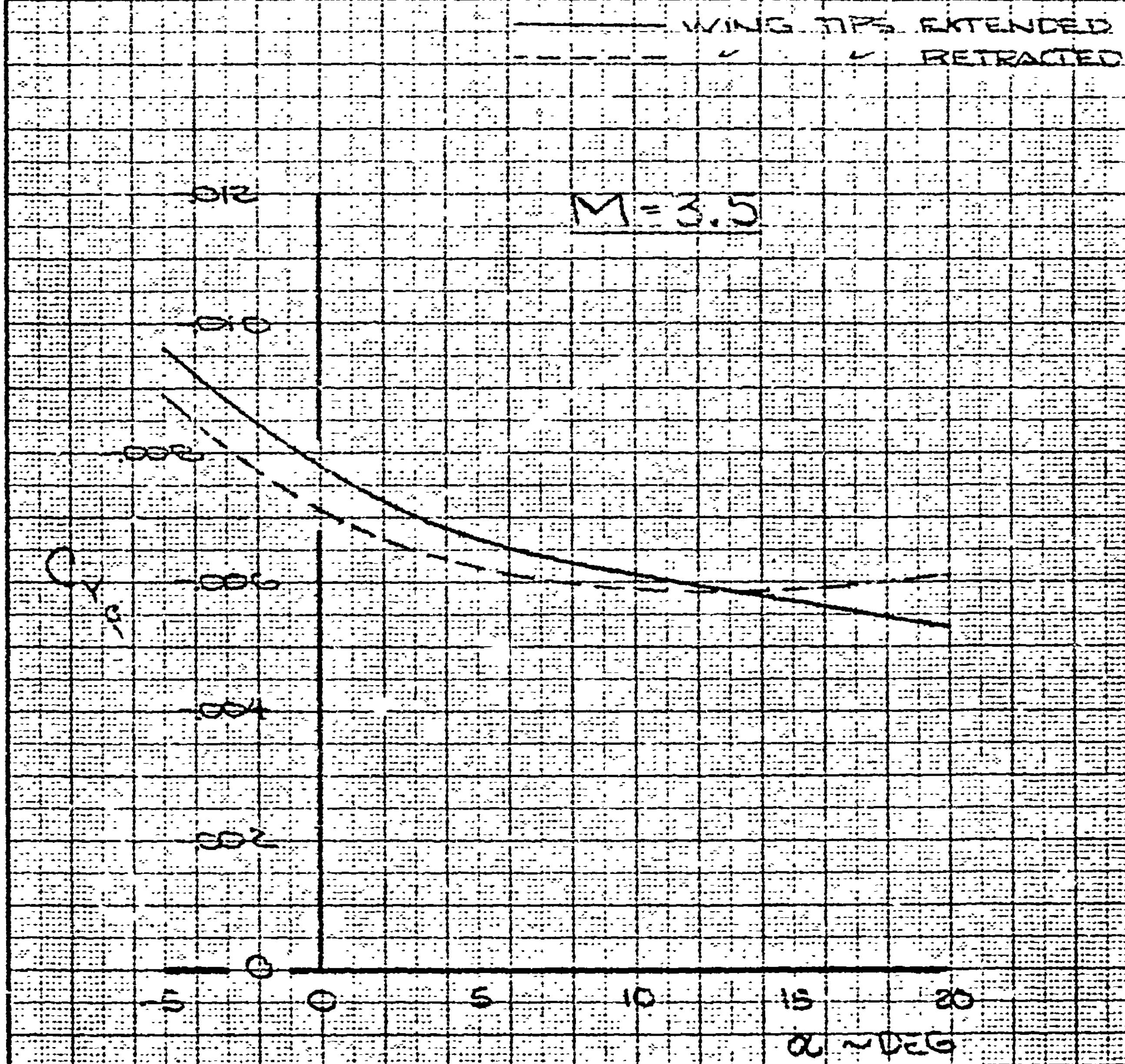

FIG. 6.20

CALC	BYR	2-2-0	REVISED	DATE	SIDE FORCE M = 3.5	844-2035
CHECK					129	D2-8174
APR					BOEING AIRPLANE COMPANY	PAGE 6.23
APR						

109

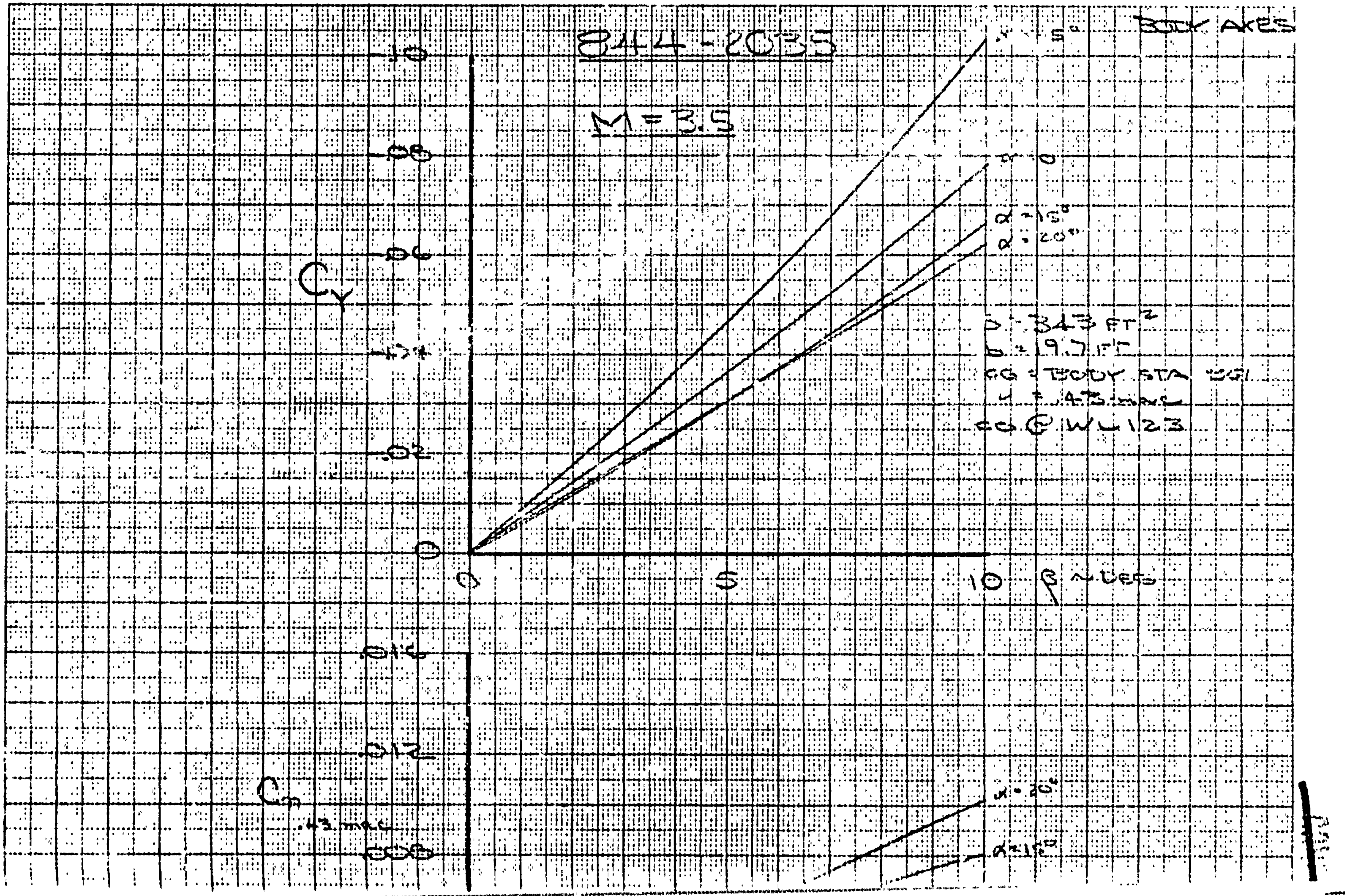
844-2035
BODY AXES
M = 3.5
α = 5°
α = 0
α = 15°
α = 20°
S = 343 FT²
b = 19.7 FT
CG = BODY STA 551
= .43 mac
CG @ WL 123
.10
.08
.06
.04
.02
0
.016
.012
.008
Cy
Cn .43 mac
0
5
10
β ~ DEG
α = 20°
α = 15°

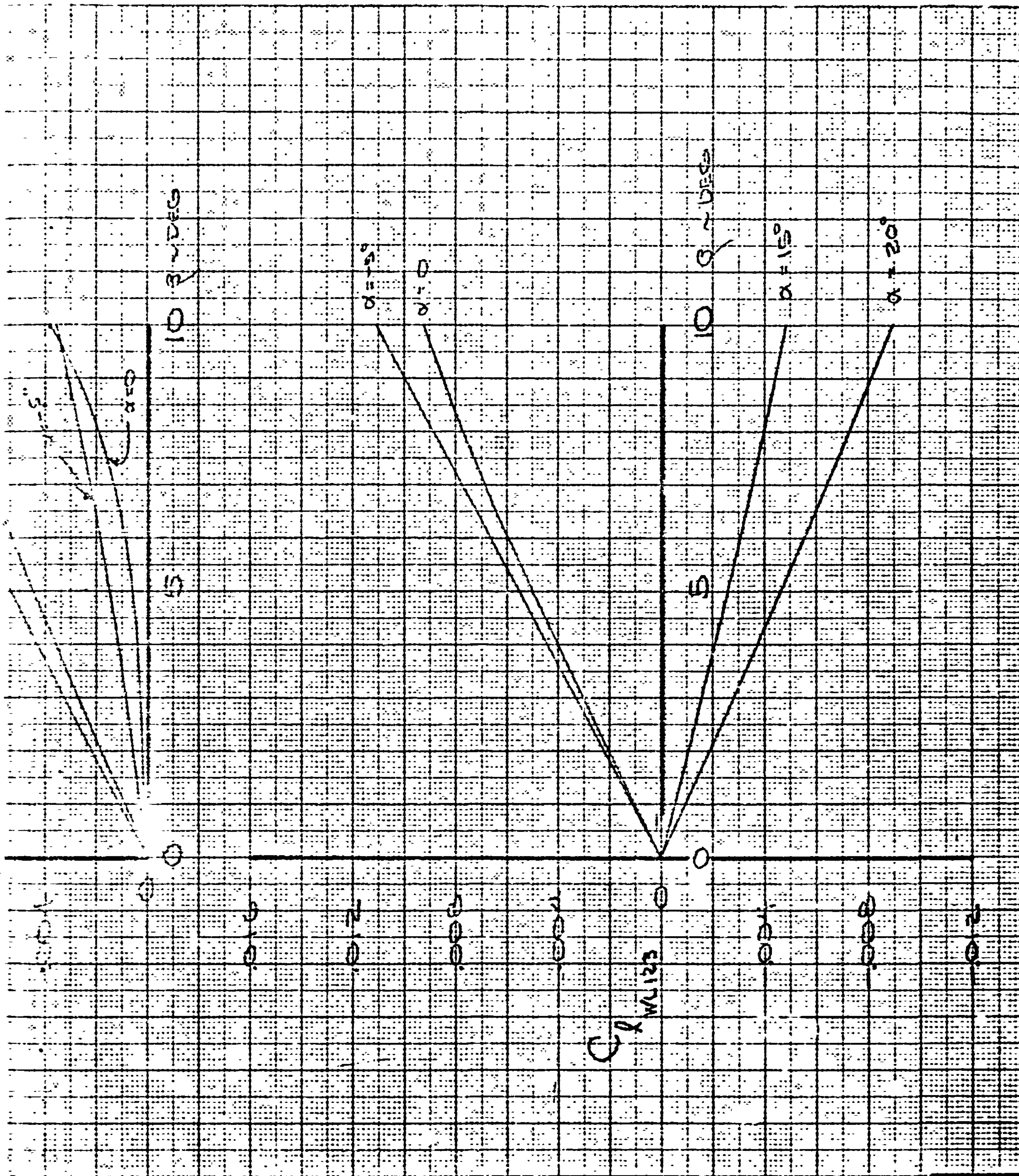

FIG. 6.21

LATERAL-DIRECTIONAL STABILITY ~ M=2.5 ~ WING TIPS RETRACTED

244-2035

D2-8174

PAGE 6.24

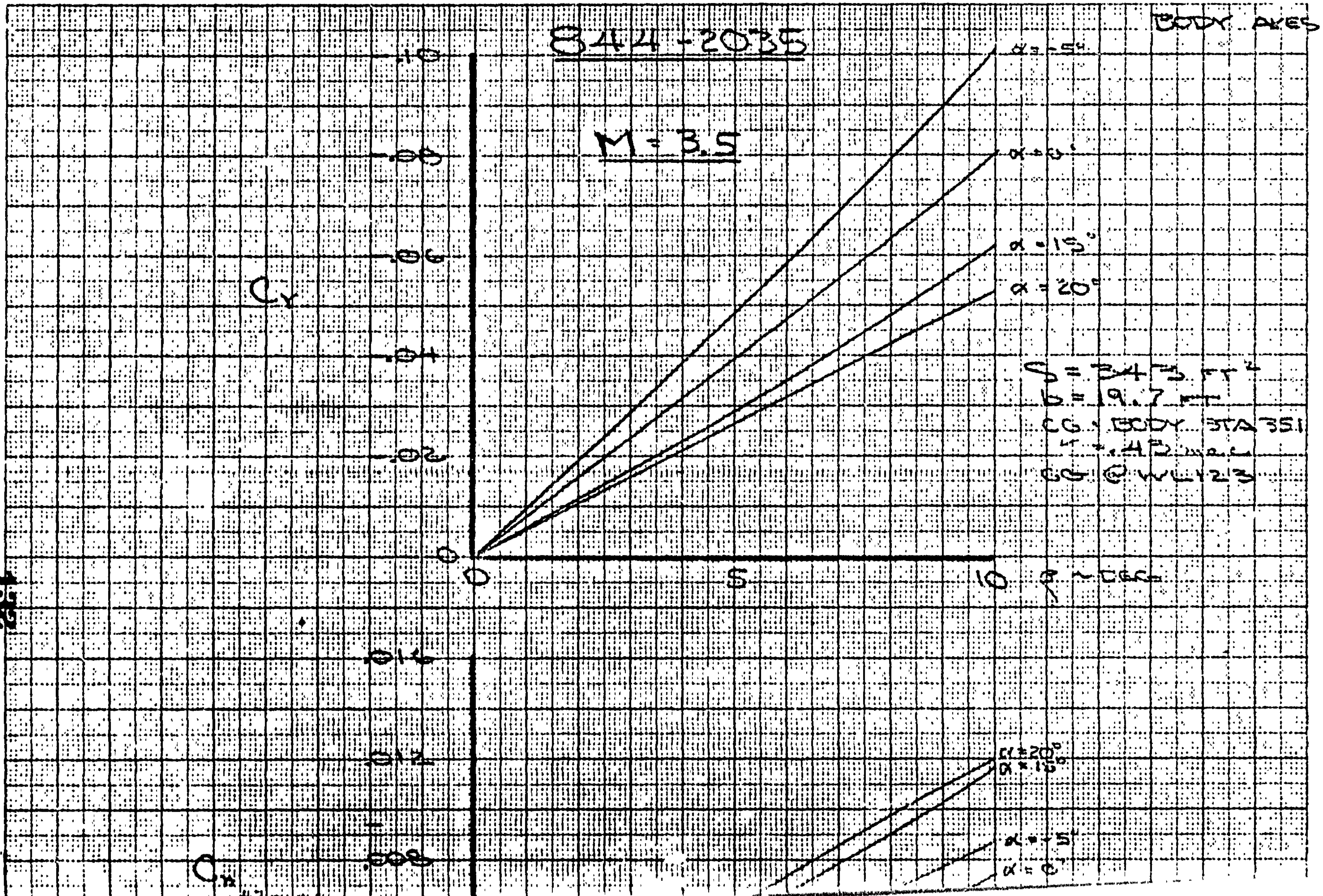

844-2035
M = 3.5
BODY AXES
C_Y
$\alpha = -5°$
$\alpha = 0°$
$\alpha = 15°$
$\alpha = 20°$
$S = 343\ FT^2$
$b = 19.7\ FT$
CG @ BODY STA 351
CG @ WL 123
β ~ DEG
.10
.08
.06
.04
.02
0
5
10
.016
.012
.008

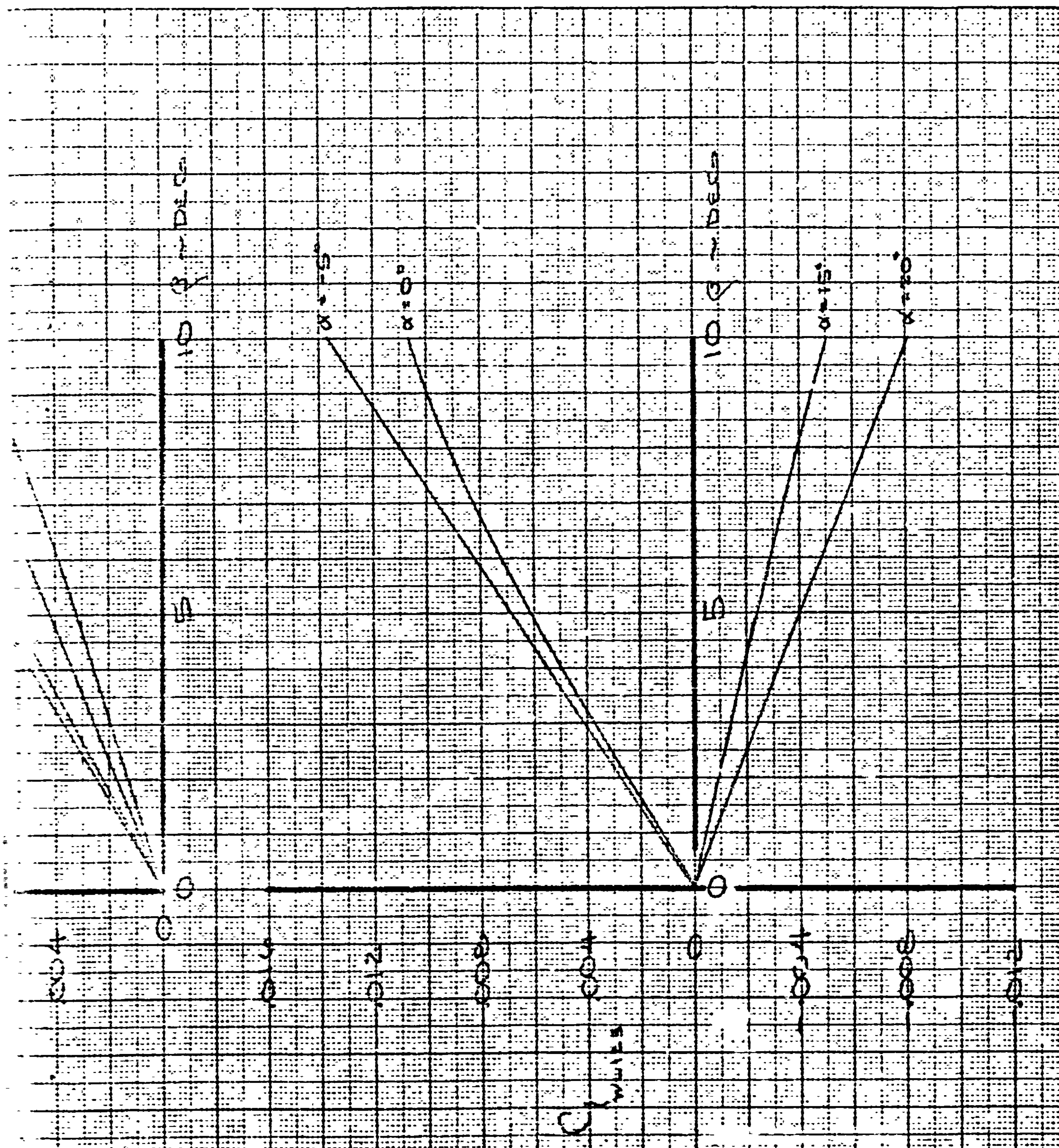

FIG. 6.22

LATERAL-DIRECTIONAL STABILITY ~ M=3.5 ~ WING TIPS EXTENDED

644-2055

D2-3174

PAGE 6.45

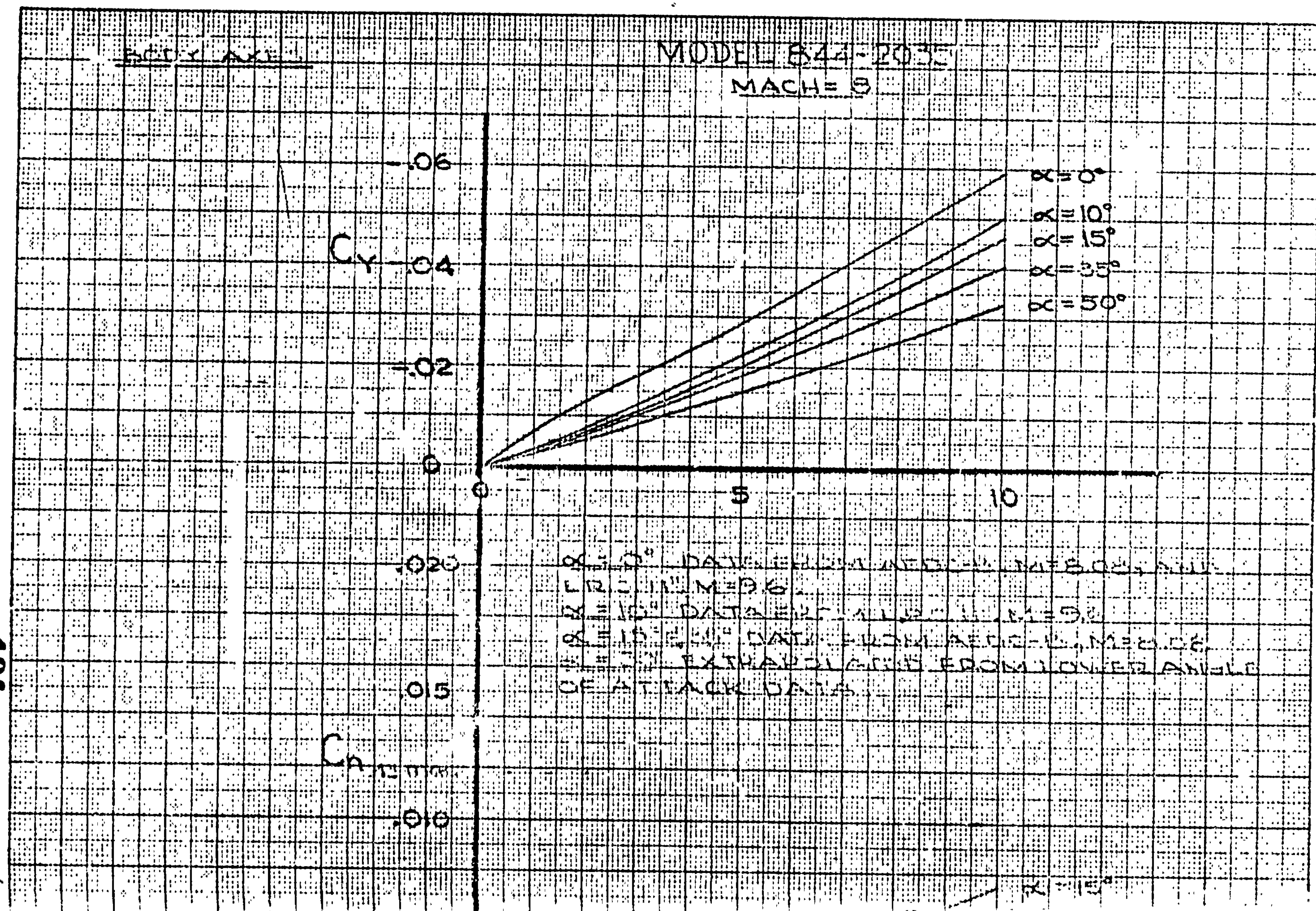

MODEL 844-2035
MACH = 8
C_Y
-.06
-.04
-.02
0
.020
.015
.010
C_n
0
5
10
α = 0°
α = 10°
α = 15°
α = 35°
α = 50°

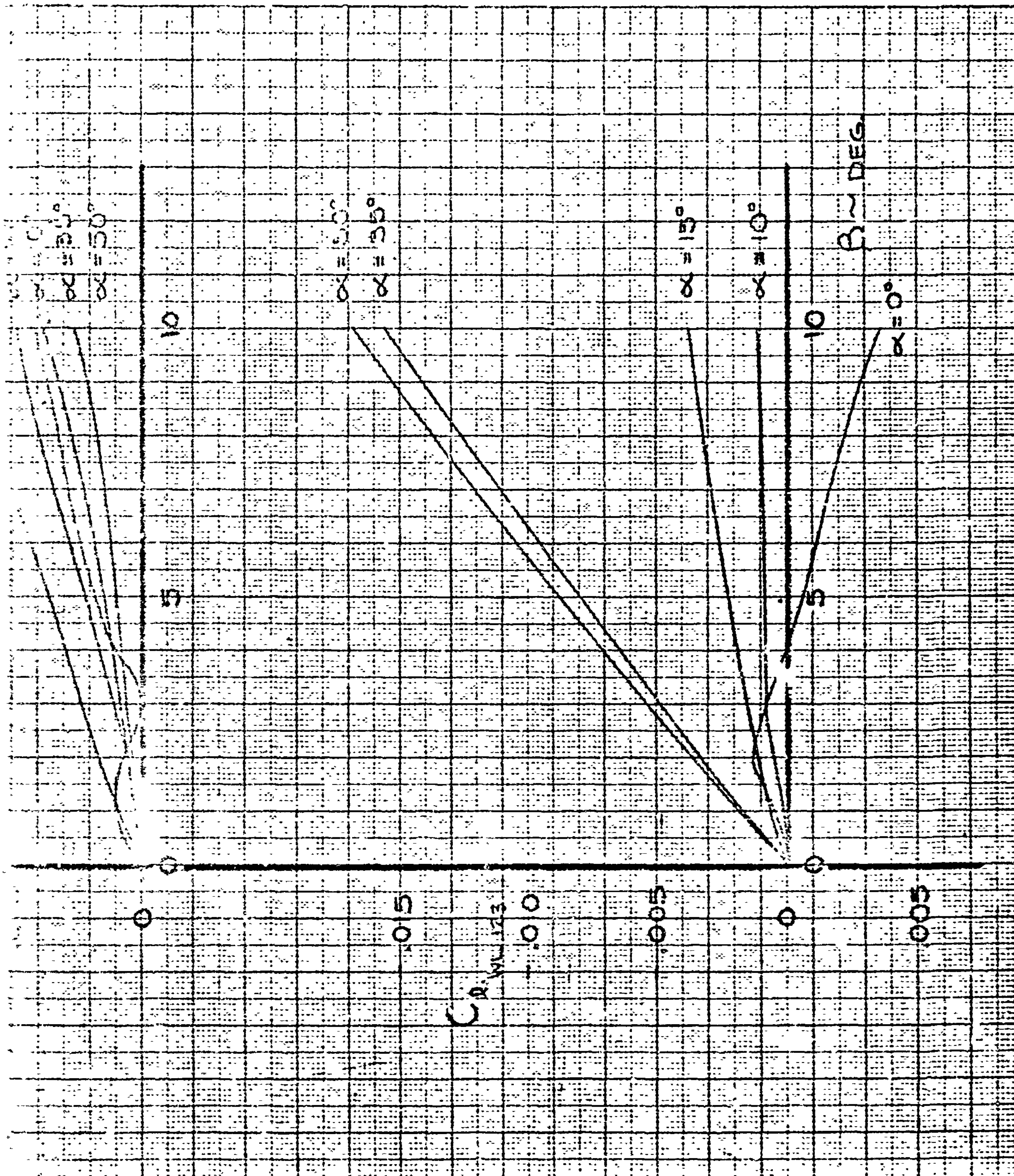

FIG. 6.23

844-2035

LATERAL DIRECTIONAL STABILITY
LOW HYPERSONIC SPEEDS

CALC JEB

D2-8374

PAGE 6.26

U3 4074 7000 (WAS BAC 1053 R1)

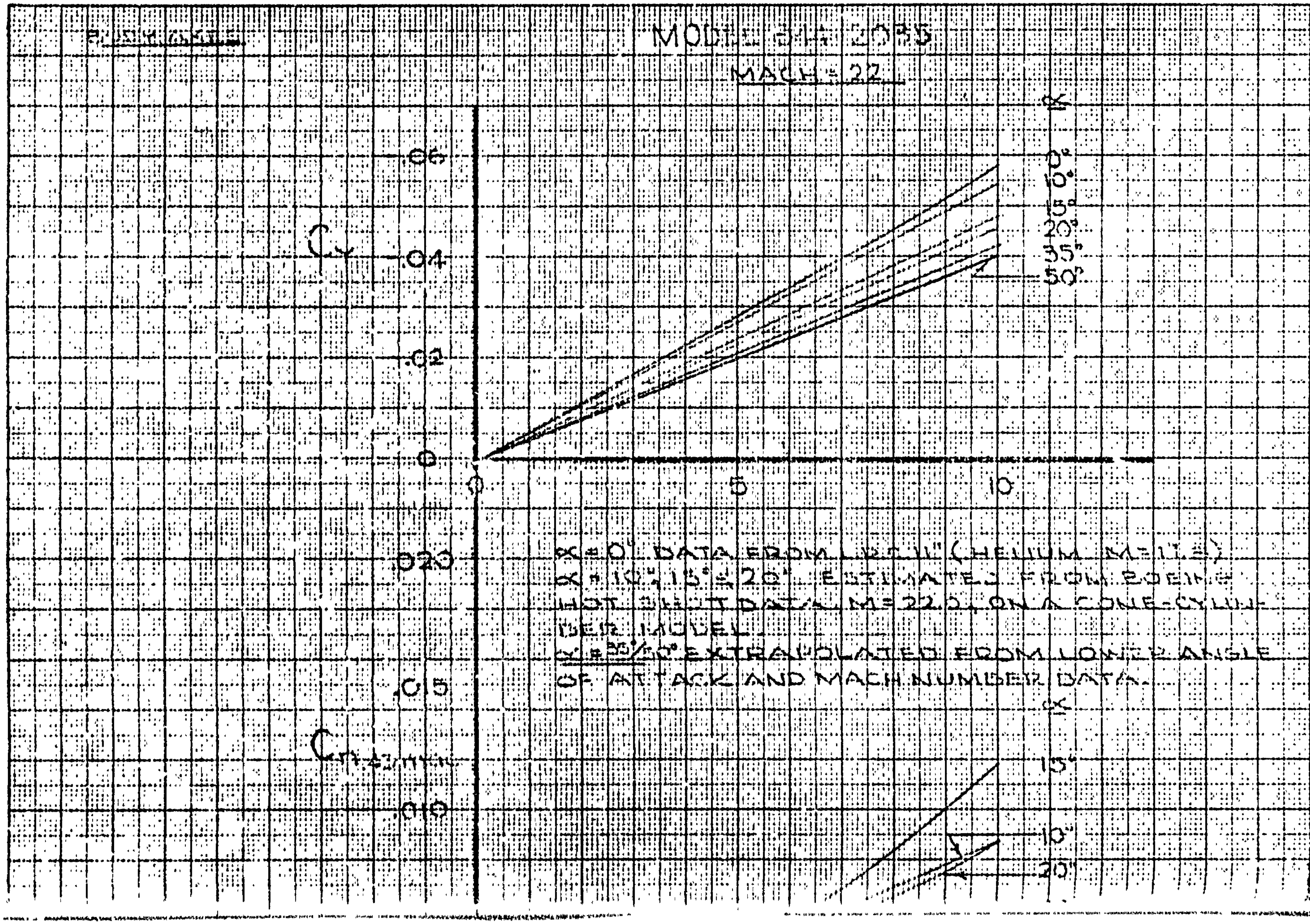
MACH = 22
α
0°
10°
15°
20°
35°
50°
.06
.04
.02
0
.020
.015
.010
0
5
10
α = 0° DATA FROM
DER MODEL
OF ATTACK AND MACH NUMBER DATA.
15°
10°
20°

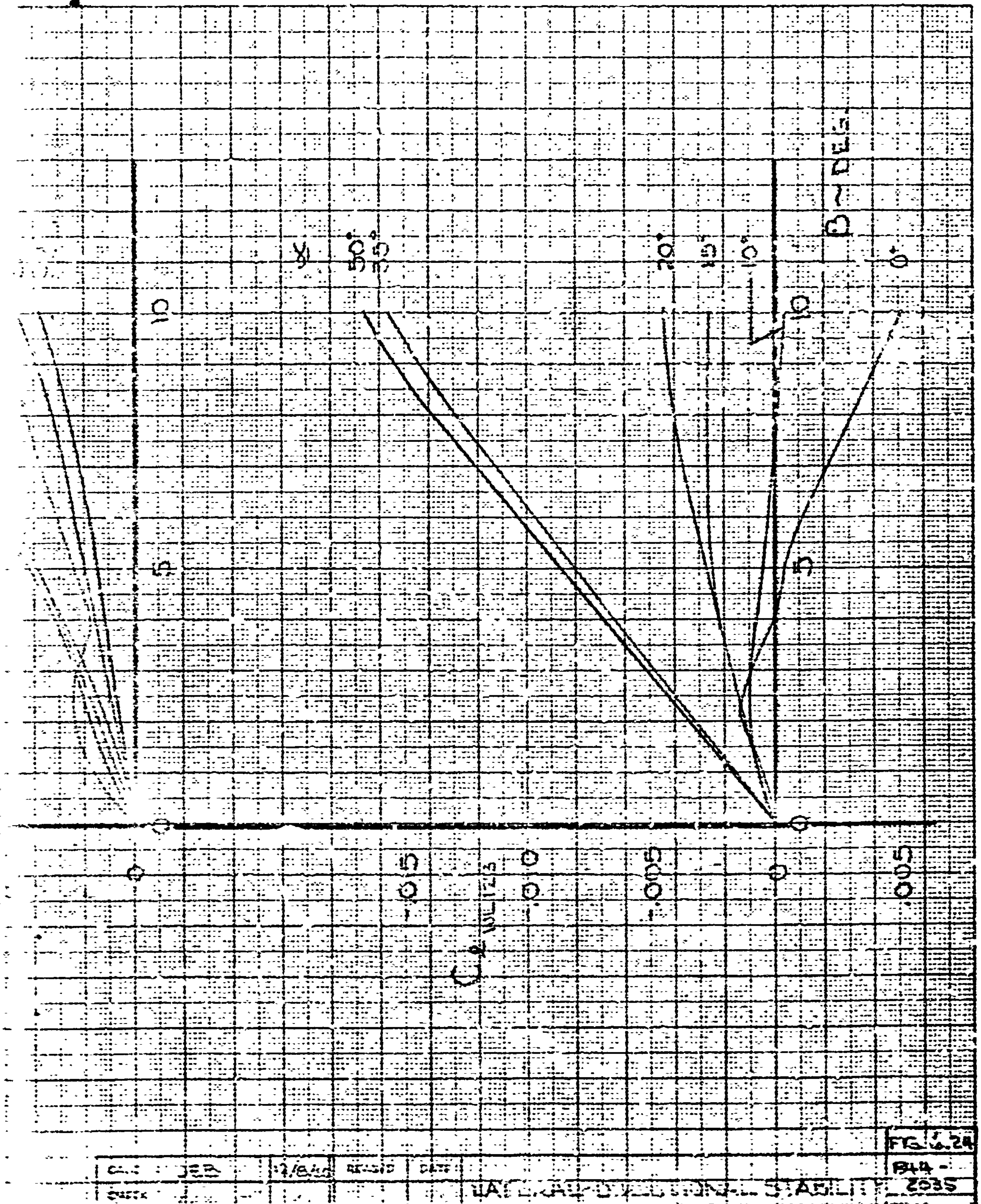

CALC JEB	12/8/66	REVISED	DATE	FIG 6.28
CHECK		LATERAL-DIRECTIONAL STABILITY		B44-2035
APPD		HIGH HYPERSONIC CRUISE		D2-874
APPD				PAGE 6.37

6.2 AILERON CHARACTERISTICS AND EFFECTIVENESS

Aileron effectiveness data for the 844-2035 configuration are presented in Figures 6.25 through 6.42. Summary curves of $C_{\ell_{\delta_a}}$, $C_{n_{\delta_a}}$ and $C_{Y_{\delta_a}}$ versus Mach number are presented on Figures 6.25, 6.26 and 6.27 to show the variation between the Mach numbers; more detailed data are presented on Figures 6.28 through 6.42.

The data presented are based on wind tunnel data on similar configurations adjusted to the dimensions of the 844-2035 configuration. All data are based on configurations with 10° swept elevon hinge lines, with the exception of the transonic region where the hinge line was unswept. The effects of hinge line sweep have not been established precisely; consequently C_n and C_Y may be changed when wind tunnel data on the 844-2035 configuration become available.

The hypersonic aileron characteristics are presented for both surfaces deflected symmetrically about δ_e of 0 and -30° and also for one elevon deflected through a range of 10° to -45° while the other is at 0° deflection. The "one-surface-deflected" data are presented in order to facilitate estimation of the effects of deflecting the ailerons unequally.

The effect of altitude (i.e., Reynolds number) on aileron effectiveness is similar to the effect on elevon effectiveness in pitch. Aileron effectiveness is influenced by a thickening boundary layer with increasing altitude which decreases the effectiveness. High hypersonic speed hot-shot data show little change in effectiveness however, and at this time it is assumed that aileron characteristics should not be changed significantly with altitude.

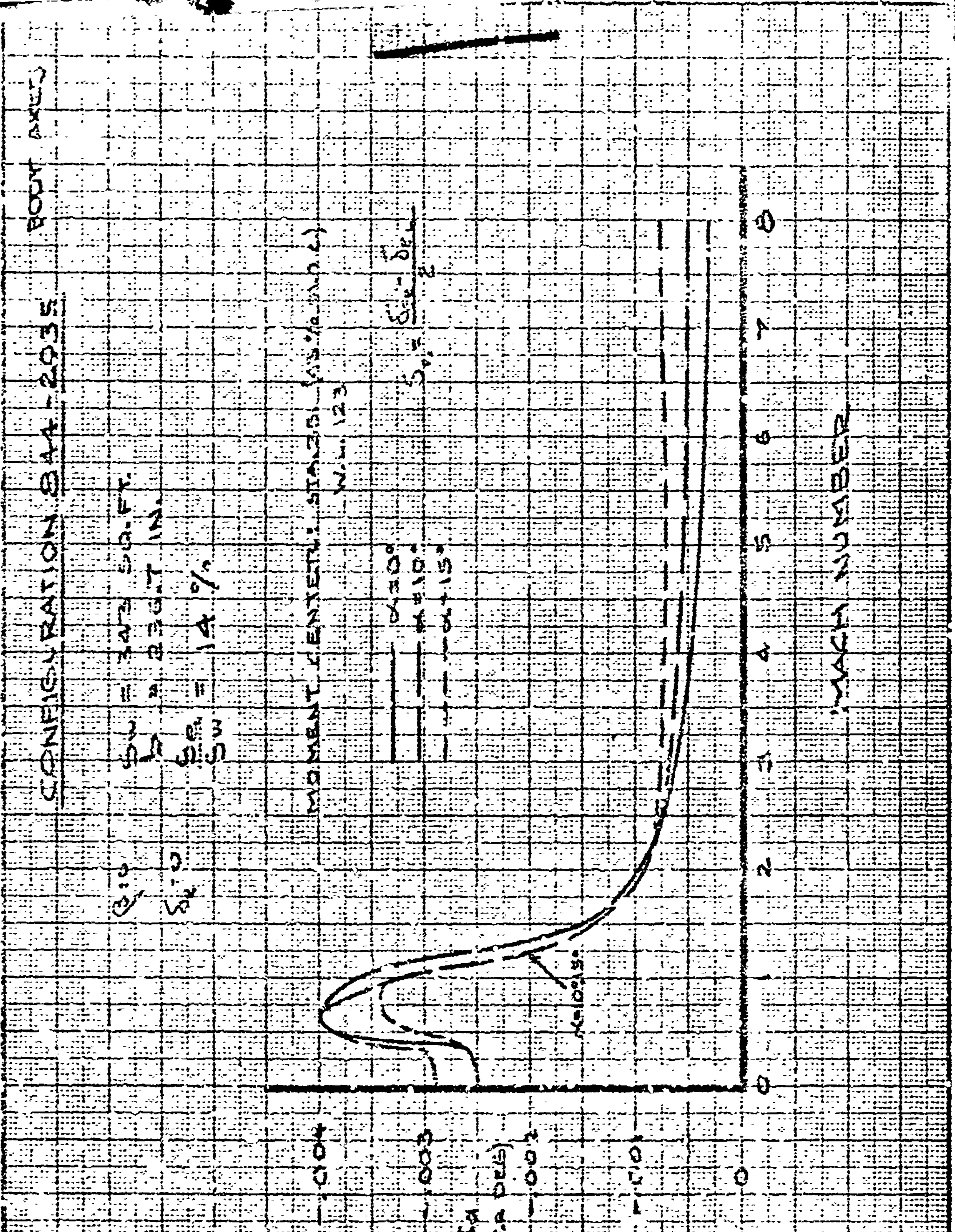

FIG. 6.25

CALC	EB	REVISE	DATE	ROLLING MOMENT DUE TO AILERON
CHECK				
APR				
APR				

844-2035

D2-8174

BOEING AIRPLANE COMPANY

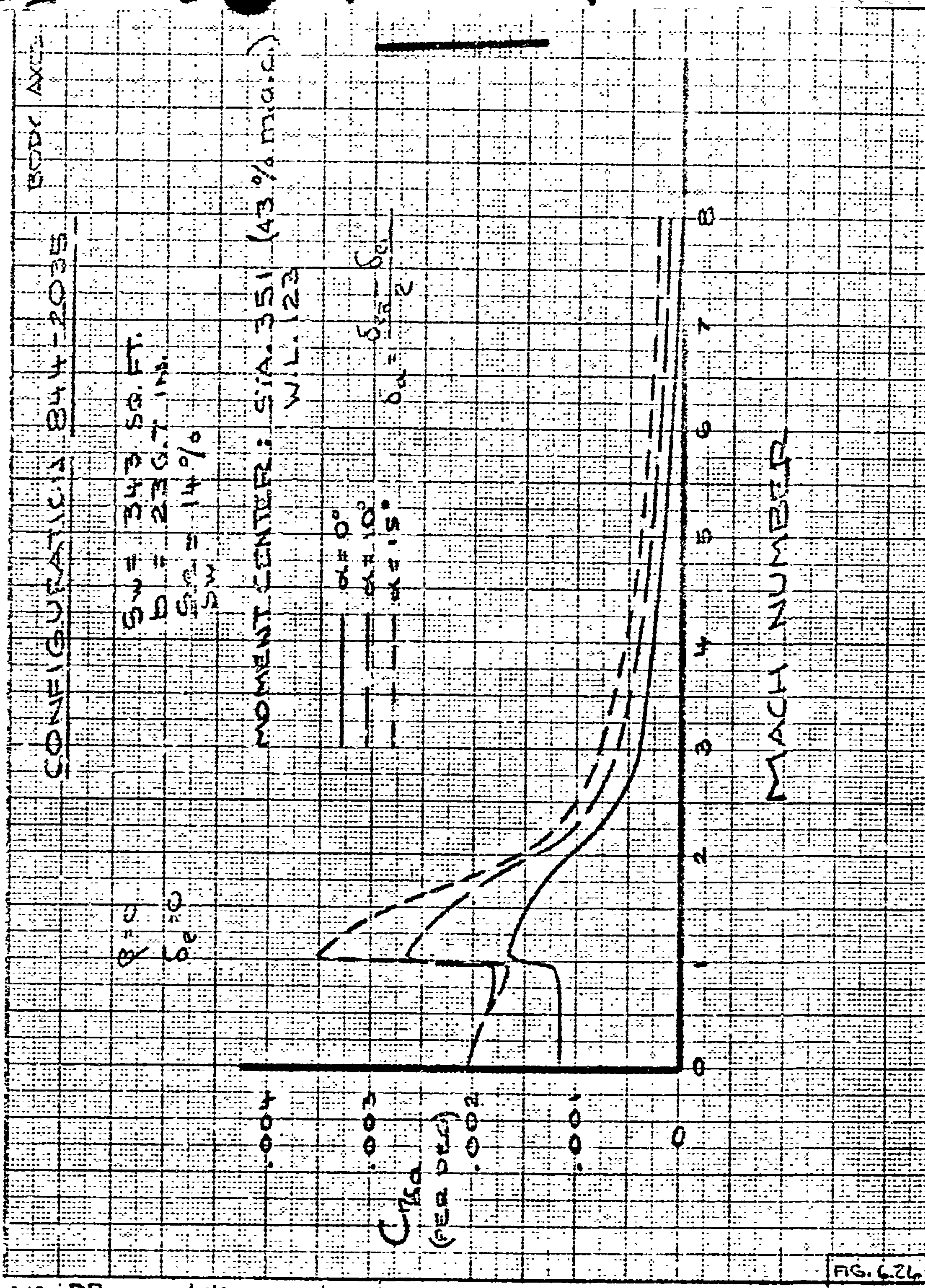

FIG. 6.26

CALC	DB	12/14/60	REVISED	DATE		844-2035
CHECK					YAWING MOMENT DUE TO AILERON	
APR						D2-8174
APR					BOEING AIRPLANE COMPANY	PAGE 6.30

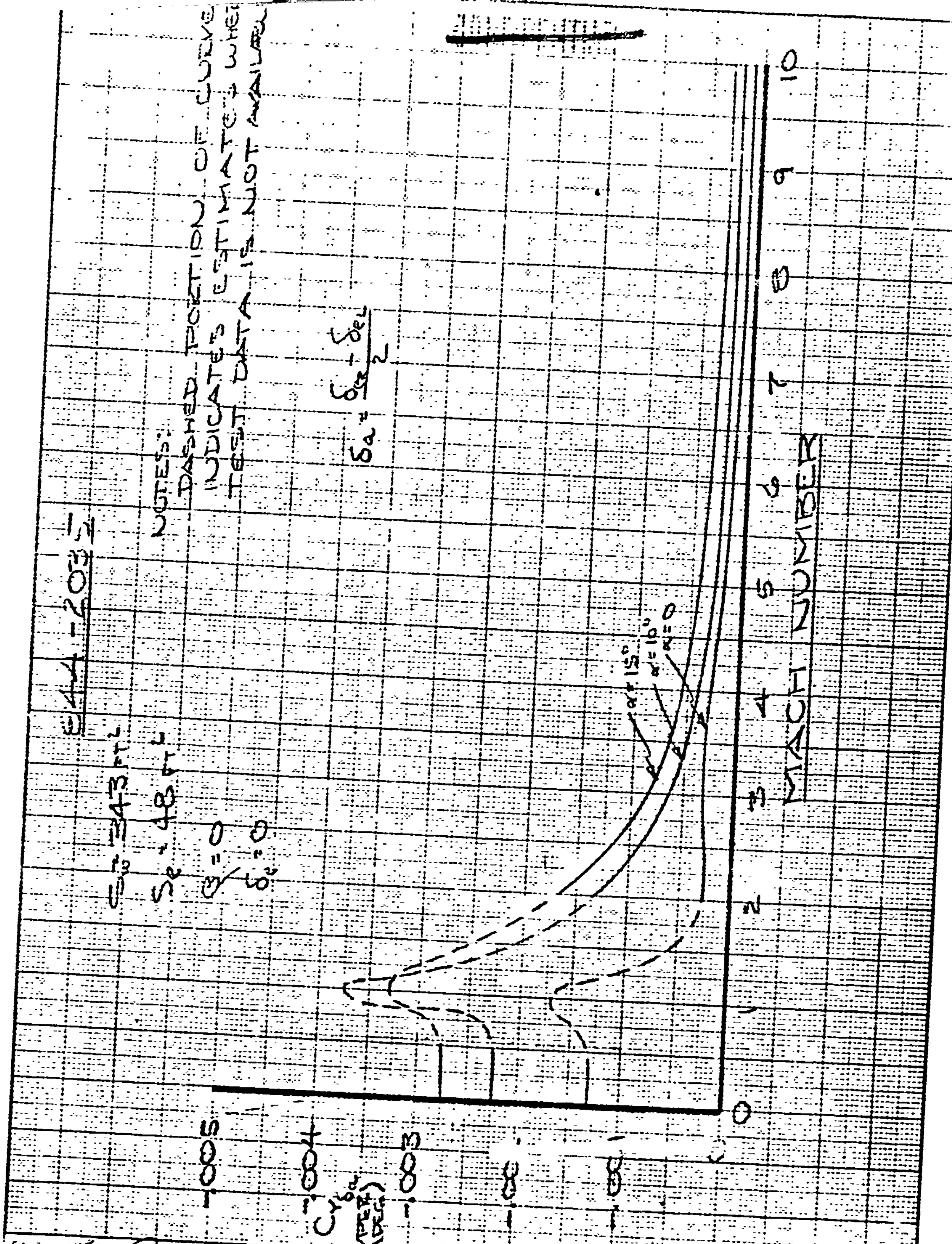

CALC RJR 12-24?	REVISED	DATE	FIG. 6.27
CHECK		SIDE FORCE DUE TO AILERON	844-2035
APR		141	D2-8174
APR		BOEING AIRPLANE COMPANY	PAGE 6.31

BAC 401 C R4

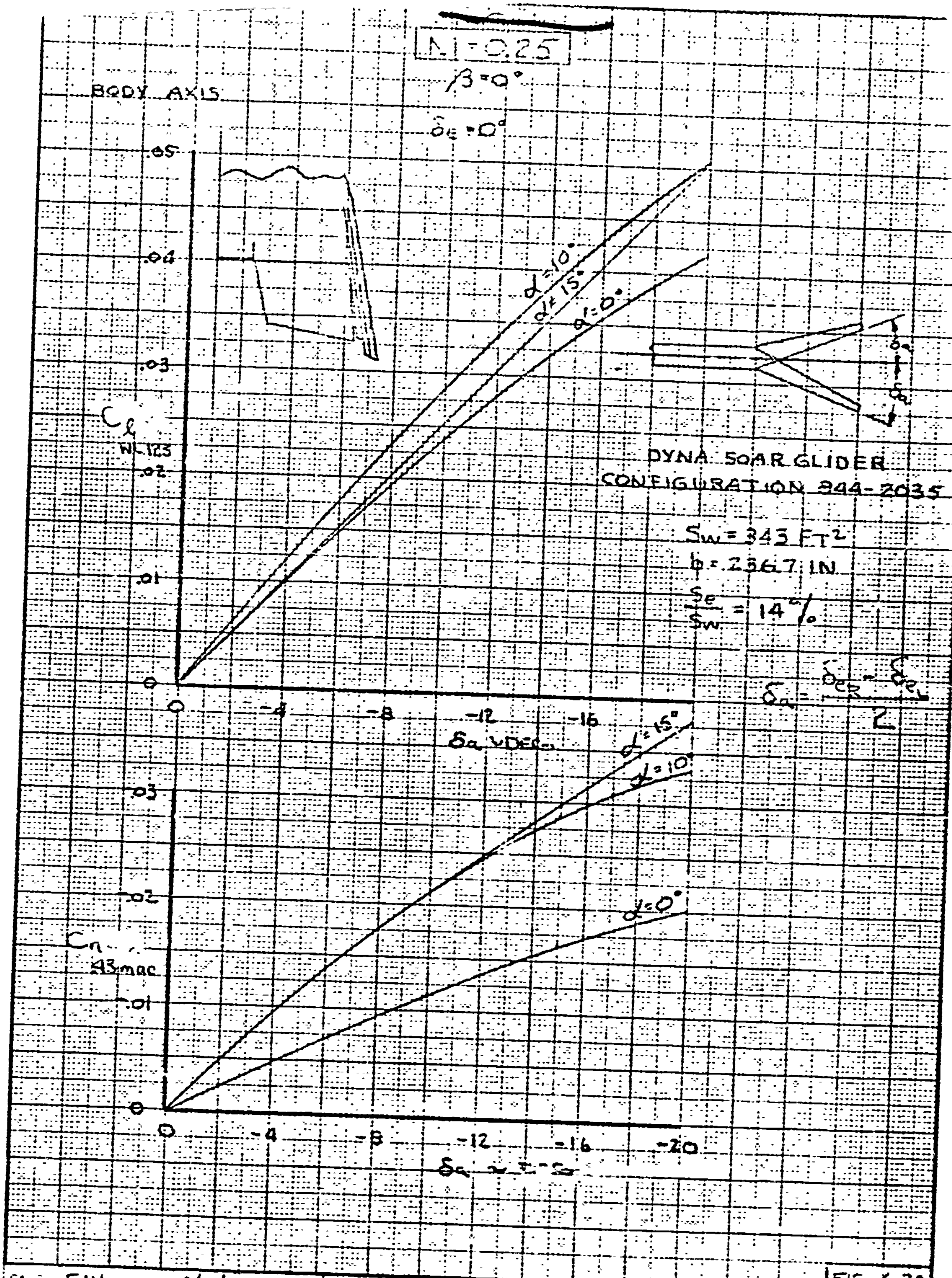

CAL	EJH	12/14/60	REVISED	DATE
CHECK	[illegible]	✓		
APR				
APR				

AILERON EFFECTIVENESS LANDING SPEED

$\delta_e = 0$

142

BOEING AIRPLANE COMPANY

FIG. 6.28
844-2035
D2-8174
PAGE 6.32

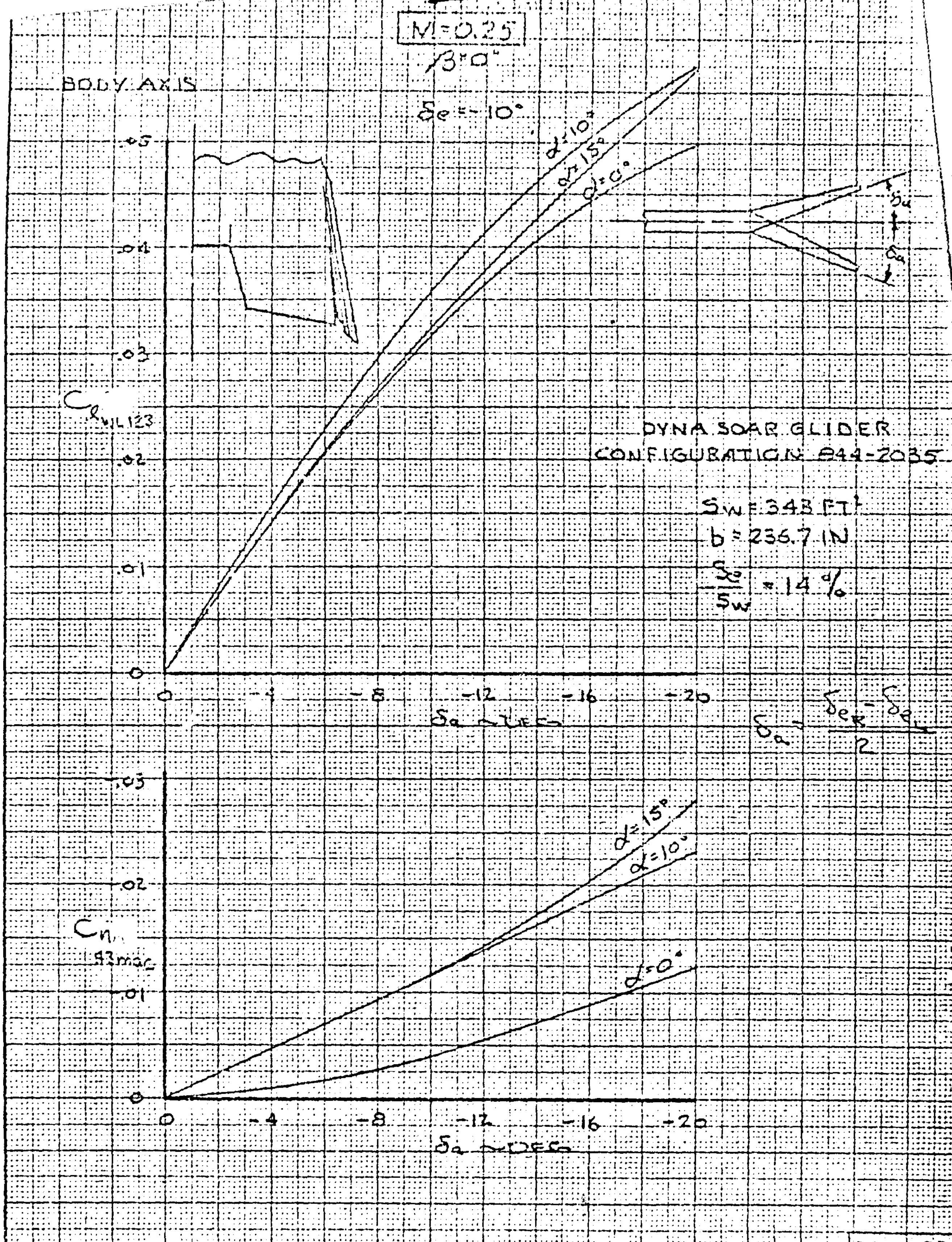

FIG. 6.29

CALC	EJH	14/14/6	REVISED	DATE	AILERON EFFECTIVENESS LANDING SPEED $\delta_e = -10°$
CHECK	[illegible signature]	—			
APR					**143**
APR					BOEING AIRPLANE COMPANY

E44-2035

D2-3174

PAGE 6.33

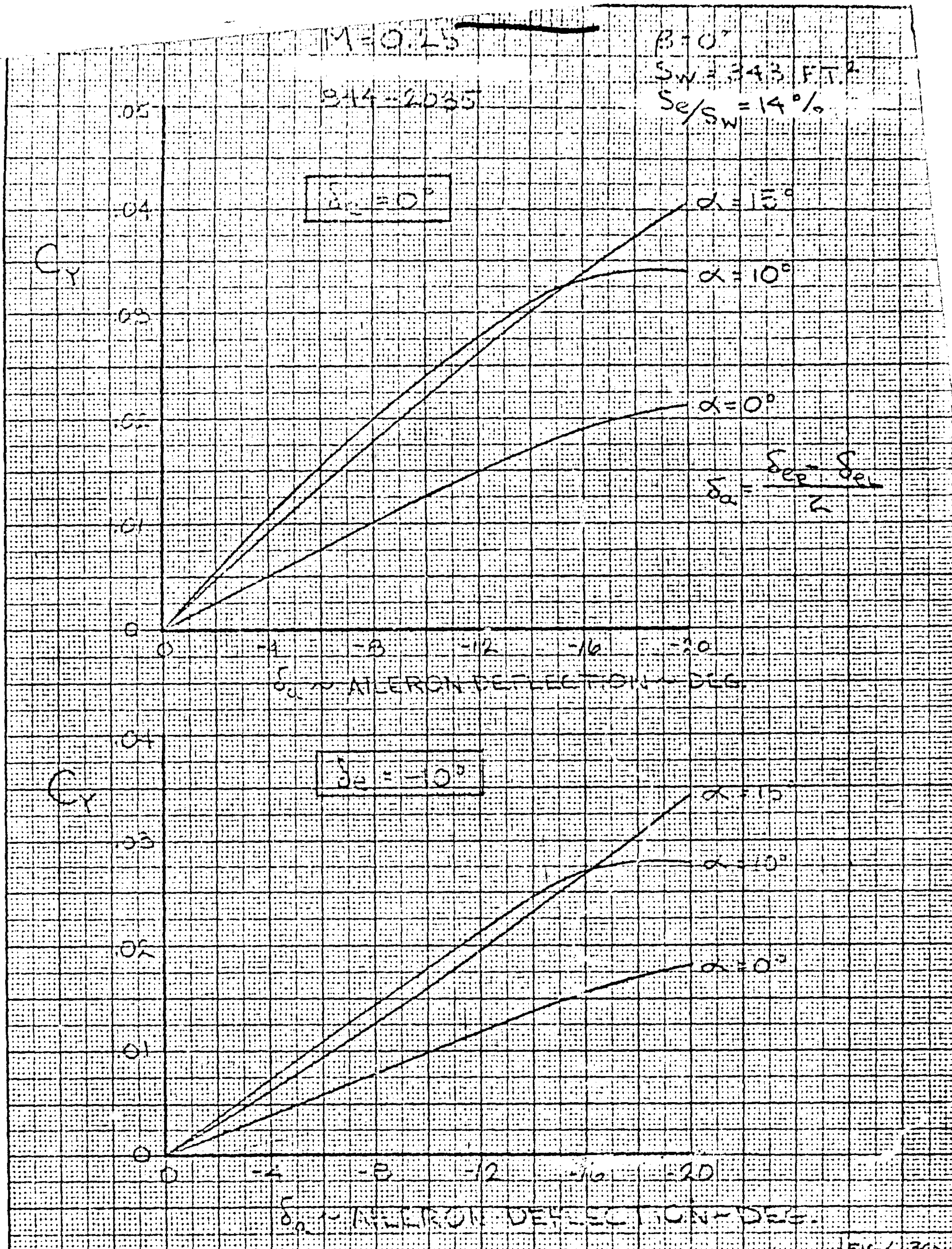

FIG. 6.30

CALC	EH		REVISED	DATE	SIDE FORCE DUE TO AILERON-LANDING SPEED	844-2035
CHECK						D2-8174
APR						
APR					BOEING AIRPLANE COMPANY	PAGE
COPIED	PTV	12-21			144	6.34

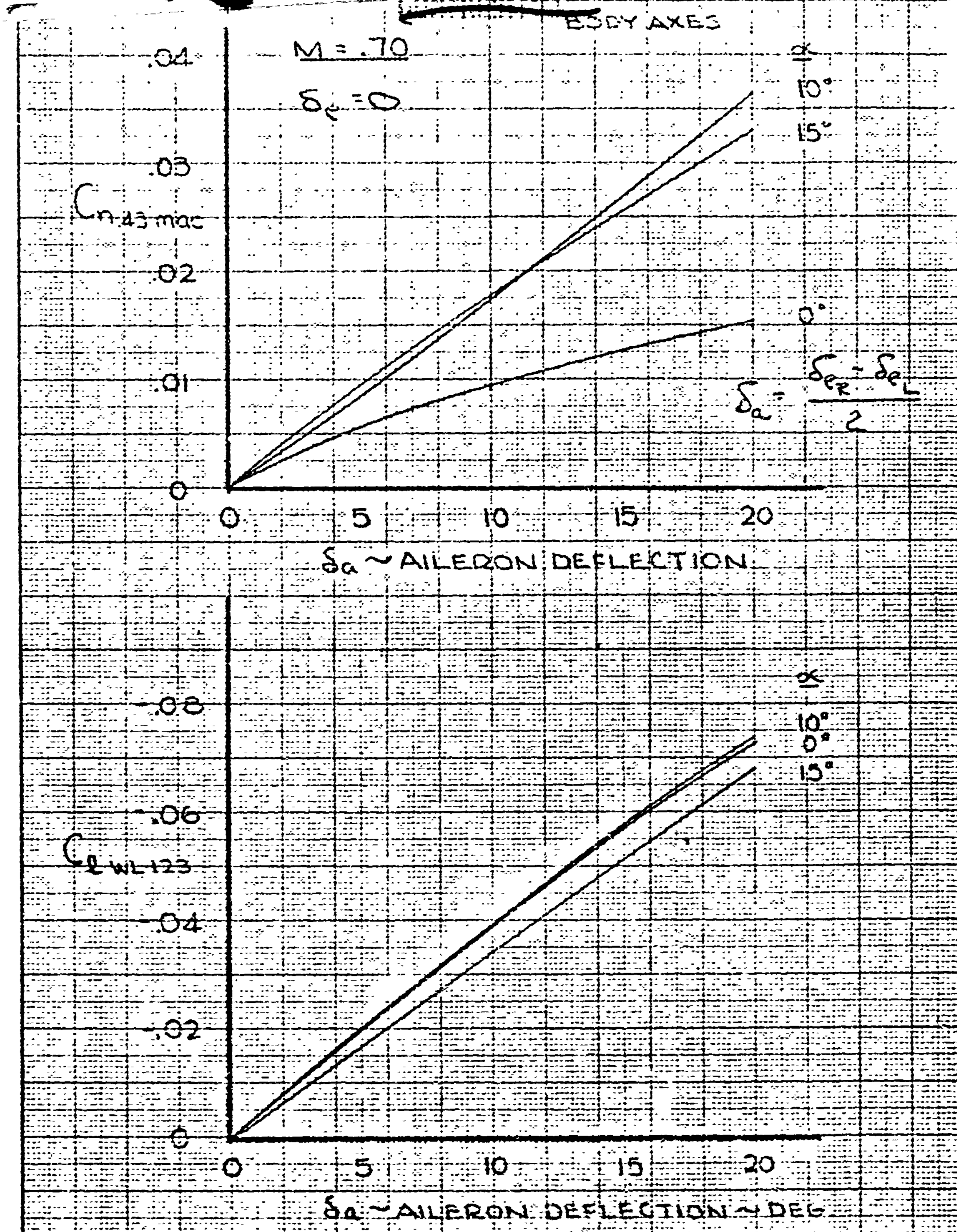

FIG 6.31

CALC JEB/RTB	12/5/60	REVISED	DATE	AILERON CHARACTERISTICS M = .70	544-2035
CHECK					D2-8174
APR					
APR				BOEING AIRPLANE COMPANY	PAGE 6.35

145

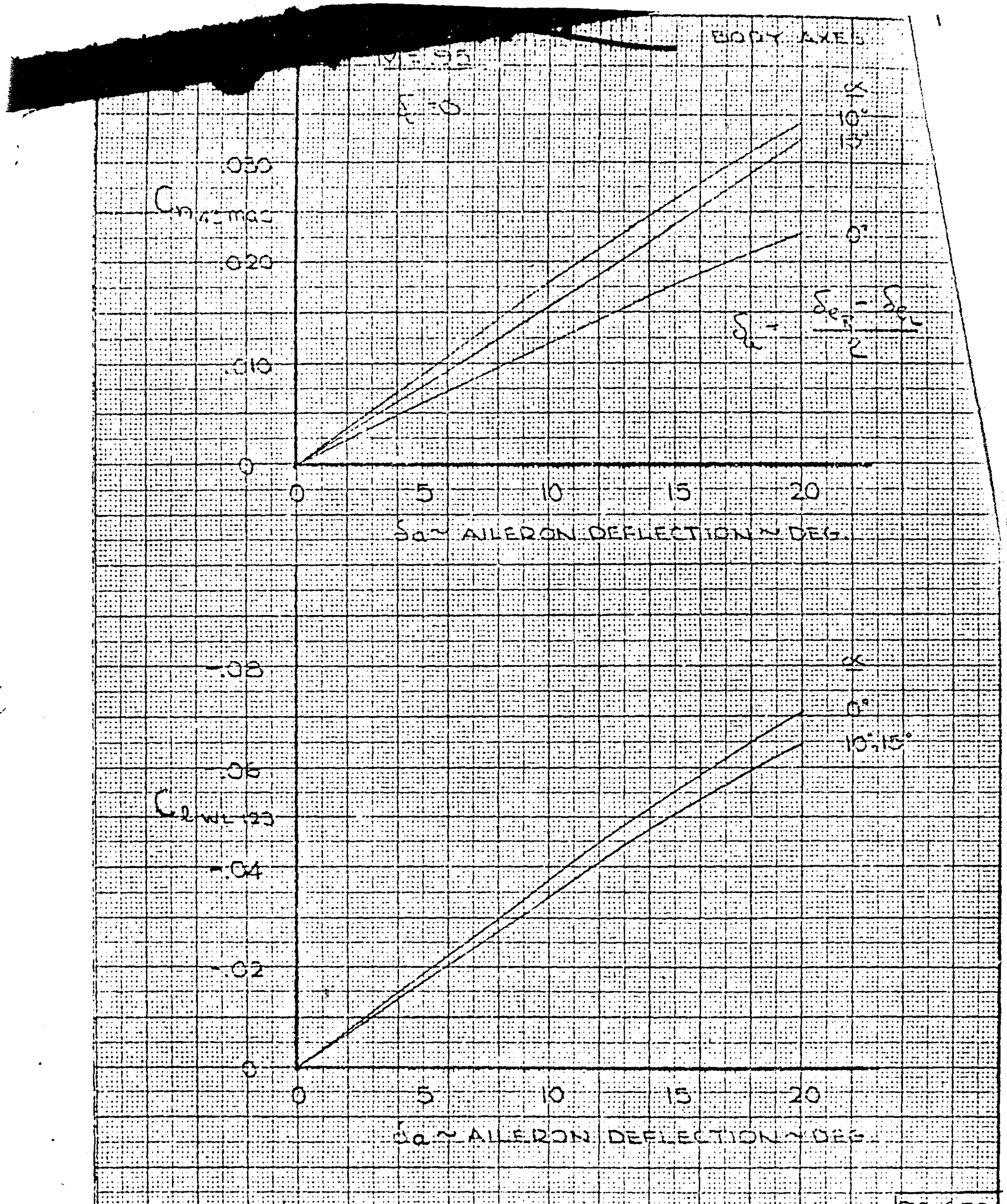

FIG. 6.32

CALC	WED/RTB	12/9/60	REVISED	DATE
CHECK				
APR				
APR				

AILERON CHARACTERISTICS

M = .95

146

BOEING AIRPLANE COMPANY

844-2035

D2-8174

PAGE

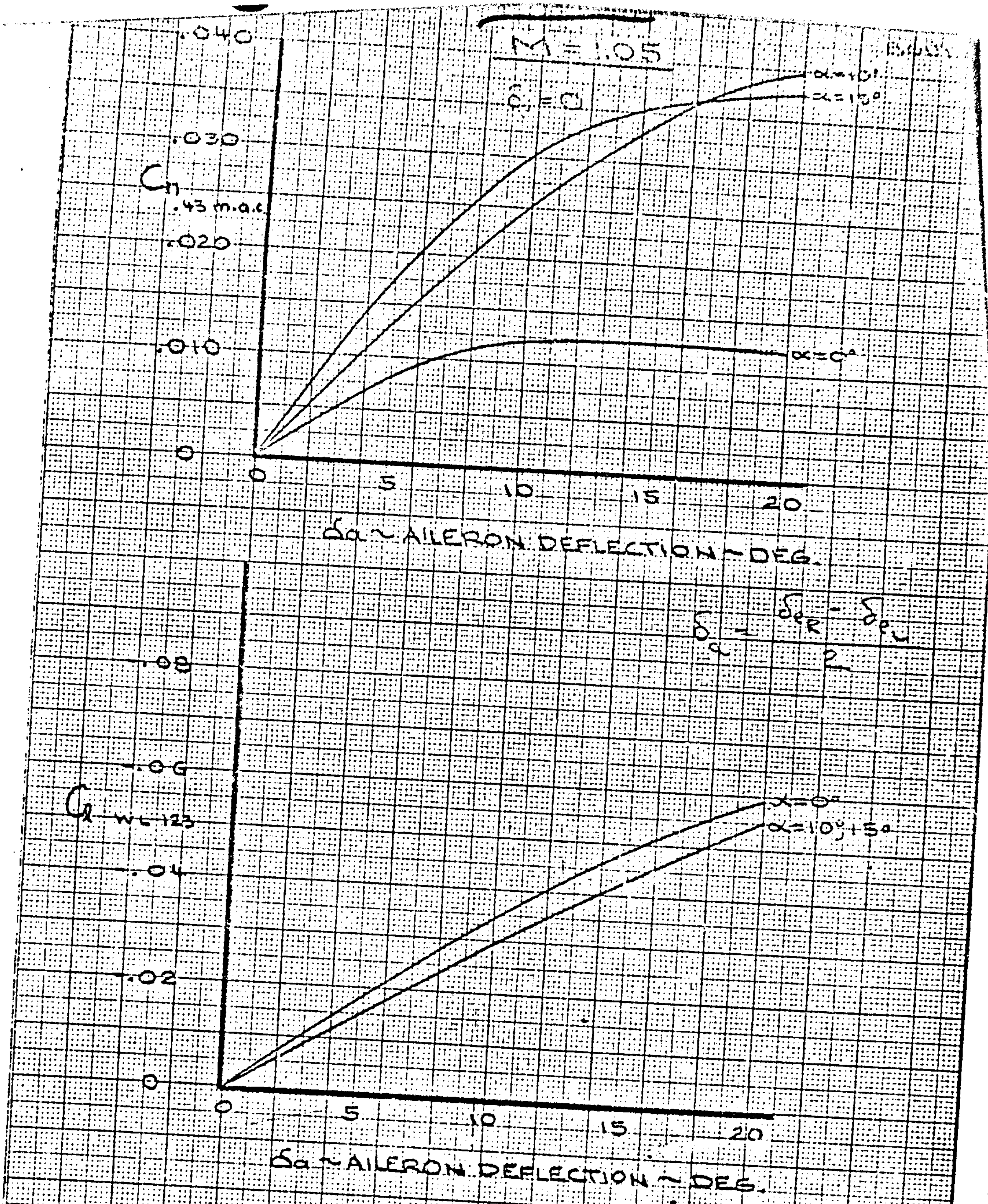

CALC	JEB/RTB	12/9/60	REVISED	DATE	FIG 6.33
CHECK					844-2035
APR					D2-8174
APR					PAGE 6.37

AILERON CHARACTERISTICS

M = 1.05

147

BOEING AIRPLANE COMPANY

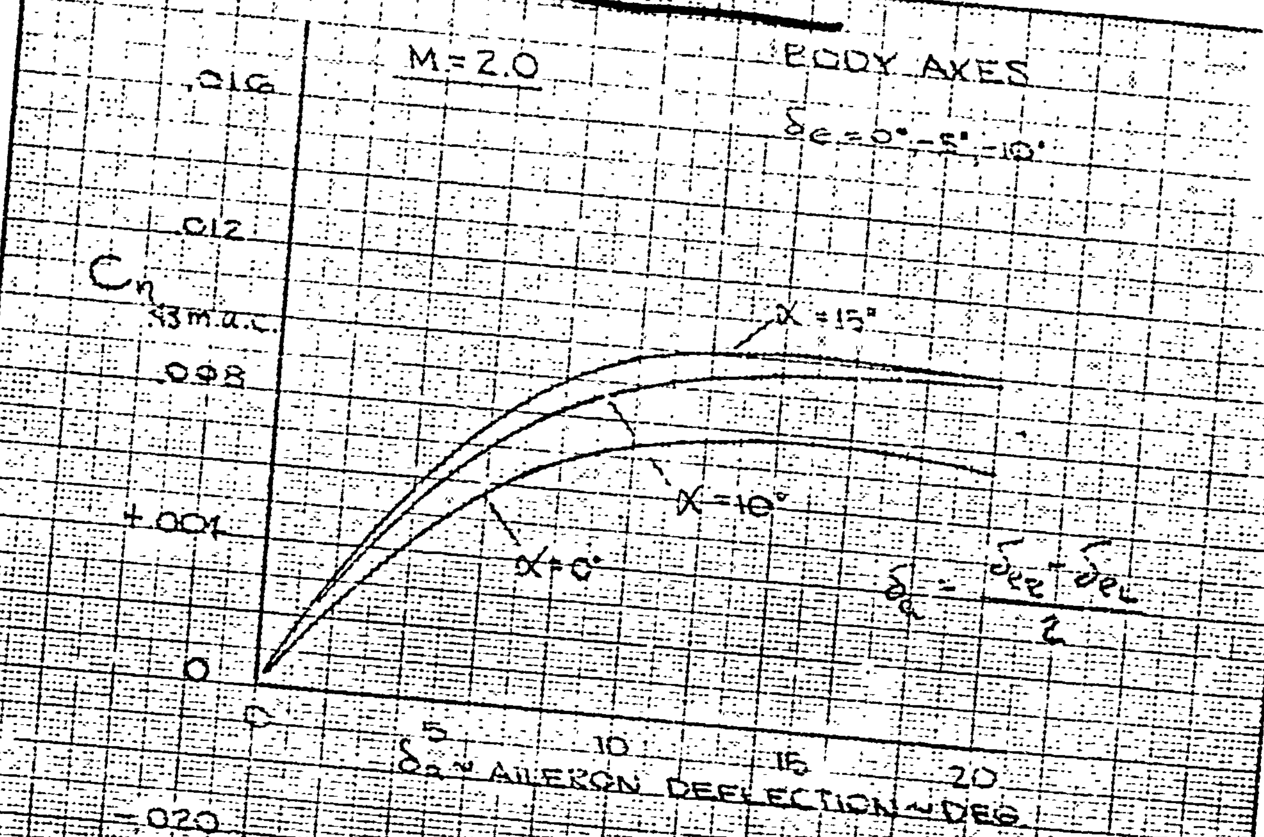

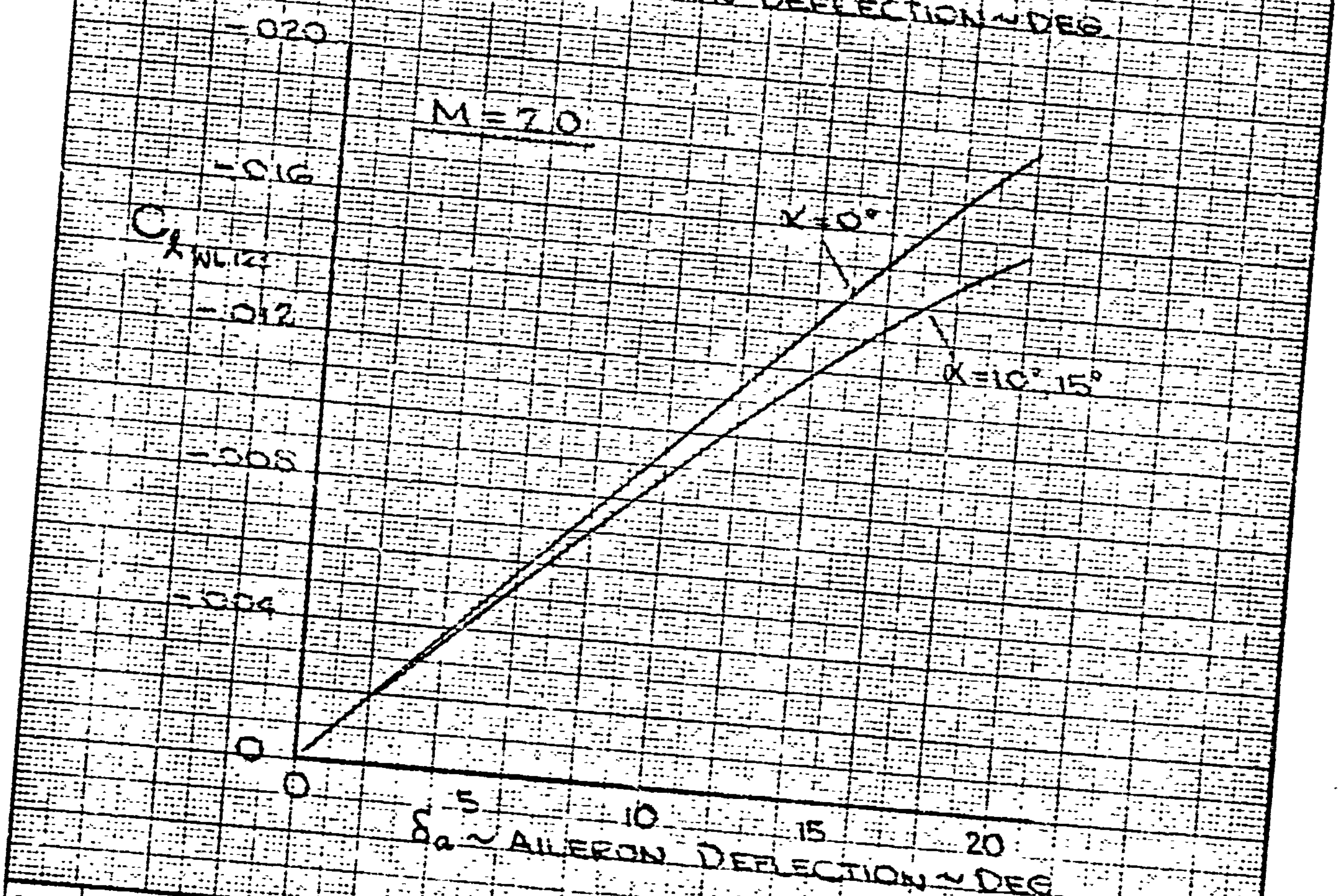

CALC	[illegible]	12-1-60	REVISED	DATE
CHECK				
APR				
APR				

AILERON CHARACTERISTICS
M = 2.0 148

FIG. 6.34
B44-2035

BOEING AIRPLANE COMPANY
SEATTLE 24 WASHINGTON

D2-8174

BAC 461 C-R4

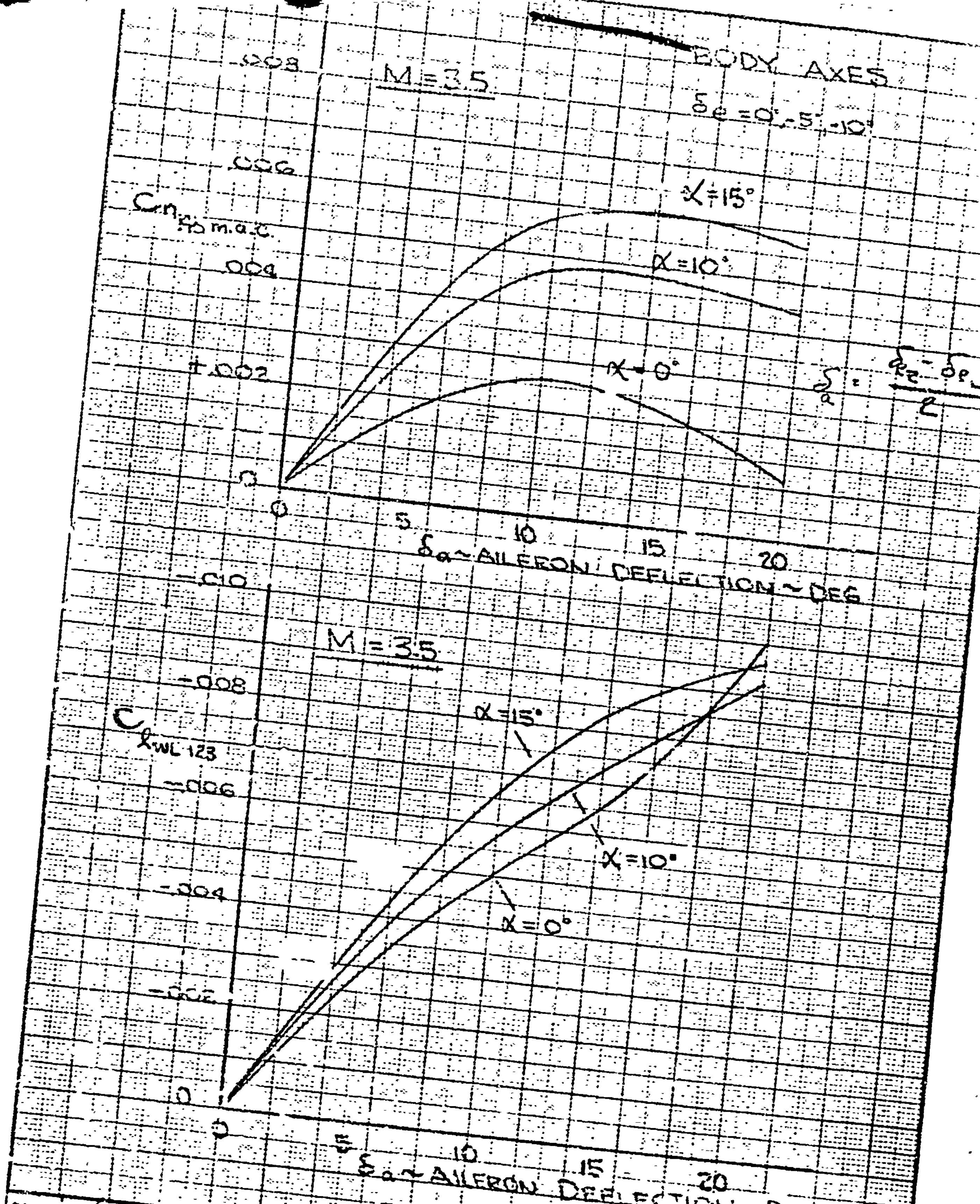

CALC	[illegible] 12/5/61	REVISED	DATE	AILERON CHARACTERISTICS	FIG. 6.35
CHECK				M = 3.5 **149**	244-2035
APR				BOEING AIRPLANE COMPANY	D2-8174
APR					PAGE 6.39

BAC 461 C-R4

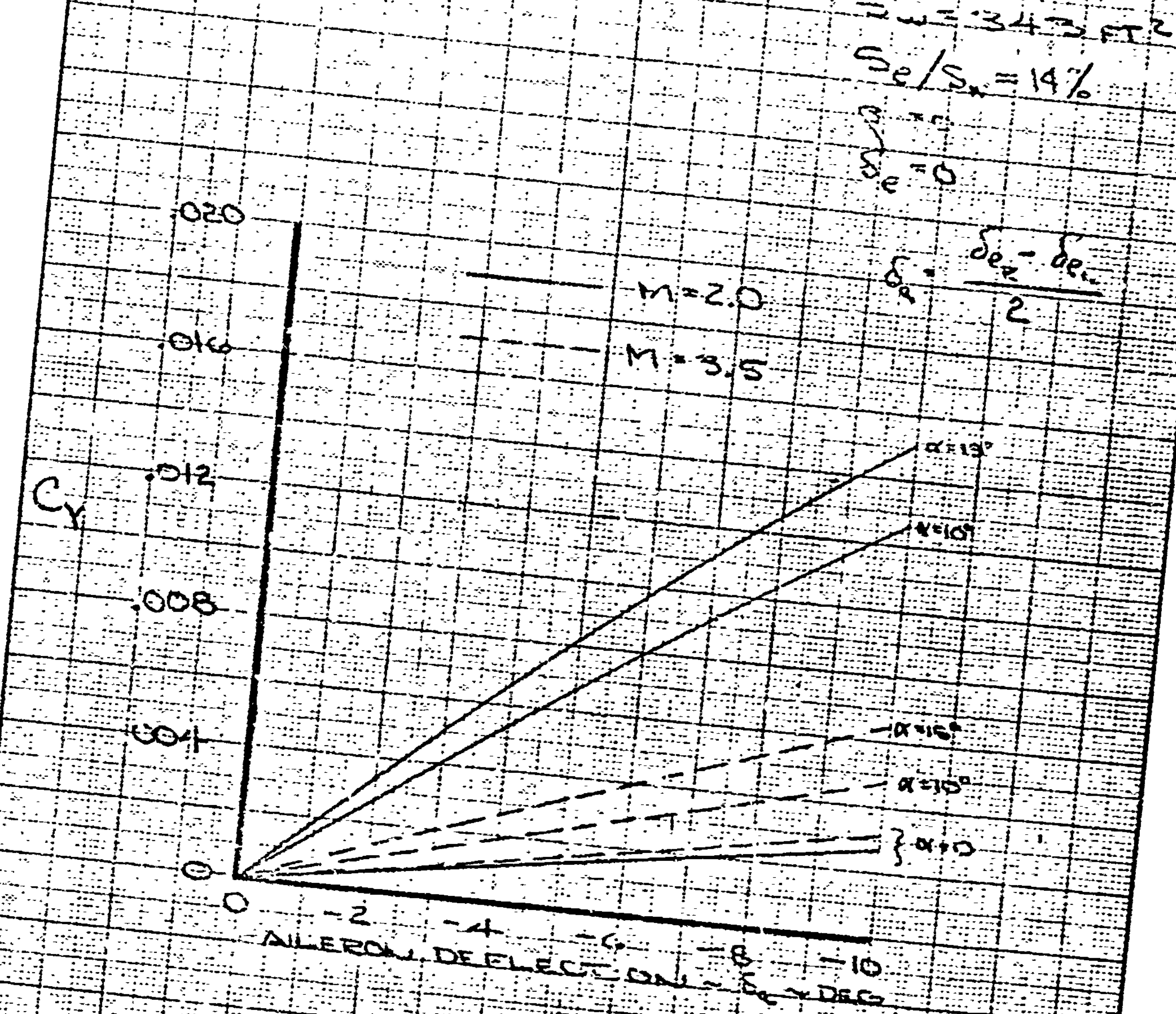

EH/EFR 12-21-?	REVISED	DATE	
CHECK			
APP			
APP			

SIDE FORCE DUE TO AILERON DEFLECTION M=2.0 AND 3.5

FIG. 36

E44-2035

D2-8124

BOEING AIRPLANE COMPANY

150

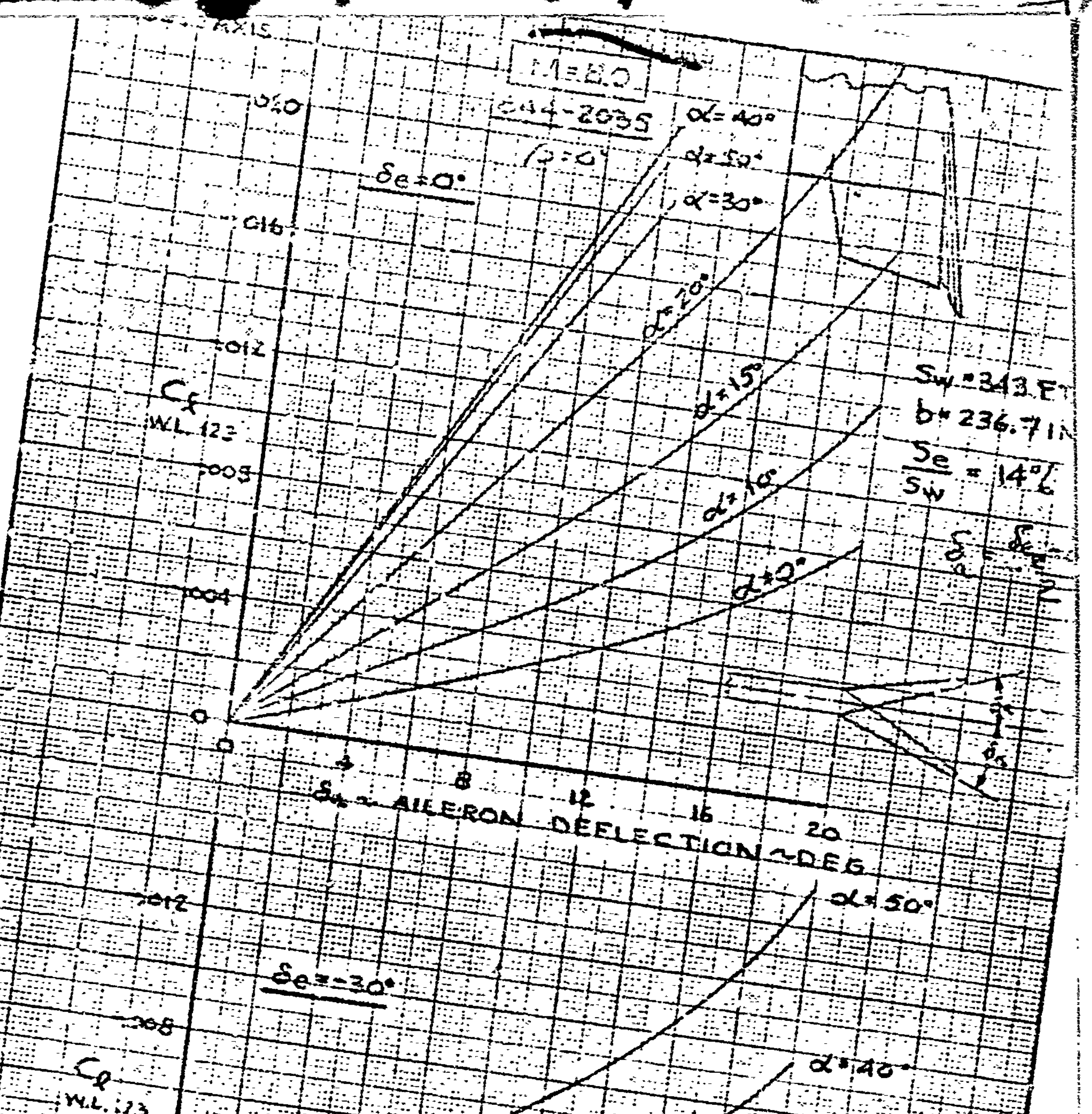

NOTE: THESE CURVES ARE BASED ON M=8.1 TEST DATA AND PARTIALLY SUBSTANTIATED BY M=9.5 TEST DATA.

CALC	EJH	8/8/6	REVISED	DATE
CHECK				
APR				
APR				

ROLLING MOMENT DUE TO AILERON HYPERSONIC SPEED

151

FIG 6.37
844-2035

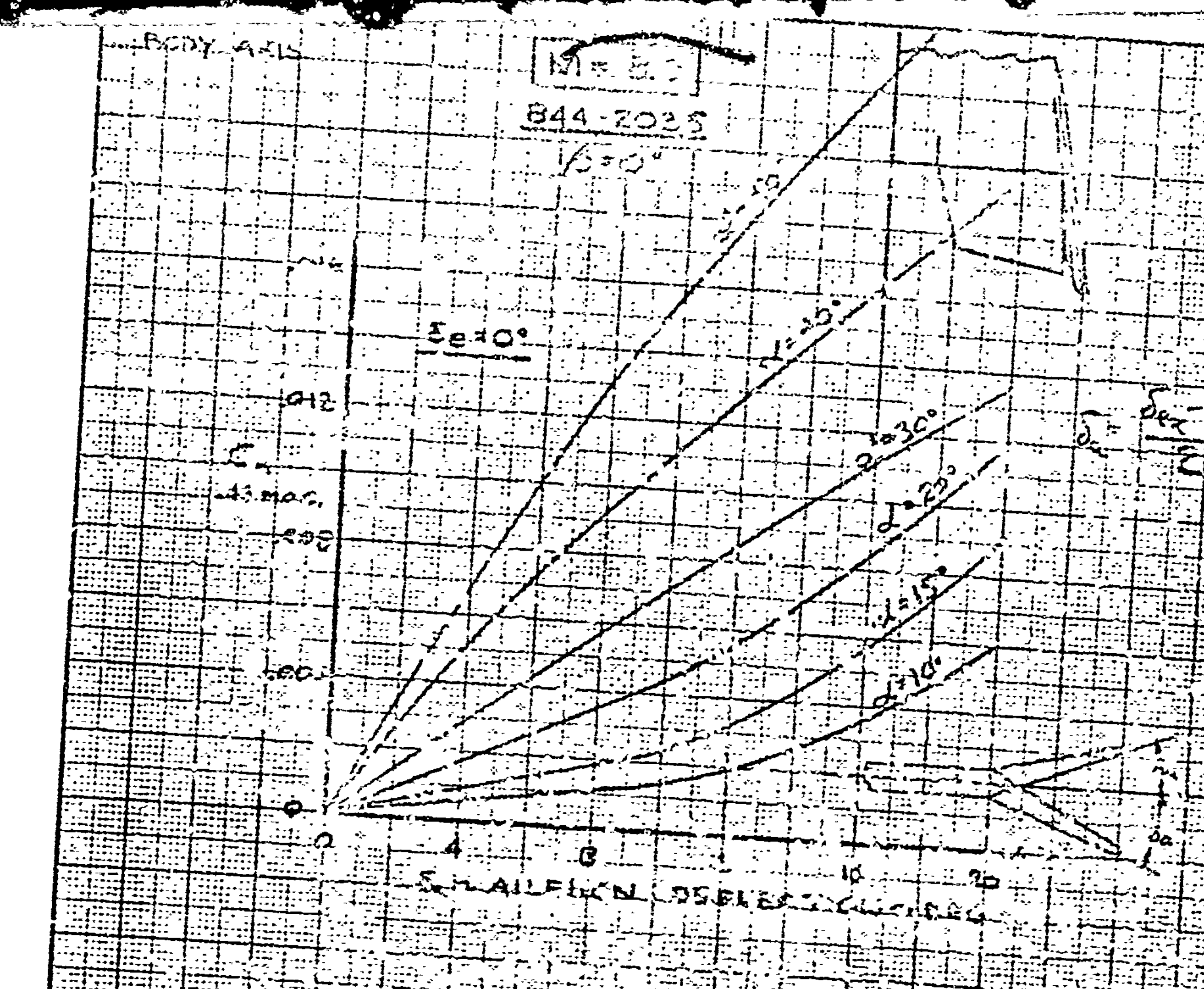

$S_W = 343\ FT^2$

$b = 236.7$ IN

$\frac{S_a}{S_W} = 14\%$

NOTE: THESE CURVES ARE BASED ON M = 6.1 TEST DATA AND PARTIALLY SUBSTANTIATED BY M = 9.5 TEST DATA.

CALC	ECH	12/9/60	REVISED	DATE
CHECK				
APR				
APR				

YAWING MOMENT DUE TO AILERON HYPERSONIC SPEED

FIGURE 152

BOEING AIRPLANE COMPANY

844-2035

T2-8174

PAGE 6.42

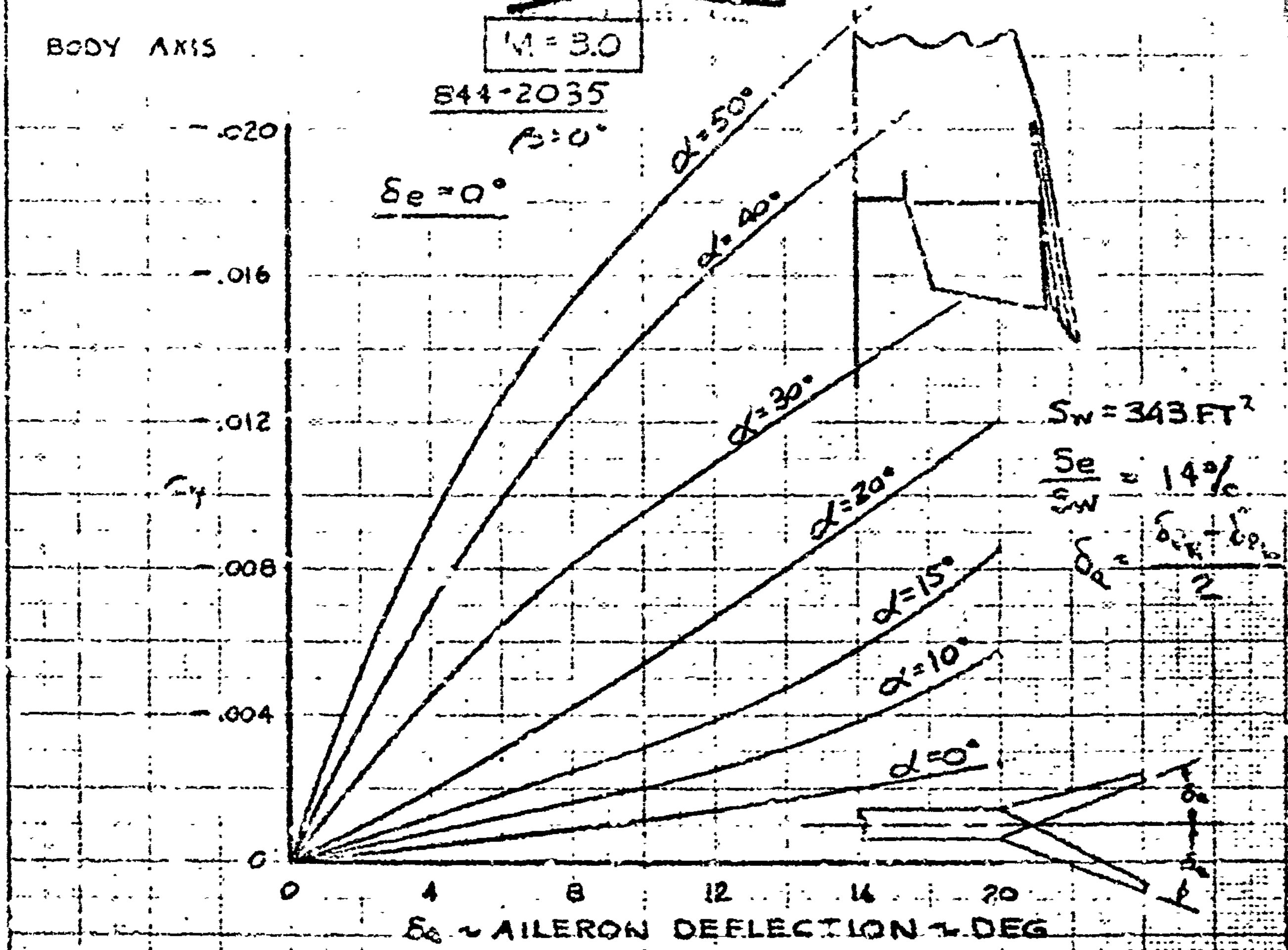

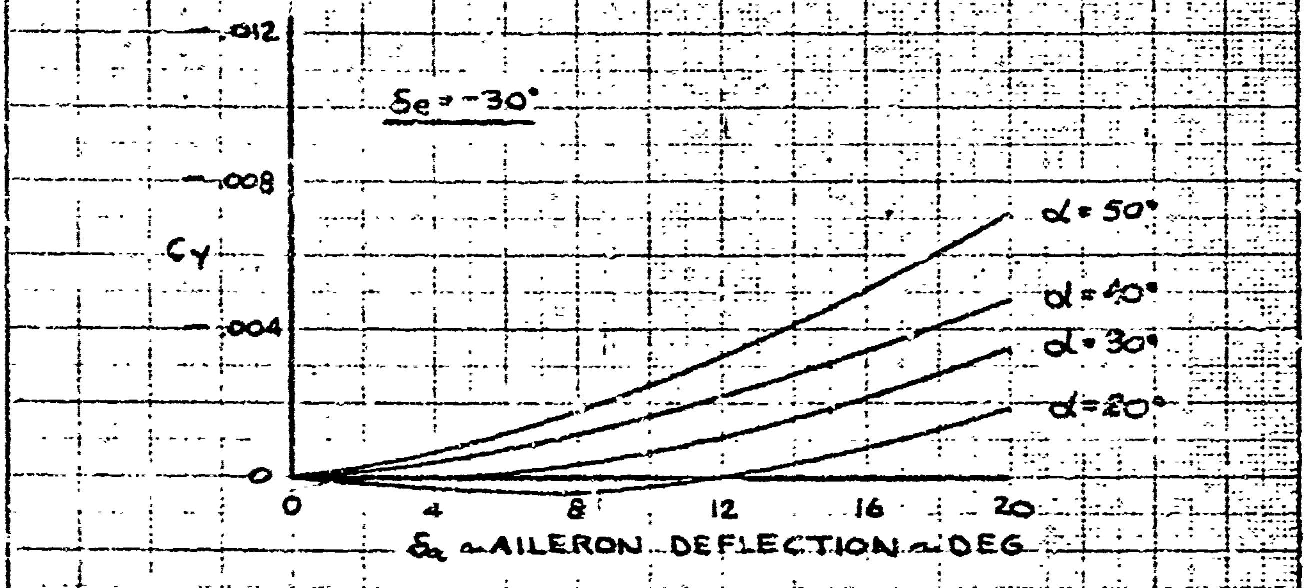

NOTE: THESE CURVES ARE BASED ON M = 8.1 TEST DATA AND PARTIALLY SUBSTANTIATED BY M = 9.5 TEST DATA.

FIG. 6.39

CALC EJH	14/8/6?	REVISED	DATE	SIDE FORCE DUE TO AILERON HYPERSONIC SPEED
CHECK				844-2035
APD				D2-8174
APD				BOEING AIRPLANE COMPANY

153

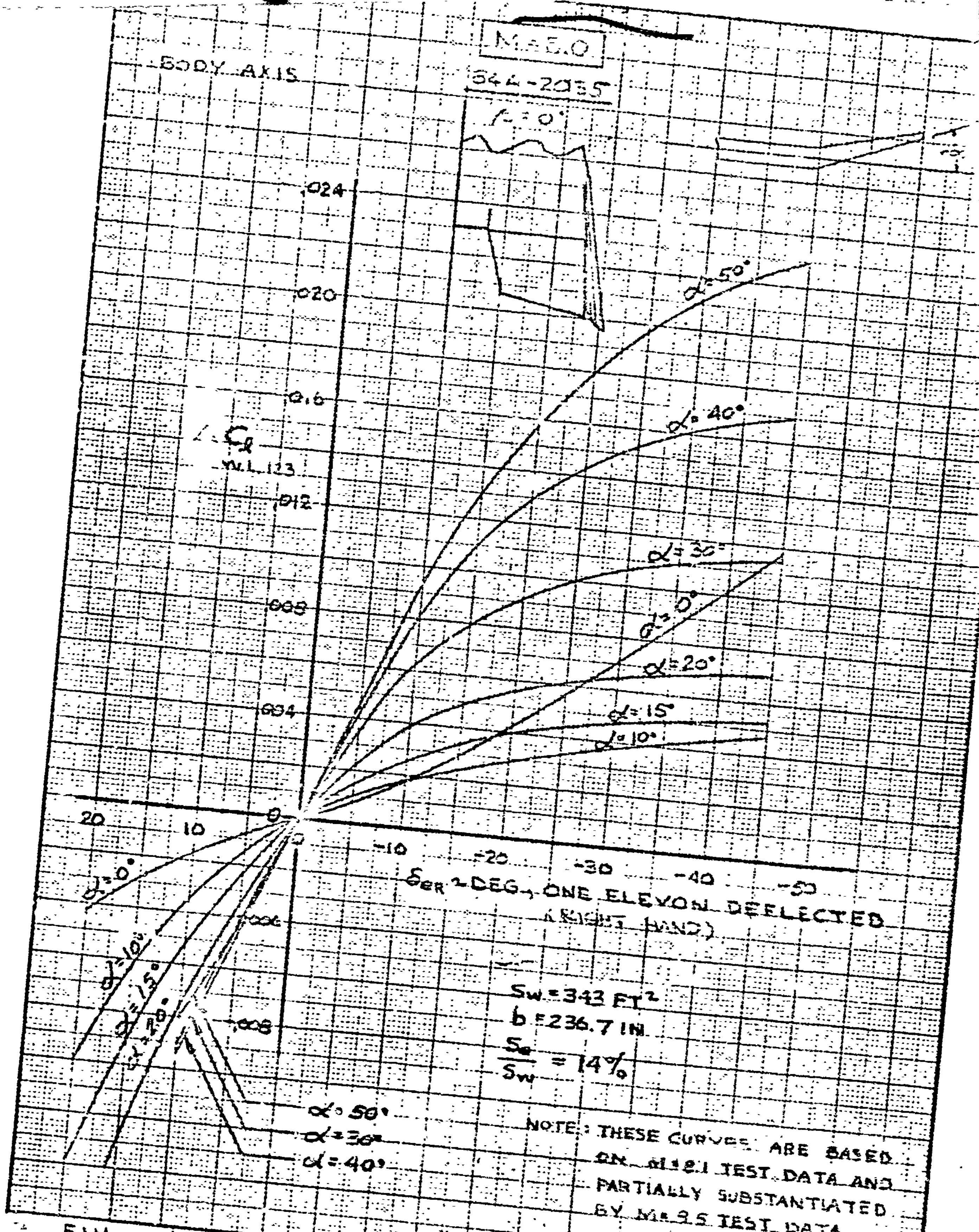

EJH	12/8/5	REVISED	DATE
CHECK			
APR			
APR			

FIG. 6.40

ROLLING MOMENT DUE TO ONE ELEVON HYPERSONIC SPEED

154

544-2035

BOEING AIRPLANE COMPANY

D2-8174

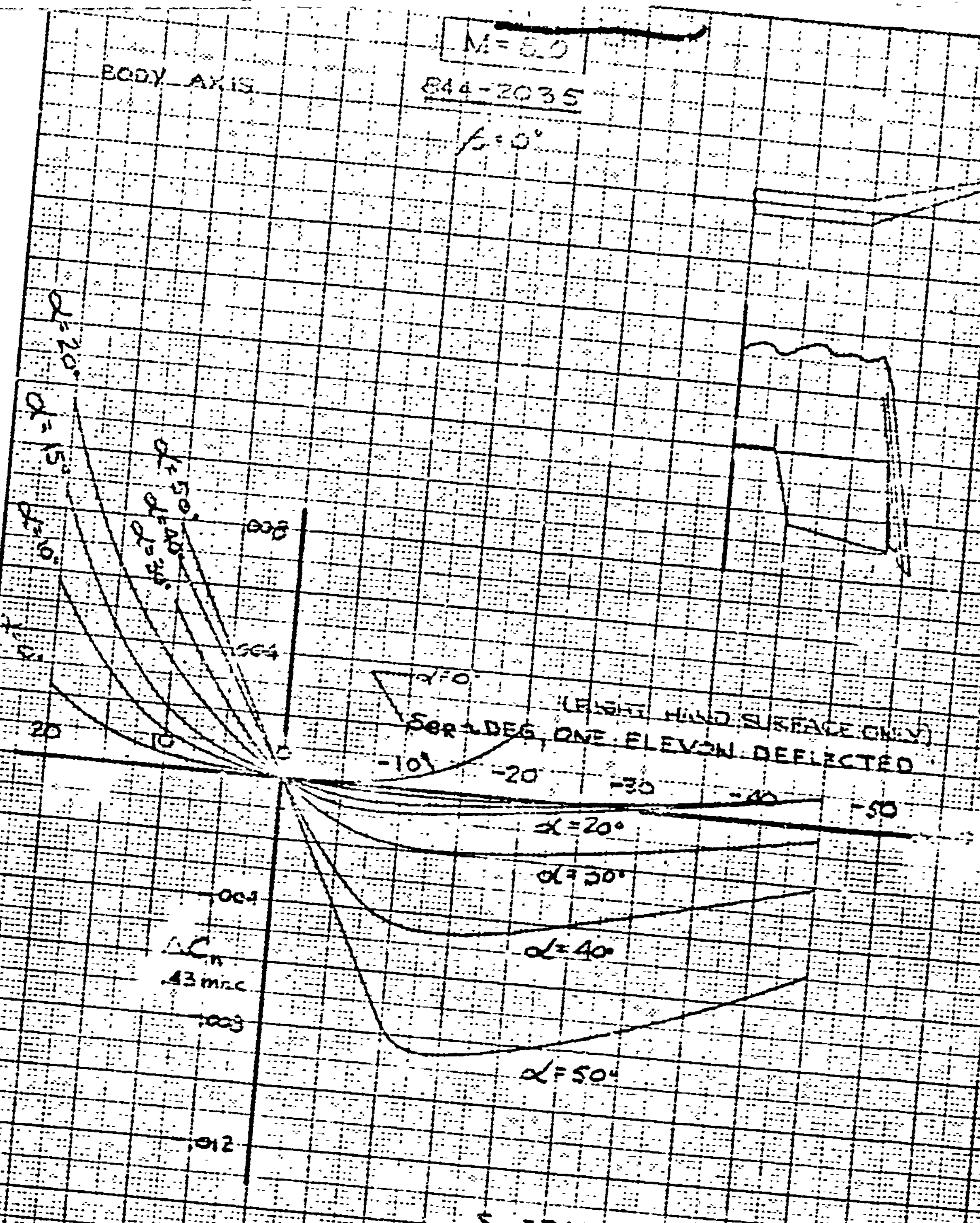

$S_w = 343\ FT^2$

$b = 236.7\ IN$

$\frac{S_e}{S_w} = 14\%$

NOTE: THESE CURVES ARE BASED ON M=8.1 TEST DATA AND PARTIALLY SUBSTANTIATED BY M=5.5 TEST DATA

CALC	EJH	11/8/0	REVISED	DATE
CHECK				
APR				
APR				

FIG. 6.41

YAWING MOMENT DUE TO ONE ELEVON HYPERSONIC SPEED **155**

844-2035

BOEING AIRPLANE COMPANY

D2-8174

PAGE 6.45

K-E

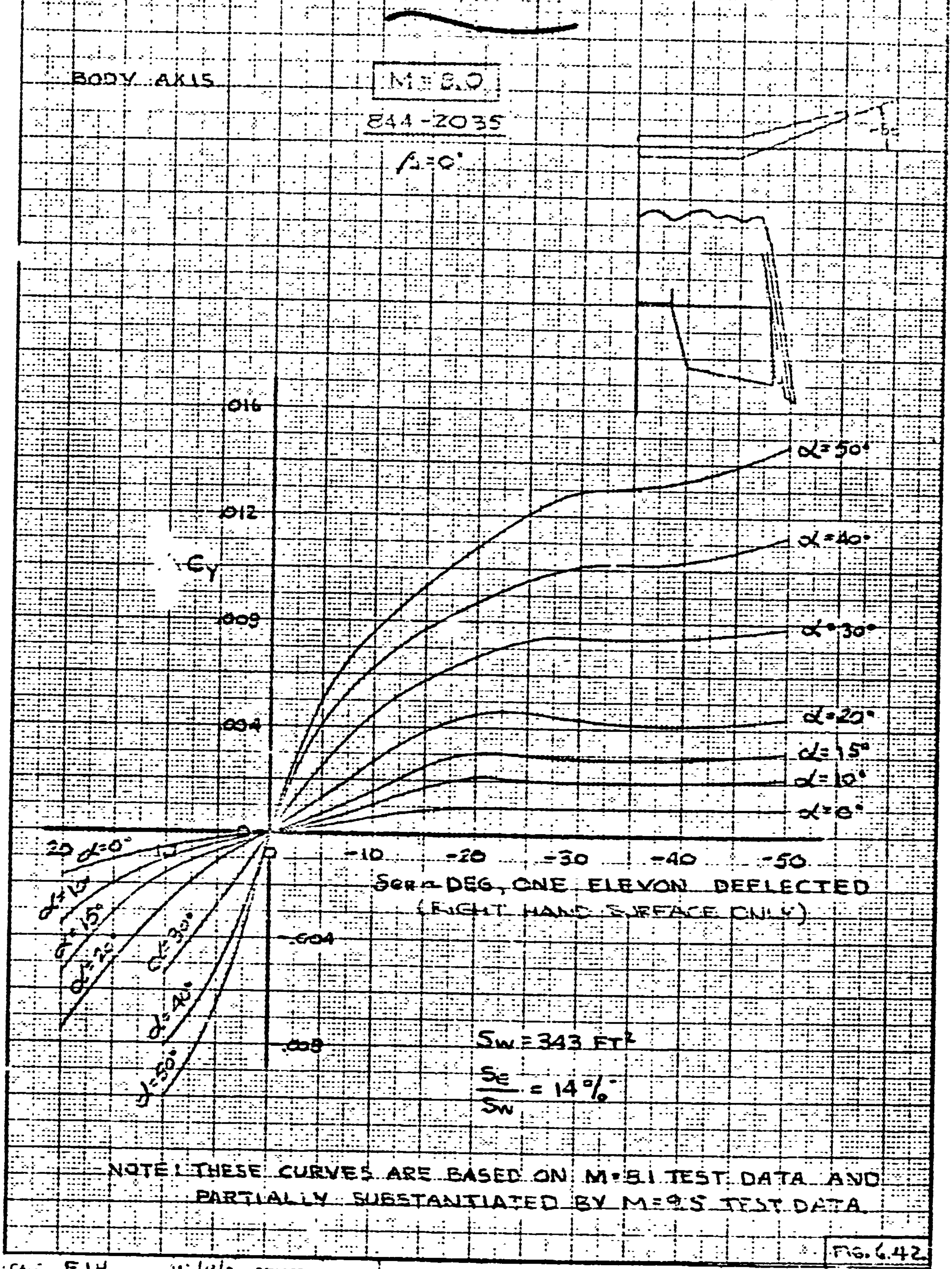

FIG. 6.42

CALC	EJH	1-18/0	REVISED / DATE
CHECK			
APD			
APD			

SIDE FORCE DUE TO ONE ELEVON HYPERSONIC SPEED

156

BOEING AIRPLANE COMPANY

844-2035

D2-8174

PAGE 6.46

6.3 RUDDER CHARACTERISTICS AND EFFECTIVENESS

Rudder effectiveness data for the 844-2035 configuration are presented in Figures 6.43 through 6.51. Summary curves of $C_{n\delta_r}$, $C_{Y\delta_r}$, and $C_{\ell\delta_r}$ versus Mach number are presented on Figures 6.43, 6.44, and 6.45; more detailed data are presented on Figures 6.46 through 6.51. The data presented are based on wind tunnel data on similar configurations adjusted to the dimensions of the 844-2035.

Landing speed rudder effectiveness is based on preliminary data from BTWT 619. Transonic and supersonic effectiveness were obtained from wind tunnel tests of a model 814-1047 at M = .905, 2.0 and 3.5. The hypersonic characteristics are presented for M = 8, based on a model similar to 814-1050 at AEDC-B (test BAC 8). These characteristics are currently considered to apply for higher hypersonic speeds. The effect of altitude (i.e., Reynolds number) is assumed to be negligible.

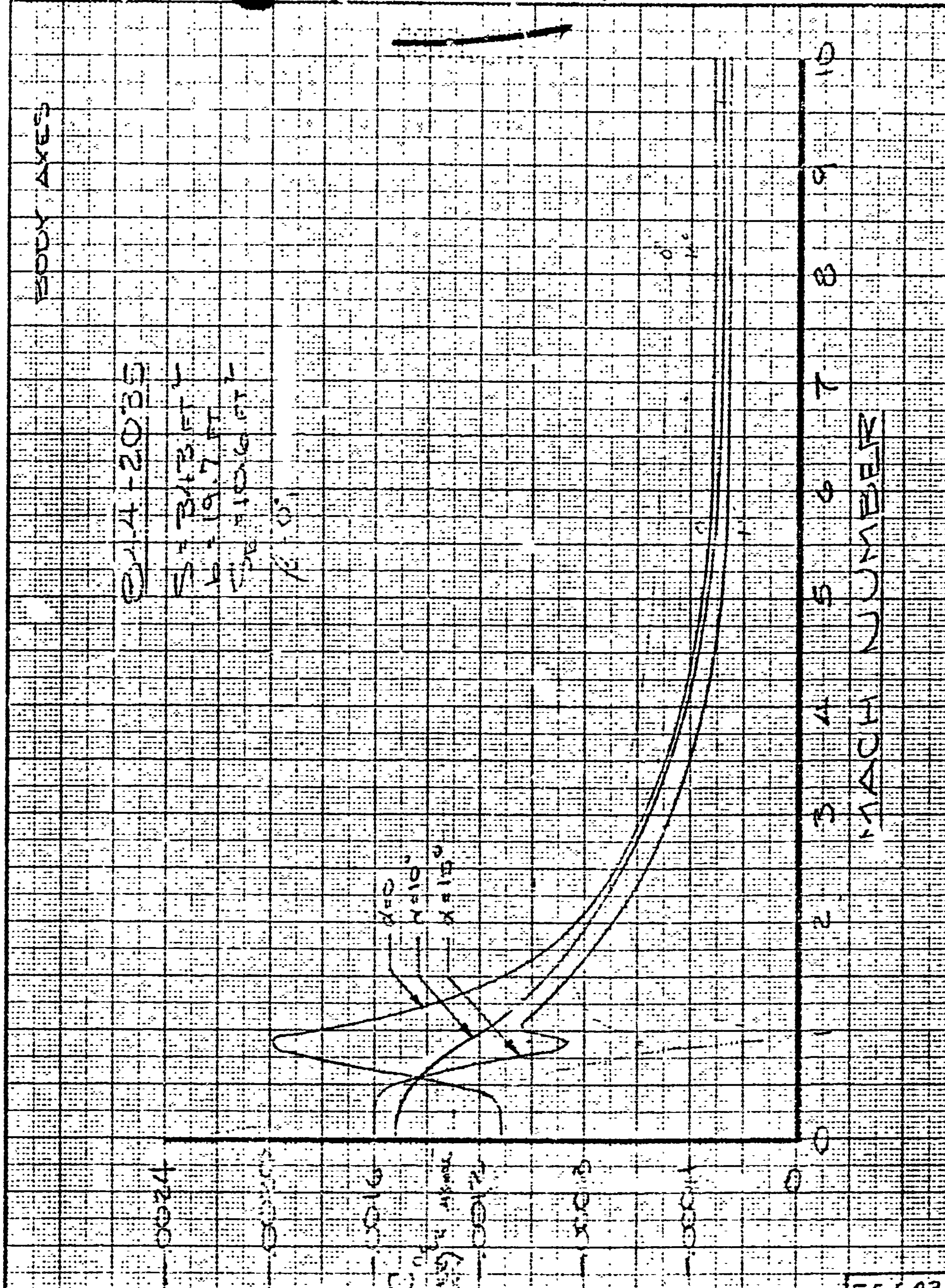

FIG. 6.43

CALC	BJK	12-8-?	REVISED	DATE
CHECK			BJK	12-15-?
APR				
APR				

YAWING MOMENT DUE TO RUDDER

BOEING AIRPLANE COMPANY

E44-2035

D2-6174

PAGE 6.48

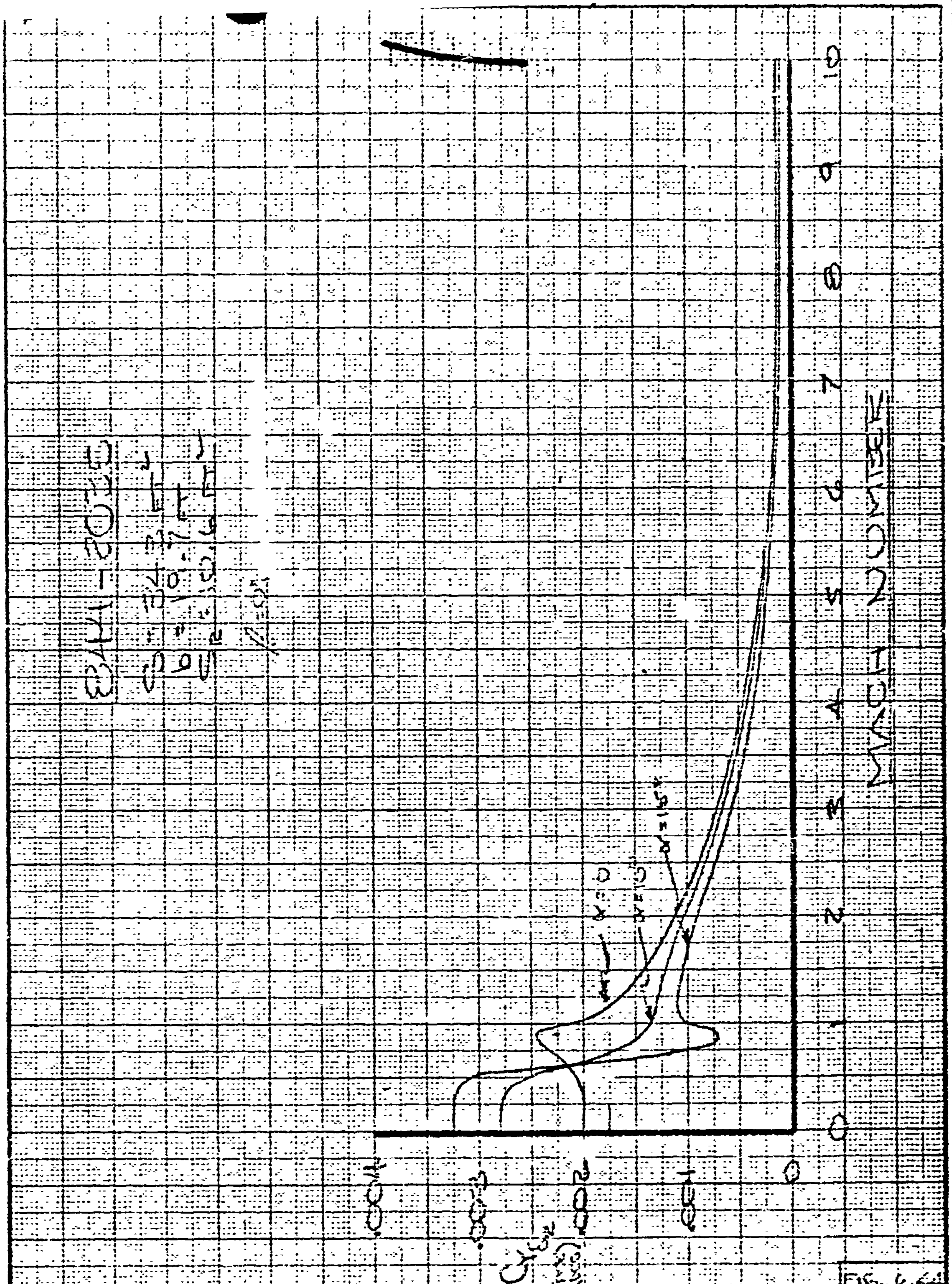

FIG. 6.44

CALC	BYR	12-8-60	REVISED	DATE	SIDE FORCE 159 DUE TO RUDDER	844-2035
CHECK			BYR	12-1-60		D2-8174
APR					BOEING AIRPLANE COMPANY	PAGE 6.49
APR						

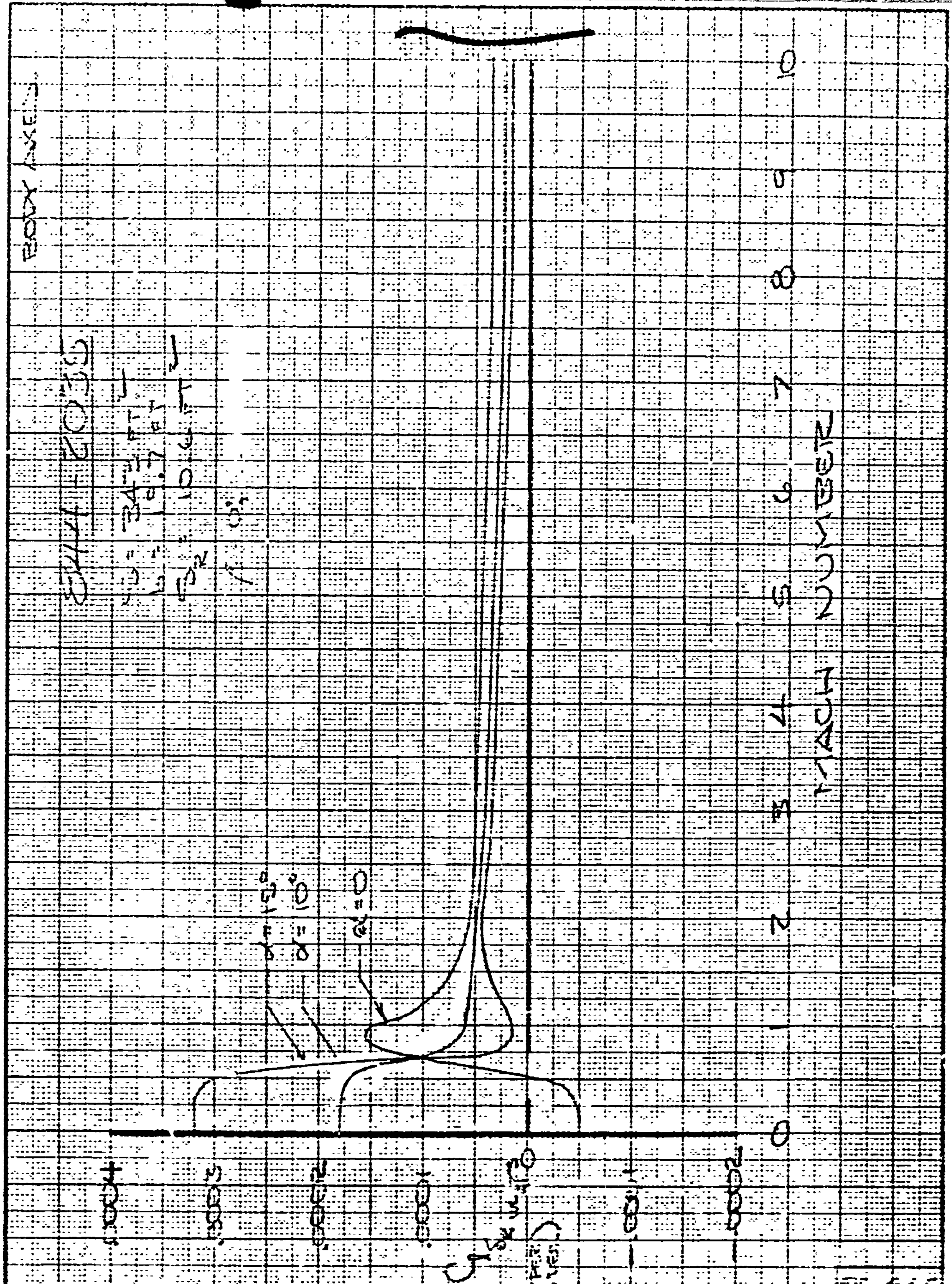

CALC			REVISED	DATE	ROLLING MOMENT DUE TO RUDDER	E44-2035
CHECK						D2-6174
APR					BOEING AIRPLANE COMPANY	PAGE 6.50
APR						

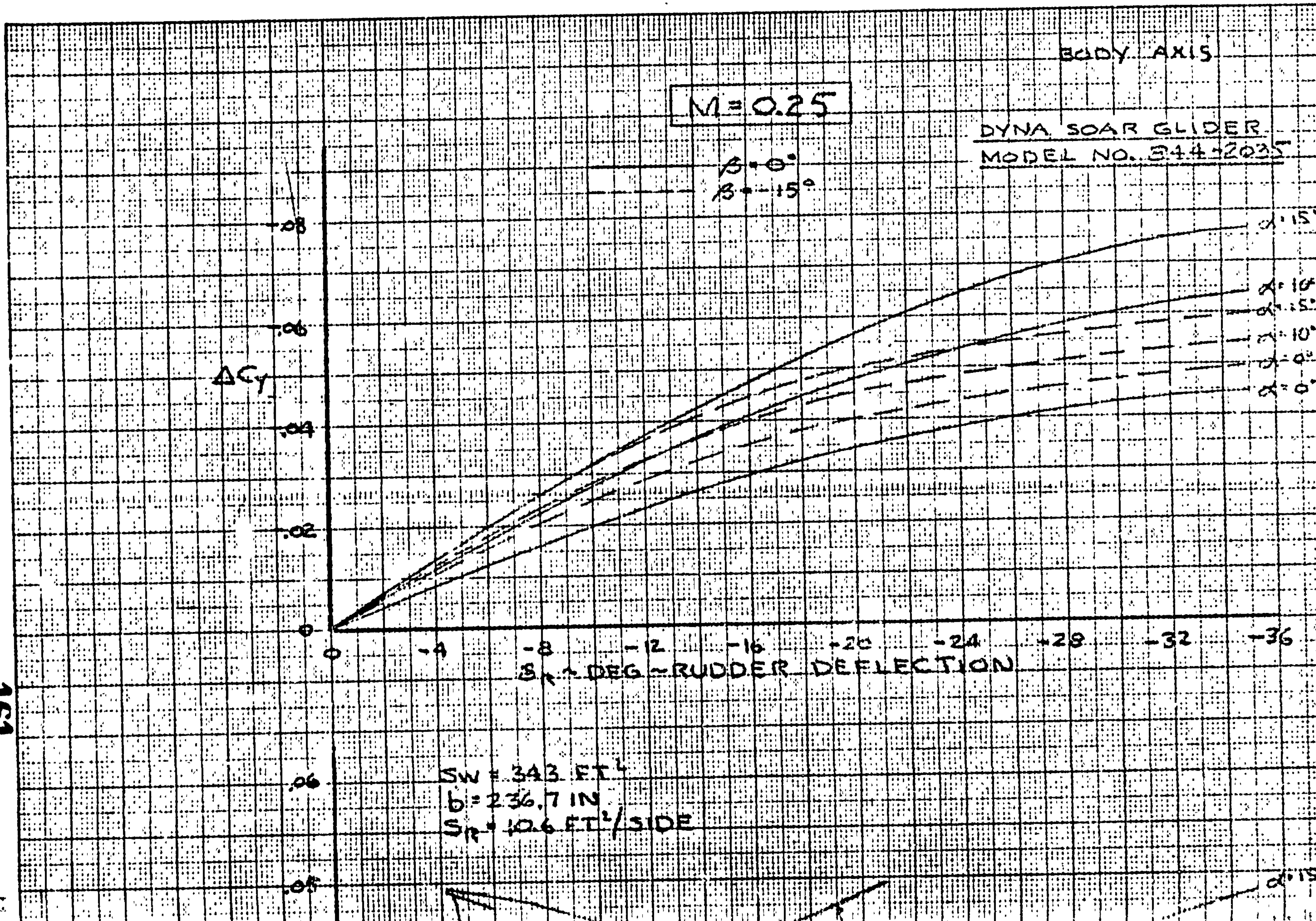
BODY AXIS
M = 0.25
DYNA SOAR GLIDER
MODEL NO. 344-2035
β = 0°
β = -15°
α = 15°
α = 10°
α = 5°
α = 10°
α = 0°
α = 0°
α = 15°
ΔCy
.08
.06
.04
.02
0
.06
.08
0
-4
-8
-12
-16
-20
-24
-28
-32
-36
δR ~ DEG ~ RUDDER DEFLECTION
SW = 343 FT²
b = 236.7 IN
SR = 10.6 FT²/SIDE

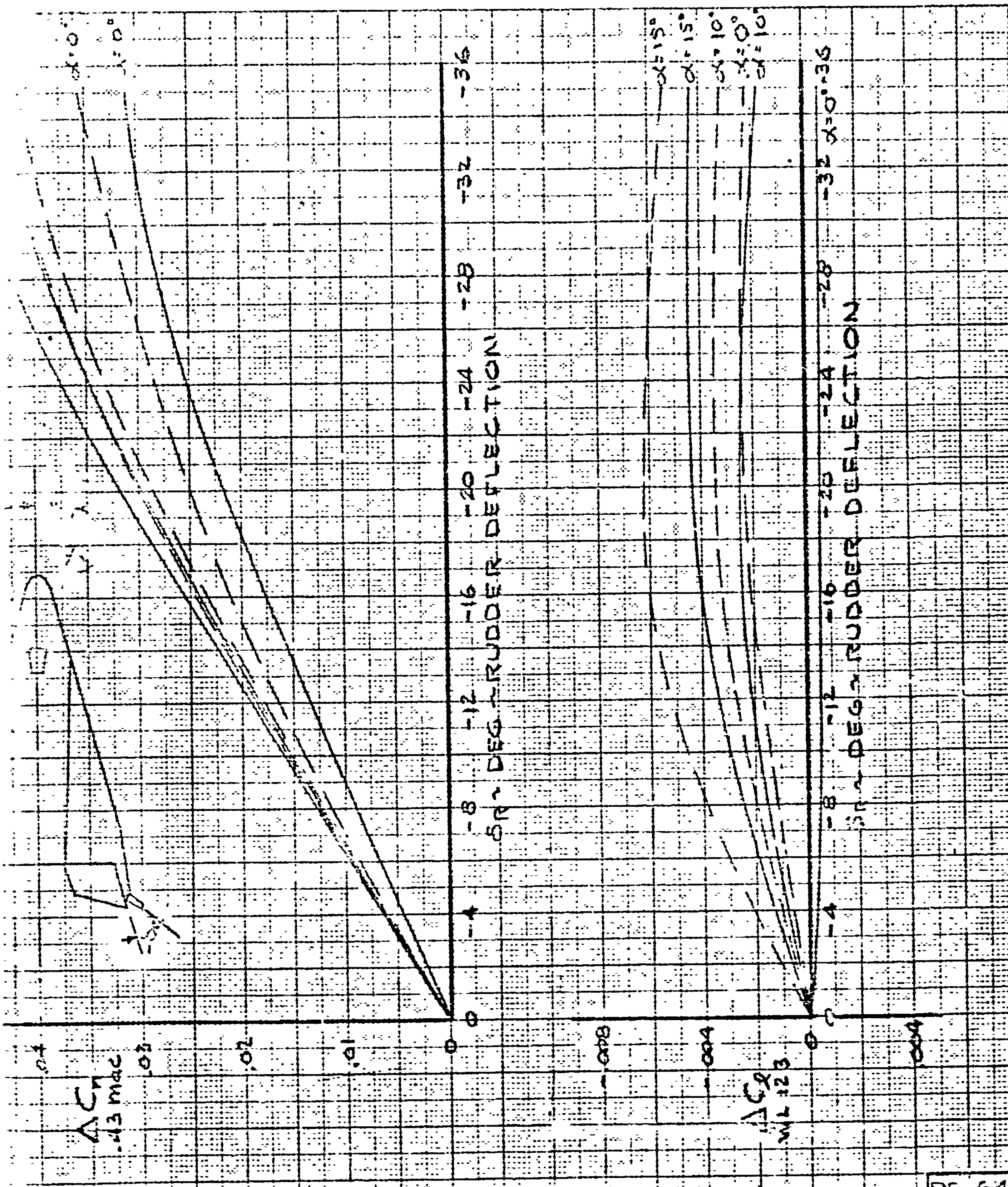

CALC	EJH	11/9/60	REVISED	DATE	RUDDER EFFECTIVENESS LANDING SPEED	FIG. 6.46
CHECK						844-2035
APPD						D2-8174
APPD						PAGE 6.51

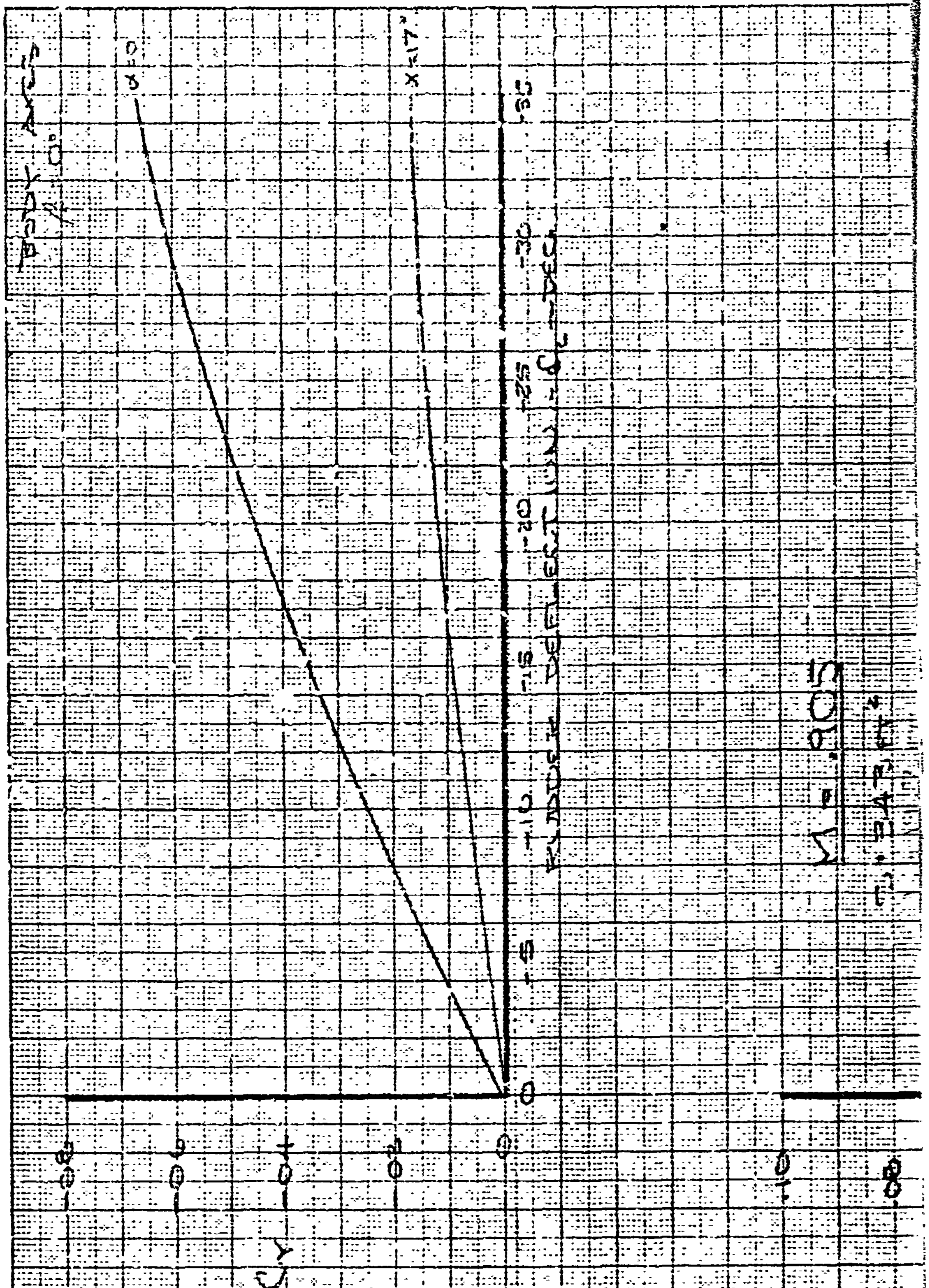
BODY AXES
β = 0°
α = 0°
α = 17°
C_Y
.08
.06
.04
.02
0
-.10
-.08
0
-5
-10
-15
-20
-25
-30
-35
RUDDER DEFLECTION ~ δr ~ DEG
M = .905

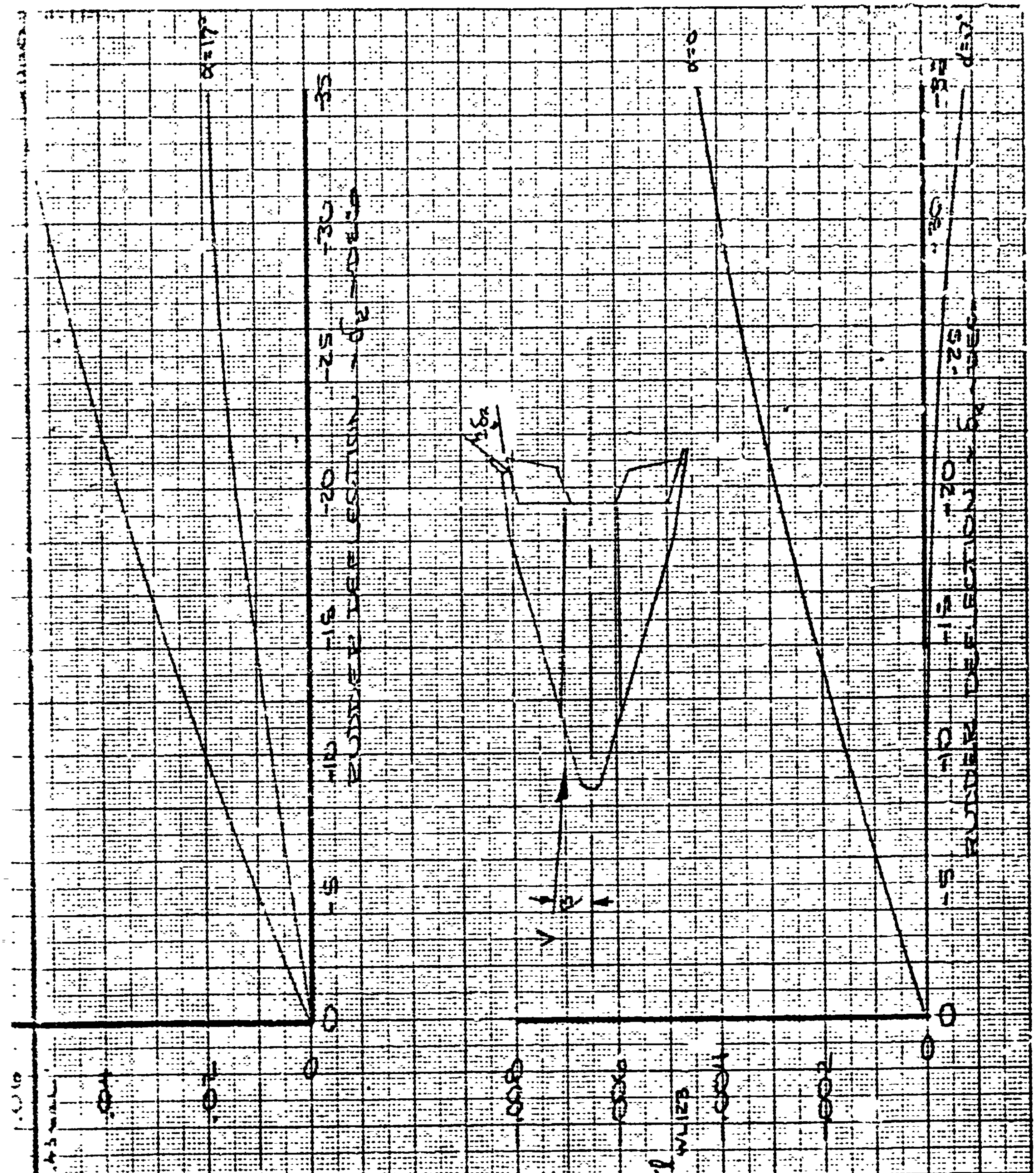

CALC	BFR	12-8-0	REVISED	DATE		FIG. 6.47
CHECK					RUDDER EFFECTIVENESS	844-2095
APPD					M = .905	D2-8174
APPD						PAGE 6.52

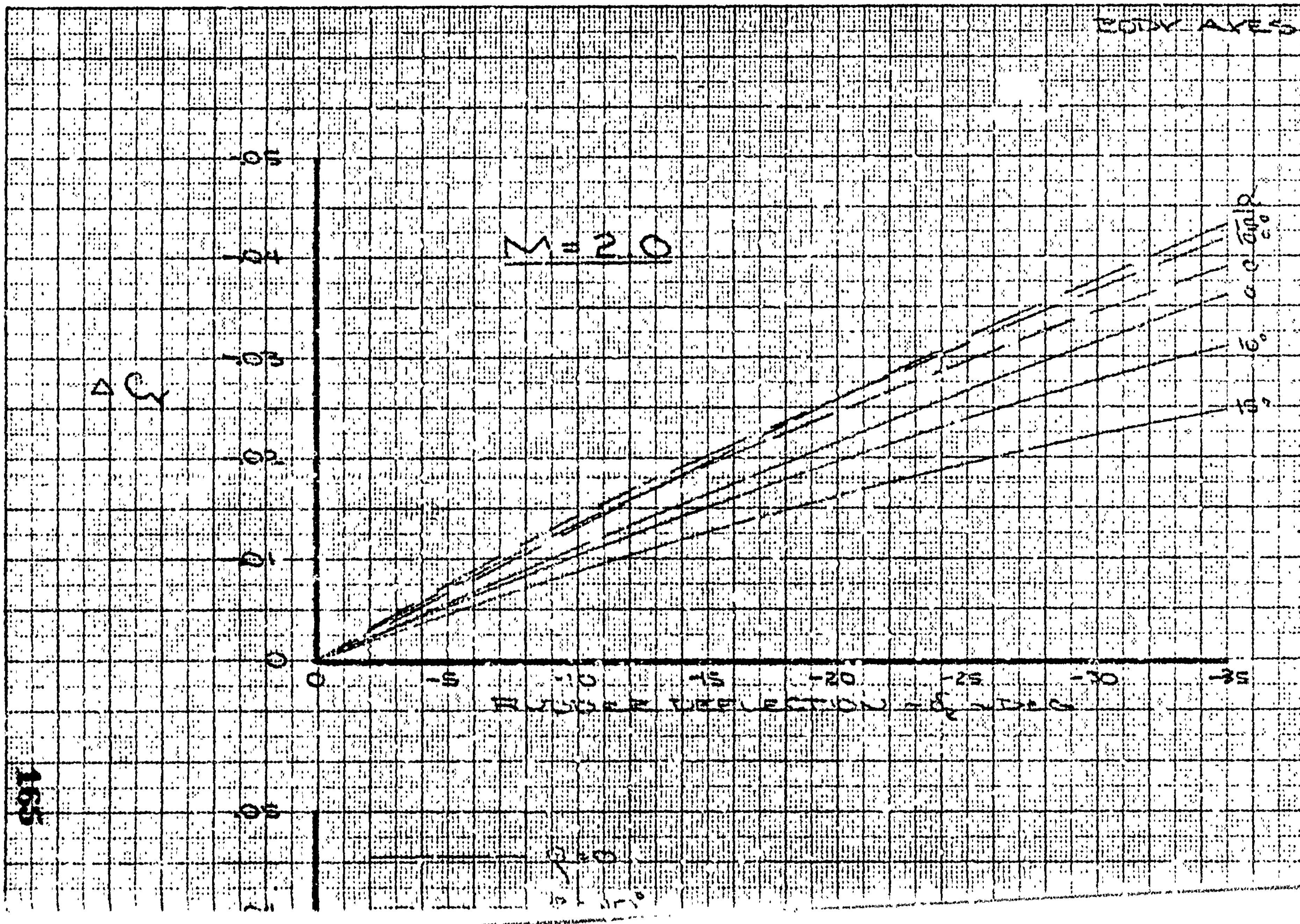
BODY AXES
M = 2.0
ΔC_Y
.05
.04
.03
.02
.01
0
-5
-10
-15
-20
-25
-30
-35
RUDDER DEFLECTION ~ δ_R ~ DEG
15°
10°

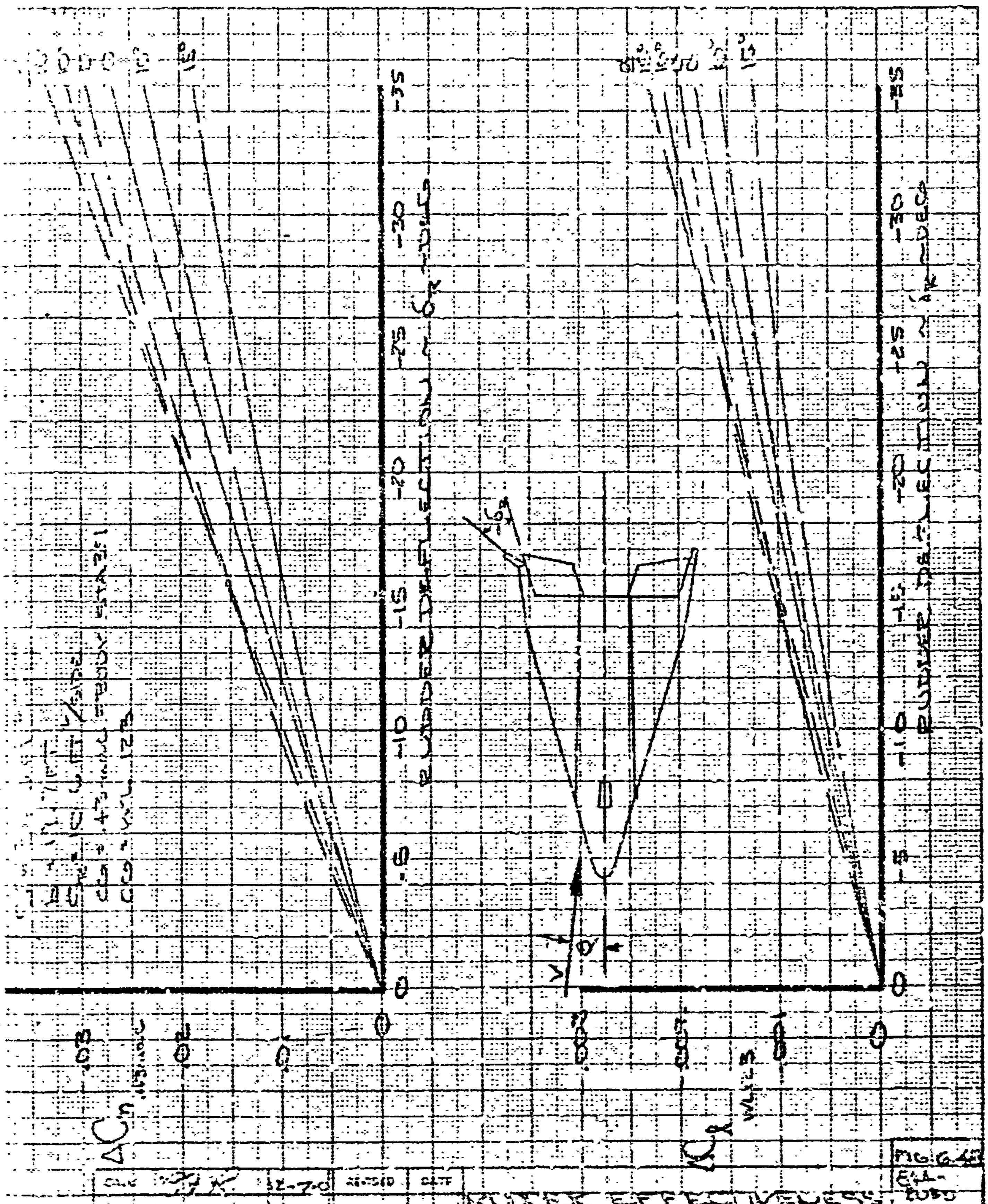

RUDDER EFFECTIVENESS
M=2.0
RUDDER DEFLECTION ~ DEG
0
-5
-10
-15
-20
-25
-30
-35
.01
.02
.03

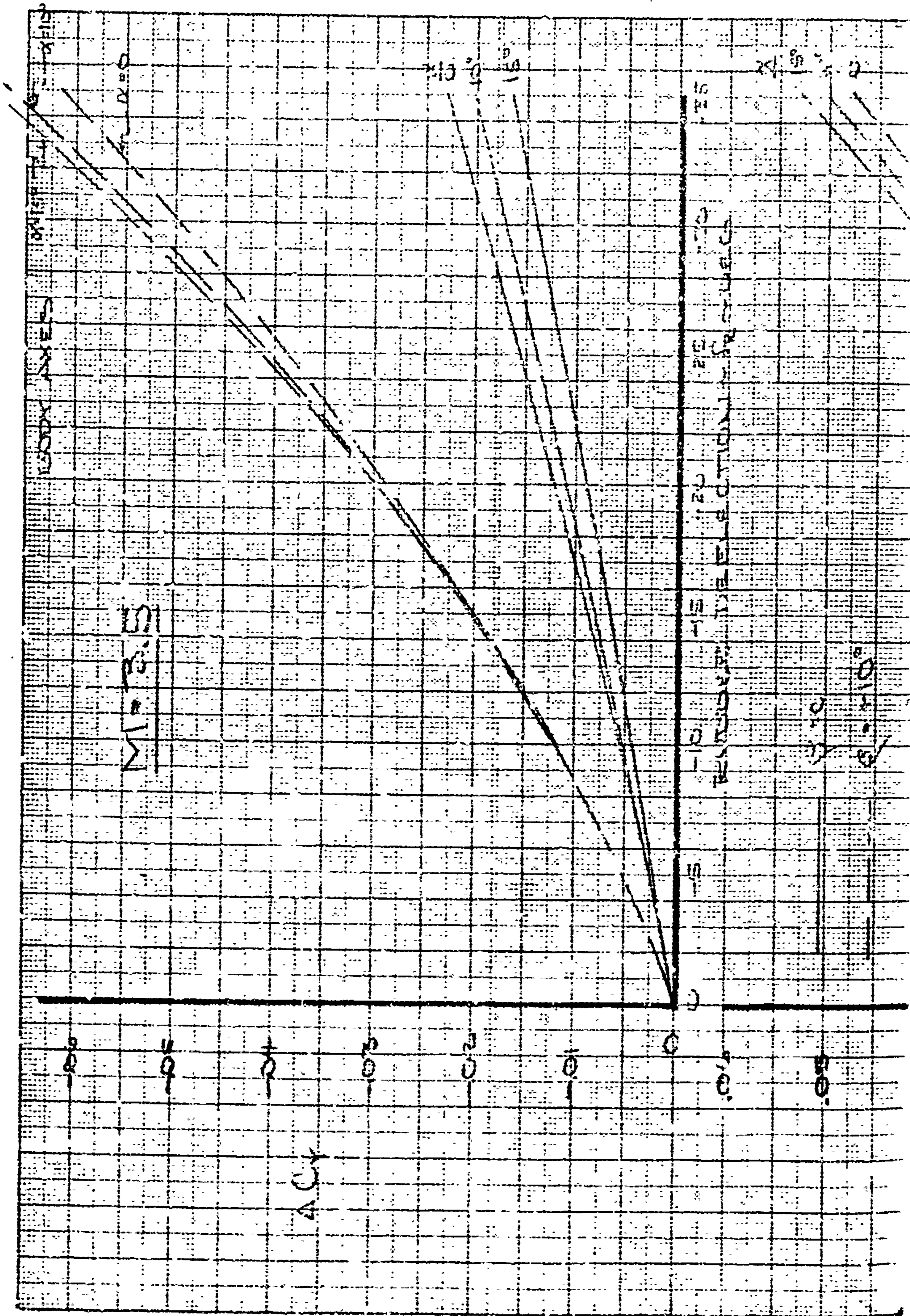

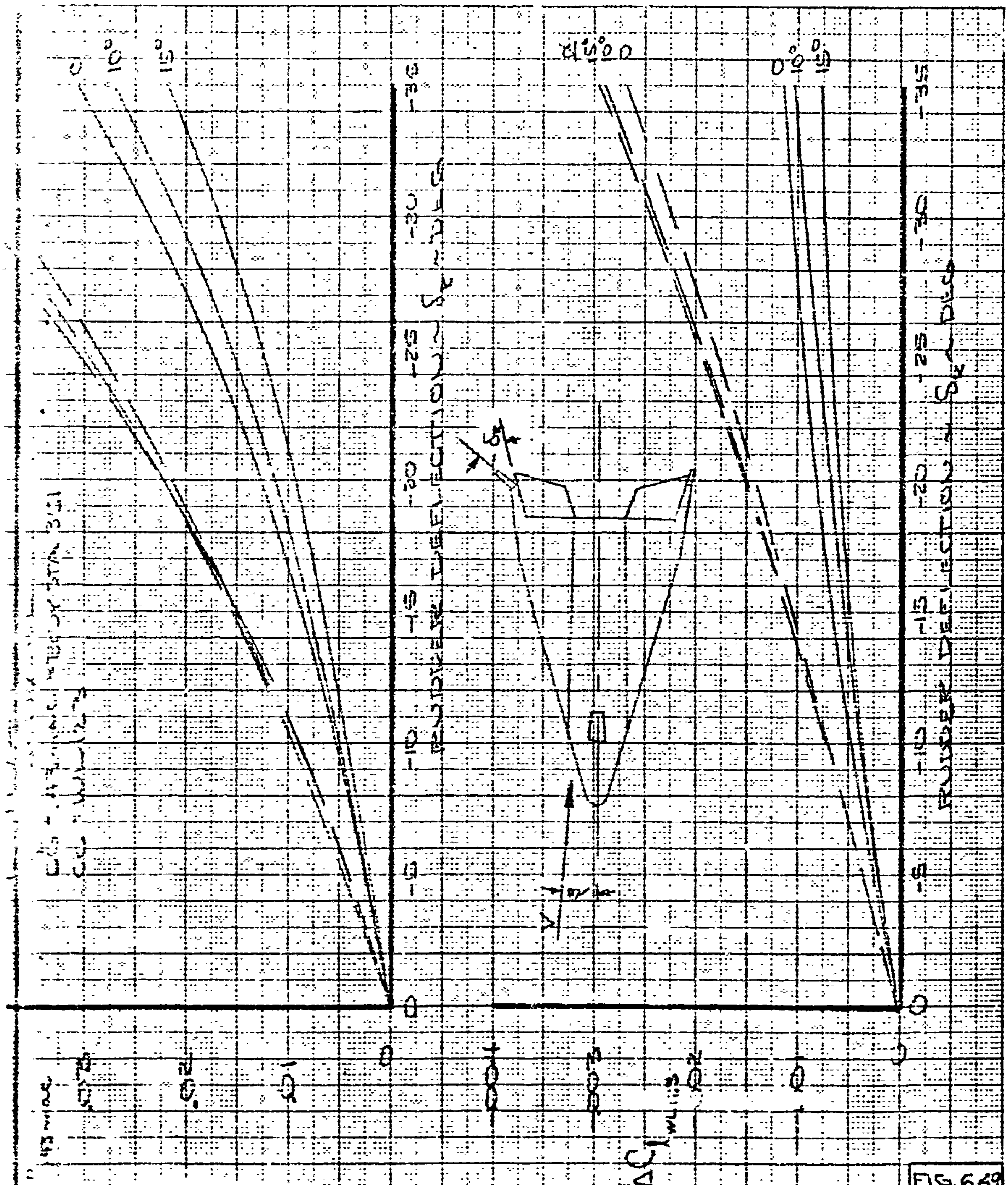

FIG. 6.49

CALC			REVISED	DATE	RUDDER EFFECTIVENESS	844-1035
CHECK					M = 3.5	D2-8174
APPD						PAGE
APPD						6.54a

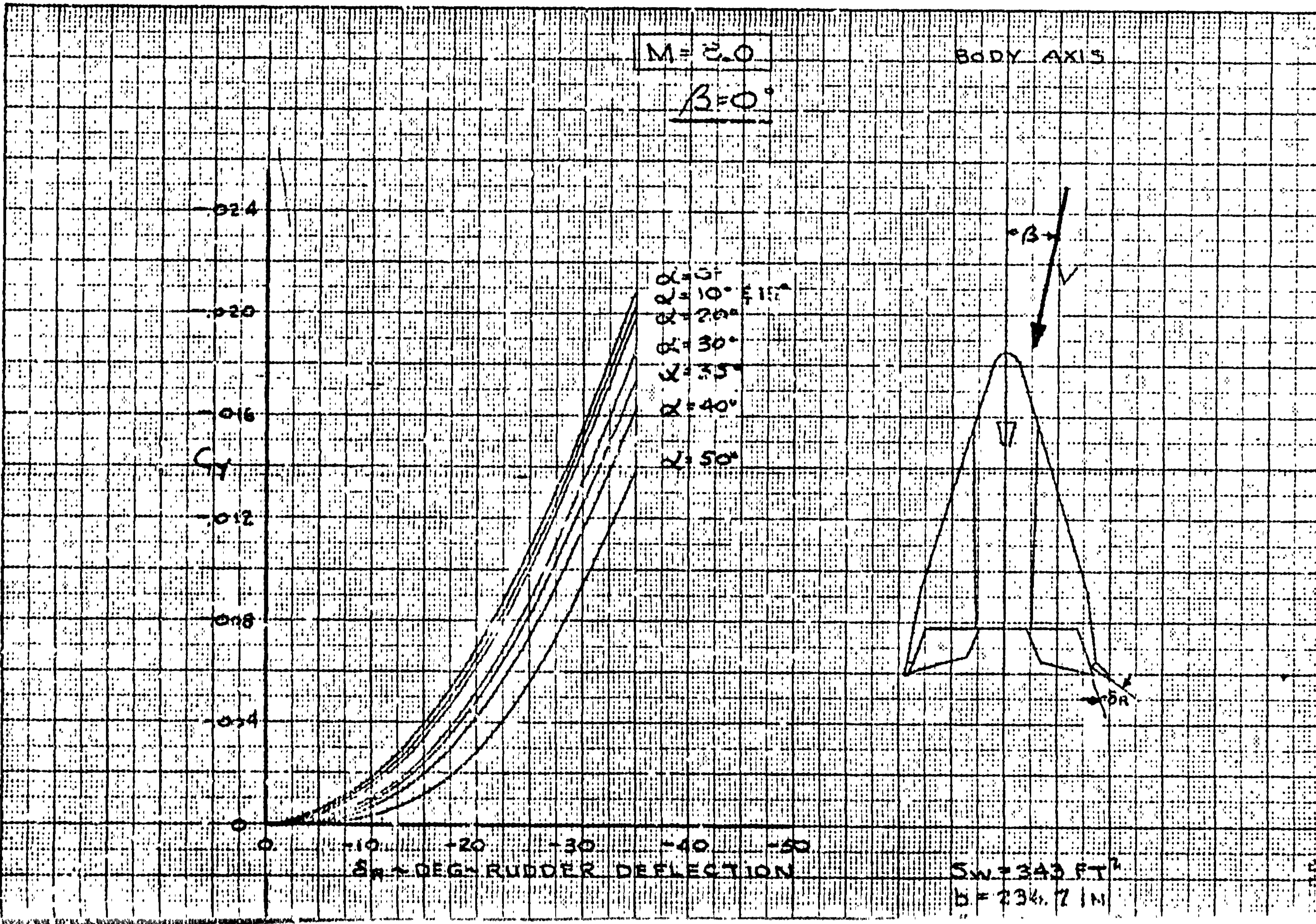
M = 2.0
β = 0°
BODY AXIS
α = 5°
α = 10° & 15°
α = 20°
α = 30°
α = 35°
α = 40°
α = 50°
C_Y
.024
.020
.016
.012
.008
.004
0
0
-10
-20
-30
-40
-50
δ_R ~ DEG ~ RUDDER DEFLECTION
β
V
δ_R
Sw = 343 FT²
b = 234.7 IN

6.54

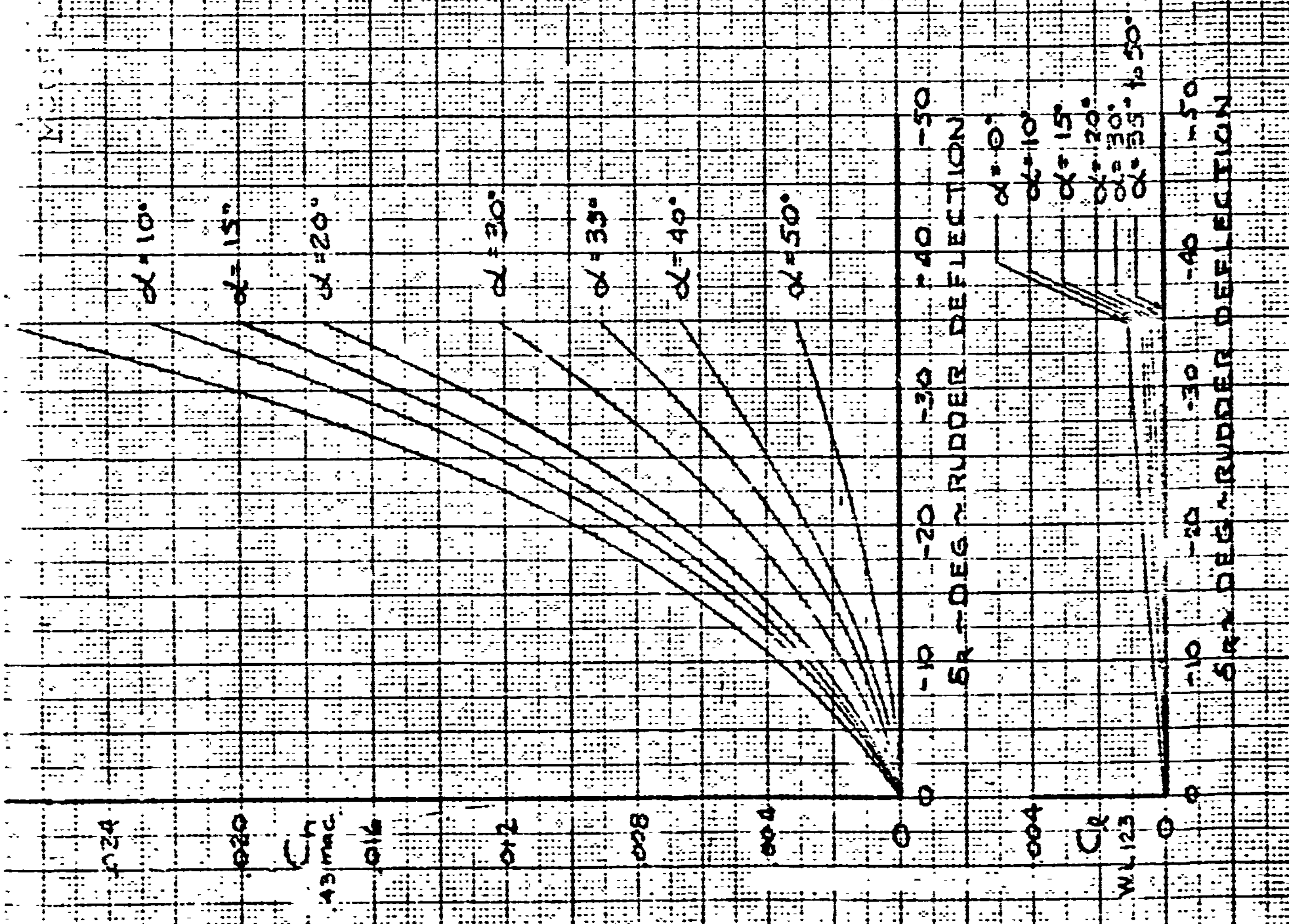

CALC	E4H	12/8/6	REVISED	DATE
CHECK				
APPD				
APPD				

RUDDER EFFECTIVENESS

HYPERSONIC SPEED ~ θ...

FIG. 6.50

844-2035

D2-8174

PAGE 6.55-a

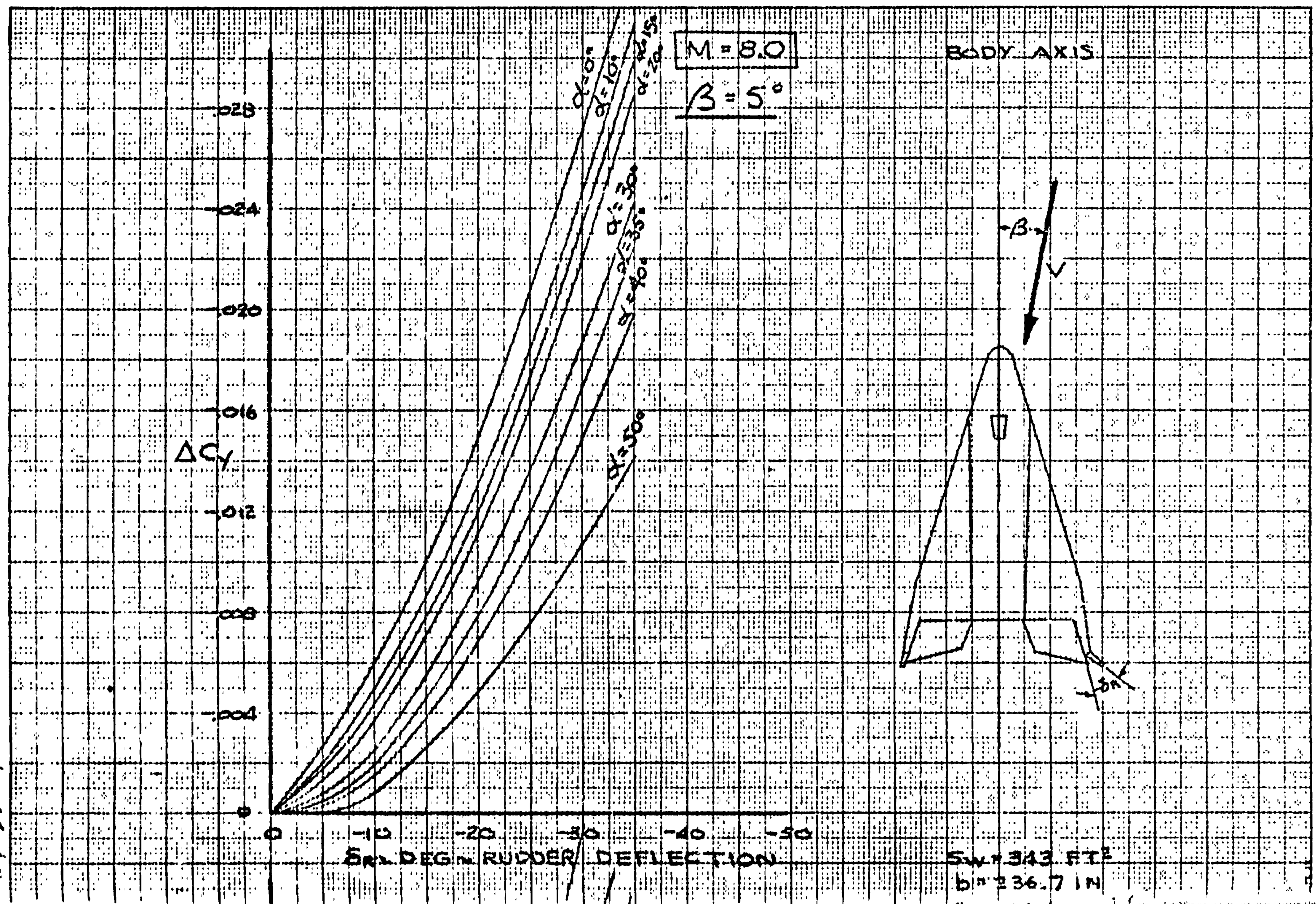

M = 8.0
β = 5°
BODY AXIS
ΔCy
.028
.024
.020
.016
.012
.008
.004
0
0
-10
-20
-30
-40
-50
δR ~ DEG ~ RUDDER DEFLECTION
α=0°
α=10°
α=15°
α=20°
α=30°
α=35°
α=40°
α=50°
β
V
δR
Sw = 343 FT²
b = 236.7 IN

6-55-7

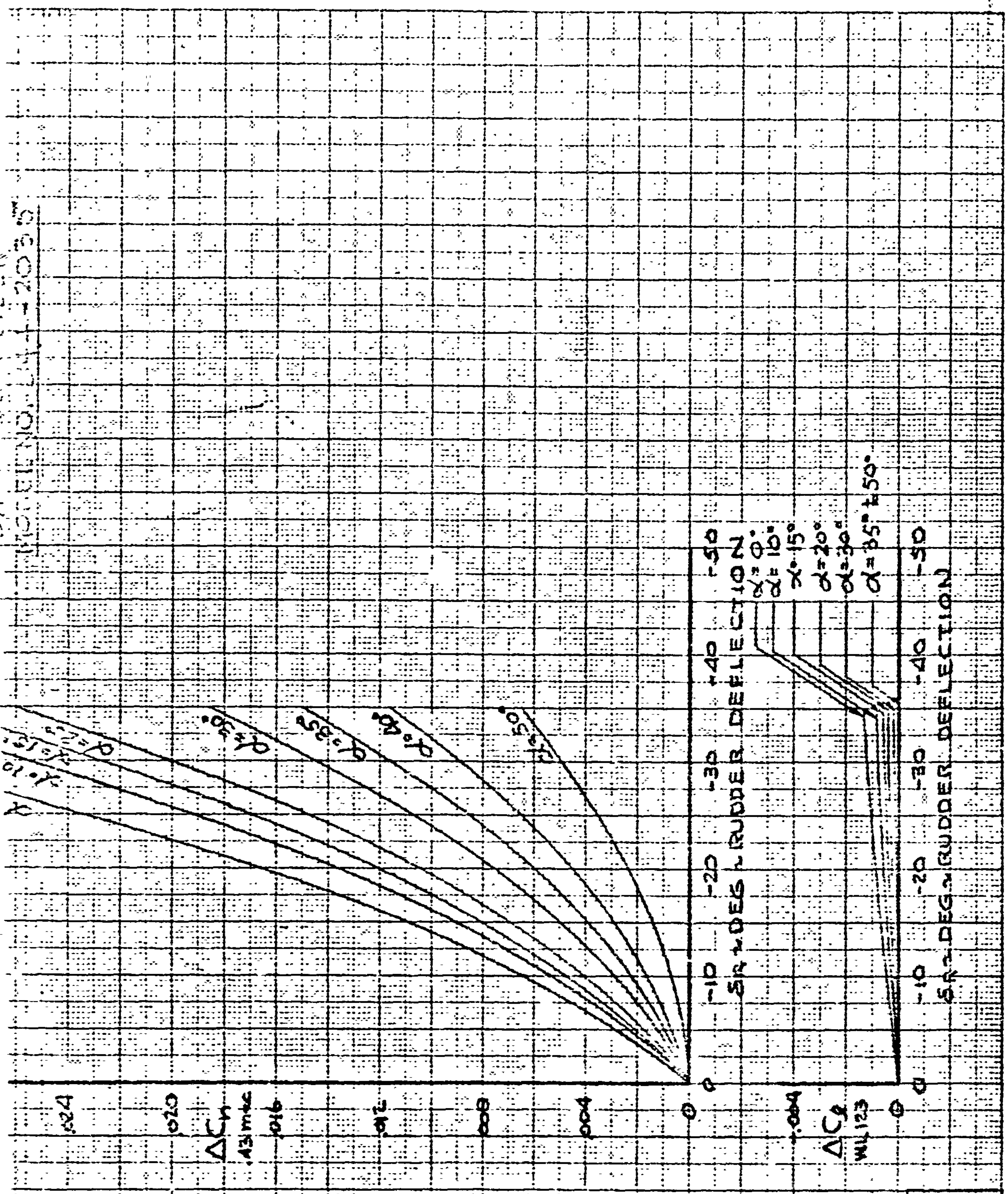

FIG. 6.51

CALC	EJH	12/8/60	REVISED	DATE
CHECK				
APPD				
APPD				

RUDDER EFFECTIVENESS
HYPERSONIC SPEED

644-2035

D2-8174

6.56

6.4 ROLL AND YAW ROTARY DERIVATIVES

The roll and yaw rate damping derivatives are presented on Figures 6.52 and 6.53 for various angles of attack at landing speed, and on Figures 6.54 and 6.55 for various Mach numbers. The landing speed derivatives are presented in the form that they would be obtained from rotary-derivative wind tunnel tests. The derivatives presented versus Mach number include a theoretical estimate of the contribution due to rate-of-change-of-sideslip. This estimate is included in order to permit use of these rotary derivatives for root-solutions and simulator studies where rate-of-change-of-side-slip may not be desired. Further study may alter this estimate significantly.

The landing speed rotary derivatives are based upon preliminary Langley Research Center rotary derivative test data on a model of configuration 814-2002, a model of the NASA Space Ferry (similar to the Dyna Soar glider), and the Bell-Martin Phase I Dyna Soar glider (Reference b). The data have been correlated by theoretical computations which are based on steady rolling or steady yawing (Reference c).

The rotary derivatives versus Mach number, Figures 6.54 and 6.55, were obtained from Figures 6.52 and 6.53 for landing speed, and the variation with Mach number was obtained from theoretical formulae and rotary derivative tests of the X-15 airplane (Reference d).

DATA SOURCE:
THEORETICAL PREDICTIONS FROM NACA TN 2409 CORRELATED WITH FREE TO DAMP OSCILLATION TESTS OF THE
① BELL-MARTIN VEHICLE (C119-ER-1044)
② NASA SPACE FERRY (PRELIMINARY DATA)
③ BAC MODEL 2007 (" ")

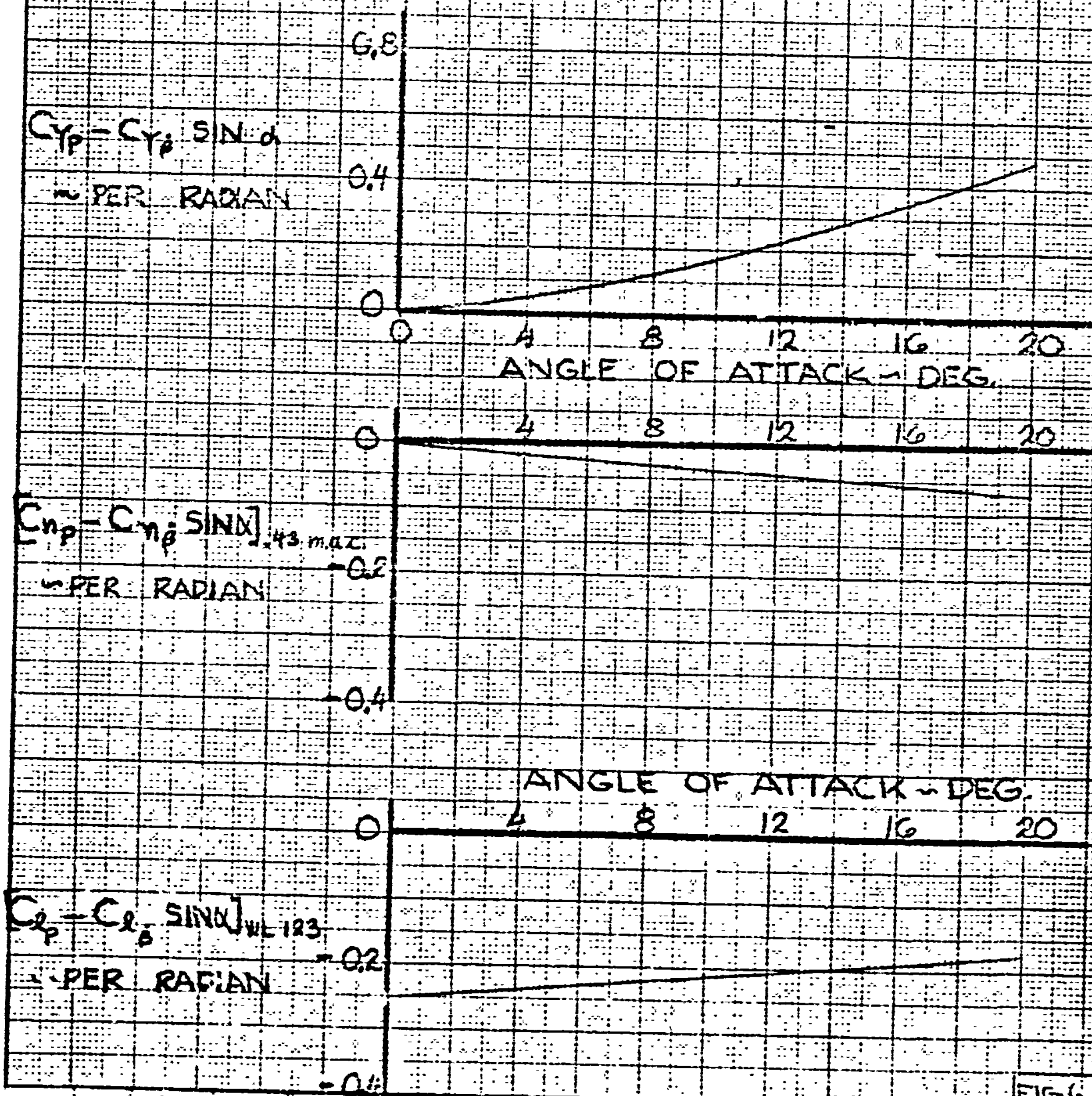

CALC	JMc	12-3-60	REVISED	DATE	EFFECT OF ANGLE OF ATTACK ON ROLLING DERIVATIVES ~ LANDING SPEED	FIG 6.52
CHECK						844-2035
APR						D2-8174
APR					BOEING AIRPLANE COMPANY	PAGE 6.58

DATA SOURCES:

THEORETICAL PREDICTIONS FROM NACA TN 2409 CORRELATED WITH FREE TO DAMP "OSCILLATION TESTS OF THE

① BELL - MARTIN VEHICLE (C119-ER-10440)

② NASA SPACE FERRY (PRELIMINARY DATA)

③ BAC MODEL 2002 (" ")

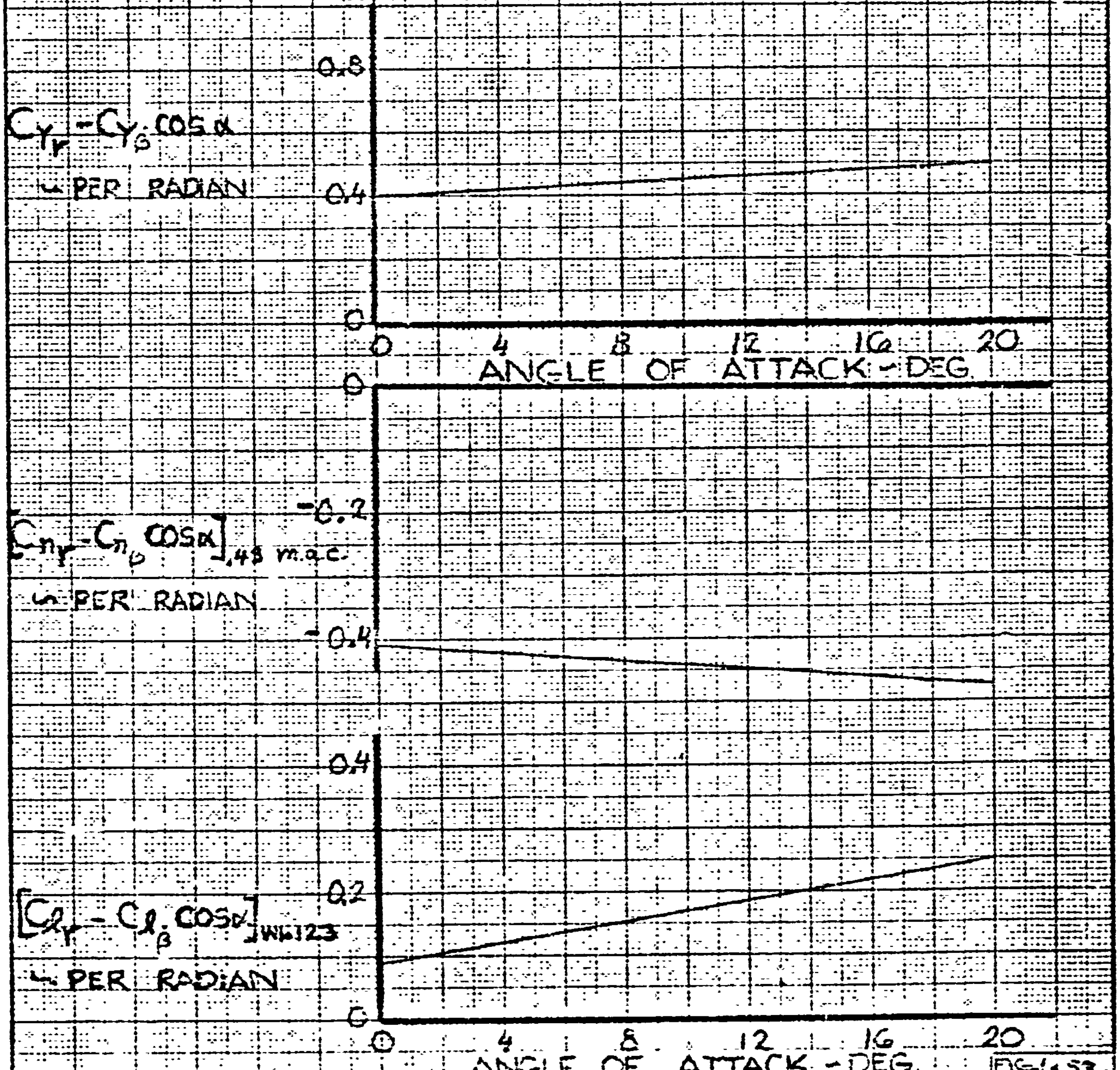

FIG. 6.53

CALC	BMS	12-5-60	REVISED / DATE
CHECK			
APR			
APR			

EFFECT OF ANGLE OF ATTACK ON YAWING DERIVATIVES ~ LANDING SPEED

944-2035

D2-8174

BOEING AIRPLANE COMPANY

BODY AXES

DATA SOURCE:

SUBSONIC DATA FROM FIGS. 6.58 & 6.53
SUPERSONIC PREDICTIONS AND TEST DATA FROM NASA TM X-287 (X-15 AIRPLANE)

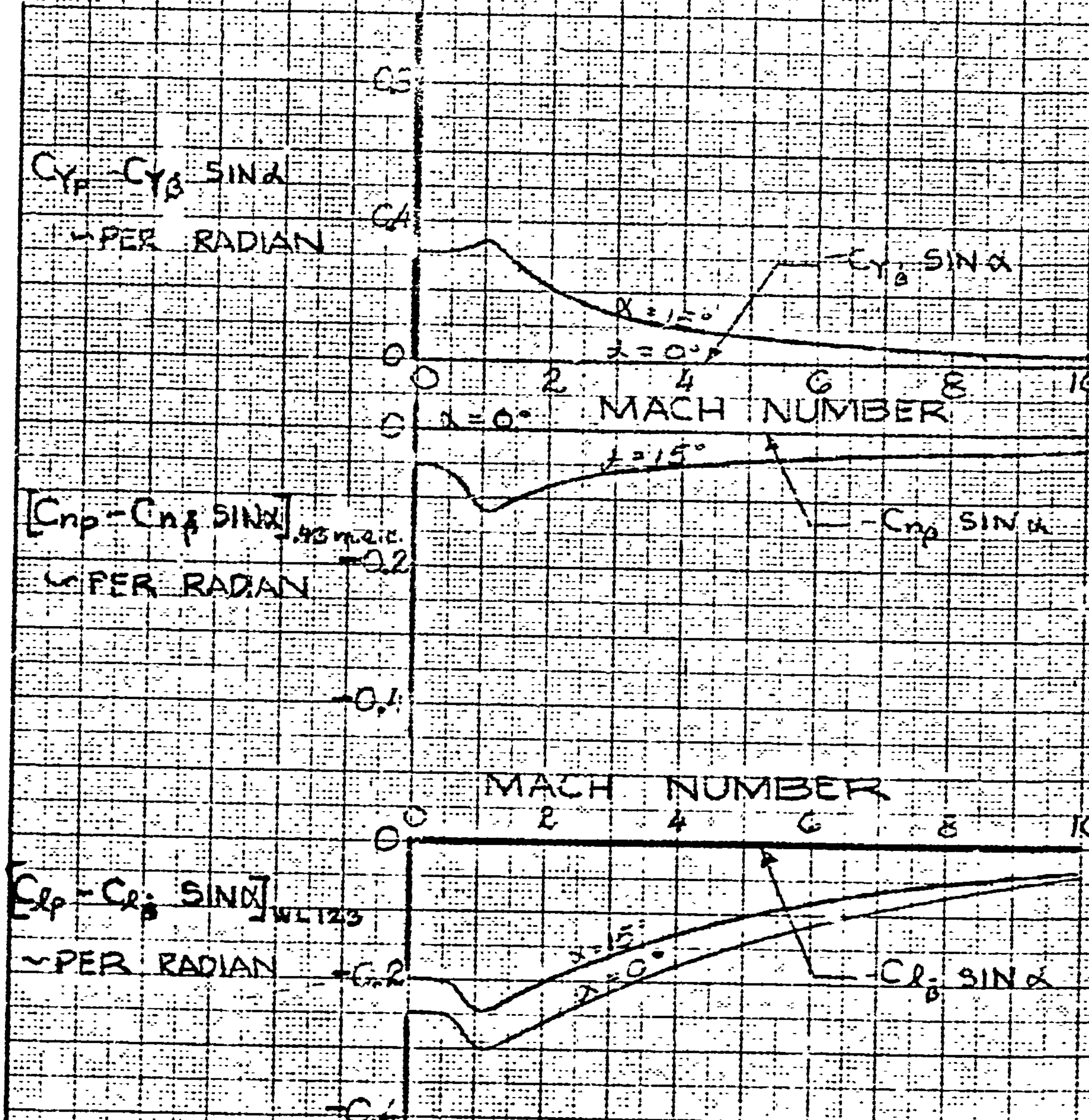

CALC	[illegible]	12-8-60	REVISED	DATE	EFFECT OF MACH NUMBER ON ROLLING DERIVATIVES	FIG. 6.54
CHECK	[illegible]					544-2055
APR						D2-8174
APD					BOEING AIRPLANE COMPANY 176	PAGE 6.60

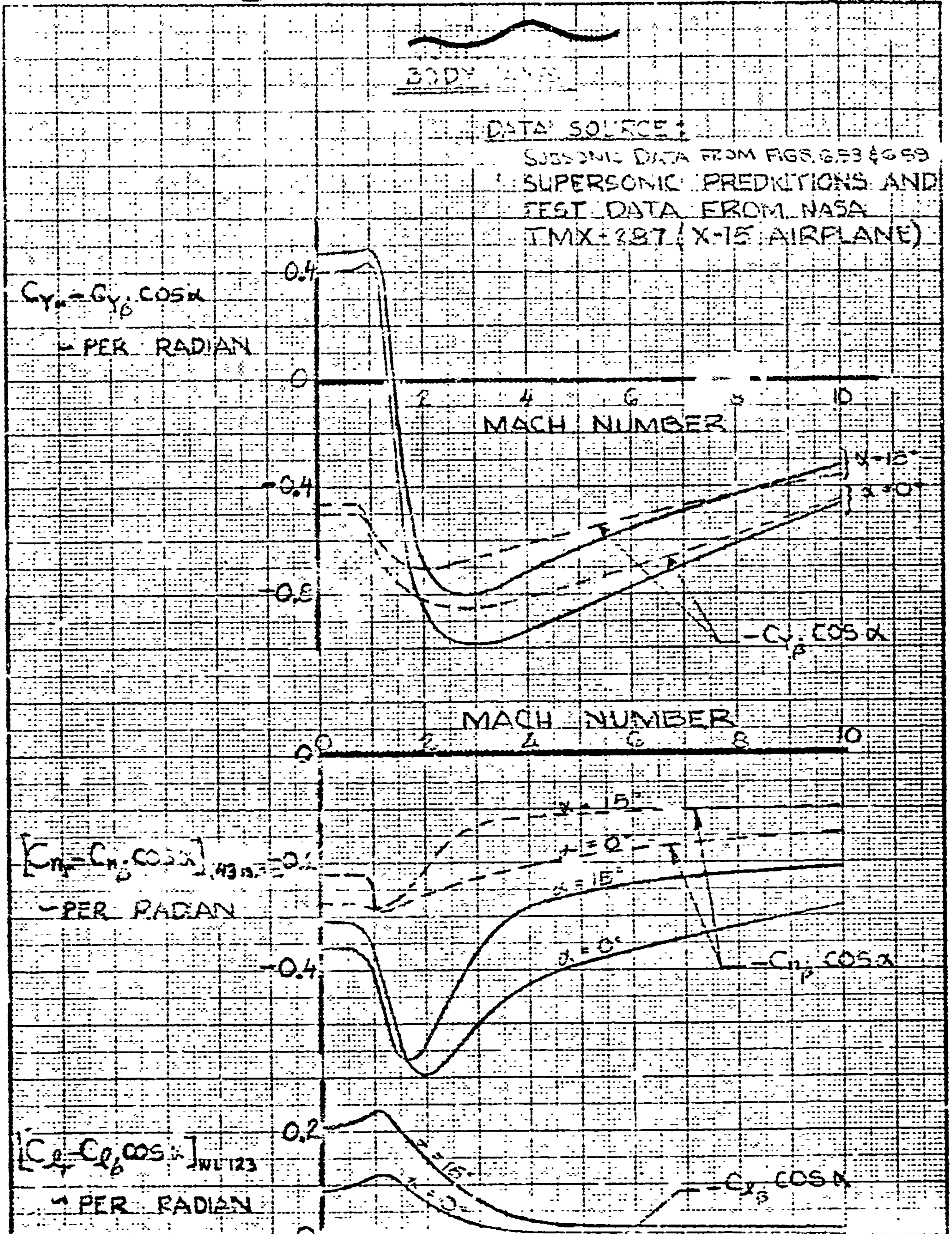

FIG. 6.55

CALC			REVISED	DATE	EFFECT OF MACH NUMBER ON YAWING DERIVATIVES	844-2?35
CHECK					177	D2-81?4
APP					BOEING AIRPLANE COMPANY	PAGE 6.61
APP						

7.0 GLIDER WITH TRANSITION SECTION

The addition of the third stage rocket and transition section to the glider moves the center of gravity rearward and changes the glider pitch and yaw characteristics. These effects are reflected in the longitudinal and lateral-directional stability data shown in Figures 7.1 through 7.13. Wind Tunnel data available for pitch characteristics were used from $M = .7$ to $M = 3.5$; at lower and higher speeds, theoretical estimations were necessary. The lateral directional data were estimated. The reference centers of gravity for the moments were those for the instant of ignition of the third stage rocket and at burn out after 19 seconds of rocket burning. The c.g. moves forward 8.8% m.a.c. during third stage powered flight. Present plans include modifying the transition shape and length from that shown to reduce the zero lift pitching moment and to increase the glider static stability at transonic speeds. The effect of change of shape to reduce the zero lift pitching moment has been estimated and included in the data shown. The effect of length to increase stability has not been included.

7.1 LONGITUDINAL STABILITY AND CONTROL

The addition of the transition section to the glider creates positive zero-lift pitching moment and reduces the vehicle normal force. This effect is most prevalent at subsonic and transonic speeds, diminishing at supersonic speeds. The increments of normal force and pitching moment for various angles of attack and Mach numbers with no elevon deflection were determined from wind tunnel tests of an early configuration and modified to reflect the current configuration. Data were available for a range of speeds from M = .7 to M = 3.5. These increments were added to the glider-alone data.

The data reflect the 66 inch transition length tested rather than the 55 inch length shown in Reference a. The transition length will be established from aerodynamic and performance requirements. The 55 inch length represents a logical separation plane from structural design considerations since the pressure bulkhead for the heat blast diaghram is located in that region. However, sufficient static stability may not be available from the 55 inch transition section.

Two center of gravity locations are shown on the plots in Figures 7.1 through 7.8. These are: (1) the initial center of gravity at the instant of separation from the second stage and (2) the center of gravity at rocket burnout.

Lines of constant elevon deflection and constant angle of attack are shown only for the initial center of gravity location at .562 m.a.c. Other fore and aft center of gravity locations can be represented on these plots by a rotation of the vertical (C_N) axis. This rotation is shown for the center of gravity at rocket burnout of .474 m.a.c. The vertical center of gravity location is assumed fixed when the C_N axis is rotated to represent a different fore and aft center of gravity location.

The following method can be used to determine the amount of rotation of the C_N axis required to represent other center of gravity locations. (1) Assume center of gravity travel linear with burn time (t).

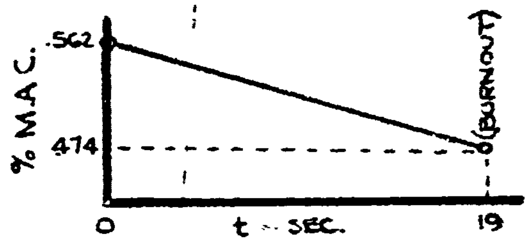

Then determine the center of gravity location in present m.a.c. for the time (t) desired as shown in the sketch above.

(2) Shift the C_N axis to reflect the center of gravity location for the time (t).

Example: Shift the center of gravity 2 percent m.a.c. forward.

(1) locate on the C_N vs C_m plot the point at C_N 1.0 and C_m = .02.

(2) Draw a line through the point and the origin as shown in the sketch below.

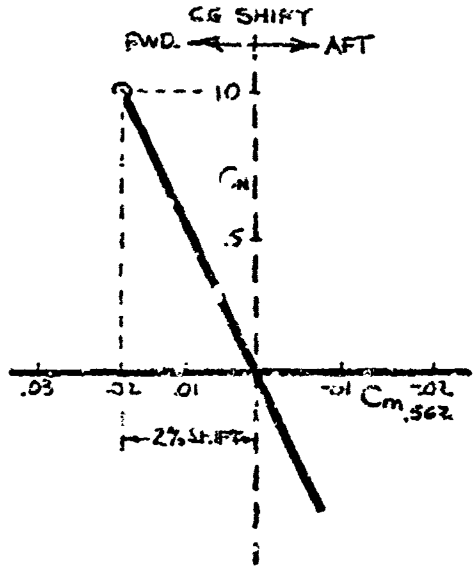

7.2 LATERAL AND DIRECTIONAL STABILITY AND CONTROL

Static directional stability characteristics are presented in Figures 7.9 and 7.10 for the effects of angle of attack, folding wing tip extensions, and center of gravity location. Theoretical estimations for the effects of the transition section were added to the glider-alone stability derivatives. The data represent the glider plus transition section aerodynamic characteristics reasonably well for ±5° sideslip. The data shows the fold down tip in the down, or extended, position to M = 3.5. The precise speed to which the folding tips will be extended is to be determined.

The effects of rudder deflection on the glider plus transition directional characteristics are shown in Figures 7.11 through 7.13 for two angles of attack. The effectiveness differs from the glider-alone characteristics because of the center of gravity location.

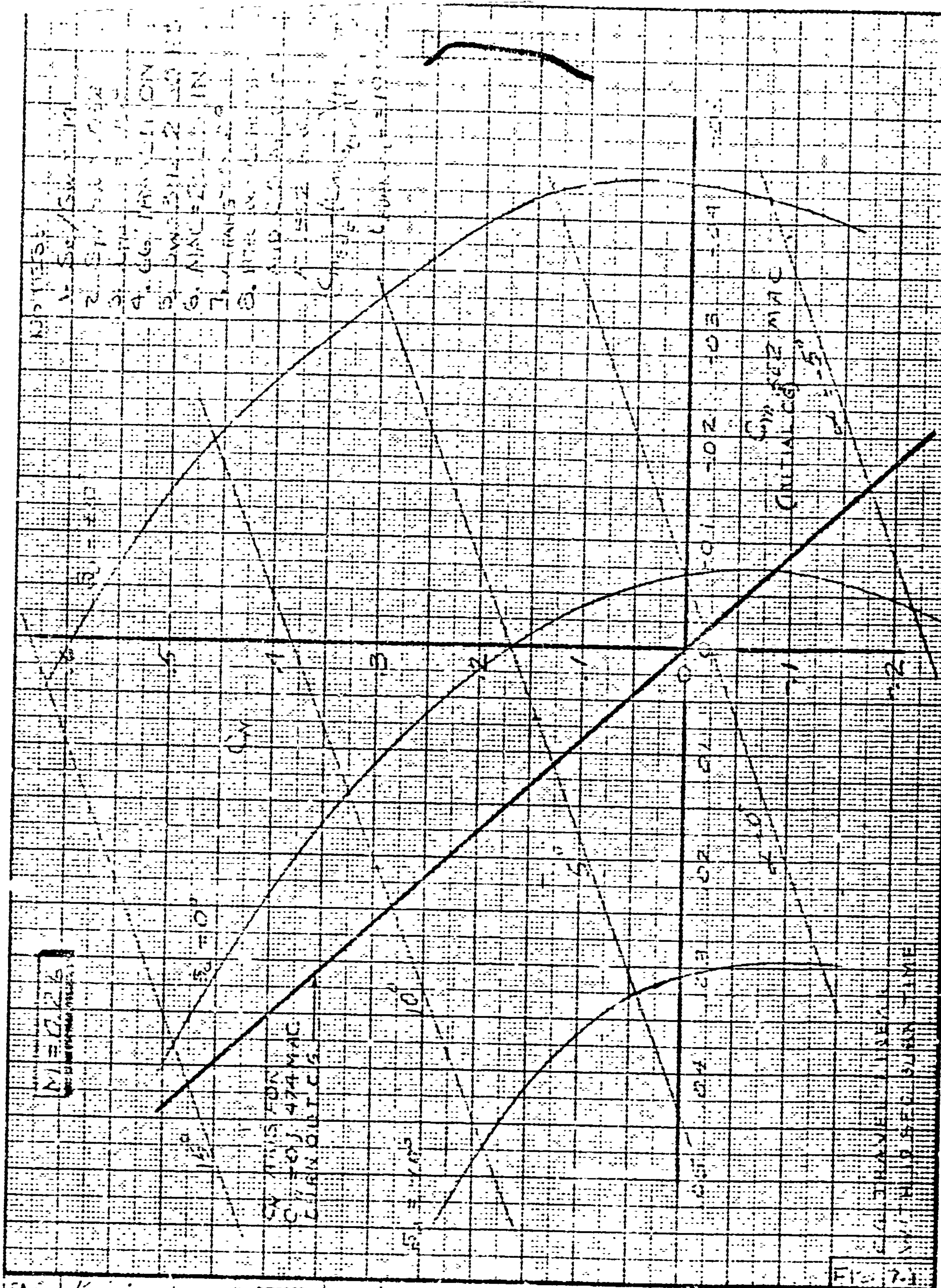

Fig. 7-1

CALC	K...	...-2...-8	REVISED	DATE
CHECK				
APR				
APR				

LONGITUDINAL STABILITY 1844-2035

TIPS EXTENDED - C6' TRANSITION D2-6174

BOEING AIRPLANE COMPANY $M=.26$ PAGE 7.5

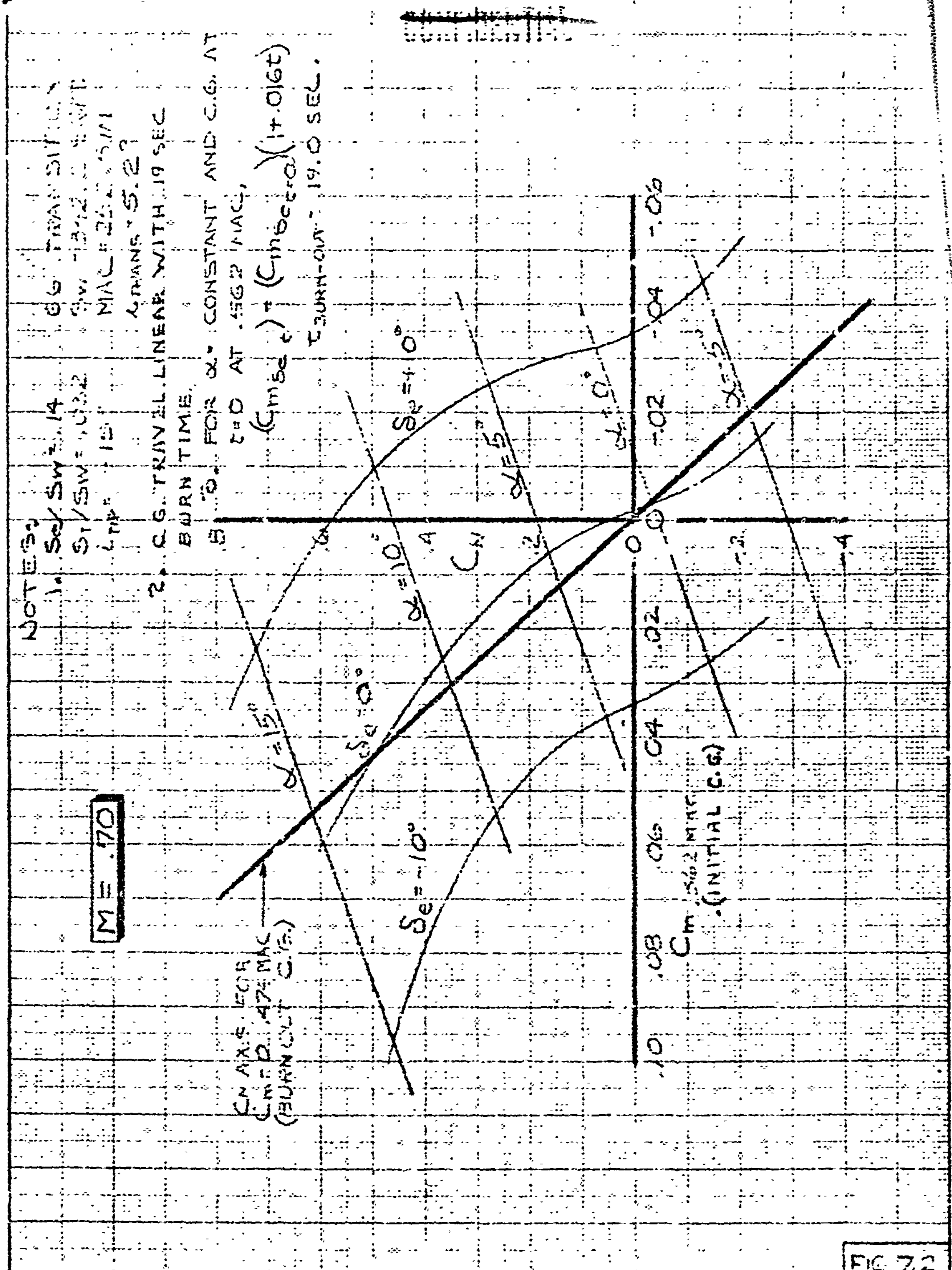

FIG 7.2

CALC DEP		REVISED	DATE	LONGITUDINAL STABILITY	SM-2035
CHECK				TIPS EXTENDED - 66" TRANSITION	D2-8174
APP				BOEING AIRPLANE COMPANY $M = .70$	7.6
APP					

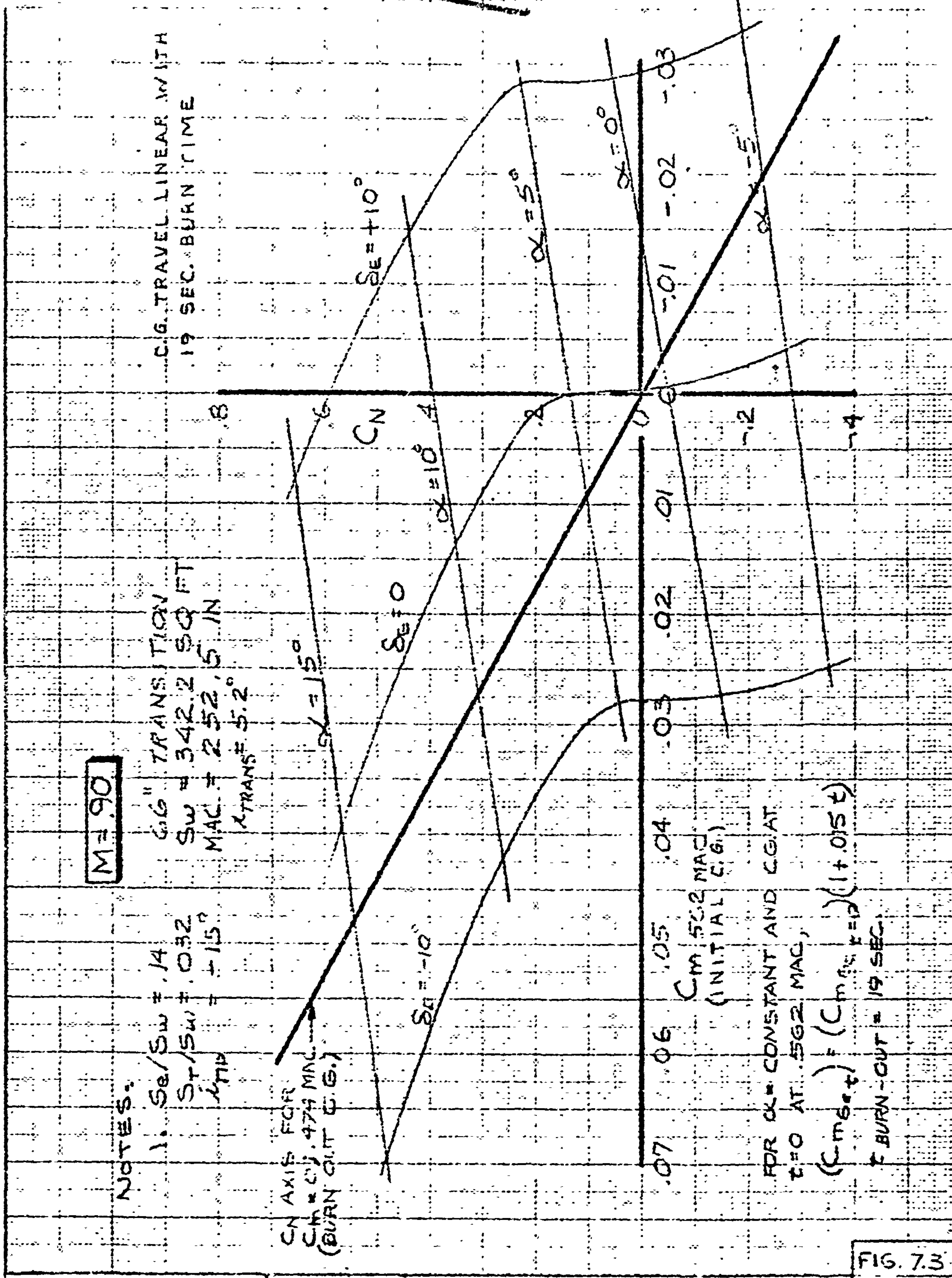

FIG. 7.3

CALC DEP 12-2	REVISED / DATE	LONGITUDINAL STABILITY 844-2035
CHECK		TIPS EXTENDED - 66" TRANSITION D2-6174
APR		
APR		BOEING AIRPLANE COMPANY M=.90 PAGE 7.7

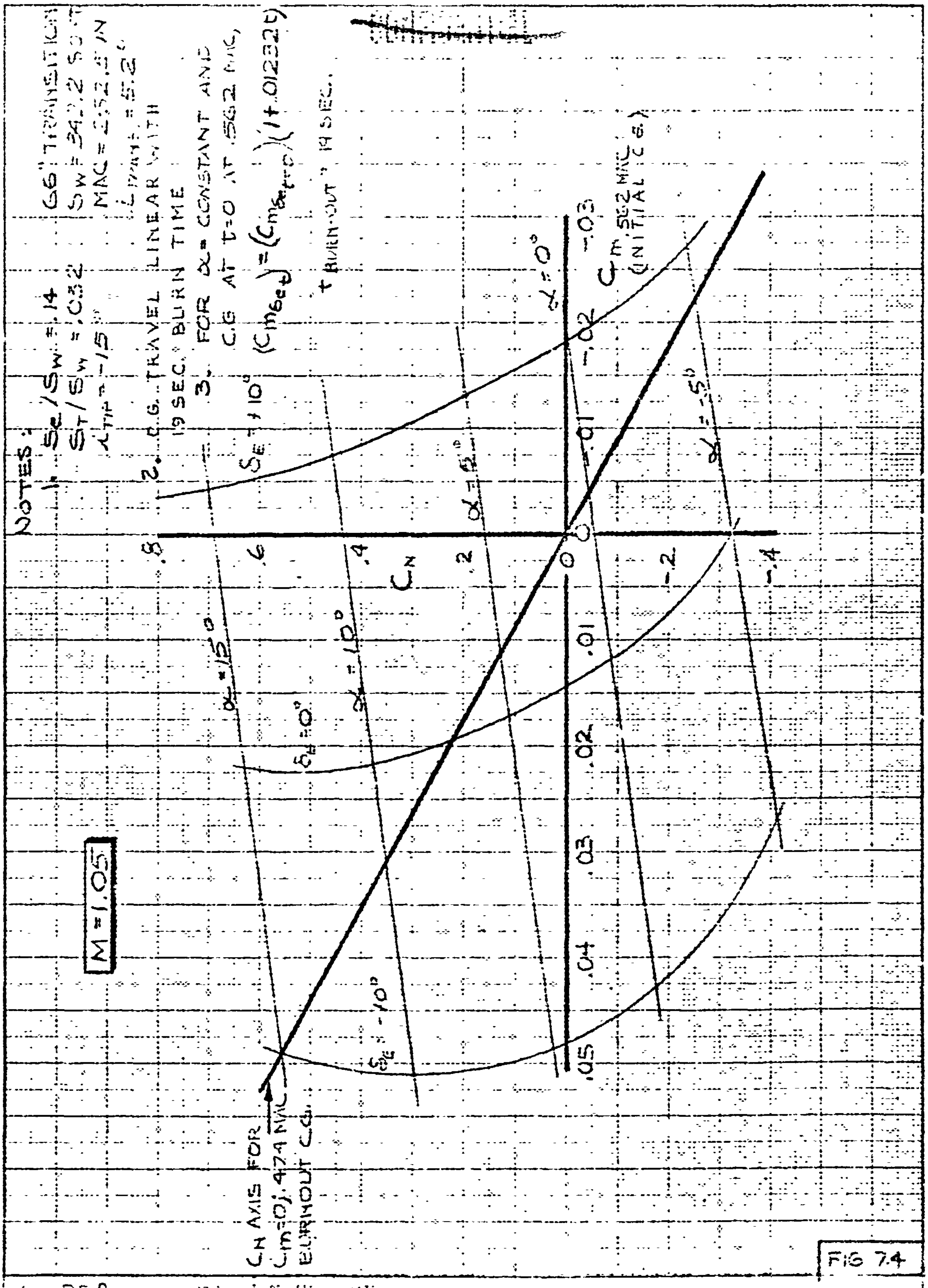

FIG 7.4

CALC DEP	REVISED	DATE	LONGITUDINAL STABILITY	844-2035
CHECK			TIPS EXTENDED - 66' TRANSITION	D2-8174
APR				
APR			BOEING AIRPLANE COMPANY M=1.05	PAGE 7.8

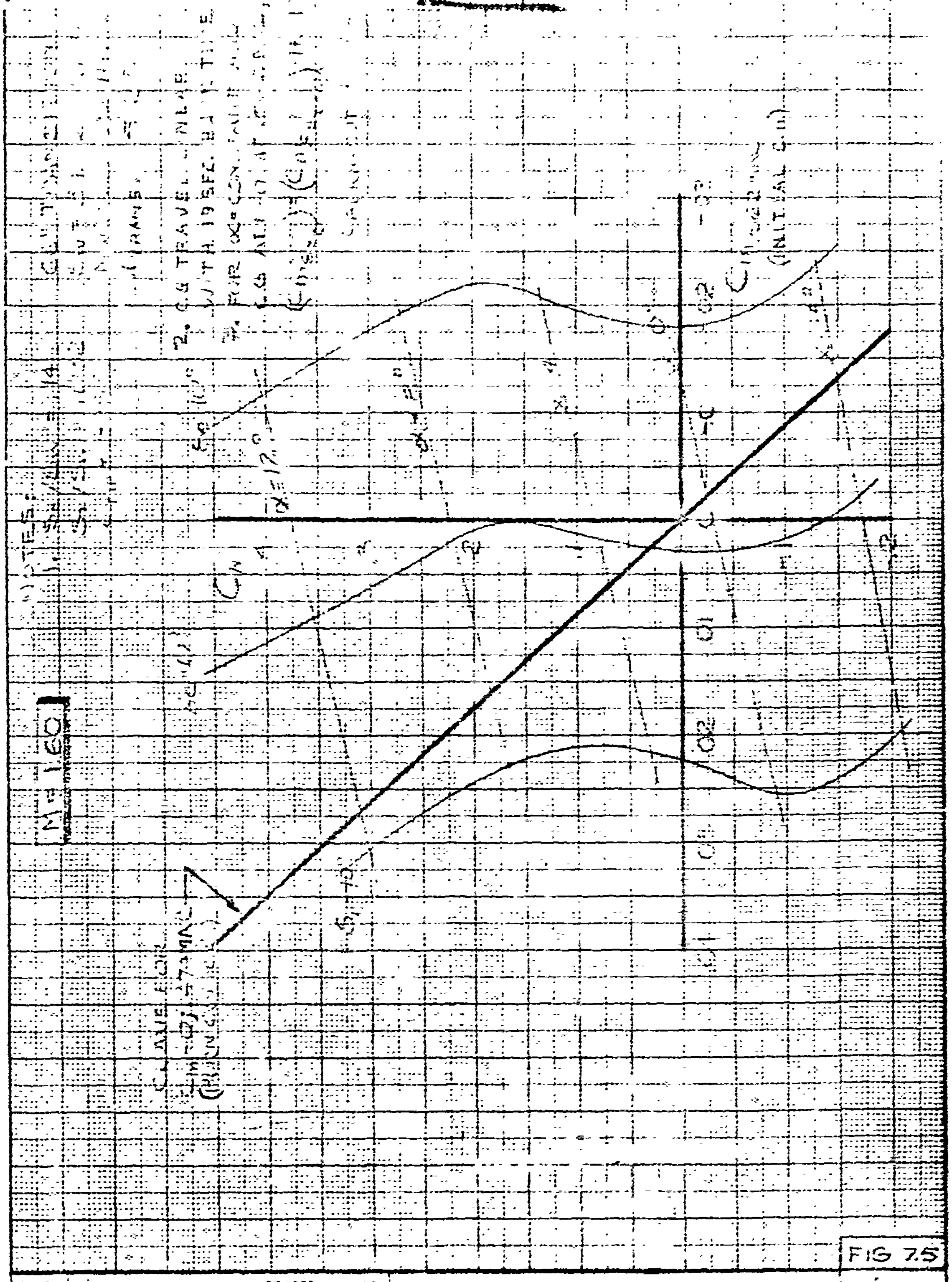

FIG 7.5

CALC			REVISED	DATE	LONGITUDINAL STABILITY	84-2035
CHECK					TIP EXTENDED	D2-8174
APR						
APR					BOEING AIRPLANE COMPANY M=1.60	PAGE 7.9

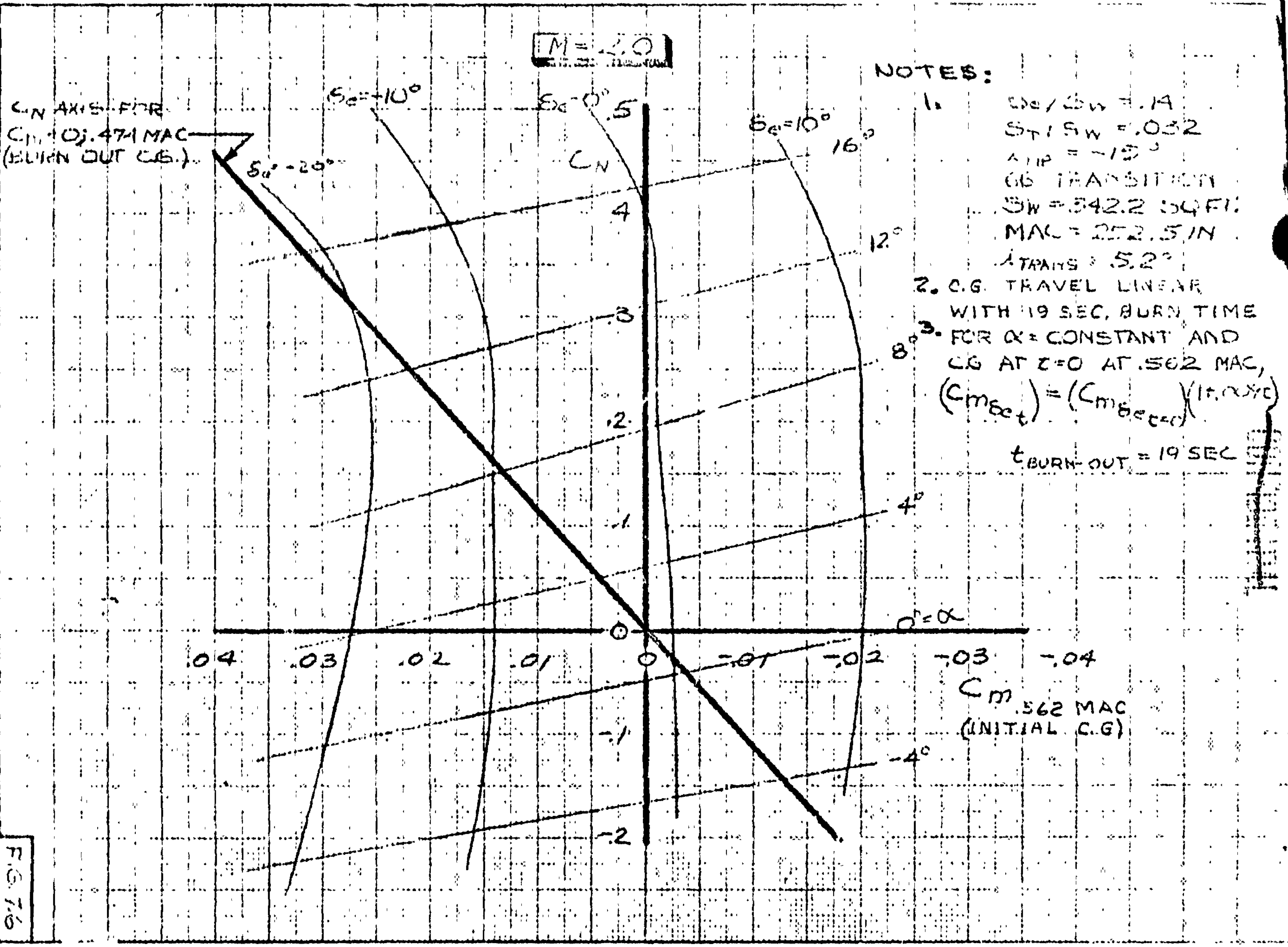

FIG. 7.6

LONGITUDINAL STABILITY

TIPS EXTENDED · CG TRANSIT...

BOEING AIRPLANE COMPANY

544-2035

D2-3174

M=2.20 PAGE 7.10

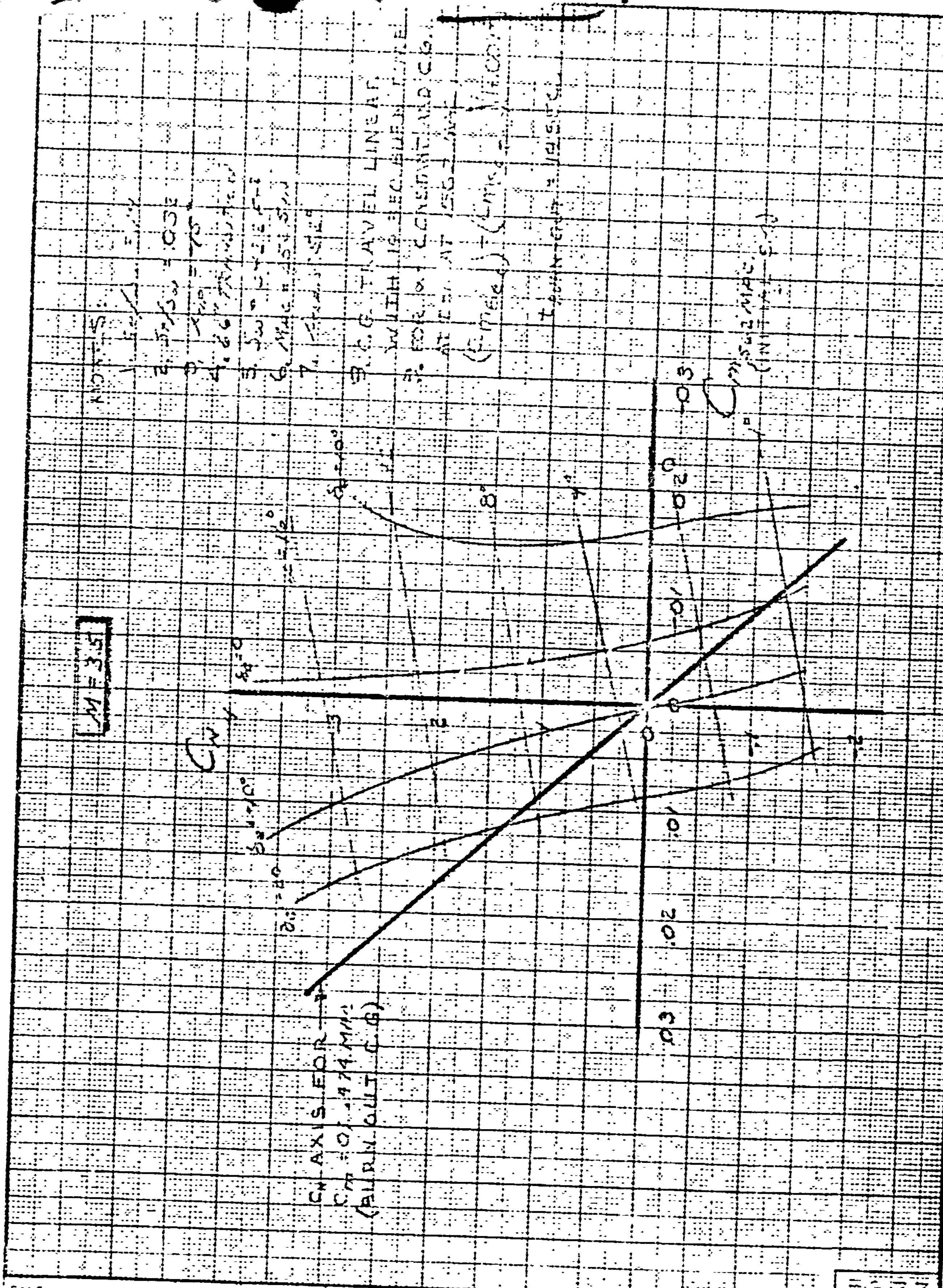

FIG 7.7

CALC	W.S.C.	119-22-0	REVISED	DATE
CHECK				
APR				
APR				

LONGITUDINAL STABILITY

TIPS EXTENDED – 66" TRANSITION

BOEING AIRPLANE COMPANY M=3.5

844-2035

D2-8174

PAGE 7.11

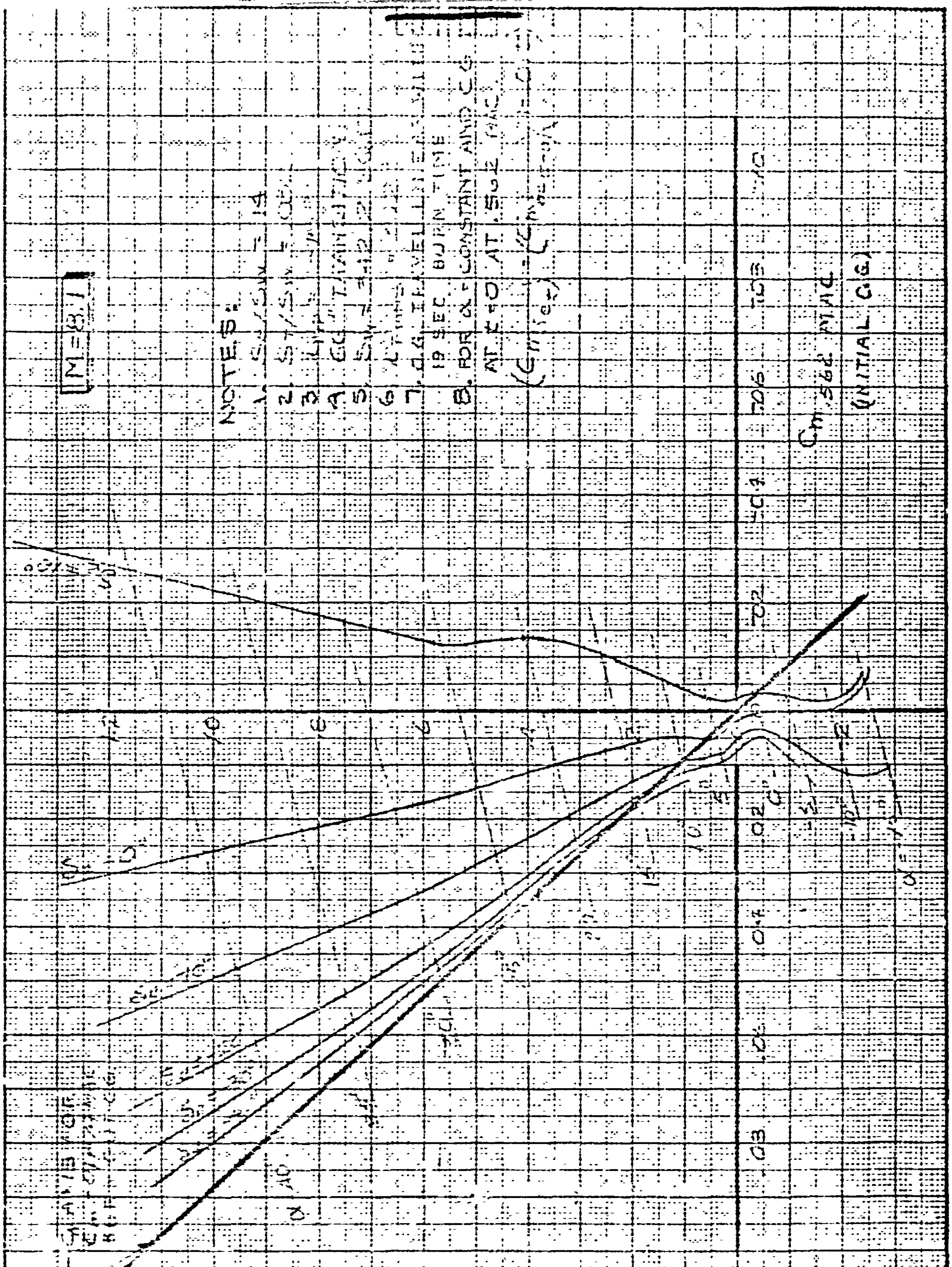

FIG 7.6

CALC	[illegible]	12-21-61	REVISED	DATE	LONGITUDINAL STABILITY	644-2035
CHECK					TIPS RETRACTED-CG TRANSITION	D2-6174
APR						
APR					BOEING AIRPLANE COMPANY M=3.1	PAGE 7.12

NOTES:

1. C.G. TRAVEL LINEAR WITH 19 SEC. BURN TIME
2. $\angle_{TIP}$ = −15°   66" TRANSITION S_W = 343 FT²
   S_T/S_W = .052 $\angle_{TRANS}$ = 5.2°   b = 19.7 FT

BODY AXIS

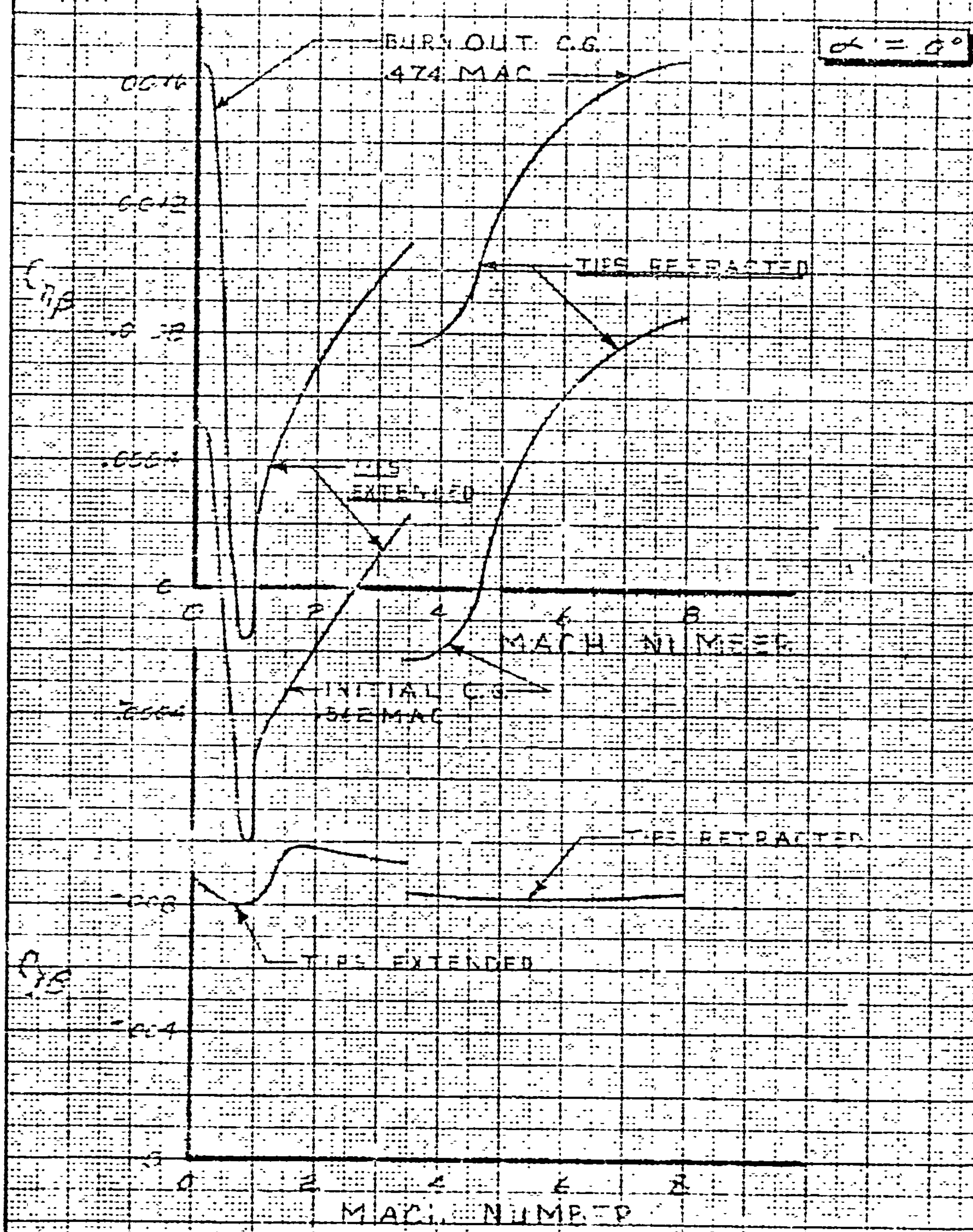

FIG. 7

CALC	K.A.N.	12-31-60	REVISED	DATE
CHECK				
APR				
APR				

DIRECTIONAL STABILITY   814-2035

$\alpha = 0°$ 190   D2-8174

BOEING AIRPLANE COMPANY

PAGE 7.13

NOTES:
1. C.G. TRAVEL LINEAR WITH 13 SEC BURN TIME
2. $i_{TIP} = -15°$ 66" TRANSITION $S_W = 343\ FT^2$
$S_{TS}/S_W = .032$ $i_{TRANS} = 5.2°$ $b = 13.7\ FT$

BODY AXIS

$\alpha = 15°$

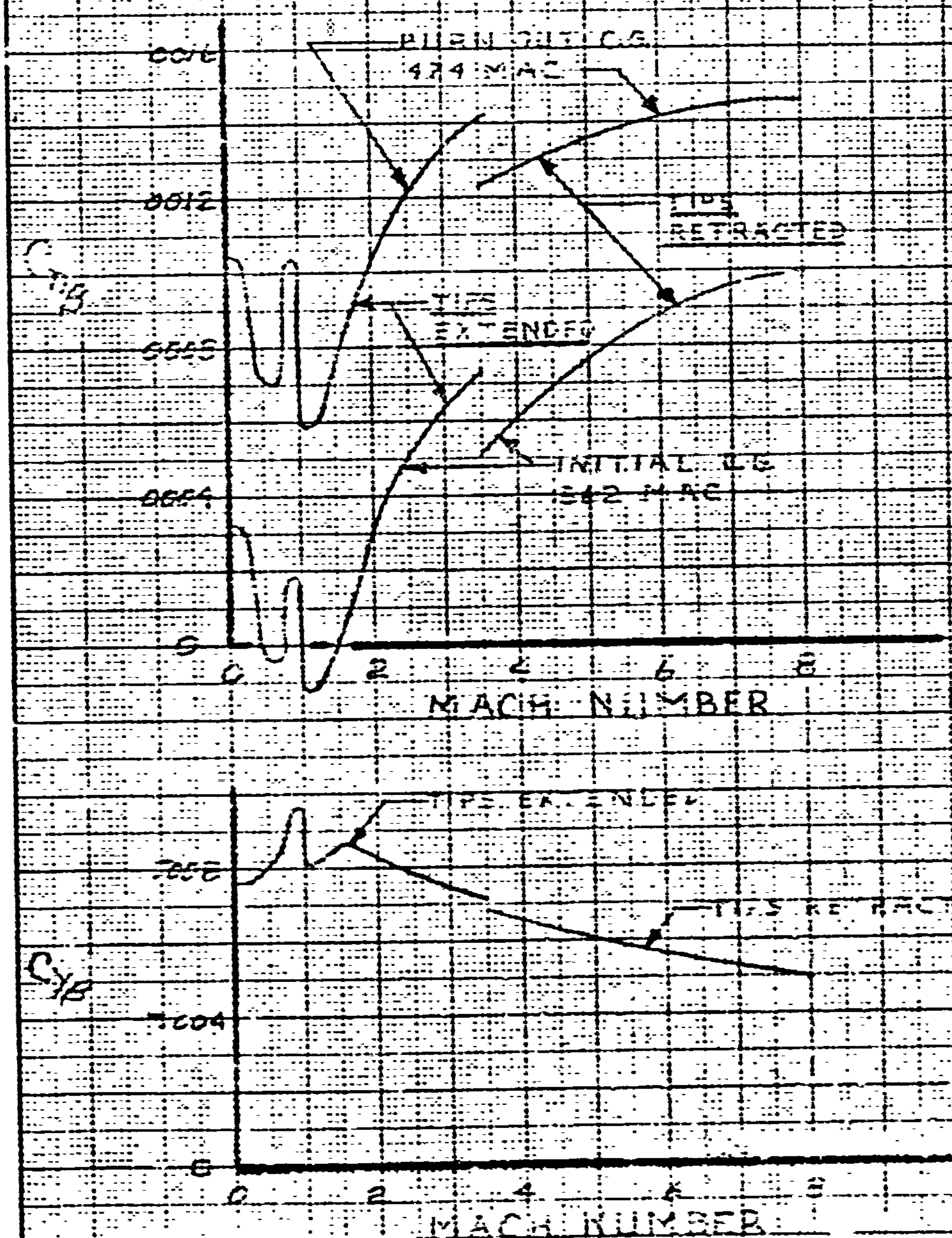

FIG 7.C

CALC	KAH	12-12-6	REVISED	DATE	DIRECTIONAL STABILITY	244-2035
CHECK					$\alpha = 15°$ 191	D2-3174
APR						
APR					BOEING AIRPLANE COMPANY	PAGE 714

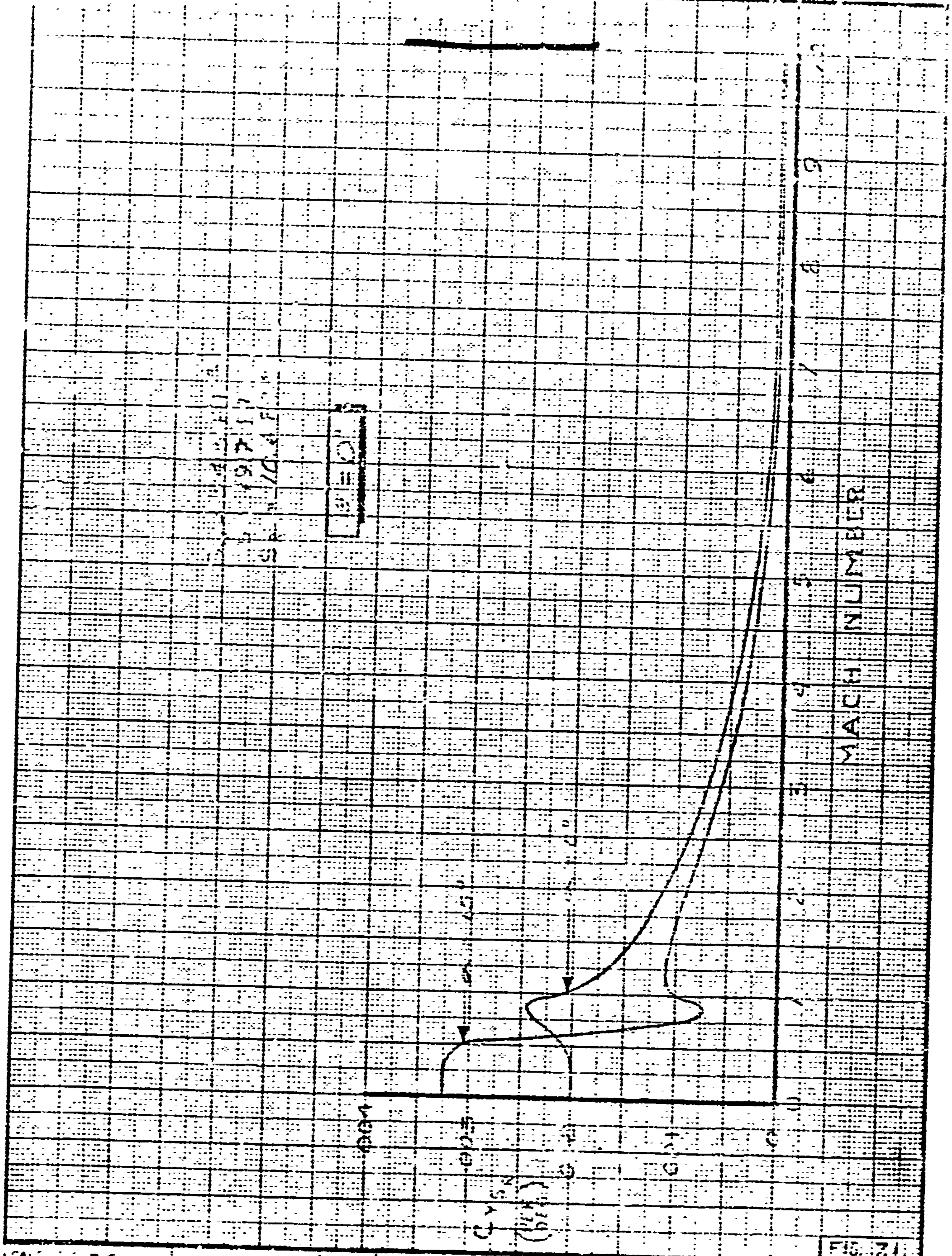

FIG. 71

CALC	PFR		REVISED	DATE
CHECK			PFR	2-15-6
APR				
APR				

RUDDER EFFECTIVENESS

192

BOEING AIRPLANE COMPANY

244-2035

D2-8174

PAGE 7.15

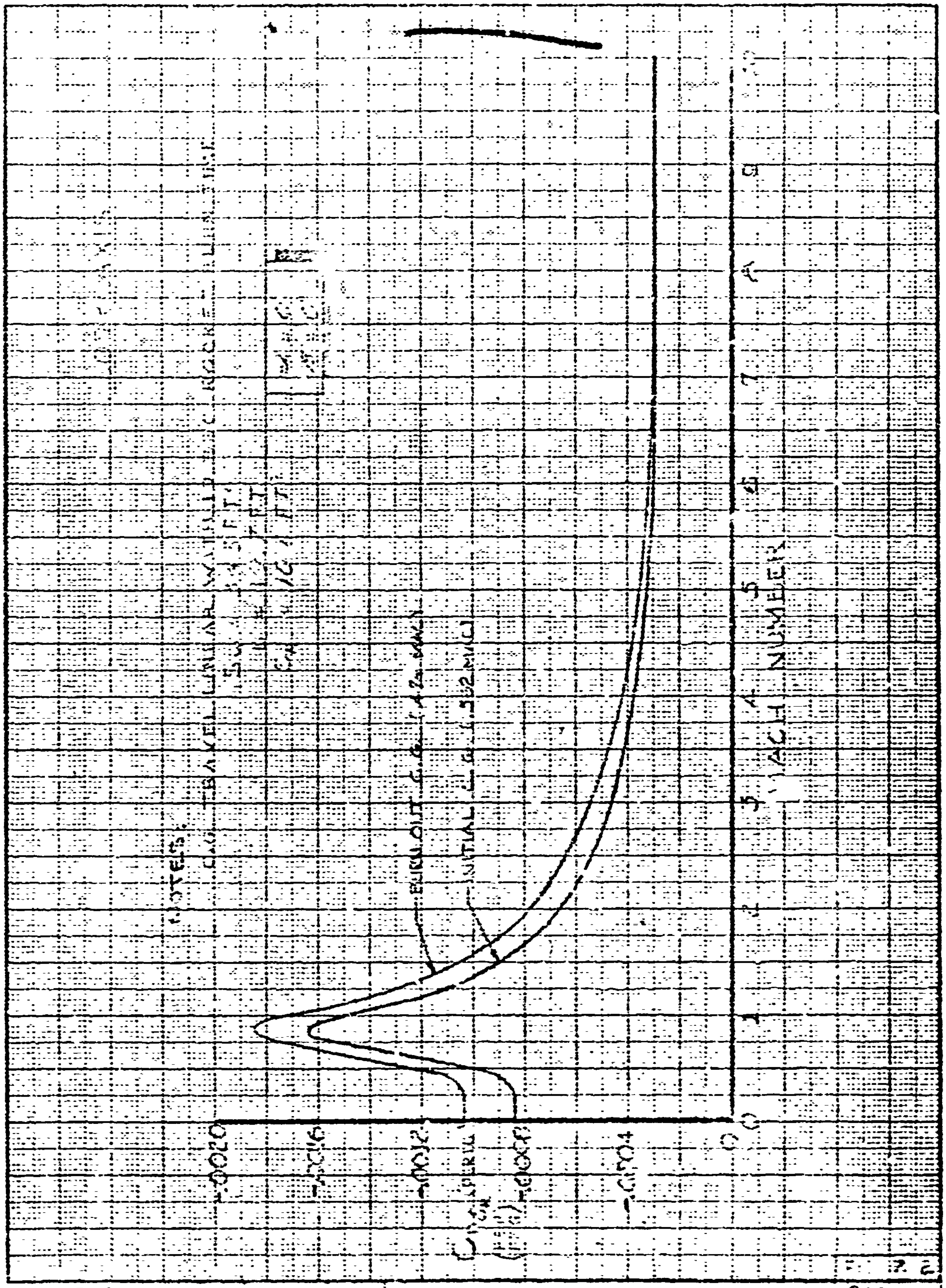

CALC DEP	12-23-?	REVISED	DATE	RUDDER EFFECTIVENESS	B44-2035
CHECK				$\alpha = 0°$ **193**	D2-8174
APR					
APR				BOEING AIRPLANE COMPANY	PAGE 7.16

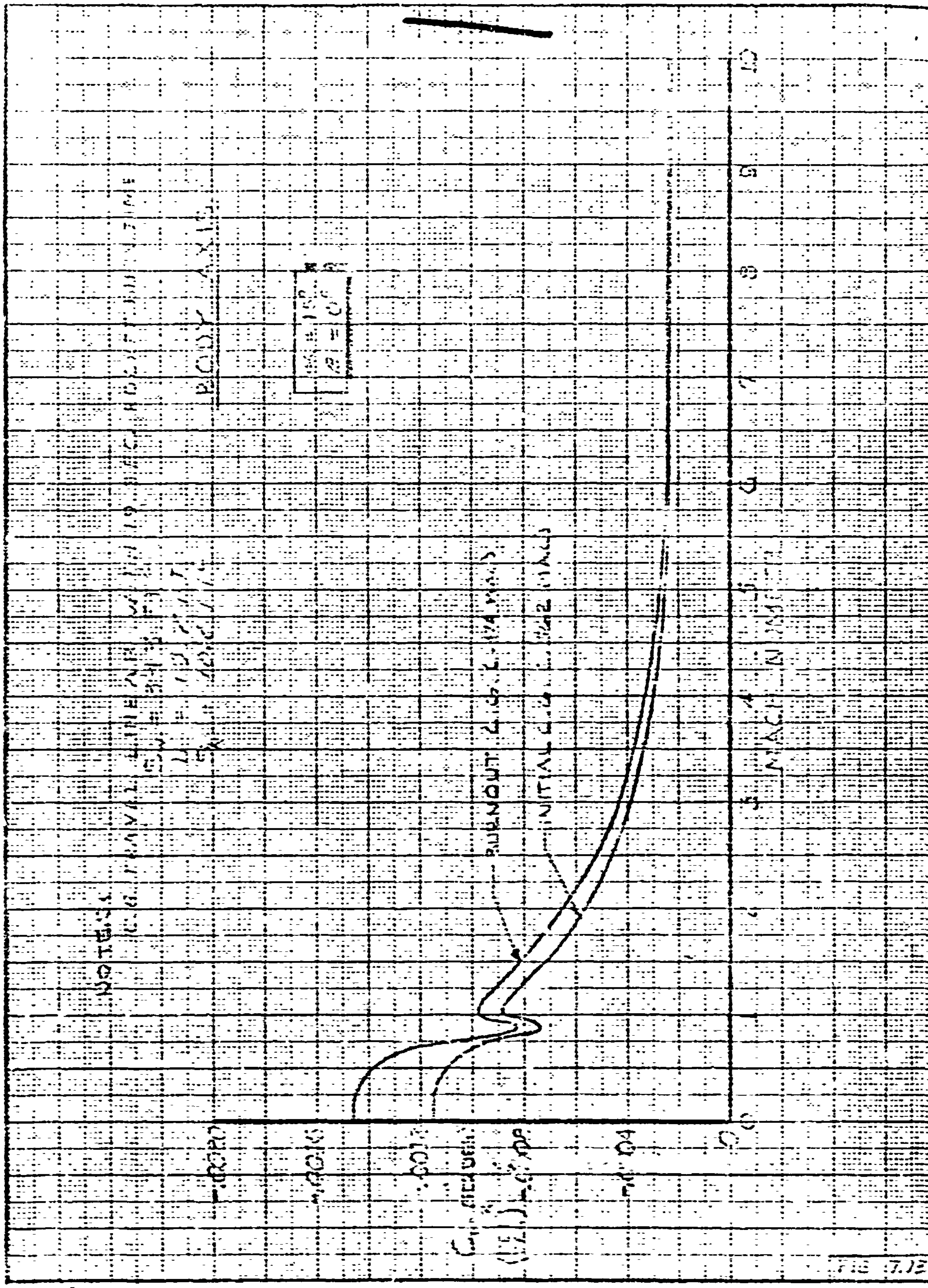

FIG 7.13

CALC		REVISED	DATE
CHECK			
APR			
APR			

RUDDER EFFECTIVENESS

$\alpha = 15°$

194

BOEING AIRPLANE COMPANY

D2-8174

PAGE 7.17